

Dissertation zur Erlangung des Doktorgrades
der Fakultät für Chemie und Pharmazie
der Ludwig-Maximilians-Universität München

The role of Integrin-linked kinase *in vivo* and *in vitro*

Carsten Grashoff
aus
Northeim

München, 2007

Erklärung

Diese Dissertation wurde im Sinne von §13 Abs.3 bzw. 4 der Promotionsordnung vom 29. Januar 1998 von Herrn Prof. Dr. Reinhard Fässler betreut und von Herrn Prof. Dr. Alexander Pfeifer vor der Fakultät für Chemie und Pharmazie vertreten.

Ehrenwörtliche Versicherung

Diese Dissertation wurde selbständig, ohne unerlaubte Hilfe erarbeitet.

München, am 08.02.2007

(Unterschrift des Autors)

Dissertation eingereicht am	08.02.2007
1. Gutachter	Herr Prof. Dr. Reinhard Fässler
2. Gutachter	Herr Prof. Dr. Alexander Pfeifer
Mündliche Prüfung am	28.03.2007

Erklärung	3
Table of contents	5
Abbreviations	9
1. Introduction	15
1.1. The integrin receptor family	15
1.1.1. The regulation of integrin activity	16
1.1.2. Structural insights into the regulation of integrin affinity	17
1.1.3. Integrin activation by cytoplasmic domain-binding proteins	18
1.2. Regulation of integrin signalling by cytoplasmic domain binding proteins	19
1.2.1. Structure and function of focal adhesions (FA).....	20
1.2.2. Mechanisms of integrin-actin interaction	22
1.2.3. Fibrillar adhesions and their role in fibronectin (FN) matrix assembly.....	23
1.2.4. Integrin signal transduction- a second level of actin reorganization	24
1.2.5. Integrin-growth factor receptor crosstalk	25
1.3. Integrin-linked kinase	27
1.3.1. Domain structure of ILK	28
1.3.2. Catalytic activity of ILK.....	28
1.3.3. Genetic studies of ILK in invertebrates	30
1.3.4. ILK- an adaptor protein at the integrin adhesion site	32
1.4. Analysis of the peri-implantation development in mice	33
1.4.1. Embryoid bodies (EBs)-a model system to study peri-implantation development.....	34
1.4.2. The role of the ECM proteins integrins during peri-implantation development.....	35
1.5. Development and analysis of the vertebrate skeleton	36
1.5.1. Bone formation by endochondral ossification	36
1.5.2. Regulation of chondrocyte proliferation and differentiation	37
1.5.2.1. Ihh-PTHrP crosstalk	38
1.5.2.2. Regulation of endochondral bone formation by growth factor signalling and transcription factors	39
1.5.3. The role of the ECM and integrins during endochondral ossification.....	40
1.5.3.1. Deletion of β 1 integrin in the cartilage	41
1.6. Epidermal morphogenesis and analysis of the murine skin	42
1.6.1. Epidermal morphogenesis	43
1.6.2. HF morphogenesis and the hair cycle.....	44
1.6.3. The role of integrins in the epidermis.....	46
1.6.3.1. Deletion of β 1 integrins from basal keratinocytes	46
1.7. Aim of the PhD thesis	47
2. Materials and Methods	49
2.1. Common chemicals	49
2.2. Animals	49
2.2.1. Breeding scheme	49
2.3. Histological analysis of ILK knockout mice	49
2.3.1. Material Histology.....	49
2.3.2. Histological methods.....	50
2.3.2.1. Preparation of paraffin sections	50
2.3.2.2. Preparation of cryo-sections	51
2.3.2.3. Skeletal whole mount staining: Alcian Blue/Alizarin Red staining.....	51
2.3.2.4. LacZ staining	51
2.3.2.5. Hematoxylin/Eosin staining.....	52
2.3.2.6. Hematoxylin/Safranin orange staining	53
2.3.2.7. Safranin-Orange von Kossa staining	53
2.3.2.8. Alkaline phosphatase staining- visualization of osteoblasts	54
2.3.2.9. Tartrate-resistant acid phosphatase staining- visualization of osteoclasts	54

2.3.3.	<i>In situ</i> hybridization on cartilaginous sections	55
2.3.3.1.	RNA labelling reaction	55
2.3.3.2.	RNA hybridization and immunological detection	56
2.4.	Immunological Methods	57
2.4.1.	Materials Immunological Analysis	57
2.4.2.	BrdU staining of cartilaginous sections	58
2.4.3.	TUNEL staining on cartilaginous sections	59
2.4.4.	Immunostaining on cartilaginous sections	60
2.4.5.	BrdU staining of adherent cells in culture	60
2.4.6.	Immunostaining of adherent cells in culture	61
2.4.7.	Cytoskeletal staining of adherent cells	61
2.4.8.	Lipid raft staining of adherent cells	62
2.5.	Cell culture methods	62
2.5.1.	Material Cell Culture	62
2.5.2.	Isolation and culture of primary chondrocytes	63
2.5.3.	Cell culture and trypsinization of immortalized mouse fibroblasts	64
2.5.3.1.	Cryo-preservation of mouse fibroblasts	64
2.5.3.2.	Thawing of cryo-preserved cells	64
2.5.4.	Establishment of clonal cell lines	64
2.5.5.	Cell substrate adhesion assay	65
2.5.6.	Cell spreading assay	65
2.5.7.	Fibronectin fibrillogenesis assay	66
2.5.8.	Dorsal ruffle formation assay	66
2.5.9.	Stable isotope labelling by amino acids in cell culture (SILAC)	67
2.5.9.1.	The SILAC principle	67
2.5.9.2.	Isotope labelling of cells in culture	68
2.6.	Biochemical methods	68
2.6.1.	Material Biochemistry	68
2.6.2.	Preparation of total protein lysates from adherent cells	68
2.6.3.	Cell fractionation	69
2.6.3.1.	Preparation of soluble and particulate fraction from adherent cells	70
2.6.3.2.	Detergent-free plasma membrane fractionation	71
2.6.3.3.	Preparation of the Triton-X insoluble cytoskeletal fraction	72
2.6.4.	Determination of the protein concentration	73
2.6.4.1.	BCA protein assay	73
2.6.4.2.	Bradford protein assay	73
2.6.5.	Immunoprecipitation	74
2.6.6.	Rac1 and Cdc42 pulldown assay	74
2.6.7.	One-dimensional SDS-polyacrylamid-gelelectrophoresis (SDS-PAGE)	75
2.6.8.	Western blotting and Immunodetection	76
2.7.	Molecular Biological Methods	77
2.7.1.	Material Molecular Biology	77
2.7.2.	Phenol/Chloroform extraction of tail DNA	78
2.7.3.	Bacteriological tools	78
2.7.3.1.	Preparation of competent bacteria	79
2.7.3.2.	Transformation of competent bacteria	79
2.7.3.3.	Cryo-preservation of bacteria	80
2.7.3.4.	Preparation of plasmid DNA from bacterial cultures	80
2.7.4.	Enzymatic manipulation of DNA	80
2.7.4.1.	Digestion of DNA with restriction enzymes	80
2.7.4.2.	Dephosphorylation of plasmid DNA	81
2.7.4.3.	Phosphorylation of DNA fragments	81
2.7.4.4.	Blunting of DNA fragments	81
2.7.4.5.	Ligation of DNA fragments	82
2.7.5.	Polymerase chain reaction (PCR)	82
2.7.5.1.	Oligonucleotides (primer)	82
2.7.5.2.	PCR reactions	86
2.7.5.3.	PCR programs	87
2.7.6.	Agarose gel electrophoresis	88

2.7.6.1. Extraction of DNA from agarose gels	88
2.7.7. Site-directed mutagenesis	88
2.7.7.1. Design of mutagenesis primers	89
2.7.7.2. Mutagenesis	89
2.7.8. Generation of siRNA constructs	90
2.7.8.1. Design of siRNA constructs	91
2.7.8.2. Cloning of siRNA constructs	92
2.7.9. Generation of retroviral expression constructs	93
2.7.9.1. Plasmids and cDNAs	93
2.7.9.2. Expression vectors	93
2.7.9.3. Generation of ILK expression constructs	94
2.7.9.4. Generation of Rac1 expression constructs	94
2.7.9.5. Generation of paxillin expression constructs	95
2.7.9.6. Generation of ELMO1 expression construct	95
2.7.10. Preparation of retrovirus	95
2.7.10.1. Calcium phosphate transfection of HEK293 cells	95
2.7.10.2. Harvest of retroviral supernatant	96
2.7.10.3. Infection of ILK fibroblasts with VSV-G pseudotyped retroviral vectors	96
2.7.11. Microscopy	97
3. Results.....	99
3.1. Analysis of ILK <i>in vivo</i>/targeted ablation of ILK in mice.....	99
3.1.1. Deletion of ILK leads developmental arrest at peri-implantation stage	99
3.1.2. ILK null EBs fail to form a mature epiblast	99
3.2. Analysis of ILK function <i>in vivo</i>/Characterization of cartilage-specific ILK knockout mice.....	101
3.2.1. Expression analysis	101
3.2.2. Chondrocyte-specific deletion of the <i>ILK</i> gene	102
3.2.3. Col2ILK mice display progressive dwarfism	102
3.2.4. Col2ILK bones have shortened growth plates	103
3.2.5. ILK is not required for chondrocyte maturation	105
3.2.6. ILK affects the G1-S transition of the chondrocyte cell cycle	107
3.2.7. ILK modulates the actin cytoskeleton of chondrocytes <i>in vivo</i> and <i>in vitro</i>	108
3.2.8. ILK is essential for proliferation and adhesion of primary chondrocytes <i>in vitro</i>	110
3.2.9. ILK is dispensable for the phosphorylation of PKB/AKT and GSK-3 β	110
3.3. Analysis of ILK function <i>in vivo</i>/characterization of keratinocyte-specific ILK knockout mice.....	112
3.3.1. Keratinocyte-specific deletion of the <i>ILK</i> gene	112
3.3.2. ILK-K5 mice display severe epidermal and HF abnormalities	113
3.3.3. Loss of ILK impairs integrin expression and BM integrity	115
3.3.4. ILK is not required for keratinocyte proliferation	115
3.3.5. Accumulation of proliferating cells in the ORS of ILK-deficient HFs	116
3.3.6. ILK is essential for directional cell migration	118
3.3.7. Loss of ILK is essential for stress fiber formation and establishment of mature FAs in keratinocytes	118
3.4. Analysis of ILK function <i>in vitro</i>/Characterization of ILK knockout fibroblasts.....	120
3.4.1. Generation of immortalized ILK knockout fibroblasts	120
3.4.2. Consequences of ILK deletion in fibroblasts	120
3.4.3. Presence of Pinch1 in FA of ILK (-/-) fibroblasts	121
3.4.4. The role of ILK during actin dynamics	122
3.4.5. ILK is essential for actin reorganization during cell spreading	123
3.4.6. ILK regulates cell spreading independently of its kinase activity	125
3.4.7. ILK is essential for fibronectin fibrillogenesis	127
3.4.8. Dorsal ruffle (DR) formation	128
3.4.8.1. DR formation during cell spreading	129
3.4.8.2. Integrin-dependency of DR formation	129
3.4.9. Localization of vinculin, talin and ILK into DR	130
3.4.10. DRs originate from the ventral side of the cell	131
3.4.11. ILK is essential for DR formation	134

3.4.12.	Stabilization of Pinch1 by N-terminal ILK is not sufficient for induction of FN fibrillogenesis in ILK (-/-) fibroblasts	135
3.4.13.	Expression of constitutive active Rac1 rescues the DR formation defect	136
3.4.14.	Expression of constitutive active Rac1 is not sufficient to overcome the FN assembly defect of ILK (-/-) fibroblasts	138
3.4.15.	Paxillin is dispensable for DR formation	138
3.4.16.	The interaction between paxillin and ILK is not essential for the organization of the actin cytoskeleton.....	141
3.4.17.	The paxillin-ILK interaction is not important for cell spreading and DR formation.....	142
3.4.18.	FAK is not essential for DR formation.....	144
3.4.19.	FAK is important for FN fibrillogenesis	146
3.4.20.	Localization of p130Cas, CrkII and ELMO1 in DRs	146
3.4.21.	p130Cas complexes with ILK and is essential for dorsal ruffling.....	147
3.4.22.	p130Cas expression is essential for dorsal ruffling.....	148
3.4.23.	The GEF Dock180 is indispensable for dorsal ruffling.....	150
3.4.24.	Normal plasma membrane organization in ILK (-/-) fibroblasts	152
3.4.25.	Cytoskeletal-associated p130Cas is hyperphosphorylated in ILK (-/-) fibroblasts	155
3.4.26.	Identification of an ILK-associated protein tyrosine phosphatase by SILAC	156
4.	Discussion	159
4.1.	The analysis of ILK <i>in vivo</i>	159
4.1.1.	General implications about the role of ILK <i>in vivo</i>	159
4.1.1.1.	A comparison of the $\beta 1$ and ILK knockout phenotypes	160
4.1.1.2.	The ILK-Pinch-parvin complex-implications from <i>in vivo</i> models.....	161
4.1.2.	Regulation of the ECM by ILK-implications from $\beta 1$ integrin and ILK knockout mice	162
4.1.2.1.	No differences in the ECM of the cartilage in the absence of ILK.....	162
4.1.2.2.	Disruption of the dermal-epidermal BM in the absence of ILK	163
4.1.3.	The impact of ILK on cell proliferation	163
4.1.3.1.	Reduced cell proliferation of ILK-deficient chondrocytes	163
4.1.3.2.	Increased cell proliferation in ILK-deficient keratinocytes	164
4.1.4.	ILK is dispensable for the phosphorylation of PKB/Akt or GSK-3 β	165
4.1.5.	ILK is essential for the regulation of the f-actin cytoskeleton.....	166
4.2.	The analysis of ILK <i>in vitro</i>	167
4.2.1.	ILK is essential for stress fiber formation and cell spreading	167
4.2.2.	ILK is required for FN fibrillogenesis.....	169
4.2.2.1.	The involvement of ILK, paxillin and FAK in FN fibrillogenesis.....	169
4.2.3.	ILK mediates integrin-RTK crosstalk during DR formation.....	171
4.2.3.1.	DR formation is integrin-dependent	171
4.2.3.2.	DRs originate at the ventral side of the cell.....	172
4.2.3.3.	ILK is indispensable for DR formation	173
4.2.3.4.	Integrin/ILK-dependent DR formation does not require paxillin or FAK.....	174
4.2.3.5.	Integrin/ILK-dependent DR formation requires p130Cas and Dock180.....	175
4.2.4.	Hyperphosphorylation of p130Cas in the cytoskeletal fraction of ILK-deficient cells	175
5.	Summary	179
6.	References	181
7.	Publications	199
8.	Acknowledgements	201
9.	Curriculum vitae	203

aa	amino acid
A	Alanin
AgNO ₃	silvernitratre
ANK	ankyrin
AP	alkaline phosphatase / arrector pili
APS	ammonium peroxodisulfate
AS	antisense
ATP	adenosine-triphosphate
BCA	bicinchoninic acid
BCIP	5-Bromo-4-chloro-3-indolyl phosphate
BM	basement membrane
BMP	bone morphogenetic protein
bp	base pair
BrdU	5-Bromo-2'-deoxyuridine
BSA	bovine serum albumine
Cas	Crk-associated substrate
CCD	charge coupled device
Cdc42	cell division cycle 42 homologue
cDNA	complementary DNA
<i>C.elegans</i>	<i>Caenorhabditis elegans</i>
CIB	calcium and integrin binding protein
CH	calponin homology
Col	collagen
CMV	Cytomegalovirus
CPI-17	protein kinase C dependent phosphatase inhibitor of 17 kDa
Crib	Cdc42/Rac interactive binding motif
CRM	caveolin-rich membrane fraction
Crk	chicken Tumour Virus 10 regulator of kinase
CYT	cytoplasm
D	aspartic acid / dermis
DAB	3-3'diaminobenzidine
Dab1	disabled-1
DAPI	4', 6-Diamidin-2-phenylindol-dihydrochloride
DIG	digoxigenin

Abbreviations

DMEM	Dulbecco's Modified Eagle Medium
DMSO	dimethylsulfoxide
DNA	deoxyribonucleic acid
dNTP	deoxynucleotide-triphosphate
Dock180	180kDa protein downstream of Crk
Dok	downstream of kinase
DP	dermal papilla
DTT	1,4-Dithiothreitol
DR	dorsal ruffle
DRAL	down-regulated in rhabdomyosarcoma LIM protein
E	embryonic day /Glutamic acid / Epidermis
<i>env</i>	envelope
EB	embryoid body
ECM	extracellular matrix
EDTA	ethylene-diamine-tetraacetic acid
EGF	epidermal growth factor
EGFP	enhanced green fluorescent protein
ELISA	Enzyme-linked Immunosorbent Assay
EMT	epithelial-to-mesenchymal transition
EPS8	EGFR-pathway substrate No. 8
ES cells	embryonic stem cells
F-actin	filamentous actin
FA	focal adhesion
FAK	focal adhesion kinase
FC	focal complex
FCS	foetal calf serum
FERM	four-point-one, ezrin, radixin, moesin
FGFR	fibroblast growth factor receptor
FN	fibronectin
g	gram
G-actin	globular actin
<i>gag</i>	group specific antigen
GEF	guanine nucleotide exchange factor
GSK-3	glycogen synthase kinase 3

GTP	guanosine triphosphate
h	hour
HBSS	Hanks' balanced salt solution
HCl	hydrochloric acid
H/E	Hematoxylin/Eosin
HeLa cells	cell line derived from cervical cancer taken from Henrietta Lacks
HEPES	N-(2-hydroxyethyl)-piperazine-N'-2-ethanesulfonic acid
HEK cells	human embryonic kidney cells
HF	hair follicle
HGF	hepatocyte growth factor
HIV	human immunodeficiency virus
HPLC	high performance liquid chromatography
HRP	horseradish peroxidase
Ihh	Indian hedgehog
ILK	Integrin-linked kinase
ILKAP	ILK-associated phosphatase
ICAP	Integrin-cytoplasmic domain associated protein
ICM	inner cell mass
IL2	Interleukin 2
IP	immunoprecipitation
IRS	inner root sheath
JAB	jun-activating binding protein
K	lysine
K5	keratin 5
K14	keratin 14
kDa	kilo Dalton
LB	lysogeny broth
LD	Leucine-Aspartic acid
Lef/Tcf	lymphoid enhancer factor/transcription factor
LIM domain	Lin-11, Isl-1, Mec-3 domain
LMW-PTP	low molecular weight protein tyrosine phosphatase
μl	micro litre
M/mM	molar/millimolar
MBP	myelin basic protein

Abbreviations

MCS	multiple cloning site
mDia	mammalian diaphanous
MEF	murine embryonic fibroblast
MIBP	muscle-specific β 1 integrin-binding protein
MIDAS	metal ion-dependent adhesion site
Mg/MgCl ₂	Magnesium/Magnesiumchloride
Mn	Manganese
mg	milligram
Mig-2	mitogen-inducible gene 2
min	minutes
MLC	myosin light chain
MTOC	microtubule organizing center
n	number
NaCl	sodium chloride
NaF	sodium fluoride
Na ₃ VO ₄	sodium-orthovanadate
α NAC	nascent-polypeptide associated complex and co-activator alpha
NBT	Nitro blue tetrazolium chloride
NCM	non-caveolin rich membrane fraction
NMR	nuclear magnetic resonance
o/n	overnight
nm	nanometer
OD	optical density
ORS	outer root sheath
p	passage
PAK	p21-activated kinase
PAT	paralyzed and arrested at twofold
PBS	phosphate buffered saline / paxillin binding site
PCR	polymerase chain reaction
PDK	3-phosphoinositide-dependent kinase
PFA	paraformaldehyde
PI3K	phosphoinositide 3- kinase
PH	pleckstrin homology
PHI-1	phosphatase holoenzyme inhibitor-1

Pinch	particularly interesting new cysteine-histidine rich protein
PIP2	phosphatidylinositol (4,5) bisphosphate
PIP3	phosphatidylinositol (3,4,5) trisphosphate
PIPES	Piperazine-1, 4-bis (2-ethanesulfonic acid)
PIPKI γ	phosphatidylinositol-4-phosphate 5-kinase type I gamma
PIX	PAK-interacting exchange factor
PKC	protein kinase C
PKL	paxillin kinase linker
PM	plasma membrane
PNK	polynucleotide kinase
PNS	post nuclear supernatant
POD	peroxidase
<i>pol</i>	polymerase
PPR	parathyroid hormone-related peptide receptor
PS	position specific
PTHrP	parathyroid hormone-related peptide
PTP	protein tyrosine phosphatase
PEST	Proline, Glutamic acid, Serine, Threonine
PVDF	polyvinylidene fluoride
R	Arginine
Rac	Ras-related C3 botulinum substrate
RACK	receptor for activated C-kinase
RGD	Arginine-Glycine-Aspartic acid
RNA	ribonucleic acid
ROCK	Rho kinase
RPM	rotations per minute
RT	room temperature
S	serine
SC	stem cells
siRNA	small interfering RNA
shRNA	short hairpin RNA
SCID	severe combined immunodeficiency
SDS	sodium dodecyl sulphate
SDS-PAGE	SDS polyacrylamid gel electrophoresis

Abbreviations

Ser	Serine
SFKs	src family kinases
SH domain	src-homology domain
SHP	src-homology protein
SILAC	stable isotope labelling by amino acids in culture
Sox9	SRY (sex determining region Y)-box 9
SSC	sodium chloride sodium citric acid
SV	simian virus
T	Threonine
TAP-20	theta-associated protein 20
<i>Taq</i>	<i>Thermophilus aquaticus</i>
TAE	Tris-acetic acid-EDTA buffer
TBS	Tris-buffered saline
TdT	terminal deoxynucleotidyl-transferase
TE	Tris-EDTA buffer
Thr	Threonine
TPA	12-O-Tetradecanoylphorbol-13-acetate
TRAP	tartrate-resistant acid phosphatase
Tris	Tris (hydroxymethyl) aminomethane
TEMED	N,N,N',N'-Tetramethylethylenediamine
TSS	transformation and storage solution
TUNEL	terminal deoxynucleotidyl-transferase-mediated dUTP nick end labelling
Tyr	Tyrosine
U	Unit
UV	ultra violet
V	Volt
VCAM	vascular cell adhesion molecule
VEGF	vascular endothelial growth factor
VN	vitronectin
VSV-G	vesicular stomatitis viral G protein
wt	wild type
X-Gal	Chloro-3-indolyl- β -D-galactopyranoside
Y	tyrosine

1. Introduction

1.1. The integrin receptor family

Integrins are heterodimeric cell surface receptors expressed in all metazoa. They consist of an α and a β subunit both of which are transmembrane type I proteins. Man and mouse have 18 α and 8 β subunits which can non-covalently assemble into 24 different heterodimeric receptors. The interaction between integrins and their ligands is considered to provide the physical support for cells in order to maintain adhesion, to permit traction forces and to organize signalling complexes which regulate cell proliferation, cell survival or differentiation (Hynes and Zhao 2000; Hynes 2002; Liddington and Ginsberg 2002).

Based on their recognition specificity integrins can be divided into different classes (Fig 1.1). One class recognizes the tri-peptide sequence RGD present in extracellular ligands such as fibronectin (FN) or vitronectin (VN). A pair of related integrins ($\alpha4\beta1$, $\alpha9\beta1$) can recognize FN and additionally interact with Ig-superfamily counter receptors such as VCAM-1 (vascular cell adhesion molecule). A second class mediates the interaction with a family of ECM molecules called laminins, a third set are the collagen receptors. The leukocyte-specific receptors are also capable of interacting with Ig-superfamily counter receptors to mediate cell-cell adhesions.

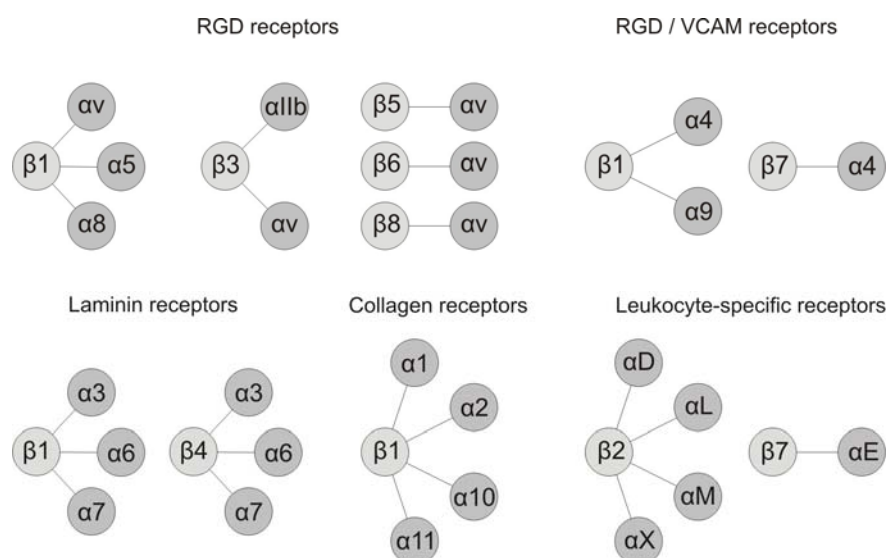


Fig 1.1. The integrin receptor family. Based on their recognition specificity integrin heterodimers can be considered in different classes (see text). Integrins are ubiquitously expressed and mediate the interaction of cells with the extracellular matrix. (Based on Hynes, 2002).

Up to now, knockout mice for all β subunits and all but three α subunits have been generated (Table 1.1). The diversity of the phenotypes observed in those mice ranging from peri-implantation lethality to perinatal lethality, defects in leukocyte function, inflammation, hemostasis, bone remodelling, angiogenesis and lack of phenotype suggests that most of the integrins have a specific, non-redundant function (Bouvard et al. 2001). Since abnormal integrin function is also associated with the progression of diseases such as Glanzmann thrombosthenia (caused by mutations in α IIb β 3) or epidermolysis bullosa (α 6 β 4) or cancer, integrin structure, function and signal transduction has been and is still extensively studied.

The following chapter will introduce the mechanisms of integrin activation, integrin signal transduction and the role of cytoplasmic integrin-binding proteins.

integrin	phenotype	Reference
β 1	peri-implantation lethality E5.5, defective BM assembly	Fässler and Meyer, 1995
β 2	viable / fertile, leukocytosis, impaired inflammatory response	Scharffetter-Kochanek, 1998
β 3	viable / fertile, no platelet aggregation, osteosclerosis	Hodivala-Dilke, 1999
β 4	perinatal lethal, severe skin blistering	van der Neut, 1996
β 5	viable / fertile, no obvious defects	Huang et al., 2000
β 6	viable / fertile, inflammation in skin and airways	Huang et al., 1996
β 7	viable / fertile, no formation of Peyer's patches	Wagner et al., 1996
β 8	lethal at E10 due to placental defects or perinatal lethal	Zhu et al., 2002
α 1	viable / fertile, reduced tumor vascularization	Gardner et al., 1996
α 2	viable / fertile, delayed platelet aggregation	Holtkotter et al., 2002
α 3	perinatal lethal, kidney tubule defects, mild skin blistering	Kreidberg et al., 1996
α 4	lethal at E11/14 due to placental defects or heart defects	Yang et al. 1995
α 5	lethal at E10-11, defective formation of posterior somites	Yang et al. 1993
α 6	perinatal lethal, severe skin blistering	Georges-Labouesse et al., 1996
α 7	viable / fertile, muscular dystrophy	Mayer et al., 1997
α 8	perinatal lethal, no or defective kidney formation	Muller et al., 1997
α 9	perinatal lethal, lymphatic duct defect	Huang et al., 2000
α 10	viable / fertile, mild skeletal defects	Bengtsson et al., 2005
α v	lethal at E10 due to placental defects or perinatal lethal	Bader et al., 1998
α IIb	viable / fertile, no platelet aggregation	Tronik-Le Roux, 2000
α E	viable / fertile, reduced numbers of intraepithelial lymphocytes	Schon et al., 1999
α L	viable / fertile, impaired leukocyte recruitment	Schmits et al., 1996
α M	viable / fertile, defective phagocytosis and apoptosis of neutrophils	Coxon et al., 1996

Table 1.1. Diversity of integrin knockout phenotypes. For all but three integrin subunits (α 11, α D, α X) knockout mice have been generated. Almost each of them displays a specific phenotype, demonstrating the non-redundant functions of integrins (Taken from: Bouvard et al. 2001; Hynes 2002 and modified).

1.1.1. The regulation of integrin activity

Integrins are not constitutively active, but are present on the cell surface either in an active or an inactive state. The regulation of integrin activity is essential for its function which becomes most evident when considering integrins on circulating platelets (Bennett 2005). The integrin

$\alpha\text{IIb}\beta\text{3}$ is highly expressed on platelets and in the absence of activating signals in an inactive state. This is essential since constitutive active integrins would lead to platelet aggregation and thrombosis. On the other hand loss of $\alpha\text{IIb}\beta\text{3}$ leads to severe bleeding disorders due to defective aggregation upon platelet activation (Table 1.1). Therefore, integrin activity needs to be tightly regulated.

1.1.2. Structural insights into the regulation of integrin affinity

The elucidation of the integrin $\alpha\text{v}\beta\text{3}$ crystal structure provided unprecedented insights into the mechanism of integrin activation and ligand binding (Xiong et al. 2001). In general, integrins are approximately 280Å long and consist of a 150-180kDa large α and approximately 100kDa large β subunit. Both proteins are comprised of a large extracellular domain, a transmembrane domain and a rather small cytoplasmic tail which usually spans around 50 amino acids (aa). An exception is the β4 integrin cytoplasmic domain which consists of more than 1000aa. The $\alpha\text{v}\beta\text{3}$ integrin consists of an ovoid head region produced by the β -propeller from the αv subunit and the βA domain from the β3 subunit (forming the ligand binding site) and two almost parallel tail regions consisting of two calf and a thigh domain in the α subunit and EGF like repeats and a hybrid domain in the β subunit (Fig 1.2). The metal ion-dependent adhesion site (MIDAS), which is essential for binding activating bivalent cations (Mg^{2+} or Mn^{2+}) is located in the βA domain adjacent to an inhibitory calcium (Ca^{2+}) binding site (ADMIDAS). Interestingly, the crystal structure of $\alpha\text{v}\beta\text{3}$ did not reveal an extended but instead a severely bent conformation (Fig 1.2A). Although the structure was solved almost 4 years ago it is still hotly debated whether this bent integrin fold represents the active or the inactive integrin conformation (Fig 1.2A, B). On the one hand Arnaout and co-workers could show that the bent conformation can bind RGD peptides (Xiong et al. 2002) and fibronectin (Adair et al. 2005) in a Mn^{2+} -dependent manner and therefore concluded that the bent structure indeed represents an active conformation. On the other hand Springer and co-workers could show with negative stain electron microscopy that a recombinant extracellular fragment of $\alpha\text{v}\beta\text{3}$ drastically changes from a bent to the extended conformation upon Mn^{2+} - or RGD-dependent activation. Moreover, they found that the affinity of soluble $\alpha\text{v}\beta\text{3}$ to its physiological ligands is much higher in the extended conformation (Takagi et al. 2002).

Most probable the extracellular domain of integrins can adopt different conformations which all can bind physiological ligands but with varying affinities (Carman and Springer 2003). The conformation and hence affinity of the extracellular integrin domain is thought to be regulated by the transmembrane as well as the cytoplasmic domains, which in turn are

modulated by their interaction with intracellular proteins. The regulation of integrin activity by intracellular proteins is called inside-out signalling (see below, 1.1.3).

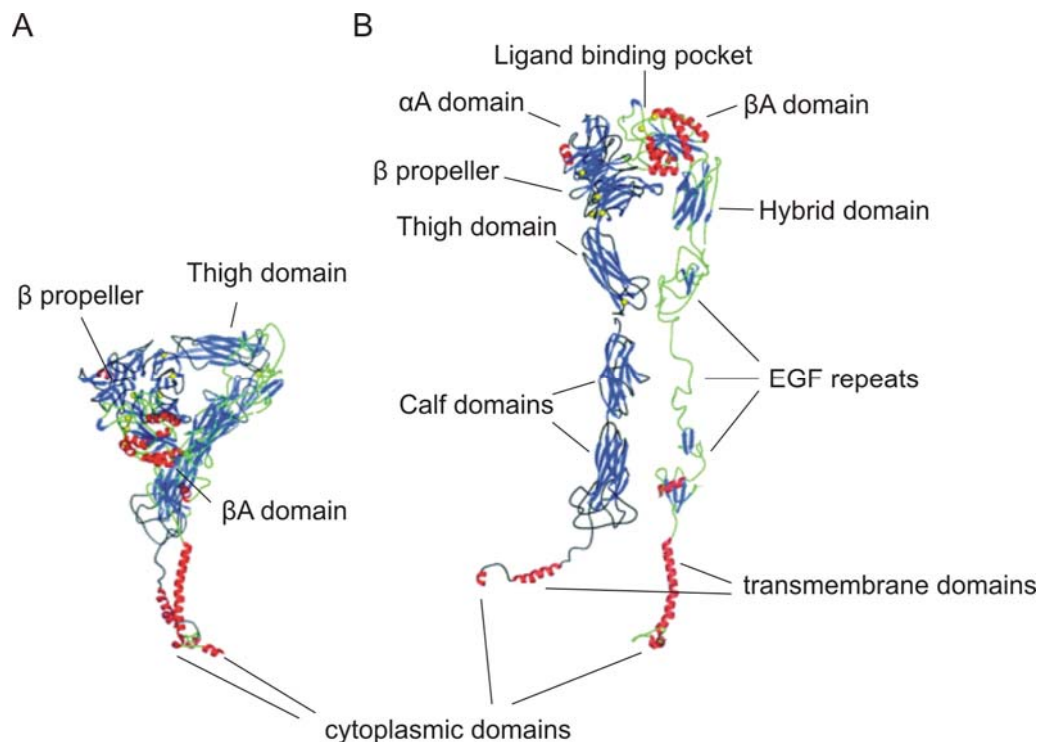


Fig 1.2 Schematic representation of the crystal structure of $\alpha v \beta 3$. *A.* Crystal structure of the extracellular domain of $\alpha v \beta 3$ (Xiong et al., 2001), including the transmembrane and cytoplasmic domains. This structure is often considered as the “inactive” (or low affinity) conformation. *B.* Model of the straightened extracellular segment of $\alpha v \beta 3$ which is considered the “active” (or high affinity) conformation. The β subunit (right) consists of a βA domain, a hybrid domain and EGF repeats, the α subunit (left) comprises an αA domain, a β propeller, a thigh domain and two calf domains. β strands are shown in blue, α helices in red. The transmembrane and cytoplasmic domains were pasted to the bottom of the extracellular domains. (Taken from Humphries et al. 2003 and modified). Note, how small the cytoplasmic domains are in comparison to the extracellular domains.

1.1.3. Integrin activation by cytoplasmic domain-binding proteins

Although integrins cytoplasmic tails are much smaller than the extracellular domains (Fig 1.2) they play a pivotal role during integrin activation (Liu et al. 2000). Overexpression of integrins which either lack the cytoplasmic domains of the β subunit (Solowska et al. 1989) or which comprise deletions of 5-15aa near the carboxyl end (Hayashi et al. 1990) exert dominant-negative effects regarding integrin localization and its ligand binding activity. Overexpression of cytoplasmic integrin β tails fused to an irrelevant extracellular domain (murine CD4 or IL2R) inhibits integrin ligand binding (Lukashev et al. 1994). Interestingly, deletion of conserved sequences in the cytoplasmic domain of the αIIb -subunit (O'Toole et al. 1994) leads to a constitutive active integrin. All these data suggest that both the α - and the β -

cytoplasmic tails contribute to the regulation of integrin activity. Recent data, using NMR spectroscopy demonstrated that the cytoplasmic tails of α IIb and β 3 weakly interact with each other in a low affinity state. Separation of the cytoplasmic tails (by unclasping of the weak interaction) leads to integrin activation and can be induced by the interaction with cytoplasmic plaque proteins such as talin (Vinogradova et al. 2002). These data further demonstrated that the regulation of integrin activity can be modulated by cytoplasmic domain binding proteins.

The function of the cytoplasmic tail-binding molecules, however, is not restricted to integrin activation. Since integrins lack enzymatic activity, the transmission of signals transduced from the extracellular space into the interior of the cell critically depends on the recruitment of cytoplasmic tail-binding proteins. This process is called outside-in signalling.

1.2. Regulation of integrin signalling by cytoplasmic domain binding proteins

More than 20 proteins have been identified to be capable of directly interacting with the cytoplasmic tail of integrins including actin-binding proteins (i.e. talin, α -actinin, filamin), adaptor proteins (i.e. ILK, Grb2, paxillin), kinases (FAK), guanine nucleotide exchange factors (cytohesin-1,-3), transcriptional co-activators (JAB1) and other transmembrane proteins (CD98) (Table 1.2; Liu et al. 2000). The diversity within this group of integrin interaction partners already points to the complexity of integrin signalling, which is far too intricate to be introduced here fully. Instead, the reader is referred to excellent reviews about integrin signalling (Giancotti 1997; Schwartz and Ginsberg 2002; Guo and Giancotti 2004).

One of the most important functions of cytoplasmic integrin binding proteins is the interconnection of integrins with the actin cytoskeleton, which occurs in a specialized integrin structures called focal adhesions (FAs). Structure and function FAs as well as mechanisms of integrin-actin interactions will be described below.

integrin binding partner	integrin subunit	Reference
α -actinin	$\beta 1, \beta 2$	Otey et al., 1990
calreticulin	α	Rojiani et al., 1991
caveolin-1	α	Wary et al., 1998
CD98	$\beta 1, \beta 3$	Zent et al., 2000
CIB	$\alpha 1b$	Naik et al., 1997
cytohesin-1	$\beta 2$	Kolanus et al., 1996
cytohesin-3	$\beta 2$	Hmama et al., 1999
DAB1	$\beta 1, \beta 3$	Calderwood et al., 2003
DAB2	$\beta 3, \beta 5$	Calderwood et al., 2003
Dok-1	$\beta 2, \beta 3, \beta 5, \beta 7$	Calderwood et al., 2003
DRAL	$\alpha 3, \alpha 7, \beta$	Wixler et al., 2000
endonexin $\beta 3$	$\beta 3$	Shattil et al., 1995
EPS8	$\beta 1, \beta 3, \beta 5$	Calderwood et al., 2003
FAK	$\beta 1, \beta 2, \beta 3$	Schaller et al., 1995
filamin	$\beta 1, \beta 2, \beta 3, \beta 7$	Pfaff et al., 1998, Goldmann et al., 2000
f-actin	$\alpha 2$	Kieffer et al., 1995
Grb-2	$\beta 3$	Law et al., 1996
ICAP	$\beta 1$	Chang et al., 1997
ILK	$\beta 1, \beta 3$	Hannigan et al., 1996
JAB1	$\beta 2$	Bianchi et al., 2000
Melusin	$\beta 1$	Brancaccio et al., 1999
MIBP	$\beta 1$	Li et al., 1999
myosin	$\beta 3$	Jenkins et al., 1998, Sajid et al., 2000
paxillin	$\beta 1, \beta 3, \alpha 4$	Schaller et al., 1995, Liu et al., 1999
Rack-1	$\beta 1, \beta 2, \beta 5$	Liliental et al., 1998
Shc	$\beta 3$	Law et al., 1996
skelemin	$\beta 1, \beta 3$	Reddy et al., 1998
TAP-20	$\beta 5$	Tang et al., 1999
talin	$\beta 1, \beta 2, \beta 3$	Horwitz et al., 1986, Knezevic et al., 1996
tensin-1	$\beta 1, \beta 3, \beta 5, \beta 7$	Calderwood et al., 2003
Unc-112 / Kindlin / Mig-2	$\beta 1$	Mackinnon et al., 2002
WAIT-1	$\beta 7$	Rietzler et al., 1998

Table 1.2. Cytoplasmic domain-binding proteins. Integrins can interact with a number of cytoplasmic proteins which connect integrins with the actin cytoskeleton or with different signalling pathways. (Taken from Liu et al., 2000 and modified).

1.2.1. Structure and function of focal adhesions (FA)

Most of our knowledge about the integrin-actin interaction stems from experiments in cell culture, where integrin ligand binding and clustering leads to the assembly of small multiprotein adhesion structures called focal complexes (FCs; 100-200 nm in size). The maturation of the rather small FCs into larger structures results in the assembly of FAs (1 μ m in size), which mediate the interaction of integrins with thick f-actin bundles called stress fibers (Fig 1.3; Zamir and Geiger 2001). Although these structures are hard to detect *in vivo*, the analysis of FAs has emerged as a powerful tool to study the role of integrins and various integrin adaptor proteins during processes such as cell adhesion or cell migration.

The organization of FAs is highly complex. More than 50 proteins have been found to localize into FAs including phosphatases (i.e. SHP-2, PTP1B), tyrosine kinases (i.e. c-src, FAK) and Ser/Thr kinases (i.e. PKC, PAK), proteases (calpainII) or GTPase modulators (i.e. Pix, Dock180) (Fig 1.4; Zamir and Geiger 2001). Moreover, mRNA and ribosomes could be detected at FAs suggesting that integrin signalling directly induces protein translation at the adhesion sites (Chicurel et al. 1998). The molecular complexity of FAs might be even higher than Fig 1.4 implies since many components are expressed in a cell-type specific manner or can be expressed in different splice variants or isoforms (i.e. Pinch1, Pinch2, α -, β -, γ -parvin). Furthermore, most of the FA components can adopt different conformations (i.e. upon phosphorylation) and most of them contain more than one protein binding site allowing FA proteins theoretically to assemble in many alternative ways producing a number of different supramolecular structures with different mechanical or biochemical functions.

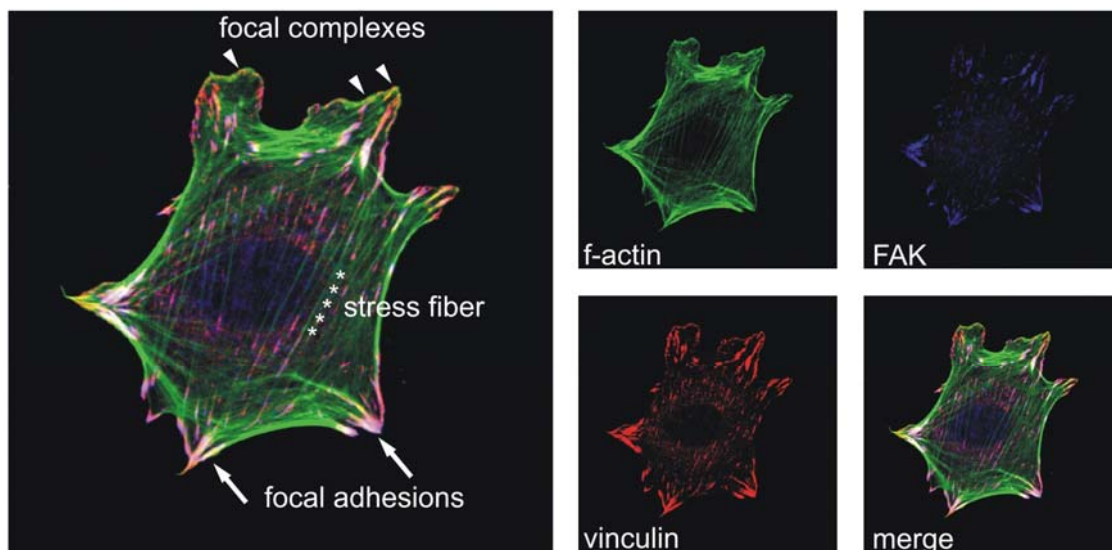


Fig 1.3. Assembly of FCs, FAs and stress fibers in cultured cells. Cells seeded on ECM proteins form large FAs (arrows), which mature from smaller FCs (arrowhead). Both types of adhesion structures can be visualized by vinculin and focal adhesion kinase (FAK) staining. Stress fibers (*) can be visualized by phalloidin staining, which specifically decorates f-actin. (Shown here: ILK (f/f) fibroblasts adherent to FN).

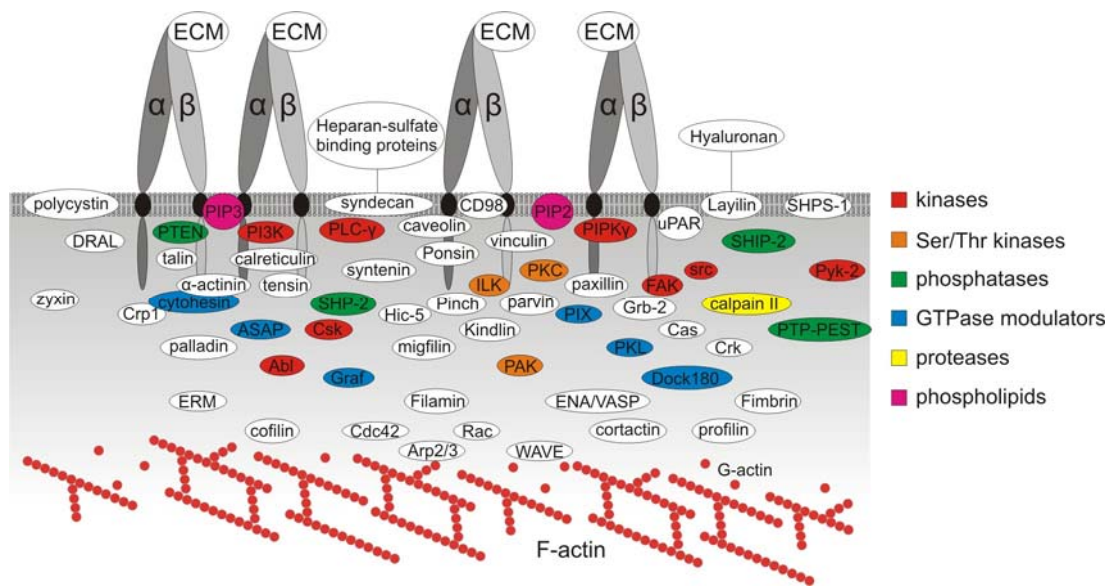


Fig 1.4. The molecular complexity of FAs. More and more proteins are identified, which can localize to FAs. In addition, ribosomes and mRNA were detected in these integrin adhesion sites. Theoretically, all these proteins can assemble into numerous different supramolecular structures. (Based on Zamir and Geiger 2001).

1.2.2. Mechanisms of integrin-actin interaction

The establishment of the f-actin cytoskeletal network as seen in Fig 1.3 requires anchorage to the integrin adhesions sites and is essential for the development of pulling and traction forces. This in turn is indispensable for the modulation of the cell shape during migration, differentiation or proliferation. Depending on the cell type the integrin-actin interaction can be highly dynamic and regulated by many signalling processes. Although most of these processes are still not fully understood on the molecular level, work over the last 20 years identified certain basic mechanisms, which seem to be applicable for almost all cell types. The most important molecular players involve talin, vinculin, α -actinin, filamin and ILK (Brakebusch and Fassler 2003). As an example, the talin-mediated establishment of the integrin-actin connection will be briefly introduced.

Talin can bind directly to integrin β subunits (Table 1.2.). This interaction does not only promote integrin activation (as discussed in 1.1.3) but in addition leads to the recruitment and activation of phosphatidylinositol-phosphate kinase type I gamma (PIP3K γ) which catalyzes the production of phosphatidylinositol (4,5) bisphosphate (PIP2) (Fig 1.5A, B). The PIP2-binding increases on the one hand the interaction of talin with β integrins but on the other hand attracts other PIP2 binding proteins like vinculin to the integrin adhesion site. PIP2-binding leads to a conformational change of vinculin exposing talin binding sites. The

interaction of talin and vinculin, in turn, increases the affinity of vinculin for f-actin, which finally leads to the recruitment of f-actin into FAs (Fig 1.5C).

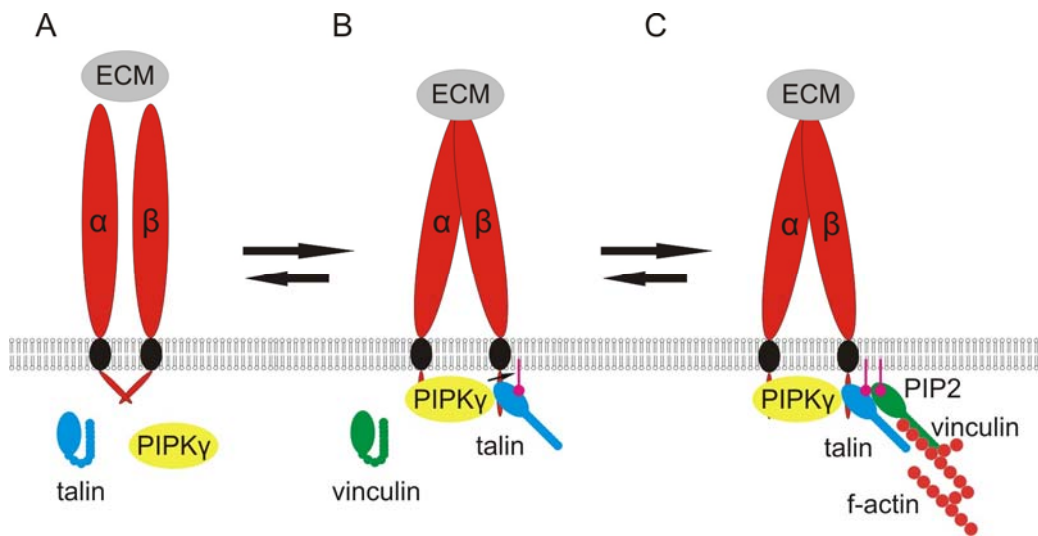


Fig 1.5. Interconnection of integrins with the f-actin cytoskeleton through talin. *A. Binding of talin to β integrin subunits is essential for integrin activation and ligand binding. B. Binding of talin to β integrin subunits induces cytoplasmic tail separation, ligand binding and the recruitment of PIPK γ , which leads to local production of PIP2. C. PIP2-binding molecules such as vinculin are attracted to the integrin adhesion site. The vinculin-PIP2 interaction induces conformational changes, which lead to a talin-vinculin interaction and the recruitment of f-actin. (Picture based on Giancotti and Tarone, 2003).*

1.2.3. Fibrillar adhesions and their role in fibronectin (FN) matrix assembly

Classical FAs are defined by oval peripheral cellular structures enriched in vinculin, paxillin and highly tyrosine-phosphorylated proteins (Fig 1.3). Fibrillar adhesions are more elongated centrally located structures, which are enriched in tensin and integrin $\alpha 5 \beta 1$ but contain less tyrosine-phosphorylated proteins (Zamir et al. 2000). The assembly of fibrillar adhesion coincides with a special type of ECM modulation namely FN fibrillogenesis.

Fibrillar adhesion formation is initiated when integrin $\alpha 5 \beta 1$ binds soluble fibronectin in FAs. Pulling forces triggered by the actin-binding molecule tensin and generated by myosin II-based contraction of the f-actin cytoskeleton lead to the translocation of $\alpha 5 \beta 1$ centripetally into the cell body to form fibrillar adhesions. This is different for all other integrins such as $\alpha v \beta 3$ for example, which primarily interacts with VN and remains localized in FAs. The mechanical tension applied to FN leads to the exposure of cryptic self assembly sites promoting self-association of FN (Fig 1.6; Yamada et al. 2003). Little is known about the FA proteins involved in the assembly of fibrillar adhesions.

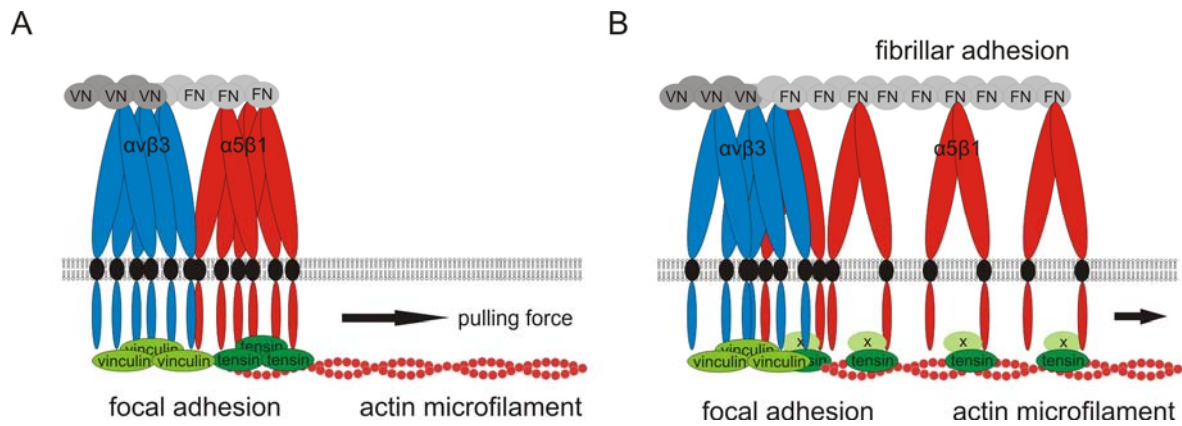


Fig 1.6. Model of FN fibrillogenesis. *A.* FAs usually contain $\alpha\beta3$ (FN/VN receptor) as well as $\alpha5\beta1$ (FN receptor). FA proteins like vinculin and the actin binding protein tensin colocalize in FAs. *B.* In response to actin-dependent pulling forces triggered by the actin-binding protein tensin integrin $\alpha5\beta1$ moves centripetally into the cell body, leading to the exposure of FN domains that promote FN self-assembly. $\alpha\beta3$ integrin remains in FAs and can not be found in fibrillar adhesions. (Picture based on Yamada et al. 2003).

1.2.4. Integrin signal transduction- a second level of actin reorganization

In addition to their important role in cell adhesion, assembly and organization of the ECM as well as the anchorage of the f-actin cytoskeleton, integrins can act as important signalling receptors (Schwartz and Ginsberg 2002). The f-actin cytoskeleton for example can be additionally modulated in response to the formation of new cell-substrate interactions by the induction of actin polymerization.

Almost all integrins activate focal adhesion kinase (FAK), a cytoplasmic tyrosine kinase which is composed of an N-terminal FERM domain, a C-terminal FA targeting domain and a central kinase domain (Cary and Guan 1999). Upon ligand binding integrins recruit FAK into FCs and FAs (Fig 1.7A, B) where FAK undergoes autophosphorylation and associates amongst others with src family kinases and the regulatory subunit of PI3K (Fig 1.7C). Activated PI3K provides a local source of PIP3 for the initiation of downstream signalling important for cell migration, survival or proliferation, while c-src is capable of phosphorylating a number of downstream targets including paxillin, cortactin or p130Cas (Cary and Guan 1999). The scaffolding protein paxillin is known to interact with a more than 20 proteins including the adaptor protein paxillin kinase linker (PKL) and the GTPase activating protein PIX/Cool which can affect the actin cytoskeleton (Turner 2000). p130Cas is able to recruit CrkII which engages with the adaptor protein ELMO1 and the guanine nucleotide exchange factor (GEF) Dock180 to activate the small GTPase Rac1, which promotes Arp2/3-dependent actin polymerization (Fig 1.7D; Chodniewicz and Klemke 2004).

This example shows that integrins do not only provide a physical linkage to the actin cytoskeleton, but also directly initiate signalling pathways that regulate f-actin polymerization and reorganization.

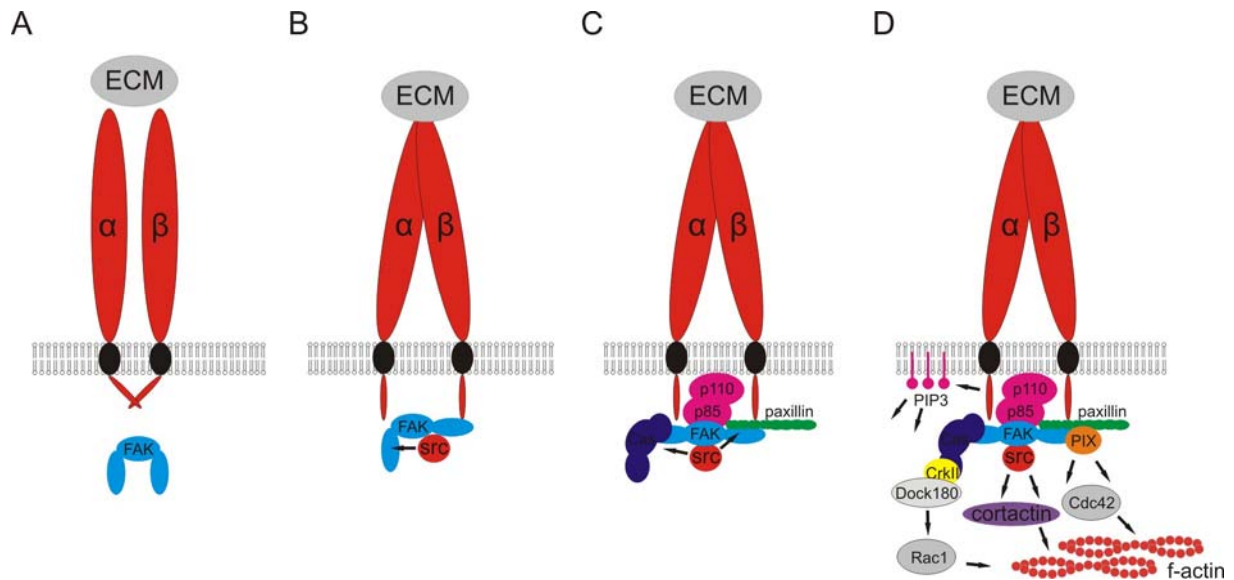


Fig 1.7. Integrins can act as signalling receptors. *A.* Before integrin activation FAK is localized throughout cytoplasm. *B.* Upon integrin engagement, FAK gets recruited to β integrins cytoplasmic domain (directly or indirectly), thereby changing its conformation. The exposure of SH-2 binding sites facilitates c-src binding, which can further phosphorylate FAK. *C.* Activated and phosphorylated FAK interacts with downstream proteins such as paxillin, p130Cas or the regulatory subunit of PI3K (p85). *D.* The activation of PI3K leads to the local production of PIP3 by the catalytic subunit (p110). p130Cas gets phosphorylated by FAK and c-src and interacts with CrkII which in turn is able to recruit the ELMO1/Dock180 complex. Paxillin is able to recruit PIX and Dock180 which activates the small Rho-GTPases Rac1 and Cdc42 leading to the induction of Arp2/3 mediated f-actin polymerization.

1.2.5. Integrin-growth factor receptor crosstalk

It is interesting to note that integrins share many common elements in their signalling pathways with other cell surface receptors especially with receptor protein tyrosine kinases (RTK) which bind to soluble growth factors and/or cytokines. In fact, it has been noted long time ago that integrin and RTK signalling pathways are interdependent. Non-transformed cells require anchorage to the matrix in order to progress through the G1 phase of the cell cycle indicating that integrin engagement can aggravate RTK signalling to promote cell proliferation (Assoian and Zhu 1997). A key feature of neoplastic cells on the other hand is their anchorage-independent growth, facilitated by the activation of dominant oncogenes or inhibition of tumour suppressor leading to the constitutive activation of signalling pathways which are normally tightly regulated by integrins and RTKs.

The crosstalk between integrins and RTKs is achieved in several ways. First, integrins and RTKs can become physically linked by certain adaptor molecules. FAK was co-immunoprecipitated with $\beta 1$ integrin but is also known to interact with RTKs upon growth factor stimulation. Although it seems unlikely that FAK binds to integrins and RTKs at the same time, it could bind with its N-terminal FERM domain to growth factor receptors and simultaneously interact with integrin binding proteins such as paxillin or talin (Fig 1.8A). Second, integrin engagement can lead to the activation of signalling proteins which directly affect RTK phosphorylation (Moro et al. 1998). p130Cas was shown to engage with the EGF-receptor in a src-dependent manner upon cell adhesion to FN, leading to phosphorylation of distinct tyrosine residues at the EGF-receptor (Fig 1.8B; Cabodi et al. 2004). *Vice versa*, the stimulation of the EGF-receptor pathway induces tyrosine phosphorylation of $\beta 4$ integrin through members of the src kinase family such as Fyn and Yes (Fig 1.8C; Mariotti et al. 2001). Finally, integrins and RTKs can be directly associated in certain plasma membrane microdomains, called lipid rafts (Fig 1.8D). In fact, it has been shown recently, that integrin engagement regulates plasma membrane order (Gaus et al. 2006). Since RTKs have been co-immunoprecipitated with integrins (Schneller et al. 1997; Moro et al. 1998) it is entirely possible, that a close if not direct interaction of these receptors at the plasma membrane accounts for the interconnection of their signalling pathways. For more detailed information about the integrin-RTK crosstalk see (Giancotti and Tarone 2003).

Taken together, integrins, which are expressed on almost all cells of the body, are indispensable for many cellular processes such as cell adhesion, cell migration, cell proliferation or cell differentiation but also important for the assembly of the ECM. Since integrins lack actin-binding sites and enzymatic activity, they regulate these processes by the recruitment of various intracellular proteins, which directly bind their cytoplasmic tails. One of these proteins is Integrin-linked kinase (ILK), which will be introduced in the following section.

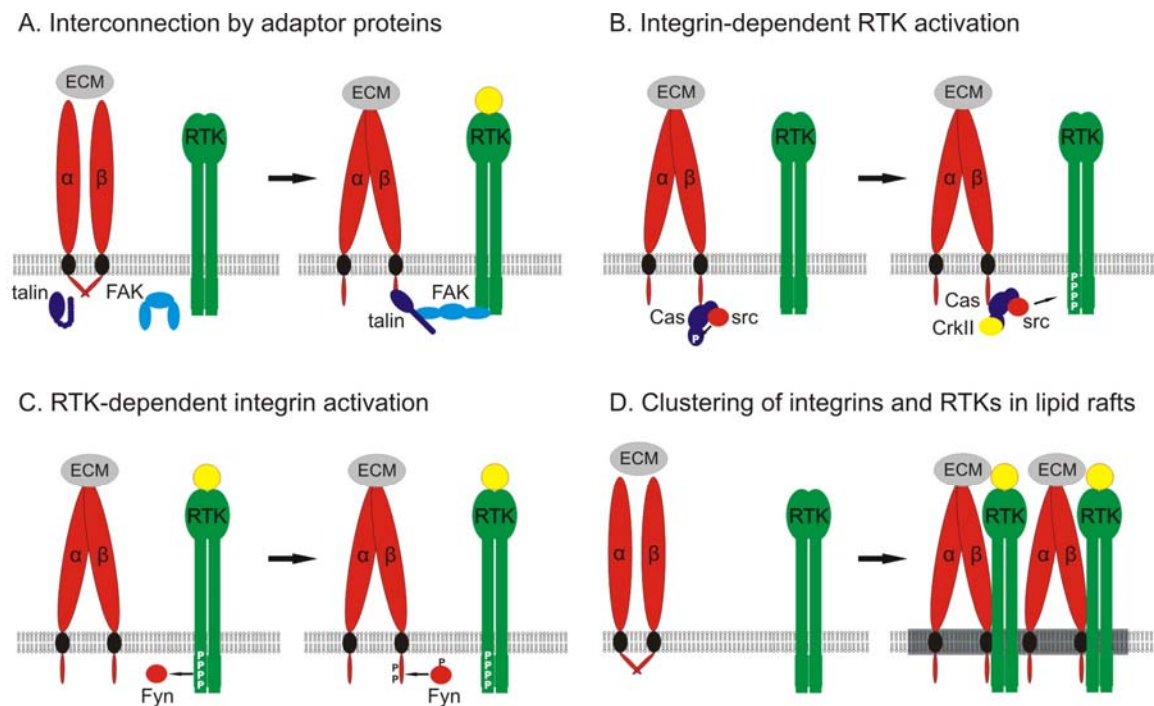


Fig 1.8. Possible mechanisms underlying an integrin-RTK crosstalk. *A. Integrins and RTK signalling can be physically linked by adaptor proteins. B. Integrin engagement can activate RTK even in the absence of growth factors. C. Fyn, which can become phosphorylated by growth factor receptors, is able to phosphorylate $\alpha\beta$ 4 integrins. D. Integrins and RTK can be clustered in specialized microdomains at the plasma membrane. (See also: Giancotti and Tarone, 2003).*

1.3. Integrin-linked kinase

Integrin-linked kinase (ILK) was originally identified as a protein capable of interacting with the cytoplasmic tail of β 1 integrin (Hannigan et al. 1996). In the original paper it was also shown that ILK can phosphorylate the integrin β subunits. The ability to bind and phosphorylate integrins gave ILK its name. However, the molecular function of ILK at the integrin adhesion site is not fully understood. Due to the frequent overexpression in tumours and metastases ILK was thought to act as a proto-oncogene downstream of integrin signalling. Moreover, ILK was believed to act as a kinase phosphorylating a number of target proteins including the survival factor PKB/Akt as well as the Wnt signalling regulator GSK-3 β (Persad and Dedhar 2003). However, data about the role of ILK in invertebrates has shed new light on the molecular function of this protein (Zervas et al. 2001; Mackinnon et al. 2002). In the following section, the domain structure of the protein, ILK's role as a kinase and as an adaptor molecule will be introduced. In addition, data from genetic experiments in invertebrates will be briefly discussed.

1.3.1. Domain structure of ILK

ILK consists of 452aa and has a molecular weight of 52 kDa, which was originally reported to be of 59kDa. It is composed of three structurally distinct domains: three ankyrin repeats at the N-terminus (a fourth ankyrin repeat was identified in human ILK but clearly lacks well conserved residues) mediating the interaction to Pinch1, Pinch2 and ILKAP (ILK-associated phosphatase), a short linker sequence, and a C-terminal domain. The linker domain, together with sequences from the C-terminal domain, shares some similarities with pleckstrin homology (PH) domains and is believed to bind PIP3. The C-terminal domain which mediates the interaction to a number of ILK binding partners like paxillin, the parvins, integrins or Mig-2/Kindlin-2 shows significant homology to Ser/Thr protein kinases. If the kinase domain is catalytically functional and if the kinase activity has any importance *in vivo* is still unclear and has been a matter of hot debates (Grashoff et al. 2004; Legate et al. 2006).

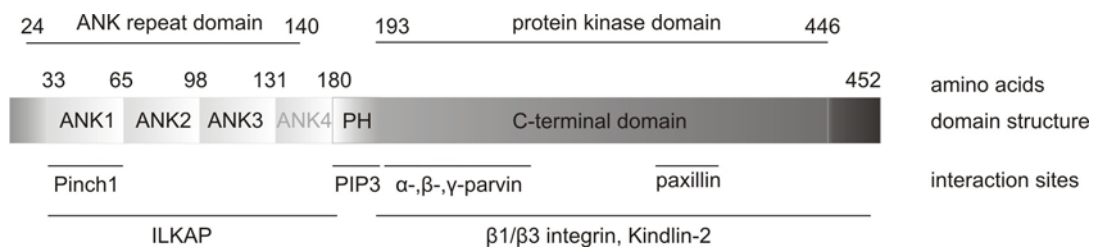


Fig 1.9. Domain structure of murine ILK. ILK comprises three distinct domains. Ankyrin repeats, a PH domain and a C-terminal domain which shares significant homology with Ser/Thr protein kinase domains.

1.3.2. Catalytic activity of ILK

Overexpression of ILK in cells results in anchorage-independent cell cycle progression and epithelial to mesenchymal transition (EMT) of non-tumourigenic as well as tumourigenic epithelial cells (Radeva et al. 1997; White et al. 2001). Inhibition of ILK kinase activity by expression of kinase-dead ILK versions on the other hand, suppresses cell growth in culture as well as growth of human colon carcinoma cells in SCID mice (Tan et al. 2001). Several lines of experimental evidence suggested that these phenotypes were largely attributed to ILK's kinase activity leading to phosphorylation of GSK-3 β and PKB/Akt, two key enzymes involved in a diverse array of cell functions including cell proliferation or survival and insulin responses (Delcommenne et al. 1998). ILK-dependent phosphorylation of GSK-3 β in epithelial cells downregulated GSK-3 β kinase activity. This in turn was associated with reduced E-cadherin expression, enhanced AP1 activity, and increased β -catenin-Lef/Tcf activity, which induces the expression of cell cycle-promoting genes such as cyclins and c-myc (Troussard et al. 1999). The reduced E-cadherin expression was interpreted to be a direct

effect of the β -catenin-Lef/Tcf complex on E-cadherin gene expression. It was also shown, however, that ILK can reduce E-cadherin levels indirectly by triggering expression of a transcriptional repressor called snail, which negatively acts on the E-cadherin gene (Troussard et al. 1999).

Several additional targets of the catalytic activity of ILK have been identified over the last years (Table 1.3A). The phosphorylation of myosin light chain or myosin phosphatase target subunits by ILK were described in platelets and smooth muscle extracts (Deng et al. 2001; Deng et al. 2002; Kiss et al. 2002). The phosphorylation of the transcriptional co-activator α -NAC has been described in COS-7 cells (Quelo et al. 2004).

Questions about the importance of the ILK kinase activity emerged with the genetic studies in *Caenorhabditis elegans* (*C. elegans*) and *Drosophila melanogaster* (see below; 1.3.3). While loss of ILK expression in both organisms led to muscle detachment and early lethality during embryogenesis, the expression of kinase-dead mutant ILK could fully rescue the severe phenotypes (Zervas et al. 2001; Mackinnon et al. 2002). Doubts about ILK kinase activity were reinforced by biochemical studies which suggested that ILK lacks an intrinsic kinase activity and is not capable of phosphorylating PKB/Akt (Hill et al. 2002). A detailed protein sequence analysis revealed that ILK (although a high homology to other kinases is evident) lacks essential catalytic amino acids which are highly conserved in other kinases: the DFG sequence which is common to almost all kinases and essential for the alignment of the γ -phosphate of ATP is missing; a conserved Lysine which neutralizes the charge on the γ -phosphate and a conserved Asparagine, important for Mg^{2+} -binding are also not present. Therefore, it is difficult to envisage how ILK can actively transfers phosphate groups to its targets (Legate et al. 2006).

A

target	phosphorylation site	Reference
ILK	Ser 343	Persad et al., 2001
β 1 integrin	Ser 785	Hannigan et al., 1996
β 3 integrin	—————	Pasquet et al., 2002
β -parvin	—————	Yamaji et al., 2001
PKB/Akt	Ser 473	Delcomenne et al., 1998
GSK-3 β	Ser 9	Delcomenne et al., 1998
MLC-20	Thr18 / Th19	Deng et al., 2001
MBP	—————	Hannigan et al., 1996
MYPT-1	Thr695, Thr495	Kiss et al., 2002
CPI-17	Thr38	Deng et al., 2002
PHI-1	Thr57	Deng et al., 2002
α -NAC	Ser43	Quelo et al., 2004

B

interactor	domain	Reference
β 1 integrin	C-term	Hannigan et al., 1996
β 3 integrin	C-term	Pasquet et al., 2002
ILKAP	ANK	Leung-Hagesteijn et al., 2001
Kindlin-2	C-term	Mackinnon et al., 2002
paxillin	C-term	Nikolopoulos and Turner, 2001
Pinch1	ANK	Tu et al., 1999
Pinch2	ANK	Zhang et al., 2002
α -parvin	C-term	Tu et al., 2001
β -parvin	C-term	Yamaji et al., 2001
γ -parvin	C-term	Chu et al., 2006
PIP3	PH	Delcomenne et al., 1998

Table 1.3. Substrates and interaction partners of ILK. **A.** List of proteins that were shown to be phosphorylated by ILK. **B.** List of proteins that were shown to interact with ILK. (Taken from Grashoff et al. 2004 and modified).

1.3.3. Genetic studies of ILK in invertebrates

In contrast to vertebrates, invertebrates have only a very small set of integrin subunits. Because of the low redundancy, model organisms like the nematode *C.elegans* or the fruit fly *Drosophila melanogaster* have become valuable tools to study integrin function and the role of their cytoplasmic plaque proteins (Brown 2000). *C. elegans* has only one integrin β subunit (β -PAT3) and two α subunits (α -PAT-2, α -INA-1), of which α -ina1/ β PAT3 binds laminin and α -PAT2/ β PAT3 to RGD-containing ligands (Fig 1.10A). The set of integrins in *Drosophila* consists of two β subunits (β PS, β v) and five α subunits (α PS1-5). While α PS1/ β PS binds laminin and α PS2/ β PS the RGD motif, the remaining integrin heterodimers cannot be classified as orthologues of any known vertebrate integrin pair (Fig 1.10B).

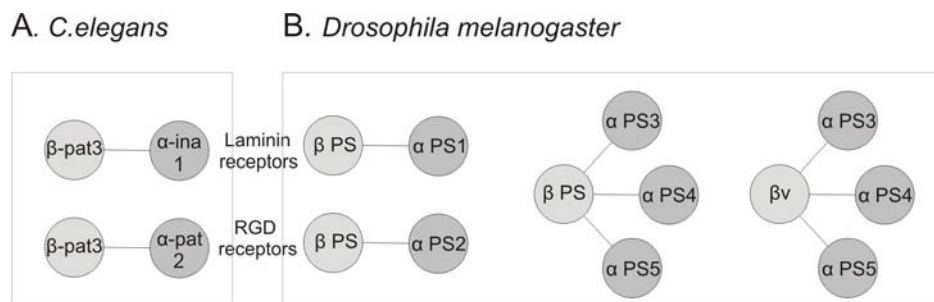


Fig 1.10. The integrin receptor family of invertebrates. **A.** The nematode *C. elegans* expresses only two integrin heterodimers which can bind laminin and RGD-containing proteins, respectively. **B.** *Drosophila* expresses two β subunits and five α subunits. Certain *Drosophila* integrins (β PS/ α PS3-5) are not comparable to any known vertebrate integrin pair. β v integrin most likely pairs with α PS3- α PS5 (N. Brown, personal communication).

Null mutations in *C. elegans* for the β integrin subunit β -PAT3 lead to a phenotype called PAT. PAT stands for paralyzed and arrested at twofold and this phenotype is caused by impaired muscle contraction resulting in early embryonic lethality (Williams and Waterston 1994). In *Drosophila* loss of β PS integrins leads to a similar phenotype characterized by detachment of muscles from the ECM and early lethality during larval development (Brown 1994). Hypomorphic integrin mutations result in viable animals which display blisters in their wings demonstrating the crucial function of integrins in cell adhesion.

Drosophila ILK consisting of 448aa is 60% identical and overall 75% similar to human ILK. Like human and mouse ILK, it lacks crucial catalytic amino acids which indicates that the divergence of ILK from other kinases was established already before the separation of invertebrates and vertebrates. Truncation of the protein as well as complete deletion of the *ILK* gene leads to a collapse of the actin cytoskeleton in the muscle similar (but milder) than

the phenotype caused by the loss of β PS expression (Fig 1.11; Brown 1994; Zervas et al. 2001). In addition, clonal expression of ILK-mutant cells during adulthood leads to severe blistering in the wing. These data point toward a crucial role of ILK during integrin-mediated cell-ECM adhesion. Interestingly, re-expression of wt-ILK and wt-ILK-GFP but also expression of several ILK kinase-dead mutants could completely rescue the lethal phenotype, indicating that ILK kinase activity – should it exist - is not essential in *Drosophila*. Moreover, the authors could show that ILK is mainly important for maintaining the integrin-actin interaction, while β PS integrin solely establishes and maintains cell-matrix interactions (Fig 1.11). These data were the first to show, that ILK plays a crucial role as an adaptor protein but is dispensable as a kinase *in vivo*.

The *C. elegans* orthologue of ILK is called PAT-4. PAT-4/ILK is 56% identical to human ILK and consists of a similar domain structure like human, mouse, and *Drosophila* ILK. Williams and colleagues (Mackinnon et al. 2002) showed that PAT-4-null nematodes failed to assemble sarcomere-like structures (called dense bodies and M-lines in worms) paralyzing the embryo and resulting in developmental arrest. Yeast-two-hybrid assays revealed that PAT-4/ILK interacts with the orthologue of Kindlin-2 called Unc-112 in nematodes. Unc-112 is important for the proper localization of PAT-4/ILK to integrin adhesion sites. Similar to the situation in *Drosophila*, kinase-dead mutant versions of ILK completely rescued the lethal phenotype (Mackinnon et al. 2002).

Upon publication of these studies, it has been hypothesized that ILK rather acts as an adaptor molecule at the integrin adhesion site, essential for the interaction between integrins and the actin cytoskeleton, and is - at least under physiological conditions - dispensable as a kinase.

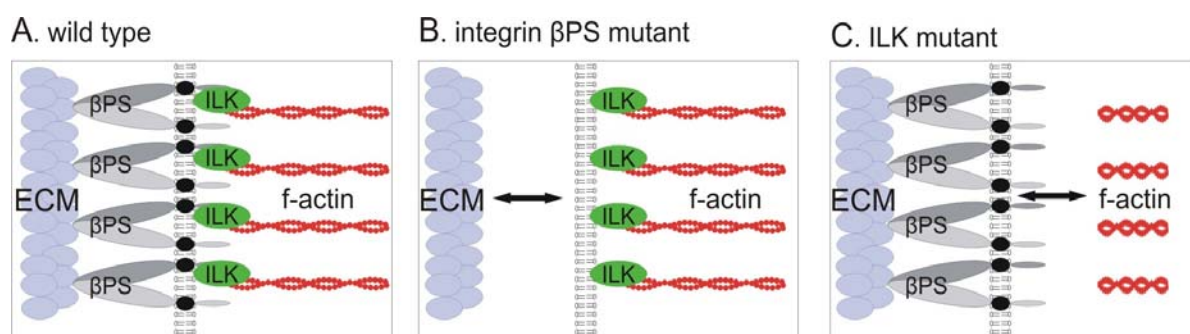


Fig 1.11. Summary of *Drosophila* phenotypes in the muscle. *A.* In the normal situation, integrins (β PS) connect the actin cytoskeleton with the ECM. This area is subject to high mechanical stress in the developing muscle. *B.* In the absence of β PS integrin the muscle collapses due to a disruption of the interaction between the ECM and the plasma membrane. *C.* In the absence of ILK, the interaction between ECM and plasma membrane occurs normally, while the connection between integrins and the actin cytoskeleton is disrupted. (Figure based on Zervas et al. 2001).

1.3.4. ILK- an adaptor protein at the integrin adhesion site

Besides its interaction with $\beta 1$ and $\beta 3$ integrins, ILK is able to bind a number of additional proteins. Almost all proteins that bind either directly or indirectly to ILK could potentially regulate the actin cytoskeleton. Pinch1 was the first interactor to be identified (Tu et al. 1999). Pinch2, a Pinch1 homologue, was subsequently identified in mice and humans (Zhang et al. 2002; Braun et al. 2003). They are both composed of five LIM domains and contain a nuclear localisation signal (NLS) at the C-terminus. The first LIM domain binds to the first ankyrin repeat of ILK. The fourth LIM domain of Pinch1 was shown to bind with very low affinity to the SH2/SH3 adaptor protein Nck2, which in turn is known to interact with growth factor receptors and recruits a large number of proteins including actin modulators such as Dock180 and the p21-activated kinase (PAK) (Tu et al. 1998; Velyvis et al. 2001).

A search for paxillin-binding proteins showed that the C-terminal domain of ILK contains sequences resembling a so-called paxillin binding site (PBS) motif, which firmly binds paxillin. The ILK-paxillin interaction is necessary but not sufficient to recruit ILK into FAs, where the complex may modulate the function of other paxillin-binding proteins such as vinculin, α -actinin, talin or FAK (Nikolopoulos and Turner 2001).

Several laboratories have simultaneously shown that parvins, a new family of f-actin binding proteins, bind the C-terminal domain of ILK (Olski et al. 2001; Tu et al. 2001; Yamaji et al. 2001). The parvin family consists of three members (α -parvin or actopaxin or CH-ILK binding protein; β -parvin or affixin; and γ -parvin) which are composed of two calponin homology (CH) domains. While α -parvin is broadly expressed at relatively high levels, β -parvin displays rather low expression levels but is also ubiquitously expressed. γ -parvin is exclusively expressed in haematopoietic cells (Chu et al. 2006). In addition to its ILK binding activity, α -parvin was shown to interact simultaneously with paxillin and f-actin (Nikolopoulos and Turner 2000). If β -parvin can also interact with paxillin is unclear. However, β -parvin was shown to interact with the GEF α -PIX, which might be important for the activation of Rac1 and Cdc42 (Rosenberger et al. 2003). Several reports indicate that α -parvin and β -parvin, although they share rather high homology, have different functions at the integrin adhesion site and even counteract each other (Zhang et al. 2004).

An additional ILK binding partner at the C-terminus was identified in *C. elegans* and named UNC-112. UNC-112 contains a FERM domain that is split by a PH domain and is important for the recruitment of the ILK orthologue, PAT-4, to muscle attachment sites (Mackinnon et al. 2002). The mammalian orthologue of UNC-112 is Mig2a/Kindlin-2 and was shown to

bind the LIM-domain containing adaptor protein migfilin, which in turn binds filamin, an actin crosslinking molecule (Tu et al. 2003).

The different ILK interactions are illustrated in Fig 1.12. It should be kept in mind, that it is not clear, if all these interactions occur at the same time at integrin adhesion site (ILK can be also found outside of these structures) and in all cells.

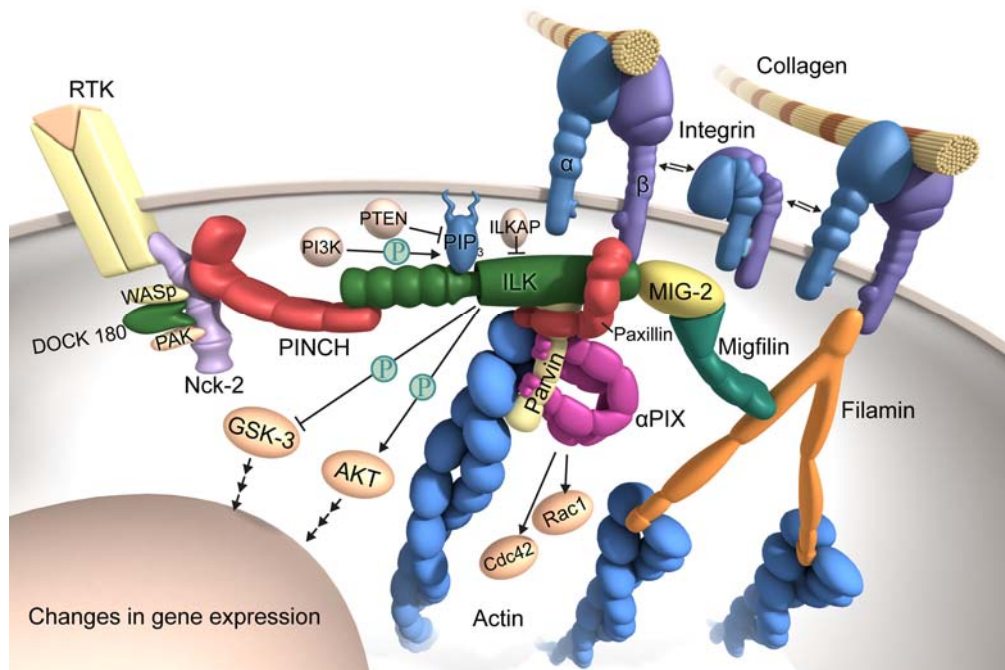


Fig 1.12. ILK as an adaptor protein at the integrin adhesion site. ILK can interact with several proteins, which link integrins to the actin cytoskeleton. However, if ILK interacts with all these proteins at the same time is questionable. Moreover, not all cell types might express the whole set of proteins as depicted here. (Picture taken from Grashoff et al. 2004).

1.4. Analysis of the peri-implantation development in mice

The first basement membrane (BM) that assembles during mouse development appears in the peri-implantation blastocysts between the visceral endoderm and the inner cell mass (ICM) and between the parietal endoderm and the trophectoderm. In the absence of BM assembly the epiblast, which is the source of the three germ layers, fails to differentiate and to polarize leading to the arrest of embryonic development. $\beta 1$ integrins are crucial for the establishment of this ECM structure. In the following sections, embryoid bodies (EBs) as a model system for the analysis of peri-implantation development and the role of $\beta 1$ integrins during this early phase of embryonic development will be introduced.

1.4.1. Embryoid bodies (EBs)-a model system to study peri-implantation development

The blastocyst develops 3.5 days after fertilization and consists of the inner cell mass (ICM) and the trophectoderm. Subsequently, the primitive endoderm differentiates from the ICM and gives rise to the visceral and the parietal endoderm. Those endodermal cell layers secrete ECM components such as laminin111 and collagen type IV which assemble into a BM between visceral endoderm and ICM and between parietal endoderm and the trophectoderm. Following blastocyst implantation at E4.5, the ICM undergoes cavitation forming the proamniotic cavity and the epiblast (Fig 1.13; Wang and Dey 2006).

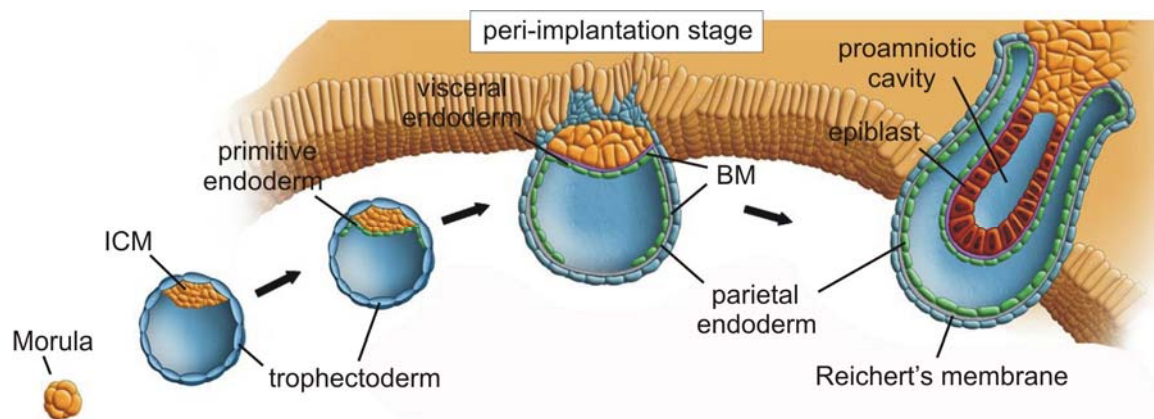


Fig 1.13. Early events of embryonic development in mice. The ICM gives rise to the endodermal cell layers, which secrete BM components such as laminin111 or collagenIV to form the first BM during development. Differentiation of ICM cells leads to the formation of the epiblast, cavitation to the formation of the proamniotic cavity. (Picture provided by R. Fässler and E. Montanez).

Since these processes are difficult to study *in utero* an *in vitro* model system was established that recapitulates most of the processes described above (Fig 1.13). Suspension culture of embryonic stem (ES) cells leads to the formation of EBs. In a series of well characterized events ES cells form compact spherical ES cell aggregates and differentiate into a two germ structure that consists of visceral as well as parietal endoderm, a BM, an epiblast and a proamniotic-like cavity. Since EB-derived parietal endodermal cells lack the trophectoderm to which they would normally attach, these cells tend to form peripheral aggregates (Fig 1.14). The lack of trophectoderm prevents the analysis of extraembryonic differentiation processes or the formation of Reichert's membrane with the EB system (Li et al. 2003).

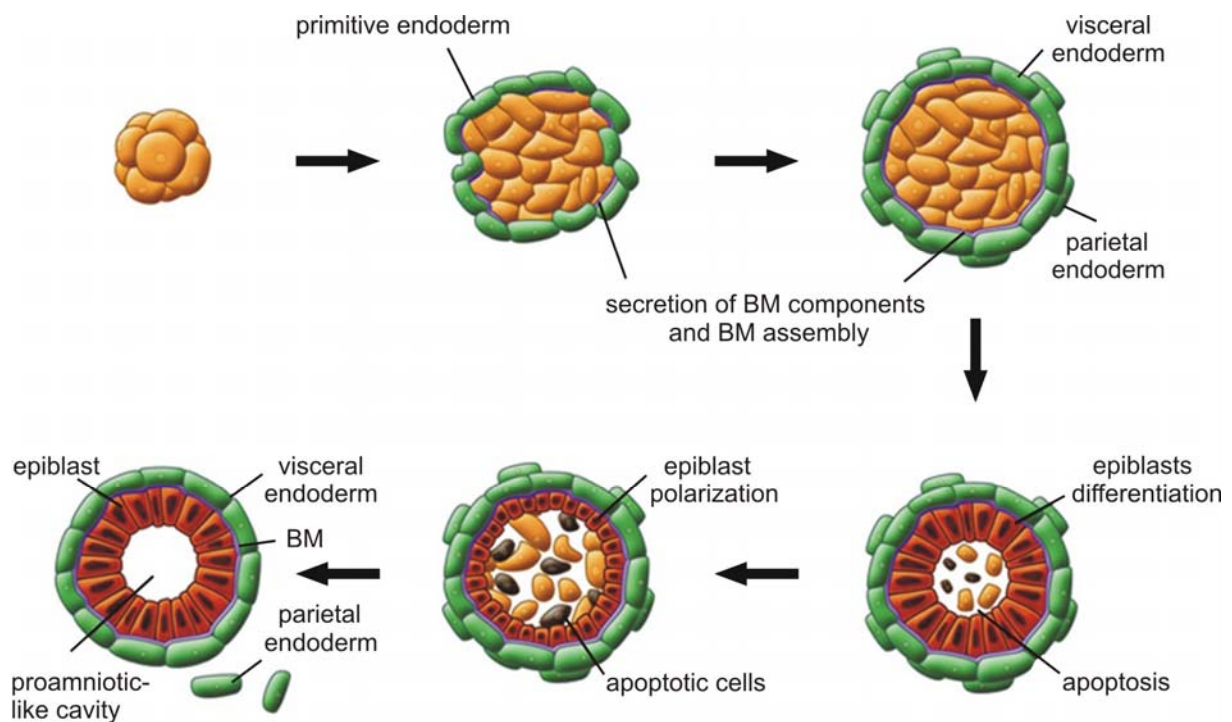


Fig 1.14. EB development. When cultured in suspension, spherical ES cell aggregates can develop into an EB. They trigger primitive endoderm formation, BM assembly, epiblast differentiation/polarization and cavitation. (Picture provided by R. Fässler and E. Montanez).

1.4.2. The role of the ECM proteins integrins during peri-implantation development

The assembly of a BM is a critical step during peri-implantation development. Deletion of laminin111 (achieved by targeted ablation of the laminin γ 1) led to developmental arrest at E5.5 due to defective BM assembly (Smyth et al. 1999). Deletion of β 1 integrin caused the same phenotype since the laminin α 1 subunit is not secreted from the endodermal cells and laminin111 can not be assembled (Fassler and Meyer 1995; Aumailley et al. 2000). Interestingly, addition of laminin α 1 to β 1-null EBs partly rescued the BM assembly defect (Li et al. 2002). It is therefore thought that β 1 integrin expression is critical for the secretion of laminin α 1 from endodermal cells but not essential for BM assembly *per se*. The formation of a laminin-rich BM between the endoderm and the ICM is critical for polarization of the ICM cells, their differentiation into the epiblast and the formation of the proamniotic cavity (Li et al. 2002).

1.5. Development and analysis of the vertebrate skeleton

The vertebrate skeleton is a complex tissue composed of more than 200 unique elements distributed throughout the body. Its development is a highly regulated process and achieved by at least two distinct mechanisms: the intramembranous ossification and the endochondral ossification. In the former, bone forms directly from mesenchymal progenitors, whereas in the latter bone formation occurs after the generation of a cartilaginous mold. Craniofacial bones and part of the clavicle are formed by intramembranous ossification, the axial and appendicular skeleton forms by endochondral ossification. Recently, it has been shown that $\beta 1$ integrins play a pivotal role during endochondral ossification (Aszodi et al. 2003). In the present study, the role of ILK during this process was analyzed.

Below, the molecular biology of cartilage and bone development as well as the role of ECM-integrin interactions during endochondral ossification will be introduced.

1.5.1. Bone formation by endochondral ossification

The formation of bone during endochondral ossification is mediated by three different cell types: chondrocytes and osteoblast, which are of mesodermal origin, and osteoclasts which are derived from the myelomonocytic lineage. While the cartilage is exclusively made up of chondrocytes, osteoblasts and osteoclasts are residing in the bone (Erlebacher et al. 1995; Karsenty and Wagner 2002).

Endochondral bone development starts with the condensation of mesenchymal cells and their subsequent differentiation into chondrocytes leading to the formation of the cartilaginous anlage (Fig 1.15). These chondrocytes start to express molecular markers such as aggrecan or collagen II in contrast to the undifferentiated cells in the perichondrium which lines the cartilaginous anlage (Fig 1.15A). Once this cartilaginous template is formed, the innermost chondrocytes further differentiate into hypertrophic chondrocytes, a population of cells that can be further subdivided into collagen II expressing pre-hypertrophic chondrocytes and hypertrophic chondrocytes which express only little amounts of collagen II but instead strongly express collagen X (Fig 1.15B). Fully differentiated hypertrophic chondrocytes become surrounded by a calcified ECM and subsequently die by apoptosis. Expression of VEGF (vascular endothelial growth factor) by hypertrophic chondrocytes initiates vascular invasion followed by the entry of chondroclasts and osteoblast progenitors leading to the formation of the trabecular bones (Fig 1.15B, C). While this process of differentiation, apoptosis and bone formation occurs, chondrocytes at each end of the forming bone strongly proliferate and acquire a flattened shape which leads to the formation of parallel columnar

chondrocyte stacks. This process is largely responsible for the longitudinal growth of bones in vertebrates and leads to the establishment of a typical structure in the cartilage called growth plate (Fig 1.15D, Fig 1.16). The sequential process of proliferation, hypertrophy, apoptosis and finally the replacement of chondrocytes by osteoblasts consumes most of the cartilaginous templates until the onset of puberty. In the final step of bone formation, cells in the distal site of the bone start to lose characteristic molecular markers such as collagen II and aggrecan but instead start to express collagen III. The differentiation of these cells leads to the formation of the secondary ossification center, vascular invasion and formation of the joint cavity. Once the adulthood stage is reached, cartilage is only left on the articular surface (Fig 1.15D; Aszodi et al. 2000).

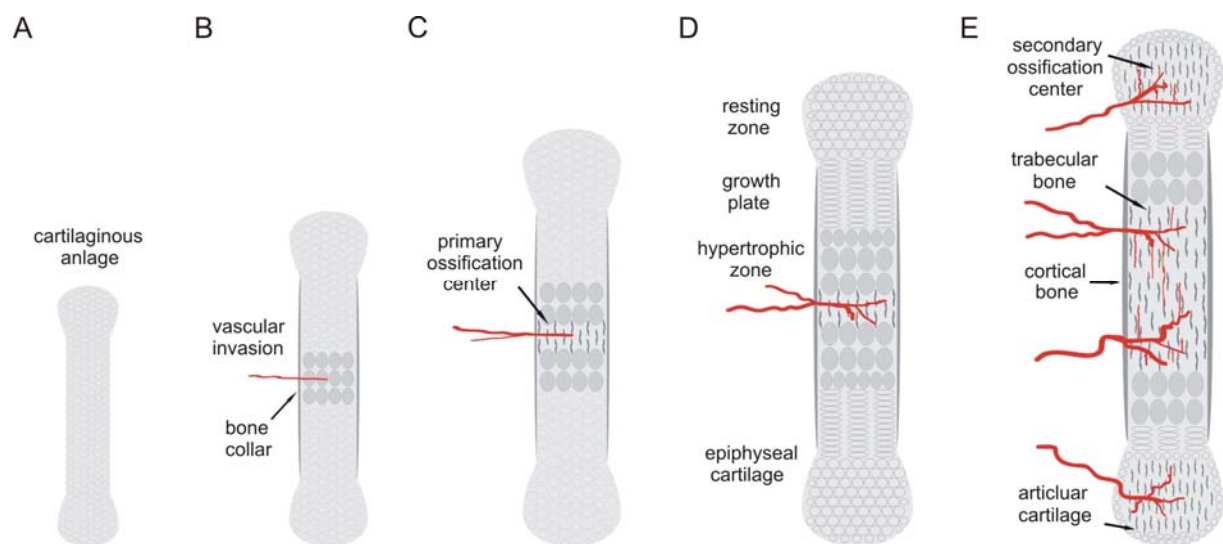


Fig 1.15. Endochondral ossification. *A. Endochondral bone formation starts with the condensation of a cartilaginous template. B. Differentiation of chondrocytes into hypertrophic chondrocytes leads to vascular invasion and C. the formation of the primary ossification center. D. Strong proliferation and dramatic cell shape changes form the growth plate. E. Differentiation of chondrocytes and another vascular invasion at the epiphyseal cartilage lead to the formation of the secondary ossification center and the formation of the joint cavity. (Figure is based on Aszodi et al. 2000).*

1.5.2. Regulation of chondrocyte proliferation and differentiation

Although the cartilage is build up of only one cell type, the chondrocyte, different subtypes can be clearly distinguished histologically. In the resting zone, chondrocytes are small and roundish, mainly express collagen II and proliferate slowly, whereas in the proliferative zone, chondrocytes appear flattened and are highly proliferative (Fig 1.15, Fig 1.16). Differentiated pre-hypertrophic and hypertrophic chondrocytes increase their size, express collagen X and cease proliferation. An obvious question is how all these events, the induction of proliferation and differentiation, the synthesis of ECM and the cell shapes changes are regulated. Recent

work has identified several regulatory mechanisms: the Indian hedgehog (Ihh)-Parathyroid hormone-related peptide (PTHrP) crosstalk, growth factor and transcription factor signalling pathways. Interestingly, integrins were also shown to play an important role during most of these processes.

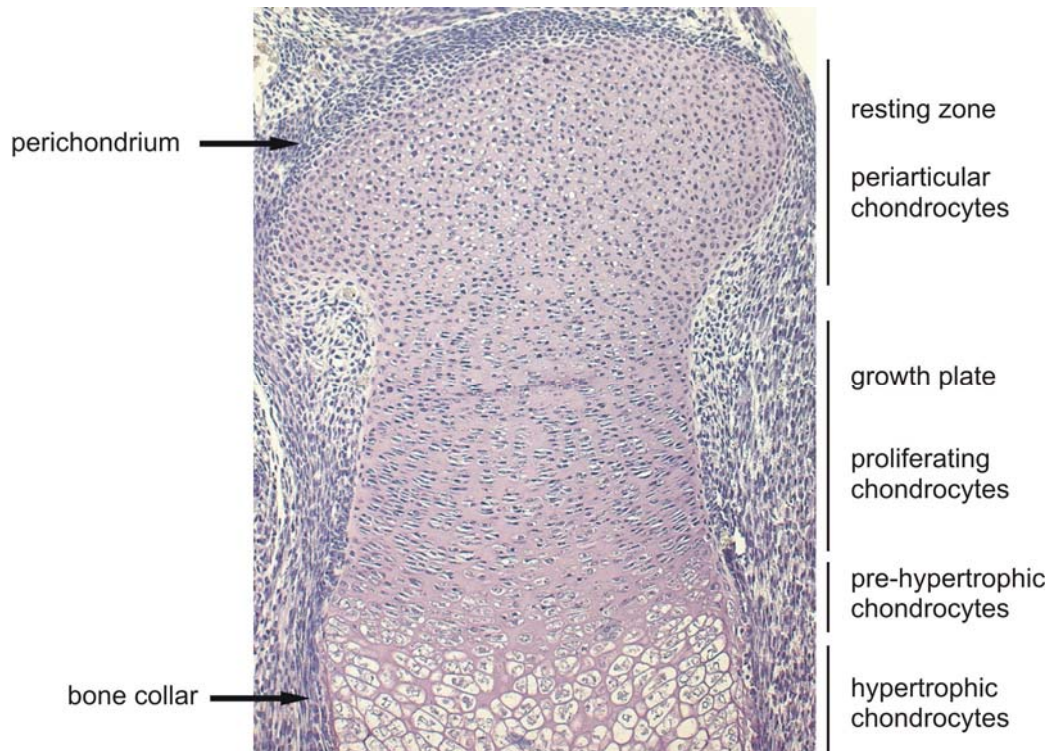


Fig 1.16. Organization of epiphyseal cartilage. Hematoxylin/Eosin staining of a cartilage section at E17.5. Cells in the resting zone are roundish, while cells in the proliferative zone appear flattened and form columnar structures. Pre-hypertrophic and hypertrophic chondrocyte are much larger. The cartilage is surrounded by a mesenchymal cell layer called perichondrium.

1.5.2.1. Ihh-PTHrP crosstalk

Targeted inactivation of PTHrP in mice leads to premature chondrocyte maturation and excessive bone formation at birth (Karaplis et al. 1994). Conversely, transgenic mice overexpressing PTHrP (using a Col2-promoter) fail to form bone in all skeletal elements which are formed by endochondral ossification (Weir et al. 1996). PTHrP is mainly secreted by cells at the periarticular cartilage, while the receptor for PTHrP (PPR) is expressed at lower levels in proliferating chondrocytes and is highly expressed in pre-hypertrophic chondrocytes. Therefore, it has been proposed that PTHrP diffuses through the bone to bind its receptor, which then antagonizes chondrocyte maturation. A somewhat similar but even more complex phenotype is caused by deletion of *Ihh*, which is at least at later time points of development, almost exclusively expressed by pre-hypertrophic chondrocytes. Although *Ihh*-

null mice initially show a normal chondrocyte condensation, mice at the newborn stage display a prominent dwarfism characterized by increased calcification of the long bones and shortening of almost all skeletal elements. Due to a strongly reduced rib cage size, *Ihh* knockout mice can not breathe and die shortly after birth. The reduced size of the long bones in *Ihh* knockout mice is caused by impaired proliferation of chondrocytes in the growth plate. Interestingly, the expression of PTHrP in periarticular chondrocytes was absent in these animals indicating that *Ihh* is essential for the maintenance of PTHrP expression thereby controlling the transition from proliferating to hypertrophic chondrocytes (St-Jacques et al. 1999). But how can *Ihh*, expressed on pre-hypertrophic chondrocytes affect the secretion of PTHrP in periarticular chondrocytes?

One possibility could be that *Ihh* triggers PTHrP expression in a direct manner early during endochondral bone formation, when the distance between *Ihh* and PTHrP expressing cells is still small. At later time points it seems more reasonable that the regulation of PTHrP secretion by *Ihh* occurs in an indirect manner. It has been suggested that this indirect regulation depends on bone morphogenic proteins (BMPs) and the transforming growth factor beta (TGF- β). More detailed information can be found in recent reviews about the *Ihh*-PTHrP feed-back loop (Lai and Mitchell 2005).

1.5.2.2. Regulation of endochondral bone formation by growth factor signalling and transcription factors

Endochondral bone formation critically depends on growth factor receptor signalling. Activating mutations in the fibroblast growth factor receptor-3 (FGFR-3) leads to achondroplasia, characterized by a virtual absence of non-hypertrophic chondrocytes. Conversely, targeted inactivation of FGFR-3 in mice leads to an increased size of the growth plate and a prolonged growth of the axial and appendicular skeleton (Deng et al. 1996). Therefore, FGFR-3 is believed to act as a negative regulator of endochondral bone formation. Several studies have indicated that the transcription factor STAT1 is a mediator of FGF signalling by regulating the expression of cell cycle inhibitors like p21 in the growth plate. Indeed, FGFR-3 knockout mice display more proliferating chondrocyte in this area of the cartilage.

Other transcription factors like Sox9, Fos and Cbfa1 have been shown to play essential roles during endochondral bone formation. Sox9 is expressed throughout cartilage during development. In ES cell-chimeric mice, Sox9 null ES cells cannot contribute to cartilaginous tissues indicating that Sox9 is an essential factor for the initial condensation of the cartilaginous template (Bi et al. 1999). Since Sox9 can directly interact with enhancers of

collagen II, it is easy to envisage that Sox9 is crucial for the onset of collagen II expression in chondrocytes.

The important role of osteoblasts during endochondral bone formation has become evident by the generation of Cbfa1 knockout mice. Targeted deletion of this transcription factor, which is essential for the differentiation of osteoblasts leads to complete loss of bone formation in mice (Komori et al. 1997).

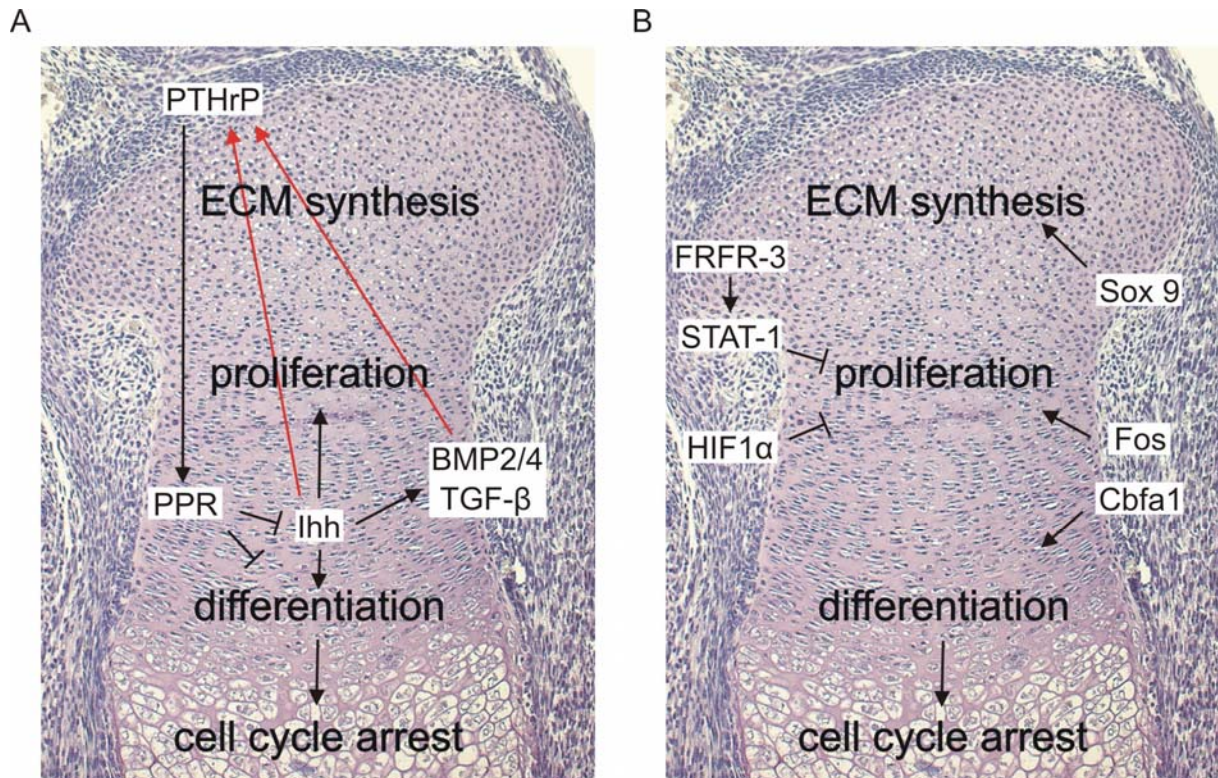


Fig 1.17. Regulatory signals and circuits during endochondral bone formation. *A.* The PTHrP-Ihh crosstalk regulates chondrocyte proliferation and differentiation. *Ihh* is expressed on pre-hypertrophic chondrocytes and induces the secretion of PTHrP. Activation of the PTHrP receptor (PPR), located at the pre-hypertrophic and hypertrophic zone, inhibits differentiation of chondrocytes. *B.* In chondrocytes, activation of the FGFR-3 pathway leads to inhibition of cell proliferation by STAT-dependent expression of cell cycle inhibitors. Several transcription factors affect endochondral bone formation by the regulation of ECM synthesis (*Sox9*), cell proliferation (*Fos*) or osteoblast differentiation (*Cbfa1*).

1.5.3. The role of the ECM and integrins during endochondral ossification

The most abundant extracellular matrix proteins in the skeleton are the collagens. Collagen I is the prominent ECM protein in the bone, whereas collagen type II is the predominantly expressed collagen in the cartilage which interacts with other less abundant collagen types like collagen IX or collagen XI to form the collagen fibrils. Collagen X is exclusively expressed by pre-hypertrophic and hypertrophic chondrocytes. The interconnection of these

various collagens with other ECM proteins like aggrecan or with proteoglycans and its binding to hyaluronan leads to the formation of a highly ordered three-dimensional network that ensures the mechanical stability of the cartilage. Mutations in the collagen genes are often associated with human disorders of the skeleton ranging from osteogenesis imperfecta (collagen I), a variety of chondrodysplasias (collagen II) to the Stickler syndrome (collagen XI) (Vikkula et al. 1994).

The interaction of the ECM with chondrocytes is mediated by $\beta 1$ and αv integrins (Fig 1.1) and therefore not surprisingly, deletion of $\beta 1$ integrin leads to an almost complete loss of the chondrocyte-ECM interaction in the cartilage. Targeted deletion of $\beta 1$ integrin in chondrocytes has demonstrated the essential role of $\beta 1$ during endochondral ossification (Aszodi et al. 2003). The phenotype of conditional $\beta 1$ knockout mice is discussed in the next chapter.

1.5.3.1. Deletion of $\beta 1$ integrin in the cartilage

Deletion of $\beta 1$ integrin exclusively in chondrocytes led to severe chondrodysplasia characterized by reduced length of the long bones which were interestingly broader than control bones. Most of $\beta 1$ integrin deficient mice died after birth due to breathing distress; the few survivors developed a severe dwarfism being 40% shorter than control littermates.

Defective collagen assembly: while FN gets assembled normally in $\beta 1$ deficient cartilage ($\alpha v\beta 3$ integrin is still present), the assembly of collagen fibrils is impaired, which is especially evident in the inter-territorial matrix of the proliferative zone. As expected, isolated chondrocytes deficient for $\beta 1$ integrin display strong adhesion defects to FN, VN or laminin and completely fail to attach to collagen substrates.

Reduced chondrocyte proliferation and apoptosis: mice with a chondrocyte specific deletion of $\beta 1$ in the cartilage display reduced cell numbers which at least in part contributes to the reduced size of the skeletal elements. BrdU incorporation assays revealed a reduced proliferation rate of chondrocytes in the growth plate whereas a slight increase in apoptosis was detectable. The reduced proliferation rate was associated with increased expression of *FGFR-3* mRNA, nuclear translocation of STAT1 and STAT5 and increased expression of the cell cycle inhibitors p16 and p21.

Impaired differentiation of chondrocytes: loss of $\beta 1$ integrin in the cartilage leads to a broadening of the pre-hypertrophic zone, but has no effect on the size of the hypertrophic zone. Although this phenotype is not fully understood, it seems likely that this rather mild differentiation defect is a result of the dramatic changes in the organization of the ECM.

Defective organization of the actin cytoskeleton: a striking phenotype of isolated $\beta 1$ -deficient chondrocytes is their inability to spread and form stress fibers *in vitro*. Similarly, f-actin distribution in chondrocytes of the growth plate is impaired. This data demonstrate the important role of integrins in the organization of the f-actin cytoskeleton.

Defective cytokinesis and chondrocyte rotation: the cartilage of $\beta 1$ -deficient mice contains a high number of bi-nucleated cells. Cell cycle analysis revealed that mutant $\beta 1$ cells accumulate in the G2/M phase of the cell cycle. In addition, these chondrocytes fail to rotate after cell division in order to form columnar stacks, but instead stay side-by-side which finally leads to the formation of a shorter but broader cartilage.

Altogether, these data indicate that integrins play crucial roles during endochondral bone formation, by regulating cell proliferation, cell differentiation and ECM assembly. In addition $\beta 1$ integrins are essential for the regulation of the cell shape most likely by modulating the organization of f-actin cytoskeleton (Fig 1.18).

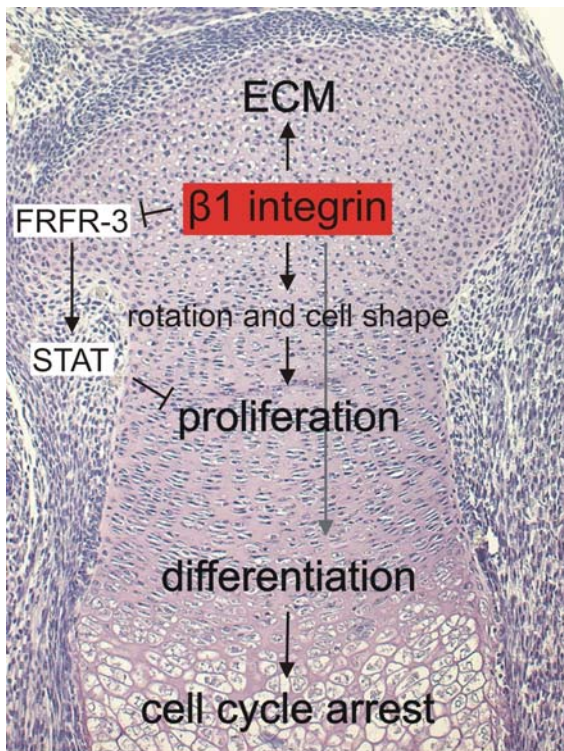


Fig 1.18. The role of $\beta 1$ integrin during endochondral bone formation. $\beta 1$ integrin is essential for collagen fibrillogenesis, cytokinesis and rotation of chondrocytes. It controls the cell shape by modulation of the f-actin cytoskeleton and suppresses the FGFR-3 signalling pathways thereby promoting cell proliferation. In addition loss of $\beta 1$ integrin leads to impaired differentiation of chondrocytes (Aszodi et al. 2003).

1.6. Epidermal morphogenesis and analysis of the murine skin

The skin is a multilayered tissue which protects the animal from loss of water, bacterial infections, radiation, extreme temperatures and mechanical stress. It is composed of more than 20 different cell types which build up the stratified epithelium (frequently called the

interfollicular epidermis), the hair follicle (HF) and as well as a mesenchymal compartment consisting of dermis, subcutis and dermal papillae. The major cell type of the epidermis is the keratinocyte.

Targeted ablation $\beta 1$ integrins from basal keratinocytes demonstrated the essential role of $\beta 1$ integrins for the maintenance of epidermis and HFs (Brakebusch et al. 2000; Raghavan et al. 2000). In the present study, the role of ILK in the epidermis and its appendages was addressed. The following sections will introduce the development of the skin and HFs and discuss the role of ECM-integrin interactions in the epidermis.

1.6.1. Epidermal morphogenesis

The epidermis of mice derives from the outer ectodermal cell layer of the postgastrulation embryo that forms a single sheet of histologically undifferentiated epithelial cells which adhere to an underlying BM (Fig 1.19A). Already at E9-E12 these cells regionally stratify to form the periderm, a cell layer which later during epidermal development is shed into the amniotic fluid (Fig 1.19B). Further stratification leads to the formation of a first intermediate cell layer (also called the *stratum intermedium*) which contains still proliferating cells (Fig 1.19C). Around this time, the expression of the typical keratinocyte marker such as keratin5 (K5) or keratin14 (K14) is induced. Further differentiation at E15-E16 gives rise to the non-proliferating suprabasal cell layers (Fig 1.19D). Terminal differentiation of suprabasal cell layers leads to the formation of the outer epidermal layer called *stratum corneum* and the shedding of the periderm (Fig 1.19E). The *stratum corneum* consists of anucleated and flattened cells, which are filled with keratin matrix and surrounded by an impermeable cornified envelope that is additionally cross-linked to external lipids. The stratification of the epidermis is completed at birth (Fig 1.19F; Blanpain and Fuchs 2006).

The epidermis constantly renews itself throughout the entire life of the animal and is able to re-epithelialize after wound injuries, which implies the existence of epithelial stem cells (eSC). Long-term labelling studies revealed that most of those eSCs are located in the hair bulge which is located at the base of the permanent part of the HF (Cotsarelis et al. 1990). There is also evidence for the existence of eSC in the interfollicular epidermis as well (Mackenzie 1997) and it has been speculated that high $\beta 1$ integrin expression is a hallmark of eSC (Jones et al. 1995). However, to which extent $\beta 1$ integrin determines the features of eSC awaits further studies.

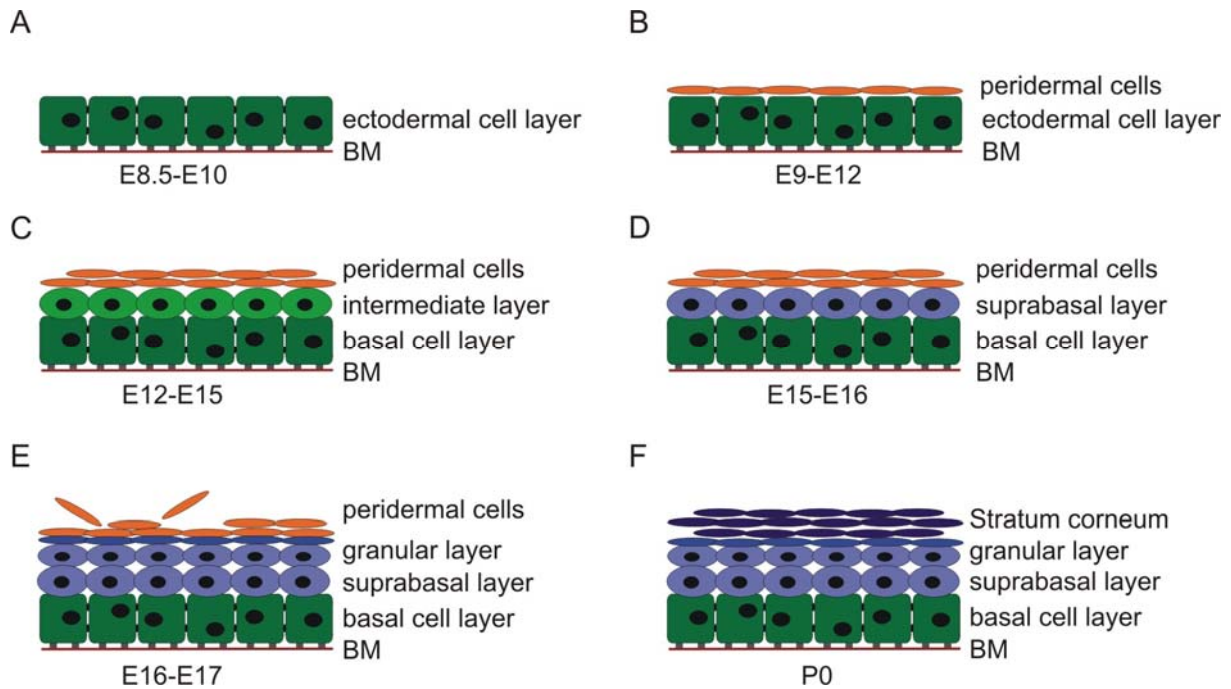


Fig 1.19. Development of the murine epidermis. *A.* The epidermis derives from an ectodermal cell layer of the postgastrulation embryo. *B.* The first stratification occurs around E9-E12 and forms the periderm, which sheds during embryonic development into the amniotic fluid. *C.* The stratum intermedium is formed between E12-E15 but is not regarded as a typical suprabasal cell layer, since the intermediate cells express basal markers and still proliferate. *D.* Further differentiation leads to the formation of suprabasal non-proliferating cell layers around E15-E16. *E.* The formation of the granular layer occurs at E16-E17. The periderm is shed into the amniotic fluid. *F.* The stratum corneum forms until birth by terminal differentiation. (Based on Blanpain and Fuchs 2006).

1.6.2. HF morphogenesis and the hair cycle

The HF is an epidermal appendage that starts to form already during embryonic development (Fig 1.20). Undifferentiated ectodermal cells are induced by the underlying mesenchymal cells to form an epidermal placode (Fig 1.20B), which in turn induces the formation of a dermal condensate that develops into the dermal papilla (DP; Fig 1.20C). Signals from the DP stimulate the proliferation and differentiation of epidermal cells resulting in the formation of the epidermal appendage (also called primary hair germ; Fig 1.20D). Those cells further differentiate into the inner root sheath (IRS), which later forms the hair shaft, and the outer root sheath (ORS), which is contiguous with the epidermis and surrounded by a BM (Fig 1.20E). Migration of ORS cells along the BM leads to the down growth of the HF into the subcutis until postnatal day 8 (P8) followed by proliferation and differentiation of hair matrix cells into six concentric layers of the IRS and the hair shaft. The development of the HF is completed around P14. A remarkable feature of the HF is its capacity to constantly renew. At

P16 proliferation of the hair matrix cells ceases and the HF degenerates (catagen), rests just below the hair bulge (telogen) until signals from the DP at P24 initiate the formation of a secondary hair germ and the downward migration of ORS cells to form a new HF. This periodic cycling of HFs continues the whole life of the animal (Blanpain and Fuchs 2006).

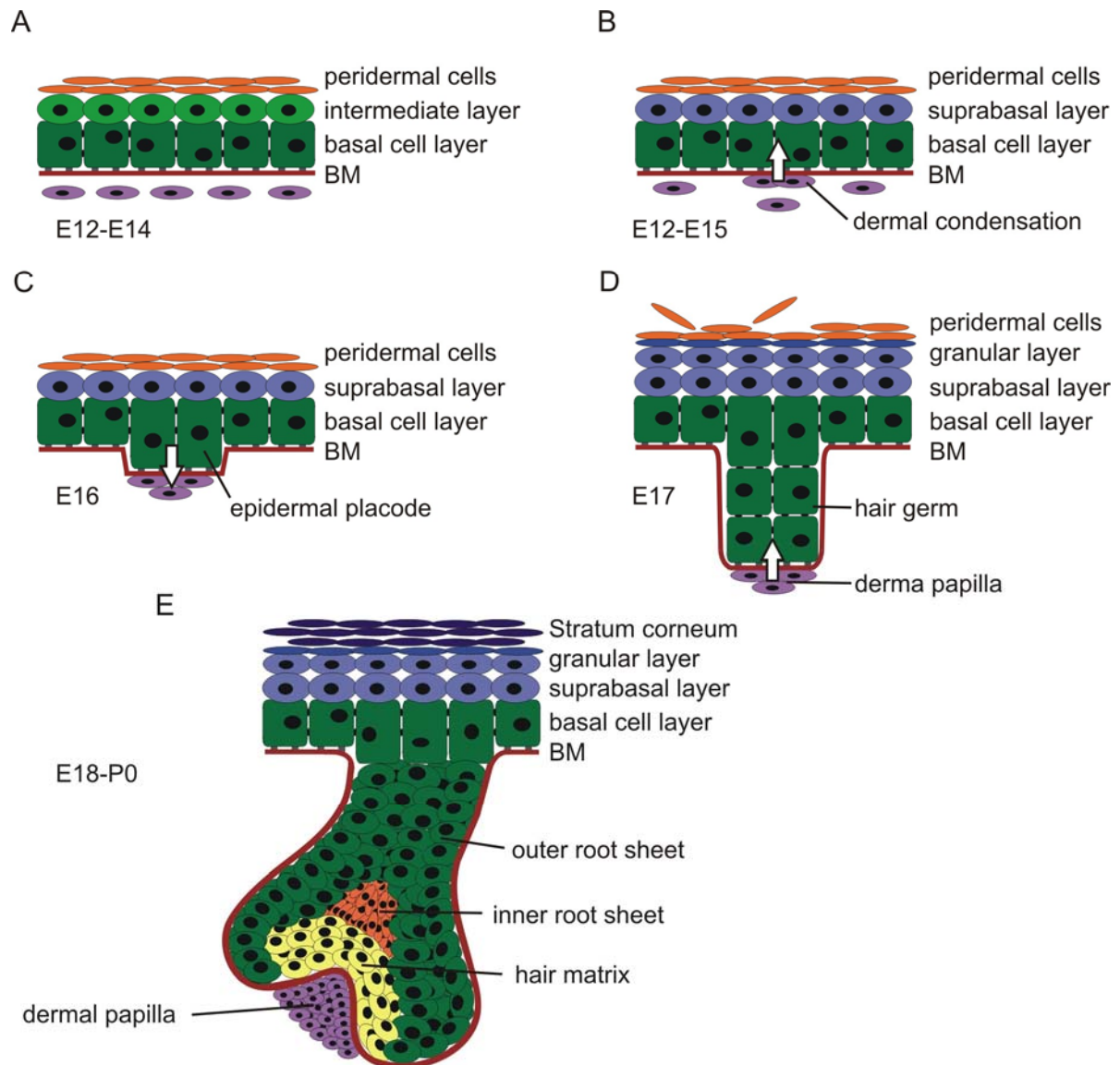


Fig 1.20. Morphogenesis of the murine HF. *A.* The HF is formed after a series of dermal-epidermal cues. *B.* The condensation of mesenchymal cells induces the formation of an epidermal placode. *C.* The epidermal placode induces the formation of a DP in the dermis. *D.* The DP stimulates cell proliferation and differentiation leading to the formation of a hair germ. *E.* Migration of ORS cells drives the downward growth of the HF, which further differentiates into inner root sheath and hair matrix. The DP remains attached to the HF. (Based on Blanpain and Fuchs 2006).

1.6.3. The role of integrins in the epidermis

The most abundant integrins expressed in basal keratinocytes are $\alpha 2\beta 1$, $\alpha 3\beta 1$, $\alpha 9\beta 1$ and $\alpha 6\beta 4$ integrins. The expression of these integrins is under normal conditions restricted to basal keratinocytes and the outer root sheath cells. While $\beta 1$ integrins are expressed around the basal keratinocyte, $\alpha 6\beta 4$, a component of hemidesmosomes, is restricted to the basal side adjacent to the BM. In humans, mutations in the genes encoding either $\alpha 6$ or $\beta 4$ integrin cause an autosomal recessive disorder called epidermis bullosa which is characterized by severe skin blistering. Similarly, $\alpha 6$ or $\beta 4$ knockout mice die shortly after birth due to epidermal disintegration indicating that the hemidesmosomal $\alpha 6\beta 4$ integrins are essential for cell attachment of basal keratinocytes to the BM (Dowling et al. 1996; van der Neut et al. 1996). Moreover $\alpha 6\beta 4$ has been implicated in skin carcinogenesis and seems to promote cell migration through mechanisms that involve integrin-RTK crosstalk (Giancotti and Tarone 2003). Deletion of the $\alpha 3$ integrin subunit also results in skin blistering, which is however much less severe as in $\alpha 6\beta 4$ -null mice. Interestingly, ablation of both $\alpha 3$ and $\alpha 6$ integrin subunits still allows stratification and HF morphogenesis (DiPersio et al. 2000).

The role of $\beta 1$ integrin has been addressed by targeted ablation of the protein specifically in basal keratinocytes. The results of these studies will be briefly discussed in the following section.

1.6.3.1. Deletion of $\beta 1$ integrins from basal keratinocytes

Two groups simultaneously reported the deletion of $\beta 1$ integrin in basal keratinocytes (Brakebusch et al. 2000; Raghavan et al. 2000). Deletion of $\beta 1$ integrin leads to skin blistering and complete loss of hair. Animals die within several weeks after birth due to impaired food uptake and disturbed development (Brakebusch et al. 2000) or shortly after birth due to severe skin blistering and dehydration (Raghavan et al. 2000).

Impaired BM maintenance in $\beta 1$ knockout mice: deletion of $\beta 1$ integrins in basal keratinocytes resulted in a defective organization of the BM caused by impaired adhesion of basal keratinocytes to the BM and aberrant processing and deposition of ECM proteins such as laminin332 or collagenVII. Although hemidesmosome can form, their number is reduced. The distortion of the dermal-epidermal junction and the reduced adhesion are the reason for the severe skin blistering. The BM of HFs was found to be unaffected, which supports the notion, that skin blistering is boosted by mechanical stress.

Reduced proliferation of basal keratinocytes and hair matrix cells: the proliferation rate of basal keratinocytes is significantly reduced in the absence of $\beta 1$ although not completely

blocked. Also the proliferation of hair matrix cells essential for the downward growth of the HF is reduced. The survival of basal keratinocytes or cells of the HF is not changed.

Delayed terminal differentiation: β 1-deficient epidermis is hyperthickened, caused by a delay in terminal differentiation. Basal keratinocytes, however, did not initiate premature differentiation and maintain their basal properties. This argues against the hypothesis that β 1 integrins are essential negative regulators of terminal differentiation.

Altogether these data indicated that β 1 integrins are indispensable for the BM integrity along the dermal-epidermal junction. They are essential for the processing and deposition of ECM proteins and necessary for cell attachment of basal keratinocytes. Similarly to the situation in chondrocytes, β 1 integrins promote proliferation of keratinocytes but only slightly impair their differentiation.

1.7. Aim of the PhD thesis

The role of ILK as an integrin-binding protein is highly controversial. While earlier studies indicated a critical role of ILK as a kinase regulating numerous signalling cascades in an integrin-dependent manner, more recent reports questioned the importance of ILK's catalytic activity and rather suggested a function of ILK as adaptor protein important for the interconnection of integrins with the actin cytoskeleton. Since all studies were using either overexpression systems or invertebrate models, the role of ILK under physiological conditions in a mammalian system was unclear. The overall goal of this study was therefore to investigate the consequences of ILK-deletion in mice.

In order to determine the importance of ILK expression during development the first aim was to complete the analysis of constitutive ILK knockout mice.

To further describe the role of ILK in mesenchymal and in epithelial cells *in vivo* the second aim was to analyze consequences of ILK deletion in the cartilage and epidermis of mice.

The third aim was to establish an *in vitro* model system to investigate the role of ILK as a kinase and during integrin-dependent f-actin reorganizations in more detail.

2. Materials and Methods

2.1. Common chemicals

All chemicals used in this study, if not further specified, were purchased from the following companies: Carl Roth GmbH (Karlsruhe, Germany), Merck (Darmstadt, Germany), Reidel de Haen (Seelze, Germany), Serva (Heidelberg, Germany) and Sigma Aldrich (Munich, Germany).

2.2. Animals

All mouse strains were maintained and bred in the animal facility of the Max-Planck-Institute of Biochemistry (Martinsried, Germany). The mice had free access to standard rodent diets and water. The light cycle was set for 12h. For breeding, mice of an age of 8 weeks were used. At an age of 3 weeks after birth, mice were separated by sex, marked with ear tags and housed in separated cages.

For genotyping, mice were clipped at the tail, which was used for DNA isolation immediately (2.7.2). All experiments were carried out according to the German Animal Protection Law.

2.2.1. Breeding scheme

In order to generate ILK knockout mice with a chondrocyte-specific deletion of the *ILK* gene, a mouse strain carrying a LoxP flanked *ILK* gene (ILK (floxed/floxed)) (Sakai et al., 2003) was intercrossed with transgenic mice expressing the Cre-recombinase under the control of the mouse collagen II promoter (Col2Cre) (Sakai et al. 2001) to obtain mice with the genotype ILK (floxed/wt) Col2Cre⁺. Male mice of this genotype were again crossed with female ILK (floxed/floxed) mice in order to obtain ILK (floxed/floxed) Col2Cre⁺ mice (called Col2ILK hereafter). To generate ILK knockout mice with a specific deletion of the protein in keratinocytes, ILK (floxed/floxed) mice were intercrossed with mice expressing the Cre-recombinase under the control of a keratin5 (K5) promoter (Ramirez et al. 2004).

2.3. Histological analysis of ILK knockout mice

2.3.1. Material Histology

Equipment

Light microscope: Leica, MZFLIII

embedding machine: Shandon, HistoCentre 2

microtome: Microm, Cool-Cut, HM355S

cryostat: Microm, HM 500 OM

embedding matrices

cryomatrix: Shandon, 676 900 6

mounting media

Entellan mounting medium: Merck, 1.07960

Aquatex: Merck, 1.08562

2.3.2. Histological methods

One of the most important steps in histochemical approaches is the fixation and embedding of the tissue, which on the one hand should preserve the tissue and maintain its morphology, but on the other hand should not affect the biological activity of the specimen. Therefore, different methods are used depending on the tissue or the experiment following the fixation.

The most widely used fixatives are paraformaldehyde or glutaraldehyde which react with basic amino acid residues thereby crosslinking neighbouring proteins. Alcoholic fixatives like methanol or ethanol are also used but preserve the tissue to a lesser extent than aldehydes. Since alcohols keep the tissue in a relatively undenatured state there are of interest in immunofluorescence approaches.

Paraffin wax is the most widely used embedding medium since it is solid enough to support the tissue but yet soft enough to enable rather thin sections to be cut (2.3.2.1). Freezing of tissue in order to obtain a solid block that can be cut is another widely used method (2.3.2.2).

2.3.2.1. Preparation of paraffin sections

Mice were sacrificed at selected time points and dissected under a light microscope. In order to assure fast penetration of the fixative into the cartilage, skin and muscles were carefully removed. The isolated skeletal elements were collected in phosphate buffered saline (PBS), subsequently transferred to freshly prepared, ice-cold paraformaldehyde (3.7% PFA in PBS) and incubated overnight (o/n) at 4°C. Next, tissue samples were dehydrated by subsequent washes in ethanol of ascending concentrations (50%, 70%, 80%, 90% and 100%) for 1h each incubated 2 times for 1h in Xylol and placed in paraffin solutions 3 times for 3h at 56°C. Embedding into paraffin was done using an embedding machine. Paraffin blocks were stored until cutting at 4°C. Paraffin blocks were cut in 6µm thick sections using a microtome. Quality and orientation of the tissue was frequently checked under a light microscope. Slides were dried at 37°C for 1-2h and finally stored at 4°C.

10xPBS

NaCl..... 80g

Na₂HPO₄..... 14.4g

KH₂PO₄..... 2.4g

KCl..... 2g

filled up to 1000ml with H₂O and adjusted to pH 7.4 with HCl

2.3.2.2. Preparation of cryo-sections

Tissue samples were embedded directly after dissection in cryomatrix on dry ice. Frozen blocks were stored on -80°C. Cryo-blocks were cut at -20°C into 6µm thick sections using a cryostat. Sections were air dried at RT for 30min and stored at -80°C.

2.3.2.3. Skeletal whole mount staining: Alcian Blue/Alizarin Red staining

This technique is most widely used for studying the skeletal morphology of mice. It is based on the ability of Alcian Blue to stain mucins that are abundant in cartilage. Alizarin Red S forms a chelate complex with calcium salts and therefore stains mineralized tissue like bone.

The skin of completely eviscerated mice was removed and corpses were fixed in 95% ethanol for 5 days at RT, transferred to acetone and incubated for another 2 days at RT. Staining was performed by incubation of the specimen in Alcian Blue/Alizarin Red S staining solution for 3 days at 37°C. Samples were washed in H₂O and cleared for 48h in 1% KOH solution followed by subsequent incubations in 0.8% KOH + 20% glycerol, 0.5% KOH + 50% glycerol and 0.2% KOH + 80% glycerol for 1 week each.

Alcian Blue/Alizarin Red S staining solution

ethanol 90%

acetic acid..... 5%

H₂O 4.8%

Alcian Blue 0.015%

Merck (Cat.No.1.01647)

Alizarin Red S..... 0.005%

Merck (Cat.No. 1.06279)

2.3.2.4. LacZ staining

The *lacZ* gene is frequently used to test gene expression in mice. The expression product is β-galactosidase and can be detected by fluorogenic or chromogenic substrates. 5-Bromo-4-Chloro-3-indolyl-β-D-galactopyranoside (X-Gal) is a chromogenic substrate that gets hydroxylated by β-galactosidase forming intense blue precipitates. It is therefore often used to visualize *lacZ* reporter gene activity.

Cryo-sections or embryos were fixed with solution B for 5min, washed 3 times 5 min with solution C and incubated o/n with solution D at 37°C. Whole embryos were incubated in solution D for even longer times depending on their size.

Sections were counterstained with Hematoxylin (2.3.2.5) and mounted with Entellan (2.3.1).

10x solution A

1M K_2HPO_4 (pH 7.4)

4x solution A2

10x solution A 400ml

1M $MgCl_2$ 128ml

EDTA 7.6g

1x solution B

1x solution A2 250ml

25% glutaraldehyde..... 2ml

2x solution C

4x solution A2 500ml

Na-deoxycholate 0.2g

NP-40..... 400 μ l

X-Gal solution

X-Gal 1g Roth (Cat.No. 2315.3)

DMSO 20ml (stored at -20°C)

1x solution D

2x solution C..... 250ml

100mM $K_3Fe(CN)_6$ 50ml (stored in the dark)

100mM $K_4Fe(CN)_6$ 50ml (stored in the dark)

X-Gal solution..... 5ml

H_2O 145ml

2.3.2.5. Hematoxylin/Eosin staining

This technique is a widespread histological stain, which can demonstrate a large number of different tissue structures. The major oxidization product of Hematoxylin is Hematein which is responsible for the colour properties. It stains cell nuclei with good intranuclear detail in blue, while Eosin stains the cytoplasm and connective tissue in varying shades and intensities with a pink colour.

In order to perform a Hematoxylin/Eosin stain, paraffin sections were treated 2 times for 5min in Xylol (deparaffinization) followed by incubation in 100%, 95%, 90%, 80% and 70% ethanol for 2min each (rehydration). Slides were then treated for 1min with Hematoxylin (Mayers hemalaun) and blued in tap water. Subsequently, slides were stained with Eosin for 1min and again washed in tap water. Sections were dehydrated in 70%, 90%, 95% and 100% ethanol for 2min each, washed for 2 times 5min in Xylol and finally mounted in Entellan.

Mayers hemalaun, Merck (Cat.No. 1.09249)

Eosin G, Merck (Cat.No. 1.09844)

2.3.2.6. Hematoxylin/Safranin orange staining

A common counterstaining method to visualize cartilage is staining with safranin orange (safranin O), which specifically stains proteoglycans. Paraffin sections were treated as described above (2.3.2.5) but instead with Eosin were counterstained with a 0.5% safranin orange staining solution for 30sec. Sections were directly washed with 95% ethanol, dehydrated in 95% and 100% ethanol for 3min each, incubated 2 times for 5min in Xylol and mounted in Entellan.

Safranin O, Merck (Cat.No. 1.15948)

2.3.2.7. Safranin-Orange von Kossa staining

The classic von Kossa method is used to demonstrate the deposition of calcium or calcium salts. To perform this staining, tissue sections are incubated in silver nitrate solution and treated with strong light. The calcium (for example in the bone) gets reduced and is replaced by silver deposits, which appear as a black staining on the section.

Sections were deparaffinized and rehydrated as described above (2.3.2.5). After washing 2 times 5min in distilled water, sections were incubated in silver nitrate solution under a 100W light bulb for 30-60min. Slides were washed once in distilled water and placed again for 15min under strong light. Slides were washed subsequently with distilled water 3 times for 5min, before cartilage was counterstained with safranin-orange staining solution (2.3.2.6) for 30sec. Sections were washed with 95% ethanol, dehydrated in 95% and 100% ethanol for 3min each, incubated 2 times for 5min in Xylol and mounted in Entellan.

Silver nitrate solution

AgNO₃.....5g

Merck (Cat.No.101512)

Fast Garnet GBC solution..... 500 μ l
sodium nitril solution..... 500 μ l
acetate solution..... 2ml
tartrate solution..... 1ml

Acid phosphatase, Leukocyte TRAP Kit, Sigma (Cat. No. 386A)

2.3.3. *In situ* hybridization on cartilaginous sections

In situ hybridization is a technique that allows for precise localization of a specific nucleic acid in histological sections. The underlying basis of this approach is that nucleic acids, if preserved adequately, can be detected through the application of a complementary nucleic acid to which a reporter module (fluorescent compounds or enzyme) is coupled or which is labelled by radioisotopes. Non-radioactive labels are biotin, which can easily be detected by avidin, but displays rather low sensitivity. Digoxigenin (DIG) is another frequently used non-radioactive label. It can be directly linked to nucleotides and detected by a highly sensitive anti-digoxigenin antibody (Kessler et al. 1990). In the present work, *in situ* hybridization was performed by non-radioactive labelling of RNA with DIG-UTP.

2.3.3.1. RNA labelling reaction

DIG-UTP labelling of RNA was performed with the DIG RNA Labelling Kit according to the instructions of the manufacturer. Plasmid DNA of rat parathyroid hormone-related peptide receptor (PPR) or plasmid DNA of mouse Indian hedgehog (Ihh) (Brandau et al. 2001) were placed into a RNase-free reaction vial and the following labelling reaction was prepared:

plasmid DNA..... 1 μ g
NTP labelling mixture 2 μ l
transcription buffer..... 2 μ l
RNase inhibitor..... 1 μ l
RNA polymerase T7..... 2 μ l
filled up to 20 μ l with H₂O and incubated for 2h at 37°C

DIG RNA Labeling Kit, Roche (Cat.No. 11 175 025 910)

Non-incorporated nucleotides were removed by passing the labelled mixture over a Quick Spin column for RNA preparations. Purified probes were stored at -20°C.

2.4. Immunological Methods

2.4.1. Materials Immunological Analysis

LabTek Chamber Slides, NUNC (Cat.No.177402)

Antibodies: see below

Name.....	manufacturer	Cat.No.....	WB.....	IF	IP
actin.....	Sigma	A2066	1:1000	---	---
aggrecan	Dr.Heinegard (Lund University)	---	---	1:400	---
AKT	Cell Signaling.....	9272.....	1:1000	---	---
AKT pThr308...	Cell Signaling.....	9275.....	1:1000	---	---
AKT pS473	Cell Signaling.....	9271.....	1:1000	---	---
AKT pS473	Cell Signaling.....	3787.....	---	1:50	---
BrdU-POD.....	Roche	1585860	---	1:30	---
cholera-toxin ...	Molecular Probes....	C-22841	---	5µg/ml.....	---
Caveolin-1	BD Bioscience.....	610059.....	1:2500	---	---
Cdc42	BD Bioscience.....	610929.....	1:500	---	---
Collagen II.....	Dr. Holmdahl (Lund University).....	---	---	1:800	---
Cortactin.....	Upstate	05-180.....	1:1000	1:150	---
CrkII.....	BD Bioscience.....	610036.....	1:5000	1:200	1µg/µl
Dock180.....	Santa Cruz	Sc-6167.....	1:200	1:50	---
FAK.....	Upstate	06-543.....	1:1000	1:150	1µg/µl
FAK pY397.....	Biosource Int.	44-624G.....	1:1000	1:200	---
Flag-tag-HRP ...	Sigma	A8592	1:10000	---	---
Gsk3-β.....	BD Bioscience.....	610201.....	1:2500	---	---
Gsk3-β pS 9/21.	Cell Signaling.....	9331.....	1:1000	---	---
integrin α6	BD Bioscience.....	555735.....	---	1:400	---
integrin β1	BD Bioscience.....	610467.....	1:2500	1:400	---
integrin β1	self made	MPI (Mayer).....	1:5000	1:800	---
integrin β4	BD Bioscience.....	553745.....	---	1:400	---
Hic-5.....	BD Bioscience.....	611165.....	1:250	1:50	---
ILK.....	BD Bioscience.....	611802.....	1:2500	1:800	---
LMW-PTP.....	Abgent.....	AP8441	1:500	1:50	---
Matrilin-2	Dr. Paulson (University of Cologne).....	---	---	1:200	---
mouse-HRP	Bio-Rad	172-1011.....	1:10000	---	---
mouse 647	Invitrogen	A21239.....	---	1:200	---
mouse Cy3.....	Jackson.....	115165146	1:400	---	---
Myc-tag	Upstate	05-724.....	1:1000	1:100	---
Migfilin	self made	MPI (Ussar).....	1:1000	1:100	---
Mig-2a.....	self made	MPI (Ussar).....	1:1000	---	---
α-parvin.....	self made	MPI (Chu).....	1:5000	1:800	---

β -parvin.....	self made	MPI (Thievensen)	1:2000	---	---
Paxillin	BD Bioscience.....	610051	1:10000	1:600	1 μ g/ μ l
p130Cas.....	BD Bioscience.....	610272	1:1000	1:200	1 μ g/ μ l
p130Cas pY410 Cell Signaling.....	4015	1:1000	1:100	---	---
p130Cas pY165 Cell Signaling.....	4011	1:1000	1:50	---	---
phalloidin 488... Invitrogen	A12379	---	1:800	---	---
Pinch1	self made	MPI (Stanchi)	1:10000	1:400	---
rat-HRP	Jackson	712 035150	1:10000	---	---
rat-Cy3.....	Jackson	---	---	1:400	---
Rac1	BD Bioscience.....	610651	1:2000	---	---
rabbit 647	Invitrogen	A21245	---	1:200	---
rabbit Cy3.....	Jackson	711165152	1:400	---	---
rabbit-HRP	Bio-Rad	172-1019.....	1:10000	---	---
Talin	Sigma	T3287.....	1:1000	1:400	---
Vinculin.....	Sigma	V9131	1:1000	1:400	---

2.4.2. BrdU staining of cartilaginous sections

During cell proliferation DNA replicates before cell division occurs. The close association between DNA synthesis and cell doubling is exploited in BrdU-based cell proliferation assays. 5-bromo-2'-deoxyuridine (BrdU) is a thymidine homolog and is incorporated into newly synthesized DNA when added to cells. The incorporated BrdU can later be detected with a BrdU-specific antibody. Therefore, newborn mice (or the pregnant mouse when embryonic stages were analyzed) were intraperitoneally injected with a BrdU solution 2h before the mice were sacrificed.

Paraffin sections were dewaxed and rehydrated as described above (2.3.2.5), washed for 5min in distilled water and treated for 20min with a 0.1%Trypsin/0.1%CaCl₂ solution. To inactivate endogenous peroxidase activity sections were washed in distilled water and treated with 1%H₂O₂ (in Methanol) for 10min. Sections were blocked 3 times for 5min in blocking solution and incubated with BrdU-specific antibody coupled to horseradish peroxidase (BrdU-POD, 2.4.1) diluted 1:30 in blocking solution for 4h followed by three washes in PBS. The signal was developed by a 3-3'diaminobenzidine (DAB) treatment. DAB is a compound which is frequently used in immunohistochemical approaches. After reaction with oxidizing reagents like peroxidases it produces an intense brownish colour. The colour reaction was controlled by microscopic examination. Reaction in DAB developing solution was stopped by washing for 10min in distilled water. Sections were counterstained with Mayers hemalaun (2.3.2.5) solution for 30sec and subsequently blued for 10min in tap water. Finally sections

were dehydrated by ascending ethanol washes, incubated for 2 times 5min in Xylol and mounted in Entellan.

BrdU solution for injection into mice

BrdU3mg/ml *Sigma (Cat.No. 858811)*
dissolved in PBS, stored at -20°C. 30µg BrdU/gram bodyweight was injected.

BrdU blocking solution

BSA 0.5%
Tween-20 0.1%
PBS 94%

Stock solution I

3-3'-diaminobenzidine.....27mg *Sigma (Cat.No. D 8001)*
H₂O5ml

Stock solution II

H₂O 500µl
30% H₂O₂ 100µl

DAB developing solution

Stock solution I 5ml
H₂O45ml
Tris-HCl.....49.88ml *pH 7.6*
Stock solution II..... 120µl

2.4.3. TUNEL staining on cartilaginous sections

The hallmark of apoptosis is DNA degradation. DNA cleavage results in double-stranded or single-stranded DNA breaks (called nicks). Both types of DNA breaks can be detected by labelling the free 3'-OH termini with modified nucleotides such as fluorescent dUTP. The terminal deoxynucleotidyl-transferase (TdT) is catalyzing this labelling reaction and used in the method that has been termed TUNEL (TdT-mediated dUTP-nick-end labelling).

For TUNEL staining paraffin sections were deparaffinized in Xylol and rehydrated by descending ethanol washes as described above (2.3.2.5). After treatment with proteinase K solution for 20min at 37°C, sections were washed 2 times for 5min in PBS. Apoptotic cells were detected by using the *In Situ* Cell Death Detection Kit. All steps were carried according to the protocol of the manufacturer.

In Situ cell Death Detection Kit, Fluorescein, Roche (Cat.No. 1 684 795)

2.4.4. Immunostaining on cartilaginous sections

Immunostaining of cartilaginous tissue sections was carried out on both paraffin- and cryo-sections. Paraffin sections were dewaxed and hydrated as described before (2.3.2.5). Cryo-sections were fixed for 15min at 4°C in acetic acid/ethanol fixative. Sections were then washed for 3 times 5 min in PBS.

To quench endogenous peroxidase activity, sections were treated in peroxidase solution for 30min at RT, followed by 2 washes in PBS. Next, sections were treated with hyaluronidase solution for 30min at RT, subsequently washed 3 times in PBS and blocked in blocking solution for 1h at RT. Primary antibody was diluted in blocking solution and incubated on the slide for 1h at RT. Sections were washed 3 times 5min in PBS, before the secondary antibody at the appropriate dilution was added for 1h at RT.

Cryo-section fixative

acetic acid..... 5%

ethanol..... 95%

Peroxidase solution

30% H_2O_2 1%

methanol 99%

Hyaluronidase solution

bovine testicular hyaluronidase..... 2mg *Sigma (Cat.No. H3506)*

PBS 1ml *pH 7.4*

Blocking solution

Bovine serum albumine (BSA)..... 2mg

PBS 1ml *pH 7.4*

2.4.5. BrdU staining of adherent cells in culture

Cell proliferation of adherent cells was determined by using a cell proliferation ELISA Kit. 2×10^3 cells were seeded per 96-well and cultured in 100µl DMEM+10%FCS (three 96-wells per cell line per time point). 10µg BrdU-labelling solution was added to one 96-well. The labelling was stopped at the indicated time points by removal of the culture medium and fixation of the cells in 70% ethanol. Next, 100µl BrdU-POD antibody solution was added per 96-well and incubated with the cells for 2h at RT. After washing, 100µl substrate solution was added and the colour reaction was monitored at various time points with an ELISA reader (2.5.1) at a wavelength of 370nm and a reference wavelength at 492nm.

Cell Proliferation ELISA, BrdU (colorimetric), Roche (Cat.No. 1 647 229)

2.4.6. Immunostaining of adherent cells in culture

For immunostaining of cells in culture, 1×10^4 cells were seeded in one well of a FN-coated LabTek chamber slides (2.4.1). At the indicated time points, slides were washed once in PBS and fixed for 10min in freshly prepared PFA. After three washes in PBS slides were blocked in blocking solution for 1h at RT. The indicated primary antibodies were diluted in blocking solution and incubated for 1h at RT, following four washes with PBS and incubation with the appropriate secondary antibodies for 1h. Finally slides were washed 4 times 5min each in PBS and mounted in Elvanol.

Immunostaining fixative for adherent cells

Paraformaldehyde (PFA) 3.7%
dissolved in PBS (pH 7.4), boiled for 1min and cooled on ice

Blocking solution

bovine serum albumin (BSA) 2%
Triton-X-100 0.1%
dissolved in PBS (pH 7.4)

Elvanol

Mowiol 4-88 12g Roth (Cat.No.0713)
H₂O 30ml
mixed for 10min, incubated 2-3h at RT, then addition of
0.2M Tris-HCl 60ml pH 8.5
87% glycerol 30ml
mixed for 10min, and then kept at 4°C overnight, aliquoted and stored at -20°C

2.4.7. Cytoskeletal staining of adherent cells

In order to prevent the compression of cells that usually occurs during PFA fixation the protocol described in 2.4.6 was modified.

Cells were carefully rinsed in PBS, then incubated for 1min in fixative I at RT, rinsed in cytoskeletal buffer and fixed for additional 10min in fixative II. All subsequent steps were carried out in PBS+1%BSA blocking solution.

Cytoskeletal buffer

NaCl 137mM

<i>MgCl₂</i>	<i>2mM</i>	
<i>KCl</i>	<i>5mM</i>	
<i>EGTA</i>	<i>2mM</i>	
<i>PIPES</i>	<i>5mM</i>	<i>pH 6.1</i>
<i>Na₂HPO₄</i>	<i>1.1mM</i>	
<i>Glucose</i>	<i>5.5mM</i>	
<i>KH₂PO₄</i>	<i>0.4mM</i>	
<i>Cytoskeletal fixative I</i>		
<i>Triton-X-100</i>	<i>200μl</i>	
<i>25% glutaraldehyd</i>	<i>2ml</i>	
<i>Cytoskeletal buffer</i>	<i>100ml</i>	
<i>Cytoskeletal fixative II</i>		
<i>25% glutaraldehyde</i>	<i>4ml</i>	
<i>Cytoskeletal buffer</i>	<i>100ml</i>	

2.4.8. Lipid raft staining of adherent cells

To demonstrate plasma membrane domains such as lipid rafts in adherent cells, the immunostaining protocol as described in 2.4.6 was modified. In order to keep the membrane structures intact, milder fixation conditions were used (20min in 2% PFA); permeabilization with Triton-X-100 was restricted to 5min. All subsequent steps were carried out in blocking solution (2.4.6) lacking any detergent such as Triton-X-100.

Visualization of lipid rafts was done with Alexa-488-labelled cholera-toxin (dilution 5μg/ml). Cholera-toxin binds to the ganglioside GM1, which is highly enriched in lipid rafts and therefore frequently used as a marker.

2.5. Cell culture methods

2.5.1. Material Cell Culture

ELISA reader: Tecam sunrise absorbance reader, Tecam 300 1055 0

5ml Pipette: Corning, Costar Stripette, 4487

15ml Pipette: Corning, Costar Stripette, 4488

25ml Pipette: Corning, Costar Stripette, 4489

96-well: Corning, 35 3799

12-well: Corning, 35 3043

6-well: Corning, 35 3046

15ml tube: Corning, 43 0791

50 ml tube: Falcon BlueMax, 35 2070

Cryogenic vial: Corning, 43 0489

100mm dish: Falcon, 353003

140mm dish: NUNC, 168381

DMEM: DMEM, + 4500mg/ml, + Glutamax, + Pyruvat; Gibco, 31966-021

Foetal bovine serum: Gibco, 10270-106

Trypsin: Trypsin / EDTA (10x), Gibco, 15400-054

P/S: Penicillin, Streptomycin (100x), PAA, P11-010

Fibronectin: bovine plasma fibronectin, Calbiochem, 341631

2.5.2. Isolation and culture of primary chondrocytes

Chondrocytes from rib, epiphyseal, and growth plate cartilage were isolated from newborn mice. Rib cages and joints were dissected in DMEM supplemented with foetal bovine serum and streptomycin/penicillin (dissection medium). Adherent tissues and the perichondrium were physically removed under a light microscope after a collagenase type II treatment for 30 min at 37°C. Chondrocytes were released by an additional collagenase type II treatment for 2-4 h.

Primary chondrocytes were maintained in growth medium in a humidified atmosphere (5%CO₂, 95%H₂O).

Dissection medium

foetal bovine serum (FBS) 1ml

100x Penicillin /Streptomycin (P/S) 1ml

DMEM 98ml

Digestion medium

collagenase type II 2mg *125U/mg*

Dissection medium 1ml

collagenase type II, Worthington (LS 004196)

Growth medium

FBS 10ml

P/S 1ml

DMEM 100ml

wells until confluence was reached. Finally 50% of the cells were frozen down (2.5.3.1) while 50% were expanded further and then subjected to the appropriate screening assays.

2.5.5. Cell substrate adhesion assay

Cell substrate adhesion assays were performed in 96-well plates. Plates were coated o/n at 4°C with FN (10µg/ml), VN (10µg/ml) or collagen type I (20µg/ml) and washed the next day with PBS. To prevent unspecific binding in non-coated areas plates were treated with blocking solution for 1h at RT and washed with PBS.

Cells were trypsinized, washed in culture medium, resuspended in growth factor-reduced medium (containing 0.2% FCS) and seeded on the 96-wells (1×10^5 cells per 96-well). Cells were allowed to attach for 30min-45min, the supernatant was removed, and plates were carefully washed 2 times with PBS. Attached cells were fixed for 10min at RT and stained for 30min at RT in staining solution. Next, plates were washed three times in PBS and finally treated with permeabilization solution. Colorimetric detection was carried out using an ELISA reader at a wavelength of 595nm (2.5.1).

Blocking solution

BSA 1g

PBS 100ml

Adhesion assay fixative

ethanol 70% (diluted in H_2O)

Adhesion assay staining solution

crystal violet 0.1% (diluted in H_2O)

Permeabilization solution

Triton-X-100 0.25% (diluted in H_2O)

2.5.6. Cell spreading assay

Cells spreading assays were performed on LabTek chamber slides (for immunohistochemical approaches), on Glass Bottom Microwell Dishes or 6-wells (for live cell imaging) or on 10cm dishes (for biochemical approaches). Surfaces were coated o/n at 4°C and washed the next day with PBS.

Cells were trypsinized, washed and resuspended in prewarmed growth medium (2.5.2) and seeded in following dilutions:

LabTek chamber slide: 1×10^4 cells / well

Glass Bottom Microwell 14mm: 1×10^5 cells / dish
6-well plate: 2×10^5 cells / well
10cm: 4×10^6 cells /dish

The experiment was continued depending on the approach and according to the protocols that are described elsewhere.

2.5.7. Fibronectin fibrillogenesis assay

To analyze the capability of fibroblasts to perform FN matrix assembly, cells were seeded on FN-coated LabTek chamber slides in growth medium (2.5.2, 2.5.6). 5-10 μ g Cy5-labelled FN (obtained from Dr. Walter Göhring, MPI) was added to each well and cells were cultured o/n. The next day, medium was removed and cells were subjected to immunostaining (2.4.6) with the indicated antibodies.

2.5.8. Dorsal ruffle formation assay

In order to monitor dorsal ruffle (DR) formation, cells were starved o/n in starvation medium, washed in PBS, trypsinized and resuspended in starvation medium. Cells were seeded on LabTek chamber slides (for immunostaining) or on Glass Bottom wells or on 6-wells for live cell imaging (2.5.6). Depending on the experiment wells were coated with FN (2-10 μ g/ml) or poly-lysine (100 μ g/ml) o/n at 4°C. Cells were allowed to spread for 2h and subsequently stimulated with EGF (20ng/ml).

For c-src inhibition, cells were incubated 30min before stimulation with 5 μ M PP1 analog. After stimulation the experiment was continued depending on the subsequent readout with protocols that are described elsewhere (2.4.6, 2.6.2).

For SILAC experiments, cells were grown in the presence of isotopically-labelled amino acids as described in (2.5.9) and starved in the respective SILAC medium without any FBS for 4h. Cells were washed in PBS, trypsinized and resuspended in the respective FBS-deficient SILAC medium and seeded on FN-coated 140mm dishes. After 2h of cell spreading, Arg6-labelled cells were stimulated with EGF (20ng/ml) and lysed after 2min as described in 2.6.5. Arg10-labelled cells were stimulated and lysed after 6min. Un-labelled cells were not stimulated at all and directly lysed.

The DR formation frequency was quantified using live cell microscopy. Cells were seeded on a 6-well plate and pictures were taken every 90sec. Approximately 100 cells were counted in one experiment per timepoint.

Starvation medium

FBS 200 μ l

S/P 1ml

DMEM 100ml

Epidermal growth factor (EGF), Sigma (Cat.No. E6135)

PP1 analog, Calbiochem (Cat.No.529579)

2.5.9. Stable isotope labelling by amino acids in cell culture (SILAC)**2.5.9.1. The SILAC principle**

The labelling of amino acids with stable isotopes leads to an increase in the molecular mass of all proteins in a cell. This is exploited in SILAC-based mass spectroscopy, which has emerged as a powerful tool in quantitative proteomics (Mann 2006).

Cells are grown in medium containing normal or heavy amino acids, for example 2H instead of H , or ^{13}C instead of ^{12}C , or ^{15}N instead of ^{14}N . Incorporation of these heavy amino acids into a peptide leads to a well defined mass shift compared to the unlabelled peptide. In the case of Arginine, Arg6 leads to a 6Da and Arg10 to an additional 4Da mass shift of a given peptide (as illustrated in Fig 2.1). In this way, the differently labelled cells can be lysed, pooled and subjected to a given experiment (in my case a FLAG-IP). The two different proteomes can later be distinguished, since all peptides of Arg6 cells are 6Da heavier and Arg10 peptides are 10Da heavier than unlabelled control cells (Fig 2.1B). By combining different lysates in one experiment unspecific effects and experimental variations are eliminated.

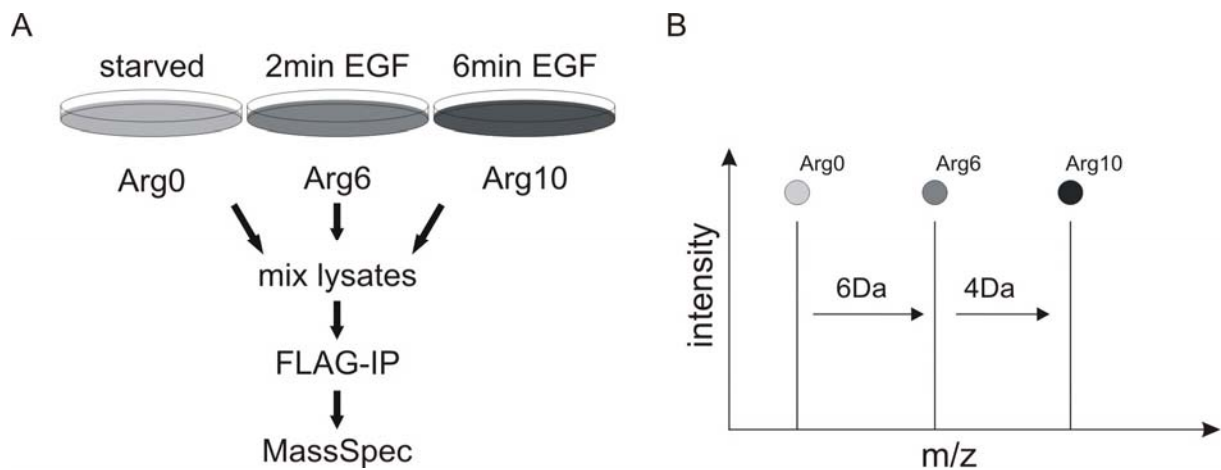


Fig 2.1. The SILAC principle. *A.* Cells are labelled using heavy amino acids such as Arg6 or Arg10 during a 1-2 week culture. In subsequent experiments cells are pooled, which eliminates unspecific effects that always occur within two separate experiments. *B.* All peptides of the differently treated cells can be distinguished later again, since all proteins of cells grown in Arg6 or Arg10 display a defined mass increase. (Taken from Blagoev and Mann 2006 and modified).

2.5.9.2. Isotope labelling of cells in culture

For SILAC experiments, cells were grown in DMEM (deficient in L-Arginine) supplemented either with “normal” L-Arginine hydrochloride (Arg0), or with L-arginine- $^{13}\text{C}_6$ hydrochloride (Arg6) or with L-arginine- $^{13}\text{C}_6$, $^{15}\text{N}_4$ hydrochloride (Arg10) in the presence of 10% FBS for 10days. Cells were split every 2 days and subjected to the DR experiment (2.5.8) using the same SILAC media with or without FBS.

2.6. Biochemical methods

2.6.1. Material Biochemistry

Centrifuge: Beckman Coulter, GS-15R

Ultracentrifuge (small): Beckman Coulter, TL-100 Ultracentrifuge

Ultracentrifuge rotor: Beckman Coulter, TL-100

Ultracentrifuge (large): Beckman Coulter, L8-60M

Ultracentrifuge rotor: Beckman Coulter, SW41

Protease inhibitor cocktail: complete Mini, EDTA-free, Roche, 12740900

2.6.2. Preparation of total protein lysates from adherent cells

Before cell lysis, cells were washed once in ice-cold PBS. The appropriate amount of cell lysis buffer was added to the cells, incubated for 10min on ice and then scraped with a cell

scraper. Cell lysates were centrifuged at 15000xg for 10min at 4°C and the protein concentration of the supernatant was determined using a bicinchoninic acid protein assay kit (2.6.4.1). After the protein concentrations were adjusted, lysates were either directly processed (2.6.5) or the appropriate amount of 4x SDS sample buffer was added. Those lysates were incubated for 5min at 95°C and either frozen on -80°C or directly subjected to SDS-PAGE (2.6.7).

Cell lysis buffer

<i>Tris-HCl</i>	<i>50mM</i>	<i>pH 7.6</i>
<i>NaCl</i>	<i>150mM</i>	
<i>Triton X-100</i>	<i>1%</i>	
<i>NaF</i>	<i>10mM</i>	
<i>Na₃VO₄</i>	<i>1mM</i>	
<i>protease inhibitor cocktail</i>	<i>1 tablet/10ml</i>	

4x SDS sample buffer

<i>20%SDS</i>	<i>16ml</i>	
<i>1M Tris</i>	<i>8ml</i>	<i>pH 6.8</i>
<i>0.5M EDTA</i>	<i>0.32ml</i>	
<i>87% glycerol</i>	<i>16ml</i>	
<i>bromphenol blue</i>	<i>0.001%</i>	

before use, mercaptoethanol was added to a final concentration of 4% and stored at RT

The following volumes of cell lysis buffer were used:

<i>6-well plate</i>	<i>200-400µl</i>
<i>10cm dish</i>	<i>0.5-1ml</i>
<i>140mm dish</i>	<i>1-2ml</i>

2.6.3. Cell fractionation

Cell fractionation is a useful preparative and analytical method for separating cellular compartments. The separation of distinct organelles results from their different physical properties, like size, shape, buoyant density or surface charge density. The basic principle of cell fractionation by centrifugation is represented by the Svedberg-equation, which describe mathematically the sedimentation of a spherical particle in solution:

$$\frac{dx/dt}{\omega^2 x} = \frac{2r^2(\rho_p - \rho_m)}{9\eta}$$

x: distance from rotor axis..... *r*: radius of particle
ω: angular velocity..... *ρ_p*: density of particle
ρ_m: density of medium..... *η*: viscosity of medium *t*: time

The most commonly used solute for cell fractionation is sucrose, since it can easily be prepared in densities that span the range of densities of most organelles. Since sucrose solutions are rather viscous at high concentrations, iodinated non-electrolytes like OptiPrep are often added, which increase the density of the fractionation medium without significantly increasing the viscosity. Another possibility to achieve high density at low viscosity is the addition of colloidal silica like Percoll.

2.6.3.1. Preparation of soluble and particulate fraction from adherent cells

Cells were washed in ice-cold PBS, then hypotonic lysis buffer was added and cells were incubated for 5min on ice. Cells were scraped and homogenized. Depending on the volume of the lysates homogenization was carried out either by using a Dounce homogenizer or by sucking the cell lysates 10 times through a 26G needle. In order to remove intact cells and cell nuclei the homogenized lysate was centrifuged for 3min at 4°C with 700g. The resulting postnuclear supernatant was transferred to a new reaction tube and centrifuged for 30min at 4°C with 30000xg. The supernatant (soluble fraction) was removed and stored on ice. The pellet was carefully washed in hypotonic lysis buffer and resuspended in resuspension buffer (particulate fraction). The protein concentration was determined by Bradford protein assay (2.6.4.2).

Hypotonic lysis buffer

Tris-HCl.....10mM *pH 7.6*
KCl.....5mM
MgCl₂.....1.5mM
Dithiothreitol (DTT)1mM
NaF10mM
Na₃VO₄.....1mM
protease inhibitor cocktail.....1 tablet/10ml

Resuspension buffer

Triton-X-100..... 1ml
Hypotonic lysis buffer..... 100ml

2.6.3.2. Detergent-free plasma membrane fractionation

In order to fractionate the plasma membrane and to separate the caveolin-rich membrane fraction the method established by Anderson and colleagues (Smart et al. 1995) was slightly modified. Since the caveolin-rich membrane fraction is very small a large amount of starting material is needed. For one experimental condition six 140mm dishes of subconfluent cells were used.

Plasma membrane preparation: Cells were washed two times in buffer A and scraped in 5ml buffer A on ice. Cells were collected by centrifugation for 5min at 1000g at 4°C, the pellet was resuspended in 1ml buffer A and placed in a 2ml Dounce homogenizer and homogenized with 20 strokes. The suspension was transferred into a 1.5ml centrifuge tube and centrifuged at 1000xg for 10min at 4°C. The postnuclear supernatant (PNS) was removed and stored on ice. The pellet was resuspended in 1ml buffer A, homogenized again, and centrifuged for additional 10min at 1000xg. This PNS was combined with the first one and layered on top of 8ml Percoll solution (30% Percoll in buffer A). Cells were centrifuged in a SW41 ultracentrifugation rotor at 84000xg for 30min at 4°C. The plasma membrane fraction bands in the middle of the tube, the cytoplasmic fraction stays located on top. Both fractions were isolated by tube puncture. In order to keep the layering of the gradient it is important not to use any brakes for deceleration of the ultracentrifuge.

Isolation of caveolin-rich membrane fraction: The volume of the plasma membrane fraction was adjusted to 2ml with buffer A. Samples were sonicated 6 times for 6sec with 1-2min on ice in between times. The sonicated samples were mixed with 1.84ml buffer C and 0.164ml buffer A and placed at the bottom of a 12ml ultracentrifuge tube. On top, an 8ml 20%-10% Optiprep gradient was poured. The 10% and 20% Optiprep gradients were produced by mixing buffer A in buffer C. Samples were then centrifuged at 52000xg for 90min at 4°C. The lower 3ml of the gradient represents the non-caveolin-rich membrane fraction. The top 5ml were collected and mixed with 4ml buffer C, placed at the bottom of a new ultracentrifuge tube and overlaid with 2ml of 5% Optiprep (made by diluting buffer C in buffer A). Samples were centrifuged at 52000xg for 90min at 4°C. The caveolin rich membrane fraction appears as an opaque band at the 5% Optiprep interface.

Buffer A

sucrose.....250mM

tricine.....20mM *pH* 7.8

EDTA1mM

Buffer B

sucrose.....250mM

tricine.....120mM *pH* 7.8

EDTA6mM

Buffer C

Optiprep..... 50%

sucrose.....250mM

tricine.....20mM *pH* 7.8

EDTA1mM

Optiprep Density Gradient Medium, Sigma (Cat.No. 1556)

Percoll, Sigma (Cat.No. P1644)

2.6.3.3. Preparation of the Triton-X insoluble cytoskeletal fraction

To isolate the cytoskeletal fraction of adherent cells, a 140mm dish of sub-confluent fibroblasts was washed once with ice-cold PBS followed by addition of 1.5ml cytoskeletal extraction buffer. Dishes were incubated for 15min on ice, cells were scraped off and the lysate was collected in a 2ml centrifugation tube. Lysates were centrifuged at 4°C with 15000g for 15min. The supernatant representing the soluble fraction was taken off and stored on -80°C. The pellet was washed two times with 2ml cytoskeletal extraction buffer and finally resuspended in 400µl RIPA buffer. The RIPA lysate was sonicated once for 5-10sec and centrifuged at 4°C with 15000g for 5min. The cytoskeletal rich supernatant was taken off and either directly processed or frozen down on -80°C.

Cytoskeletal extraction buffer

NaCl.....50mM

sucrose.....150mM

PIPES.....10mM *pH* 6.8

Triton-X-100 0.5%

NaF 10µM

Na₃VO₄.....2mM

protease inhibitor cocktail.....1 tablet/10ml

RIPA buffer

NaCl.....150mM

<i>Tris-HCl</i>	<i>50mM</i>	<i>pH 7.6</i>
<i>EDTA</i>	<i>1mM</i>	
<i>Na-deoxycholate</i>	<i>1%</i>	
<i>SDS</i>	<i>0.1%</i>	
<i>Triton-X-100</i>	<i>1%</i>	
<i>NaF</i>	<i>10mM</i>	
<i>Na₃VO₄</i>	<i>1mM</i>	
<i>protease inhibitor cocktail</i>	<i>1 tablet/10ml</i>	

2.6.4. Determination of the protein concentration

Protein concentration was determined by the use of two different assays that are described below (2.6.4.1, 2.6.4.2). While the BCA assay was used for all standard procedures (total protein lysate), the Bradford assay was used to determine protein concentrations of plasma membrane preparations, since the buffers used in fractionation assays contain either DTT or sucrose which interfere with the BCA assay.

2.6.4.1. BCA protein assay

This method is based on the reduction of Cu^{2+} - to Cu^{1+} -ions by proteins under alkaline conditions (Biuret-reaction). The detection of Cu^{1+} -ions is mediated by bicinchoninic acid, which is chelated by cuprous cations forming a complex with a strong absorbance at 562nm. The assay was performed according to the instructions of the manufacturer.

BCA Protein Assay Kit, Pierce (Cat.No.23225)

2.6.4.2. Bradford protein assay

The Bradford assay is based on the coomassie brilliant blue G-250 dye which specifically interacts with Arginine, Tryptophan, Tyrosine, Histidine and Phenylalanine residues. While the free dye displays an absorbance maximum at 470nm the bound dye has an absorbance maximum at 595nm. This assay is very fast and specific but it should be kept in mind that the relation between protein concentration and absorbance is not-linear over wide ranges (0.1-1mg/ml). The assay was performed according to the instructions of the manufacturer.

Bradford Reagent, Sigma (Cat.No.B6916)

2.6.5. Immunoprecipitation

Before cell lysis, cells were washed once in ice-cold PBS. Cell lysis buffer (2.6.2) was added and cells were incubated for 10min on ice. Cell lysates were centrifuged at 15000xg for 10min at 4°C and the protein concentration of the supernatant was determined using a BCA protein assay (2.6.4.1). Typically lysates with a concentration of 0.5-1.5 mg/ml were used.

Standard IP: For immunoprecipitation of endogenous proteins mouse IgG1 antibodies were bound to protein G sepharose beads by incubating beads and antibodies for 1.5-2h at 4°C (1µg antibody per IP). Polyclonal rabbit antibodies were bound to protein A sepharose. After binding, beads were washed 3 times with PBS and once with lysis buffer. Cell lysates were incubated for 2.5h with antibody-coupled beads, followed by 5 washes with TBS. Beads were resuspended in 40µl 2x SDS sample buffer (2.6.2) and boiled for 5min at 95°C.

FLAG-IP: For immunoprecipitation of FLAG tagged proteins cell lysates were incubated for 2h with anti-FLAG M2 sepharose (40µl per IP, equilibrated in TBS) followed by 5 washes with TBS. Immunoprecipitated FLAG fusion proteins were eluted by incubation with a FLAG-peptide solution (100µl per IP) for 30min at 4°C. Beads were centrifuged, the supernatant was added to SDS sample buffer and boiled at 95°C for 5min.

FLAG-IP for SILAC: For SILAC experiments, cells were labelled with normal (Arg0), light (Arg6) and heavy (Arg10) amino acids (2.5.9) and subjected to the DR experiment (2.5.8). 4 subconfluent 140mm dishes were used per time point. After EGF-stimulation cells were lysed in 1ml lysis buffer, scraped and centrifuged for at 4°C with 15000xg for 15min. Supernatants were taken off and the protein concentration was measured by a BCA protein assay. The concentration of the cell lysates was adjusted to 1mg/ml and the lysates of the differently labelled cells were pooled. FLAG-immunoprecipitation and elution of ILK-FLAG was performed as described above.

Anti-FLAG M2 affinity gel, Sigma (Cat.No.A2220)

3xFLAG peptide, Sigma (Cat.No.F4799)

Protein G sepharose, Fast Flow, Sigma (Cat.No3296)

Protein A sepharose, Fast Flow, Sigma (Cat.No.9424)

2.6.6. Rac1 and Cdc42 pulldown assay

In order to determine the activity of Rho-GTPases cells were washed once in ice-cold PBS and lysed in NP-40 lysis buffer containing a biotinylated peptide corresponding to the Cdc42/Rac interactive binding motif in PAK1B to which only activated (GTP-loaded)

GTPases can bind (Crib peptide). Lysates were clarified by centrifugation with 15000xg for 10 min at 4°C and the protein concentration of the supernatant was determined by BCA protein assay (2.6.4.1). Protein concentration of all samples was equally adjusted (0.5-1.5mg/ml). Samples were incubated for 45min at 4°C followed by sedimentation with streptavidin-conjugated agarose beads for additional 30min at 4°C. Beads were washed three times in NP-40 lysis buffer, resuspended 2x SDS sample buffer (2.6.2) and boiled for 5min at 95°C.

NP-40 lysis buffer

<i>Tris-HCl</i>	50mM	<i>pH 7.6</i>
<i>NaCl</i>	100mM	
<i>Nonidet P-40</i>	1%	
<i>glycerol</i>	10%	
<i>MgCl₂</i>	2mM	
<i>NaF</i>	1mM	
<i>Na₃VO₄</i>	1mM	
<i>protease inhibitor cocktail</i>	1 tablet/10ml	

Streptavidin-Agarose from Streptomyces avidinii, Sigma (Cat.No.S1638)

2.6.7. One-dimensional SDS-polyacrylamid-gelelectrophoresis (SDS-PAGE)

SDS-PAGE under denaturing conditions is the most widely used method for separation of proteins, which can be subsequently visualized by silver staining, protein dyes or Western blotting. After proteins are solubilized by boiling in the presence of sodium dodecyl sulphate (SDS) the individual proteins are separated electrophoretically. 2-Mercaptoethanol or dithiothreitol (DTT) is added during solubilization to reduce disulfide bonds.

To perform discontinuous gel electrophoresis differentially buffered separating and stacking gels are poured on top of each other. The proteins that pass first through a stacking gel get concentrated at the stacking/separating gel interface. In the separating gel the proteins are separated according to molecular size in a denaturing gel (containing SDS), according to molecular shape, size, and charge in a nondenaturing gel.

Proteins were separated in the Minigel format (7.3mm x 8.3mm x 1.5mm) by means of the Mini Protean III System (BioRad). After polymerization of the polyacrylamid gel and assembly of the electrophoresis module protein samples were mixed with 4x SDS sample buffer and boiled for 5min at 95°C. Samples were collected by centrifugation and loaded on

the stacking gel. Finally, the electrophoresis module was filled with SDS-PAGE running buffer and electrophoresis performed at 100V at RT.

separating gel (10ml) 8%.....10%..... 12% 15%
H₂O 4.6ml..... 4.0ml3.3ml 2.3ml
 30% ProtoGel..... 2.7,ml..... 3.3ml 4.0ml 5.9ml
 1.5M Tris-HCl 2.5ml..... 2.5ml2.5ml 2.5ml.....pH 8.8
 10%SDS..... 0.1ml..... 0.1ml.....0.1ml 0.1ml
 10% APS..... 0.1ml..... 0.1ml.....0.1ml 0.1ml
 TEMED..... 0.006ml..... 0.006ml.....0.006ml 0.006ml

stacking gel (5ml)..... 5%
H₂O 3.4ml
 30% ProtoGel..... 0.83ml
 1M Tris-HCl 0.63ml.....pH 6.8
 10%SDS..... 0.04ml
 10% APS..... 0.04ml
 TEMED..... 0.004ml

10x SDS-PAGE running buffer (1l)
 Glycine..... 144g
 Tris-HCl..... 30.3g
 SDS 10g

N,N,N',N'-Tetramethylethylenediamine (TEMED), Serva (Cat.No.35925)
 ProtoGel (Ultra Pure), National Diagnostics (Cat.No.EC-890)

2.6.8. Western blotting and Immunodetection

Western blotting is used to identify specific proteins by polyclonal or monoclonal antibodies. Proteins are first separated by SDS-PAGE and then electrically transferred onto a PVDF membrane. Proteins bound to the surface of this membrane can be visualized by immunodetection reagents.

After separation of proteins by SDS-PAGE (2.6.7) the stacking gel was removed while the separating gel was placed in Western blotting transfer buffer. After short equilibration of the

polyacrylamid gel and a methanol-activated PVDF membrane in blotting buffer a transfer sandwich was assembled.

Proteins were then electrically transferred o/n with 25V at 4°C or for 1.5h with 100V at 4°C. After disassembly of the transfer sandwich, membranes were stained for 30sec with Ponceau S solution, rinsed in H₂O in order to visualize proteins bands on the membrane and to confirm the successful transfer. Membranes were subsequently washed in TBS-T and blocked for 1 h at RT in blocking buffer. Next, the primary antibody was incubated on the membrane either o/n at 4°C or for 2h at RT (depending on the instructions of the antibody manufacturer), membranes were washed 4 times 5min each with TBS-T and the appropriate secondary antibody was incubated with the membrane for 1.5h at RT. After 4 washes for 5min in TBS-T membranes were subjected to a chemiluminescence-based detection kit.

Western Blotting transfer buffer (1l)

Tris-HCl..... 6g

Glycine..... 28.8g

Methanol..... 200ml

10x TBS (1000ml)

Tris-HCl..... 24.3g

NaCl..... 80g

TBS-T (1000ml)

Tween-20 1ml

10x TBS..... 100ml *in H₂O*

Blocking buffer

skim milk powder..... 5% *in TBS-T*

Ponceau S solution, Sigma (Cat.No. P3504)

Chemiluminescence Reagent Plus, Western Lightning (Cat.No.NEL104)

2.7. Molecular Biological Methods

2.7.1. Material Molecular Biology

Autoclave: KSG, KSG-112

Centrifuge: Eppendorf, 5417C

Centrifuge: Beckman Coulter, Avanti J-25

Centrifuge rotor: Beckman Coulter J 14 / J 25.50

Microwave: Daewoo, KOR 63D7

Thermocycler: Biometra T3

Thermomixer: Eppendorf 5350

2.7.2. Phenol/Chloroform extraction of tail DNA

For genotyping of mice, a small biopsy of the mouse tail was digested with 500µl DNA lysis buffer in an Eppendorf tube o/n. The next day, 500µl Phenol/Chloroform (1:1) was added, the DNA solution was mixed and centrifuged for 5min at 15000xg. The uppermost layer was taken off and added to 500µl chloroform/isoamylalcohol solution (24:1), mixed and centrifuged again for 5min at 15000xg. The upper DNA rich layer was taken off and DNA was precipitated by addition of 500µl isopropanol. The white DNA precipitates were pelleted by centrifugation for 1min at 15000xg. Pellets were air-dried for 1-2min and subsequently resuspended in 50-100µl H₂O.

DNA lysis buffer

<i>NaCl</i>	20mM	
<i>Tris-HCl</i>	100mM	pH 7.6
<i>EDTA</i>	5mM	
<i>SDS</i>	0.2%	
<i>proteinase K</i>	100µg/m	

Rothi-Phenol, Roth (Cat.No 0038.2)

2.7.3. Bacteriological tools

Escherichia coli (E.coli) cultures were cultured in lysogeny broth (LB) rich medium. Media were prepared and autoclaved for 20min at 120°C. Antibiotics were added after the solutions were cooled below 50°C. LB plates were poured into 100mm Petri dishes and stored at 4°C.

LB medium

<i>NaCl</i>	10g
<i>Trypton</i>	10g
<i>Yeast extract</i>	5g

filled up to 1000ml with H₂O, autoclaved and stored at 4°C

LB plates

<i>LB medium</i>	1000ml
------------------------	--------

Agar-Agar 15g
autoclaved, poured into 100mm Petri dishes, stored at 4°C

Additives

Ampicillin..... 50µg/ml
Kanamycin..... 25µg/ml
Tetracycline 12.5µg/ml

2.7.3.1. Preparation of competent bacteria

An *E.coli* (XL-1 blue) bacterial culture was grown o/n in 10ml LB +Tetracycline (2.7.3) at 37°C shaking 180rpm. The next morning, 100ml of LB+Tetracycline was inoculated with 2ml overnight culture and grown until an optical density at 550nm (OD₅₅₀) of 0.5 was reached. The bacterial culture was placed on ice for 10min and then centrifuged for 15min at 4°C with 1000xg. The pellet was resuspended in 10ml TSS and 2.9ml glycerol (87%) was added. This bacterial suspension was aliquoted in volumes of 200µl and immediately frozen in liquid nitrogen. Competent cells were stored at -80°C.

TSS (500ml)

polyethylenglycol..... 50g
Tryptone..... 5g
Yeast extract 2.5g
NaCl..... 2.5g
DMSO..... 25ml
1M MgCl₂ 25ml
filtrated and stored at 4°C

2.7.3.2. Transformation of competent bacteria

100µl of competent bacteria were thawed on ice, DNA was added and incubated on ice for 30min. Cells were then placed on 42°C for 90sec (heat shock) and subsequently placed on ice for at least 2min. 750µl prewarmed LB medium (w/o antibiotics) was added and cells were incubated for 1h at 37°C shaking at 200rpm. Next, bacteria were carefully pelleted by 30sec centrifugation at 4000xg, resuspended in 100µl LB medium and spreaded on LB plates. Plates were incubated o/n at 37°C. Colonies appeared within 8-12h depending on the transformed DNA construct.

2.7.3.3. Cryo-preservation of bacteria

In order to freeze bacterial cultures 250µl glycerol (87%) was added to 750µl bacterial overnight culture. Cryo-cultures were stored at -80°C.

2.7.3.4. Preparation of plasmid DNA from bacterial cultures

Bacterial colonies were inoculated with 4ml LB medium containing the appropriate antibiotics o/n at 37°C. 750µl of this bacterial culture were frozen down as described in 2.7.3.3, 3ml were used for DNA isolation, which was performed by using the Qiagen Plasmid Mini Kit. This method is based on an alkaline bacterial lysis, followed by binding of the DNA to an anion-exchange resin under low salt and low pH conditions. Impurities like proteins or RNA are removed by medium salt washing steps. DNA is eluted from the resin under neutral or alkaline pH conditions.

Large amounts of DNA were prepared by the same method using larger volumes (Qiagen Plasmid Maxi Kit). DNA concentration was determined by photometric measurement at 260nm. DNA was stored at -20°C.

Qiagen Plasmid Mini Kit, Qiagen (Cat.No. 12125)

Qiagen Plasmid Maxi Kit, Qiagen (Cat.No. 12162)

2.7.4. Enzymatic manipulation of DNA

Restriction enzymes are widely used in molecular biology in order to cleave DNA at specific sites. They can be divided into three subgroups. The type I restriction enzymes are complex multi-subunit enzymes that cut the DNA random far from their recognition sequence. The type II enzymes bind to specific DNA sequences and cut the DNA within or close to this binding motif. The type III restriction enzymes are complex and cleave the DNA outside of their recognition sequence. Type II restriction enzymes are widely used as a molecular biological tool.

2.7.4.1. Digestion of DNA with restriction enzymes

All restriction enzymes used in this study were purchased from New England Biolabs (NEB). Digestion was performed according to the instructions of the manufacturer. In general, the following reaction conditions were used:

DNA digestion

DNA 3-5µg

NEB buffer (+/- BSA) 3 μ l
Restriction enzyme..... 5U
filled up to 30 μ l with H₂O, incubated for 2h at 37°C

2.7.4.2. Dephosphorylation of plasmid DNA

Digestion of DNA with restriction enzymes generates a reactive 5'-phosphate group and a 3'-hydroxyl group. In order to prevent self-ligation of digested plasmids, the 5'-phosphate group was removed by the use of shrimp alkaline phosphatase (sAP). Digestion enzymes were heat inactivated (according to the instructions of the manufacturer) and subsequently incubated at high pH conditions for 2x 30min with sAP.

Dephosphorylation of DNA

DNA 3-5 μ g
sAP buffer 3 μ l
sAP..... 5U
filled up to 30 μ l H₂O, incubated for 2 times 30min at 37°C

2.7.4.3. Phosphorylation of DNA fragments

T4 polynucleotide kinase (PNK) was used in order to generate reactive 5'-phosphate ends for subsequent ligation. PNK catalyzes the transfer of the γ -phosphate from ATP to 5'-hydroxyl-termini of polynucleotides. DNA was incubated with PNK in the presence of ATP for 30min at 25°C. The following conditions were used:

Phosphorylation of DNA

DNA fragment..... 3-5 μ g
T4 PNK reaction buffer 3 μ l containing 1mM ATP
T4 PNK 10U
filled up to 30 μ l with H₂O, incubated for 30min at 25°C

2.7.4.4. Blunting of DNA fragments

In order to generate blunt-ends of PCR- or digestion products DNA was treated with the large Klenow fragment. The Klenow fragment is a proteolytic product of *E.coli* DNA polymerase type I which retains polymerization and 3'-5' exonuclease activity but lost 5'-3' exonuclease activity.

Blunting of DNA

DNA fragment..... 3-5 μ g
NEB buffer 2 3 μ l
dNTPs 10 μ M
Klenow fragment..... 1U/ μ g DNA
filled up to 30 μ l with H₂O, incubated for 20min at 25°C

For heat inactivation of the Klenow fragment, EDTA was added to a final concentration of 10mM. This reaction mix was subsequently incubated for 20min at 75°C.

2.7.4.5. Ligation of DNA fragments

For DNA ligation, the generation of a phosphodiester bond between a 3'-hydroxyl group and a 5'-phosphate group, the following protocol was used.

DNA ligation

DNA backbone (vector) 0.5-1 μ g *dephosphorylated*
DNA insert 5 μ g *PCR product or digested DNA*
ATP (10mM) 1.5 μ l
Fast link ligase buffer 1.5 μ l
Fast link ligase 1 μ l
filled up to 15 μ l with H₂O, incubated for 45min at RT, then heat-inactivated for 10min at 70°C. 2-5 μ l of the ligation products were used for transformation as described before (2.7.3.2).

2.7.5. Polymerase chain reaction (PCR)

PCR is a widely used method for enzymatic DNA amplification (Saiki et al. 1988). The reaction is carried out in the presence of three nucleic acid segments (DNA template, primer1, primer2), DNA polymerase (*Taq* polymerase or high fidelity polymerase) and dNTPs. The amplification occurs in three different steps: denaturation (95°C), annealing of the primers to the DNA template (58-68°C depending on the primer) and DNA synthesis (72°C).

2.7.5.1. Oligonucleotides (primer)

All oligonucleotides were synthesized and purified by Metabion international (Martinsried, Germany). Oligonucleotides used for cloning of siRNA constructs were 5'-phosphorylated and HPLC purified.

Name	5'-3' sequence	application
ILK-for	GTCTTGCAAACCCGCTCTGCG	genotyping
ILK-rev	CAGAGGTGTCAGTGCTGGGATG	genotyping
Cre-for	AACATGCTTCATCGTCGG	genotyping
Cre-rev	TTCCGATCATCAGCTACACC	genotyping
ILK-Eco-Koz	AAAGAATTCACCATGGACGACATTTTCACTCAG	Cloning ILK full length
ILK-Bam-end	GCGGATCCCTTGTCTGCATCTTCTCCAAG	Cloning ILK full length
Not-3xFLAG	ATAGTTTACGCGCCGATTCTTATTCACTACTTGTCATC GTCATCCTTGTAGTCGATGTCATGATC	Cloning ILK-3 x FLAG
Ank-del	AAAGGATCCACCATGGGGACCCTGAACAAACTCC GGTATTG	Cloning ANK-deletion
Kin-del-rev	GGGGATCCATTTTCGGGGCCTTGTGCGAGTGGTCCCC TTCC	Cloning Kinase-deletion
R211A-for	CTTGAAAGGCGCCTGGCAGGGCAATGATATTG	ILK- Mutagenesis
R221A-rev	CAATATCATTGCCCTGCCAGGCGCCTTCCAAAG	ILK- Mutagenesis
S343A-for	GCTGATGTAAATTTGCTTTCCAGTGCCCTGGG	ILK- Mutagenesis
S343-rev	CCCAGGGCACTGGAAAGCAAATTTAACATCAGC	ILK- Mutagenesis
S343D-for	GCTGATGTAAATTTGATTTCCAGTGCCCTGGG	ILK- Mutagenesis
S343D-rev	CCCAGGGCACTGGAAATCAAATTTAACATCAGC	ILK- Mutagenesis
386/387-for	CTTCTGTGGAACTGGGGGACGAGAGGTGCCCTTGC	ILK- Mutagenesis
386/387-rev	GCAAAGGGCACCTCTCGTCCCCCAGTTCACAGAAG	ILK- Mutagenesis
Pax-Mfe-for	CCCCAATTGACCATGGACGACCTCGACGCCCTGCTGG	Cloning Pax full length
Pax-Bcl-rev	CCCTGATCACTAGCAGAAGAGCTTGAGGAAGCAG	Cloning Pax full length
LD1-del-for	CCCCAATTGACCATGCGGCCTGTGTTCTTGTCG GAGG	Cloning LD1-deletion
SS-siControl	GATCCCAGCAGTGCATGTATGCTTCTTCAAGAGA TCGTCACGTACATACGAAGTTTTTA	cloning siControl
AS-siControl	AGCTTAAAAAGCAATGGAACGAGTATTAATCT	cloning

Name	5'-3' sequence	application
	CTTGAATCGTCACGTACATACGAAGGGG	siControl
SS1-FAK	GATCCCCGCAATGGAACGAGTATTAATTCAAGAGA TTAATACTCGTTCCATTGCTTTTTA	cloning FAK-siRNA
AS1-FAK	AGCTTAAAAAGCAATGGAACGAGTATTAATCT CTTGAATTAATACTCGTTCCATTGCGGG	cloning FAK-siRNA
SS2-FAK	GATCCCCGTCCAACCTATGAAGTATTATTCAAGAGA TAATACTTCATAGTTGGACTTTTTA	cloning FAK-siRNA
AS2-FAK	AGCTTAAAAAGTCCAACCTATGAAGTATTATCT CTTGAATAATACTTCATAGTTGGACGGG	cloning FAK-siRNA
SS3-FAK	GATCCCCGTCCAATGACAAGGTATATTCAAGAGA TATACCTTGTCATTGGACCTTTTTA	cloning FAK-siRNA
AS3-FAK	AGCTTAAAAAGGTCCAATGACAAGGTATATCT CTTGAATATACCTTGTCATTGGACCGGG	cloning FAK-siRNA
SS4-FAK	GATCCCCGCAATATGCTAATCTCATTTTCAAGAGA AATGAGATTAGCATATTGCTTTTTA	cloning FAK-siRNA
AS4-FAK	AGCTTAAAAAGCAATATGCTAATCTCATTCT CTTGAAAATGAGATTAGCATATTGCGGG	cloning FAK-siRNA
SS5-FAK	GATCCCCGCGAACTATCTGTAGAACTTTCAAGAGA AGTTCTACAGATAGTTCGCTTTTTA	cloning FAK-siRNA
AS5-FAK	AGCTTAAAAAGCGAACTATCTGTAGAACTTCT CTTGAAAGTTCTACAGATAGTTCGCGGG	cloning FAK-siRNA
SS1-Pax	GATCCCCCAACTGGAAACCACACATATCT CTTGAATATGTGTGGTTTCCAGTTGTTTTA	cloning Pax-siRNA
AS1-Pax	AGCTTAAAAACAACCTGGAAACCACACATATCT CTTGAATATGTGTGGTTTCCAGTTGGGG	cloning Pax-siRNA
SS2-Pax	GATCCCCGAAGCCAAAGCGAAATGGATCT CTTGAATCCATTCGCTTTGGCTTCTTTTTA	cloning Pax-siRNA
AS2-Pax	AGCTTAAAAAGAAGCCAAAGCGAAATGGATCT CTTGAATCCATTCGCTTTGGCTTCGGG	cloning Pax-siRNA
SS3-Pax	GATCCCCGTCACTGTCAGATTTCAATCTCT TGAATTGAAATCTGACAGTGACGTTTTTA	cloning Pax-siRNA
AS3-Pax	AGCTTAAAAACGTCACTGTCAGATTTCAATCTCT TGAATTGAAATCTGACAGTGACGGGG	cloning Pax-siRNA
SS4-Pax	GATCCCCCGACCCATCCTGGATAAATCTCT TGAATTTATCCAGGATGGGTCCGTTTTA	cloning Pax-siRNA
AS4-Pax	AGCTTAAAAACGGACCCATCCTGGATAAATCTCT TGAATTTATCCAGGATGGGTCCGGGG	cloning Pax-siRNA
SS5-Pax	GATCCCCCGTACTGTCGTAAAGATTTCTCT TGAAAATCTTTACGACAGTACGCTTTTTA	cloning Pax-siRNA

Name	5'-3' sequence	application
AS5-Pax	AGCTTAAAAAGCGTACTGTCGTAAAGATTTCTCT TGAAAATCTTTACGACAGTACGCGGG	cloning Pax-siRNA
SS1-Cas	GATCCCCCTGGTAACCGCCTCAAGATTTCAAGA GAATCTTGAGGCGGTTACCAGTTTTTA	cloning Cas-siRNA
AS1-Cas	AGCTTAAAAACTGGTAACCGCCTCAAGATTCT CTTGAAATCTTGAGGCGGTTACCAGGGG	cloning Cas-siRNA
SS2-Cas	GATCCCCCATCATTTCGGTGTATGATTTCAAGA GAATCATAACCGAATGATGGTTTTTA	cloning Cas-siRNA
AS2-Cas	AGCTTAAAAACCATCATTTCGGTGTATGATTCT CTTGAAATCATAACCGAATGATGGGGG	cloning Cas-siRNA
SS3-Cas	GATCCCCGCTGCGTGAGGAAACCTATTTCAAGA GAATAGGTTTCCTCACGCAGCTTTTTTA	cloning Cas-siRNA
AS3-Cas	AGCTTAAAAAGCTGCGTGAGGAAACCTATTCT CTTGAAATAGGTTTCCTCACGCAGCGGG	cloning Cas-siRNA
SS4-Cas	GATCCCCGCGGCAACTACAGAAGATTTCAAGA GAATCTTCTGTAGTTGCCGGCTTTTTTA	cloning Cas-siRNA
AS4-Cas	AGCTTAAAAAGCCGGCAACTACAGAAGATTCT CTTGAAATCTTCTGTAGTTGCCGGCGGG	cloning Cas-siRNA
SS5-Cas	GATCCCCGAGGTGTCTCGTCCAATATTCAAGA GATATTGGACGAGACACCTCCTTTTTTA	cloning Cas-siRNA
AS5-Cas	AGCTTAAAAAGGAGGTGTCTCGTCCAATATCT CTTGAATATTGGACGAGACACCTCCGGG	cloning Cas-siRNA
SS1-Dock	GATCCCCGCTACACCTTAAGGAAAATTCAAGA GATTTTCCTTAAGGTGTAGCCTTTTTTA	cloning Dock180-siRNA
AS1-Dock	AGCTTAAAAAGGCTACACCTTAAGGAAAATCT CTTGAATTTTCCTTAAGGTGTAGCCGGG	cloning Dock180-siRNA
SS2-Dock	GATCCCCGTACAAATCGGTGATTTATTCAAGA GAATAAATCACCGATTTGTACTTTTTTA	cloning Dock180-siRNA
AS2-Dock	AGCTTAAAAAGTACAAATCGGTGATTTATTCT CTTGAAATAAATCACCGATTTGTACGGG	cloning Dock180-siRNA
SS3-Dock	GATCCCCCTAATCGCGGATAGGAAATTCAAGA GAATTTCTATCCGCGATTAGTTTTTA	cloning Dock180-siRNA
AS3-Dock	AGCTTAAAAACTAATCGCGGATAGGAAATCT CTTGAATTTCTATCCGCGATTAGGGG	cloning Dock180-siRNA
SS4-Dock	GATCCCCCTGAGACAGAGCTTCGAAATTCAAGA GATTCGAAGCTCTGTCTCAGTTTTTA	cloning Dock180-siRNA
AS4-Dock	AGCTTAAAAACTGAGACAGAGCTTCGAAATCT CTTGAATTTGGAAGCTCTGTCTCAGGGG	cloning Dock180-siRNA
SS5-Dock	GATCCCCAAGGACGATCCAGATAAATTCAAGA	cloning

Name	5'-3' sequence	application
	GATTTATCTGGATCGTCCTTGTTTTTA	Dock180-siRNA
AS5-Dock	AGCTTAAAAACAAGGACGATCCAGATAAATCT CTTGAATTTATCTGGATCGTCCTTGGGG	cloning Dock180-siRNA

2.7.5.2. PCR reactions

Two different PCR reactions were performed. 1) Regular PCR for genotyping using tail DNA and self-made recombinant *Taq* polymerase, 2) a cloning PCR using purified plasmid DNA and high fidelity polymerase with an additional proof reading activity.

Genotyping PCR

isolated tail DNA 1 μ l
 primer1 (10pmol)..... 1 μ l
 primer 2 (10pmol)..... 1 μ l
 dNTP (10mM) 1 μ l
 DMSO 2.5 μ l
 MgCl₂..... 1.5 μ l
 10x PCR buffer 3 μ l
 Taq polymerase..... 1 μ l
 filled up to 30 μ l with H₂O, subjected to PCR (2.7.5.3)

Cloning PCR (Mix1)

H₂O 19.25 μ l
 10x PCR buffer 5 μ l
 high fidelity polymerase..... 0.75 μ l

Cloning PCR (Mix2)

plasmid DNA.....200ng
 primer1 (10 pmol)..... 1 μ l
 primer2 (10 pmol)..... 1 μ l
 dNTP (10mM) 1 μ l
 filled up to 25 μ l with H₂O

Both mixtures were prepared separately and combined immediately before the start of the PCR reaction (2.7.5.3).

Expand high fidelity polymerase Roche (Cat.No. 3300242001)

2.7.5.3. PCR programs

The following PCR programs were used in this study:

Genotyping Cre-PCR

step.....time(sec)temp(°C)

1.....300 95

2.....30 95

3.....30 63

4.....60 72

5.....30 95

6.....30 55

7.....60 72

8.....300 72

9.....∞ 4

Genotyping-ILK-PCR

step..... time(sec)temp(°C)

1.....300 95

2.....30 95

3.....30 66

4.....60 72

5.....30 95

6.....30 58

7.....60 72

8.....300 72

9.....∞ 4

PCR's were performed for 35 cycles (step5-7), touch down from 63°C-55°C (Cre) and 66°C-58°C (ILK) in 9 cycles by sequential reduction of the annealing temperature (-1°C / cycle) (step2-4).

Cloning PCR short

step..... time(sec)temp(°C)

1.....300 95

2.....30 95

3.....30 66

4.....45 72

5.....30 95

6.....30 58

7.....45 72

8.....300 72

9.....∞ 4

Cloning PCR long

step..... time(sec)temp(°C)

1.....300 95

2.....30 95

3.....30 66

4.....120 72

5.....30 95

6.....30 58

7.....120 72

8.....300 72

9.....∞ 4

PCR's were performed for 35 cycles (step5-7), touch down from 66°C-58°C in 9 cycles by sequential reduction of the annealing temperature (-1°C / cycle) (step2-4).

Mutagenesis PCR

step..... time(sec)temp(°C)

1..... 30 95

2..... 30 95

3..... 60 55

4..... 300 68

5..... ∞ 4

PCR was performed for 18 cycles.

2.7.6. Agarose gel electrophoresis

Agarose gel electrophoresis is a simple method for separating, identifying or purifying DNA fragments. For gel preparation, the desired amount (between 1-2%) of agarose was added to 1xTAE buffer and boiled in the microwave. For 100ml agarose solution 5µl ethidium bromide was added. The melted agarose was poured into casting platform, allowed to harden at RT and placed into an electrophoresis chamber containing 1xTAE buffer. Next, DNA was mixed with 6x loading buffer and loaded on the agarose gel. Electrophoresis was carried out at 80-120V at RT. DNA bands were visualized under a UV light transilluminator at 366nm.

TAE buffer (50x)

Tris-base 242g

EDTA 37.2g

glacial acetic acid..... 57.1ml

filled up to 1000ml with H₂O

Agarose, Invitrogen (Cat.No. 15510-027)

Ethidiumbromid, Roth (Cat.No. 2218.1)

2.7.6.1. Extraction of DNA from agarose gels

Extraction of DNA fragments from agarose gels was done by using QIAEX Gel Extraction Kit (Qiagen) according to the instructions of the manufacturer.

QIAEX Gel Extraction Kit, Qiagen (Cat. No. 20021)

2.7.7. Site-directed mutagenesis

In vitro site-directed mutagenesis is a valuable tool to study protein function. The insertion of point mutations into a given DNA sequence can be used in order to switch, insert or delete

amino acids in the protein of interest. In this study, several point mutations were introduced into ILK by using a QuickChange Site-Directed Mutagenesis Kit. The principle is based on a double stranded DNA vector and two oligonucleotides encoding for the desired mutation. The oligonucleotide primers are extended during temperature cycling by PfuTurbo DNA polymerase generating a mutant plasmid. The parental plasmid (which does not contain the mutation) is digested with an endonuclease that only targets methylated DNA. Since DNA from most of the *E. coli* strains is dam methylated only the parental plasmid but not the newly synthesized plasmid is susceptible to this digestion.

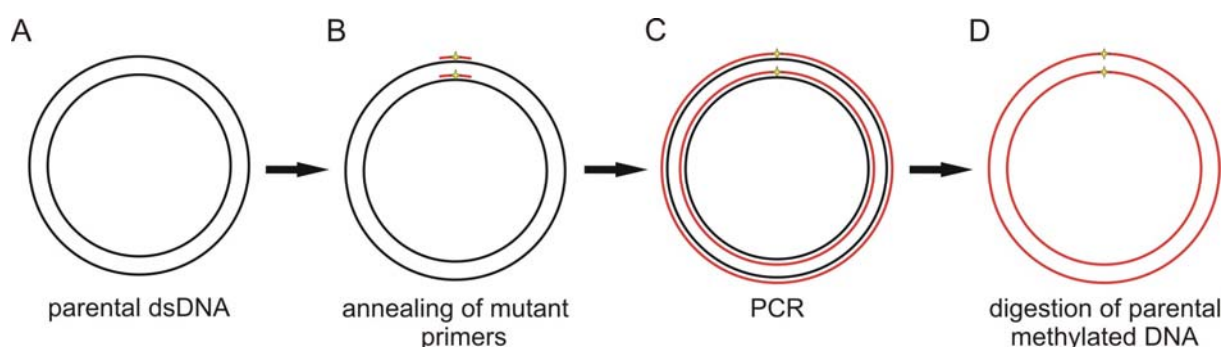


Fig 2.2. Principle of site-directed mutagenesis. A. A double-stranded (ds) parental DNA plasmid serves as a template. B. Primers, harbouring the mutant sequence are annealed to the parental DNA. C. PCR-based synthesis of two mutant DNA strands. D. Specific digestion of parental (dam-methylated) DNA. (Taken from QuickChange Site-Directed Mutagenesis Kit InstructionManual, Stratagene and modified).

2.7.7.1. Design of mutagenesis primers

All oligonucleotides used for mutagenesis (2.7.5.1) were HPLC purified and designed according to manufacturers instructions (Stratagene, QuickChange Site Directed Mutagenesis Kit, Instruction Manual). The desired mutation was inserted approximately in the middle of the primer that was flanked by 10-15 bases of correct sequence on both sides. The length of the primer was adjusted in a way that the melting temperature (T_m) of the primer was not higher than 78°C. T_m was calculated according to the following formula:

$$T_m = 81.5 + 0.41 (x \%GC \text{ content}) - 675/N - \% \text{ mismatch}$$

N: Primer length in bases

2.7.7.2. Mutagenesis

Site-directed mutagenesis was performed in two steps: mutagenesis PCR and digestion of the parental DNA.

Mutagenesis PCR: In order to perform the mutagenesis PCR (PCR program see 2.7.5.3) the following reaction was prepared:

parental plasmid DNA..... 100ng
primer1 125ng
primer2 125ng
dNTPs (10mM) 1 μ l
reaction buffer 5 μ l
PfuTurbo Polymerase..... 1 μ l 2.5U/ μ l
filled up to 50 μ l with H₂O, subjected to PCR (2.7.5.3).

Digestion of parental DNA: 1 μ l of Dpn I restriction enzyme (10U/ μ l) was added to 20 μ l of PCR product and incubated for 1h at 37°C. 2 μ l of this reaction was used for DNA transformation (2.7.3.2).

2.7.8. Generation of siRNA constructs

Introduction of double-stranded RNA directs post-transcriptional gene silencing, which is highly specific and usually does not interact with genes unrelated in sequence. However, in most mammalian cells RNA interference causes cytotoxic effects, which can be circumvented by the use of small synthetic interfering RNAs (siRNA).

Since gene silencing induced by RNAi is not caused by a genetic change these studies are often hampered by its transient nature. Therefore, stable expression of siRNAs driven by the pSUPER vector system (Brummelkamp et al. 2002) provides a powerful tool to study loss of function phenotypes in a persistent manner (pSuper RNAi system, OligoEngine, Seattle USA). The pSUPER vectors use a RNA polymerase III H1 gene promoter as it produces RNA transcripts that lack a polyadenosine tail. Moreover, start and termination of transcription are well defined and the RNA constructs can be designed in a way that the resulting transcript will form a pair stem loop structure that is rapidly cleaved within the cell to produce a functional siRNA.

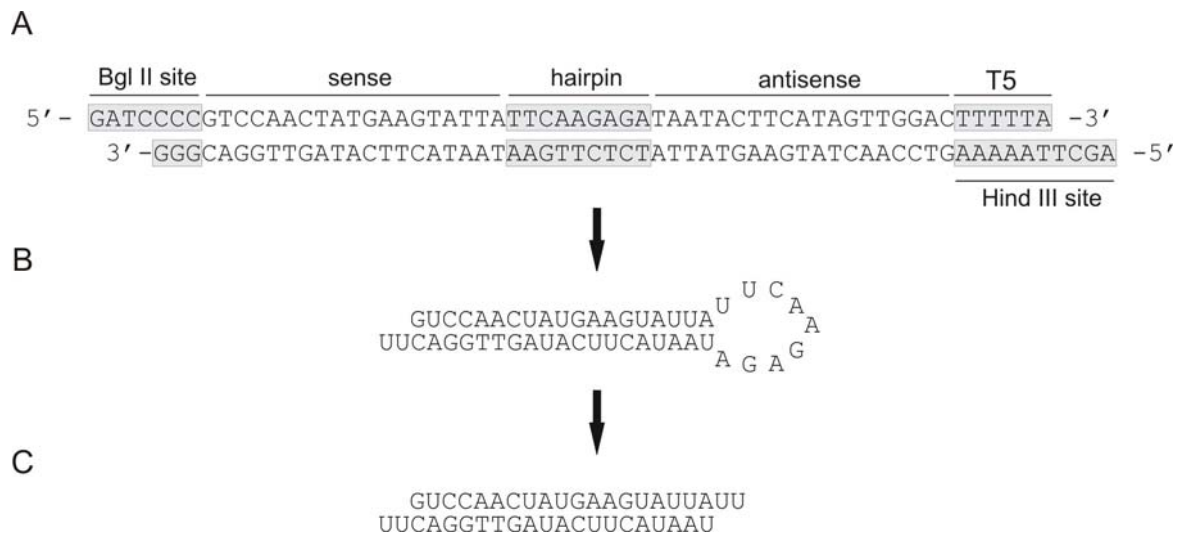


Fig 2.3. Principle of pSUPER driven siRNA expression. *A.* Annealed oligonucleotides containing the target sequence, the hairpin structure, the termination signal (T5) and BglII and HindIII compatible overhangs. *B.* The secondary structure of the RNA transcript is a pair stem loop structure. *C.* Processing of the RNA transcript within the cell leads to a functional siRNA. (Taken from the pSuper.Retro Instruction Manual, OligoEngine and modified. Shown here: knockdown construct #2 for FAK knockdown, which produced a very high knockdown efficiency).

2.7.8.1. Design of siRNA constructs

The sequence of the siRNA constructs were chosen according to the protocol from (Ui-Tei et al. 2004) and (Naito et al. 2004). Full length mRNA sequences of the target gene were checked using the online software siDirect for 19mers matching the criteria listed in Fig 2.4. Five different constructs per knockdown were designed and subsequently cloned into the pSUPER.Retro backbone.

criteria for siRNA constructs

G/C at the 5' end of the sense-strand (SS)

A/T at the 3' end of SS

AT-richness at the 3'-terminal 7bp long region of the SS

no G/C-stretches longer than 9bp

G/C content: 40%-60%

<i>annealed oligonucleotides</i>	2 μ l	
<i>linearized pSUPER</i>	1 μ l	<i>c=4μg/μl</i>
<i>Fast link ligation buffer</i>	1.5 μ l	
<i>ATP (10mM)</i>	1.5 μ l	
<i>Fast link ligase</i>	1 μ l	
<i>H₂O</i>	8 μ l	

Successful ligation leads to the destruction of the BglII restriction site. To reduce the amount of re-ligated vectors, ligation reactions were additionally treated for 30min with BglII at 37°C. 2 μ l were used for transformation 2.7.3.2.

2.7.9. Generation of retroviral expression constructs

In order to stably express the protein of interest in ILK fibroblasts, retroviral expression constructs were generated which all use the pCL vector system (Naviaux et al. 1996). The retroviral backbone used in this study, pCLMFG, was provided by Prof. Dr. Alexander Pfeifer (University of Bonn, Germany). All cDNAs were cloned into the multiple cloning site (MCS) of this vector.

2.7.9.1. Plasmids and cDNAs

cDNA	backbone	provided by	Reference
ELMO1-EGFP	pEBB.....	Dr. Ravichandran	(Gumienny et al. 2001)
ILK-EGFP (human).....	pcDNA3.1	Dr. Obbgerghen-Schilling	(Boulter et al. 2006)
ILK (mouse).....	pBluescript	Dr. Fässler	(Sakai et al. 2003)
ILK-EGFP (mouse).....	pCLMFG.....	Dr. Fässler	(Sakai et al. 2003)
myc-RacN17	pRK5	Dr. Hall	(Ridley et al. 1992)
myc-RacL61	pRK5	Dr. Hall	(Ridley et al. 1992)
paxillin.....	pLZRS	Dr. Danen.....	(Danen et al. 2005)

2.7.9.2. Expression vectors

name	approach	resistance	source
pBluescript KS	cloning	ampicillin	Stratagene (No. 200455)
p3xFLAG	cloning/expression	ampicillin/ neomycin.....	Sigma (Cat.No. E4901)
pCLMFG.....	expression	ampicillin	Dr.Pfeifer (Bonn, Germany)

2.7.9.3. Generation of ILK expression constructs

ILK-3xFLAG: an ILK cDNA with an EcoRI/BamHI restriction site was generated by PCR using full length ILK cDNA in pBluescriptKS (pBlueKS) as a template (2.7.5.1, 2.7.5.2, 2.7.5.3) and inserted into the p3xFLAG expression vector. The ILK-3xFLAG cDNA was amplified by PCR generating EcoRI/NotI restriction site and inserted into EcoRI/NotI linearized and dephosphorylated pCLMFG. Correct insertion was checked by DNA sequencing.

ANK-3xFLAG (amino acids 1-180 of murine ILK): an ILK cDNA with an EcoRI/BamHI restriction site was generated by PCR using full length ILK cDNA in pBluescriptKS as a template (2.7.5.1, 2.7.5.2, 2.7.5.3) and inserted into the p3xFLAG expression vector. The ANK-3xFLAG cDNA was amplified by PCR generating EcoRI/NotI restriction site and inserted into EcoRI/NotI linearized and dephosphorylated pCLMFG. Correct insertion was checked by DNA sequencing.

human ILK-EGFP: full length cDNA of human-ILK-EGFP (in pcDNA3.1) was released by HindIII/SphI digestion. The DNA fragment was blunt-ended by Klenow treatment (2.7.4.4) and inserted into EcoRI digested, blunt-ended pCLMFG. Direction of the insert was checked by BamHI/HindIII digestion.

ILK-R211A-EGFP: mutation of ILK was performed essentially as described (2.7.7) using ILK in pBlueKS as a template. After sequencing of the construct, a mutant ILK fragment was released by EcoRI/StuI digestion (EcoRI cuts in front of the ATG and StuI is a single restriction site located at the 3'-end of the ILK cDNA). This mutant ILK cDNA fragment was inserted into pCLMFG that was cut with the same enzymes and subsequently dephosphorylated.

ILK-S343A-EGFP: as in ILK-R211A-EGFP (see above) using different mutagenesis primers (2.7.5.1)

ILK-S343D-EGFP: as in ILK-R211A-EGFP (see above) using different mutagenesis primers (2.7.5.1)

ILK-PBS-EGFP: as in ILK-R211A-EGFP (see above) using different mutagenesis primers (2.7.5.1)

2.7.9.4. Generation of Rac1 expression constructs

myc-RacN17: mutant human Rac1 cDNA (in pRK5) was released by sequential digestion with ClaI and HindIII and subcloned into pBlueKS that was cut before with the same enzymes and dephosphorylated. Mutant Rac1 cDNA (in pBlueKS) was isolated by double digestion with XhoI and NotI and inserted into pCLMFG that was digested before with the

NaCl..... 6.54g

Na₂HPO₄..... 0,085g

filled up to 400ml with H₂O

Transfection mix (for 1x 140mm dish)

DNA of pCLMFG..... 25 µg

DNA of packaging plasmid..... 25 µg

DNA of VSV-G env plasmid..... 12.5µg

filled up to 1.16ml with sterile H₂O, then addition of

CaCl₂ (2.5M) 112µ

vortexed, then addition of

2xBBS..... 1.16ml

inverted, incubate 10-15min at RT

2.7.10.2. Harvest of retroviral supernatant

First harvest: 24h after transfection the supernatant was taken off and filtered through a 0.45µm filter. 16ml growth medium was added to the cells which were incubated for additional 24h at 37°C in 10%CO₂. Filtrate was centrifuged at 50000xg for 2h at 17°C and pellets were resuspended in 50µl HBSS, vortexed and stored at 4°C.

Second harvest: 48h after transfection the retroviral supernatant was taken off and treated as above (first harvest).

For concentration of the virus, pellets of the first and second harvest were combined, mixed with 2ml of 20% sucrose and centrifuged at 42000xg for 2h. Pellets were resuspended in 50-100µl HBSS, mixed at RT for 45min and centrifuged down. Supernatant was taken off and stored at -80°C.

Hanks' Balanced Salt Solution (HBSS), Gibco (Cat.No. 14175-046)

2.7.10.3. Infection of ILK fibroblasts with VSV-G pseudotyped retroviral vectors

The day before infection, 1.5-2x 10⁶ cells were seeded in a 6-well plate and cultured o/n. The next day in the afternoon, 800µl growth medium containing 5-10µl of the virus prep was added to the cells which were then incubated o/n. Cells were washed once in PBS, trypsinized, resuspended in growth medium and seeded again on 6-well plates.

2.7.11. Microscopy

Confocal microscopy: Confocal images were collected by using a confocal microscope (Leica DMIRE2) with 100x oil objectives at RT. Leica Confocal Software (version 2.5 Build 1227) was used for image acquisition and evaluation.

Live cell microscopy: Live cells were recorded using a Zeiss Axiovert 300M inverted microscope equipped with a CCD camera (Roper Scientific, Duluth, GA) and a stage incubator (EMBL Precision Engineering, Heidelberg, Germany). MetaMorph software (Molecular Devices, Downingtown, PA) was used for microscope control and image acquisition.

3. Results

3.1. Analysis of ILK *in vivo*/targeted ablation of ILK in mice

The generation of the ILK targeting construct as well as the generation of ILK knockout ES cells was done by Drs. Reinhard Fässler and Takao Sakai. The analysis of the EBs was performed in collaboration with Drs. Shaohua Li and Peter Yurchenco (for details see Sakai et al. 2003).

3.1.1. Deletion of ILK leads developmental arrest at peri-implantation stage

In order to delete the *ILK* gene in mice, the ILK flox targeting construct was injected into ES cells and four targeted clones were isolated, transiently transfected with a Cre-recombinase expression plasmid and subjected to selection. Two ES cell clones with a single constitutive *ILK-null* allele were again electroporated with the ILK flox targeting construct and transiently transfected with the Cre-recombinase expression construct to obtain ES cells with a homozygous deletion of the *ILK* gene. Western blot analysis of ES cell protein lysates revealed the absence of ILK protein expression (Sakai et al. 2003). When mice heterozygous for the ILK mutation were intercrossed, no homozygous mutant ILK mice were among the progeny, suggesting that deletion of ILK leads to embryonic lethality. To determine the time point of lethality, blastocysts from heterozygous intercrosses were isolated at E3.5 and stained with an ILK antibody. To analyze later time points deciduas were isolated at E5.5, E8.5 and E9.5 and histologically analyzed. While normal numbers of ILK mutant blastocysts at E3.5 were found (6 out of 33), the implantation chambers of presumptive ILK-deficient embryos at E5.5 did not contain cells from the embryo proper anymore.

3.1.2. ILK null EBs fail to form a mature epiblast

To describe in more detail the reason for the early embryonic lethality of ILK mutant embryos, control and ILK-null ES cells were cultured in suspension for 6-9 days and EBs were examined by light microscopy. While control EBs displayed endodermal cell layers, epiblasts as well as central cavities, ILK-null EBs failed to assemble well-formed epiblasts and to cavitate (Fig 3.1A). Immunostaining of control and ILK-null EBs showed that, in contrast to $\beta 1$ integrin-deficient EBs, a BM can form in the absence of ILK (Sakai et al. 2003). These experiments also revealed that ILK-null epiblasts were not able to polarize. F-actin staining is under normal circumstances restricted to the apical side of the epiblast but not along the BM between epiblast and endodermal cells. In ILK-null EBs f-actin was frequently

localized to both the apical side of the epiblasts facing the cavity but also at the side of the epiblast adjacent to the BM (Fig 3.1B, C). The distribution of E-cadherin or β -catenin was, however, not dramatically changed (Sakai et al. 2003). These data demonstrate that ILK is essential for the polarization of the epiblast and indicate an important role of ILK for f-actin reorganization *in vivo*.

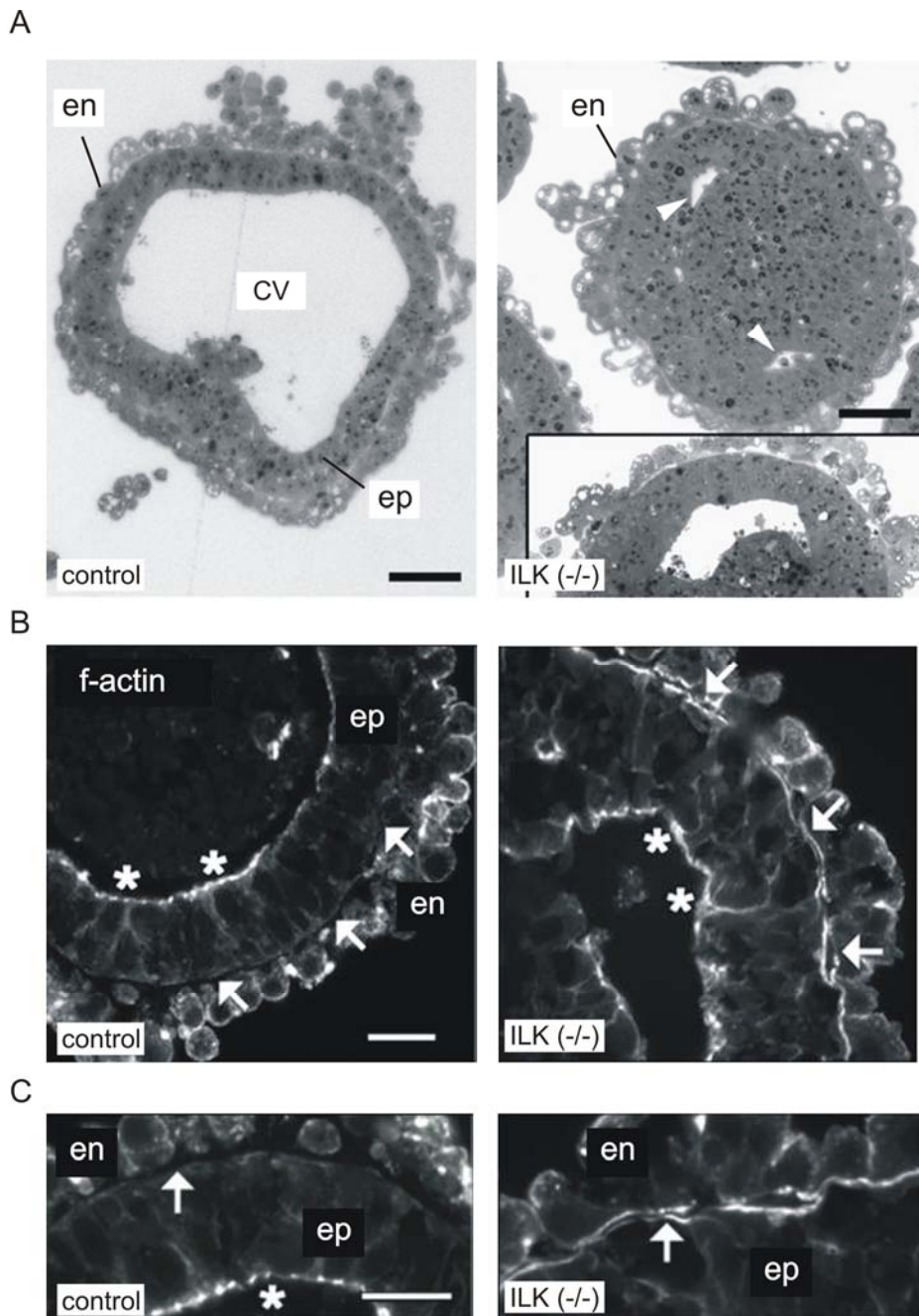


Fig 3.1. Analysis of ILK-deficient EBs. *A.* Light microscopic analysis of EBs after 7d of suspension culture. Most of the ILK (-/-) EBs failed to cavitate. Scale bars: 50 μ m. *B.* Phalloidin immunostaining revealed the defective f-actin polarization in ILK (-/-) EBs. In control EBs f-actin staining was strong in cells of the epiblast that faced the cavity (*) but not detectable in areas adjacent to the BM (arrows). In ILK (-/-) EBs f-actin was

localized in areas facing the cavity but also along the BM. **C.** Higher magnification of the phalloidin immunostaining showing the presence of α -actin staining along the endoderm/epiblast interface in the absence of ILK. Scale bars: 20 μ m. (Experiment was done by Drs. Shaohua Li and Peter Yurchenco; see also Sakai et al., 2003).

3.2. Analysis of ILK function *in vivo*/Characterization of cartilage-specific ILK knockout mice

3.2.1. Expression analysis

To determine the expression of ILK during development and adulthood, ILK *lacZ*/⁺ mice (Sakai et al. 2003) were sacrificed at distinct developmental stages to perform LacZ staining. Whole mount staining of embryos at E10.5 revealed a strong expression of ILK in the developing heart and somites and a lower expression level in almost all other tissues (Fig 3.2A). At E12.5, LacZ expression was ubiquitous, with high levels in the brain and in the condensing mesenchyme of the digits (Fig 3.2B). At E15.5, LacZ expression levels were high in chondrocytes from the epiphyseal cartilage and in the growth plates (Fig 3.2C). This high level of LacZ activity was maintained in chondrocytes from adult cartilages (Fig 3.2D).

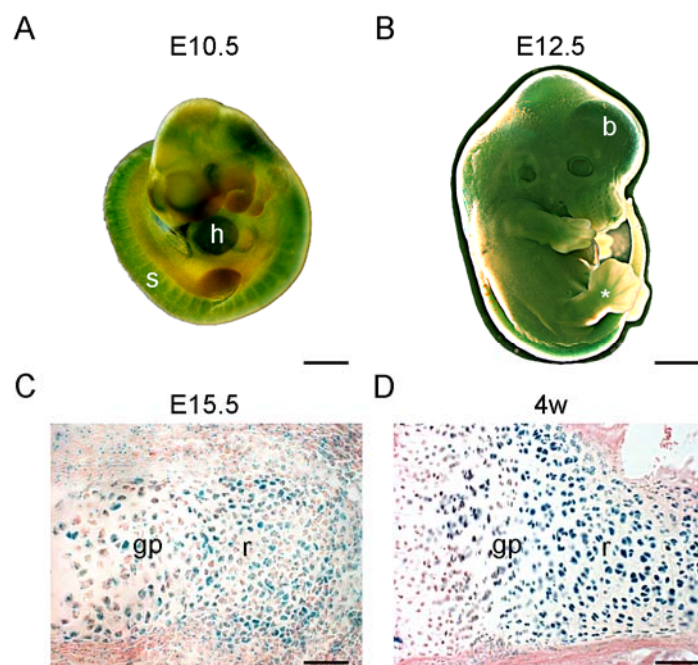


Fig 3.2. Expression analysis of ILK using ILK *LacZ*/⁺ mice. **A.** Whole mount LacZ staining of an embryo heterozygous for the ILK *lacZ* allele at E10.5. *s*: somites, *h*: heart. Scale bar: 500 μ m. **B.** Whole mount LacZ staining of an embryo at E12.5. *b*: brain, *: condensing mesenchyme of the digits. Scale bar: 1mm. **C.** LacZ staining of a metatarsal cartilage section at E15.5. *gp*: growth plate, *r*: resting zone. Scale bar: 50 μ m. **D.** LacZ staining of rib cartilage sections from a 4w-old mouse. *gp*: growth plate, *r*: resting zone. Scale bar: 50 μ m.

3.2.2. Chondrocyte-specific deletion of the *ILK* gene

To analyze the role of ILK specifically in the cartilage a mouse strain carrying a LoxP-flanked (floxed) *ILK* gene was generated (called hereafter: ILK (floxed/floxed) (Sakai et al. 2003). To delete the *ILK* gene exclusively in chondrocytes, ILK (floxed/floxed) mice were crossed with mice expressing the Cre-recombinase under the control of the mouse collagen II promoter (Col2Cre; Sakai et al. 2001) to obtain mice with the genotype ILK (floxed/floxed) Col2Cre⁺ (called Col2ILK; Fig 3.3A). The genotype of mice was determined by PCR-based genotyping (Fig 3.3B). Mice which were either heterozygous for the floxed *ILK* allele (expressing Col2Cre or not) or ILK (floxed/floxed) mice (which did not express Col2Cre) were used as controls (Fig 3.3). The control mice were indistinguishable from each other and did not show any obvious abnormalities.

To test the efficiency of ILK deletion *in vivo*, chondrocytes from control and mutant newborn mice were isolated and ILK levels in protein lysates were determined by western blot analysis. In all Col2ILK mice tested ILK expression was absent in chondrocytes (Fig 3.3C). This is in agreement with earlier results that showed Col2Cre activity already in condensing mesenchyme and cartilage (Sakai et al. 2001).

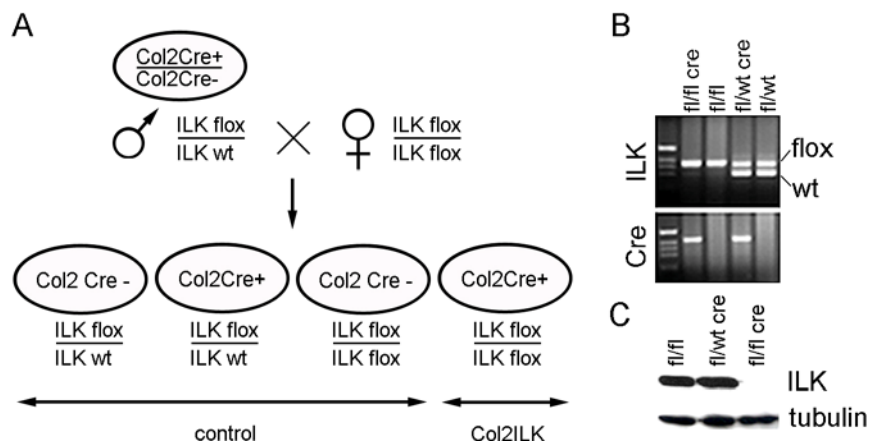


Fig 3.3. Efficient deletion of *ILK* in the cartilage. *A.* Mating scheme for the generation of cartilage-specific *ILK* knockout mice. *B.* PCR-based genotyping. *C.* Western Blot analysis of protein lysates from freshly isolated chondrocytes derived from newborn mice.

3.2.3. Col2ILK mice display progressive dwarfism

Until E16.5, the external appearance of Col2ILK embryos was indistinguishable from that of controls. At E17.5 and at the newborn stage they were approximately 5% shorter than controls (Fig 3.4A). Around 70% of the Col2ILK mice had a cleft palate (Fig 3.4B) and died 1-2 h

after birth. The remaining Col2ILK mice suffered from lung hypoplasia (Fig 3.4C) and died due to breathing distress 1–24 h after birth.

Whole-mount skeletal staining of newborn mice showed that all bones of the axial, appendicular and craniofacial skeleton formed in ILK mutant mice. However, most of the bones known to be formed by endochondral ossification were smaller than in controls. In addition, the thorax was small and narrow (Fig 3.4D), suggesting that the lung phenotype was caused by the reduced rib cage size. The growth of fore limbs and hind limbs was retarded by 10–15% (Fig 3.4D, E; Fig 3.5D).

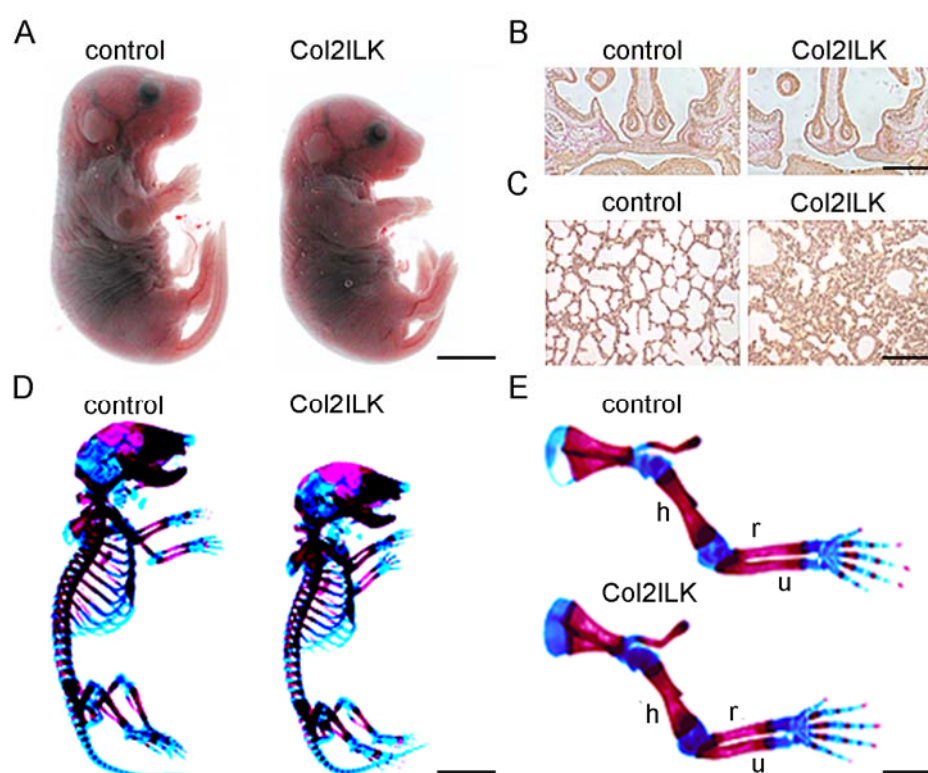


Fig 3.4. Morphological appearance of Col2ILK mice at the newborn stage. *A.* Col2ILK mice were significantly smaller than control littermates at the newborn stage. Approximately 70% of the knockout mice suffered from a cleft palate. Scale bar: 4mm. *B.* Hematoxylin/Eosin staining of frontal sections of the head at newborn stage. Scale bar: 50 μ m. *C.* Hematoxylin/eosin staining of lung sections at newborn stage. Scale bar: 2mm. *D.* Whole-mount Alcian Blue/Alizarin Red skeletal staining of mice at newborn stage. Scale bar: 4mm. *E.* Skeletal staining of fore limbs from newborn mice. Scale bar: 2mm. h: humerus, r: radius, u: ulna.

3.2.4. Col2ILK bones have shortened growth plates

At E17.5, long bones from Col2ILK mice were of normal shape, contained periosteal as well as trabecular bones (Fig 3.5A) and had a normal epiphyseal cartilage. However, the growth plates were significantly shortened (Fig 3.5B). The proliferative zone was less affected than

the hypertrophic zone, which was reduced by 30% (Fig 3.5B). At the newborn stage, the reduction in size of the growth plates became more pronounced. In addition, the columnar arrangement of chondrocytes was disorganized and the usually flattened proliferative chondrocytes appeared more roundish (Fig 3.5C). Moreover, the number of chondrocytes in the proliferative zone was reduced (Fig 3.5C).

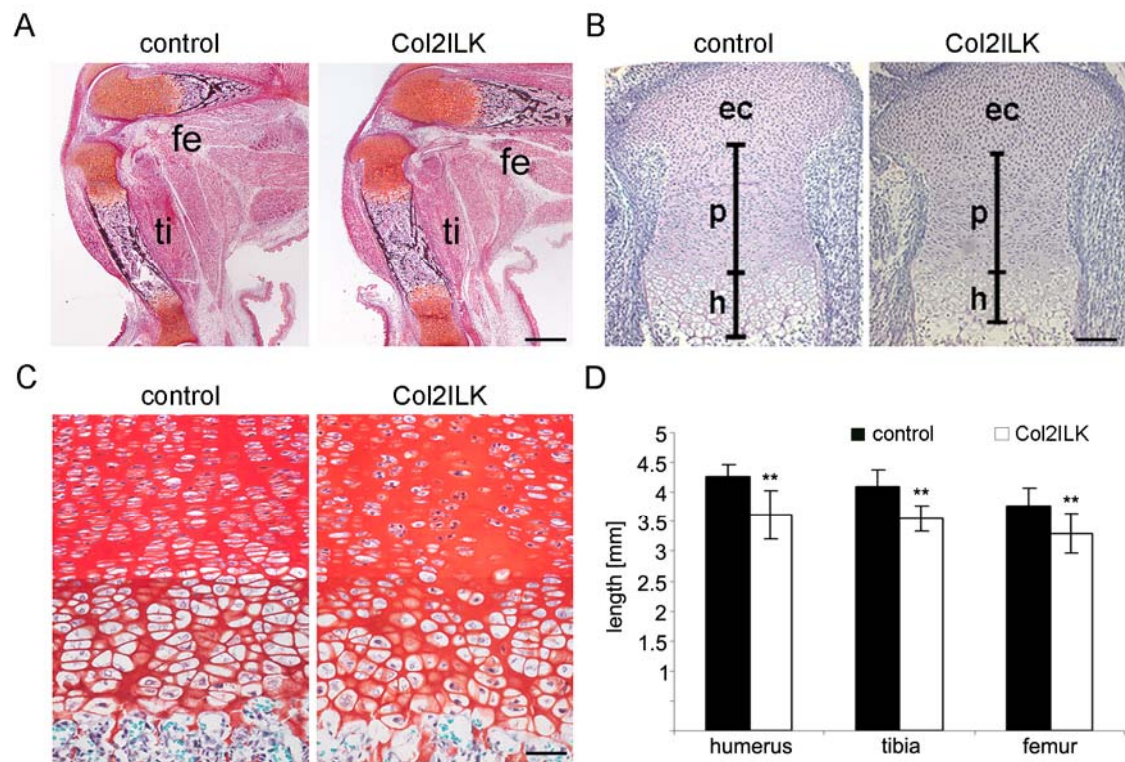


Fig 3.5. Skeletal analysis of Col2ILK mice. *A.* Safranin-orange/von-Kossa staining of tibia (ti) and femur (fe) at E17.5. Scale bar: 250 μ m. *B.* Hematoxylin/Eosin staining of tibial growth plates at E17.5. Scale bar: 100 μ m. ec: epiphyseal cartilage, p: proliferative zone, h: hypertrophic zone. *C.* Safranin-orange staining of growth plates of the proximal humerus from control and mutant newborn mice. Note, that Col2ILK chondrocytes are not as flattened as in the control cartilage and fail to form columnar stacks. Also note the reduced number of chondrocytes in the cartilage. Scale bar: 75 μ m. *D.* Quantification of the size reduction of long bones at newborn stage (** indicates $p < 0.01$ versus control, $n = 4$)

The altered shape of chondrocytes in the proliferative zone was confirmed by electron microscopy. Fig 3.6 shows the dramatically altered cell shape of chondrocytes in Col2ILK mice.

The organization of the fibrillar collagen network is dramatically affected in the absence of $\beta 1$ integrins (Aszodi et al. 2003). In Col2ILK mice the collagen organization in the resting zone as well as the proliferative zone in inter-territorial and peritorial matrix was normal (Fig 3.6B). In contrast to $\beta 1$ -deficient cartilage, no increased bi-nucleation of chondrocytes was

observed. These data indicate that ILK is not essential for integrin-mediated assembly of collagen fibrils and cytokinesis but indispensable for the regulation of the cell shape in the proliferative zone.

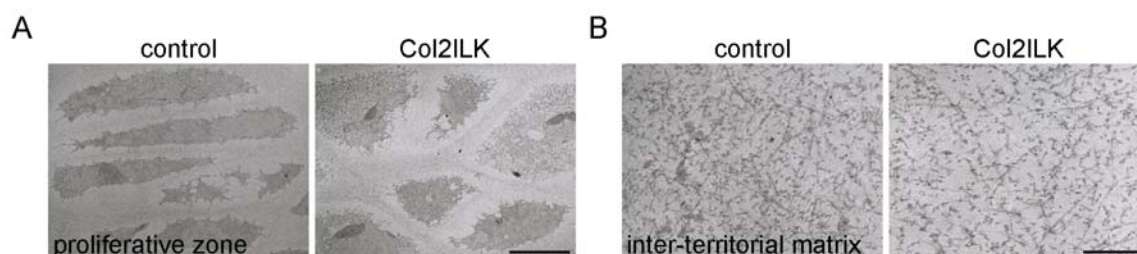


Fig 3.6. Ultrastructural analysis of newborn cartilage from control and Col2ILK mice. **A.** Electron micrographs from the proliferative zone of newborn tibiae. The formation of columnar structures is impaired in Col2ILK mice. No increased bi-nucleation was detected. Scale bar: 5 μ m. **B.** High magnifications of the inter-territorial matrix in newborn tibial growth plates. The fibrillar collagen network was found to be normal in Col2ILK mice. Scale bar: 400nm.

3.2.5. ILK is not required for chondrocyte maturation

To test the role of ILK during chondrocyte differentiation certain differentiation markers were visualized by *in-situ* hybridization. Expression of Ppr and Ihh mRNA was seen in the pre-hypertrophic zones in both control and Col2ILK mice indicating that differentiation of pre-hypertrophic chondrocytes could occur normally in the absence of ILK (Fig 3.7A,B).

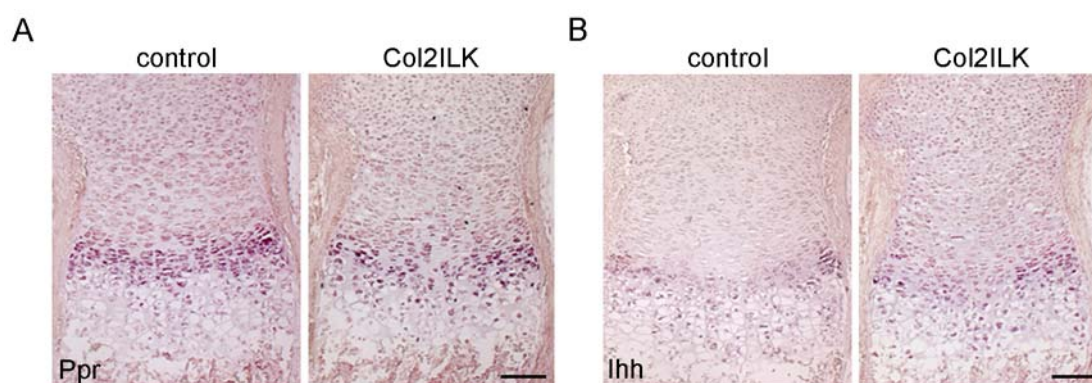


Fig 3.7. In situ hybridization analysis of chondrocyte differentiation markers. **A.** Non-radioactive *in situ* hybridization using an antisense complementary RNA probe against Ppr mRNA. Scale bar: 100 μ m. **B.** Non-radioactive *in situ* hybridization against Ihh mRNA. Sale bar: 100 μ m.

In addition immunostaining for several matrix proteins revealed no obvious differences between control and mutant mice. Matrilin-2 which is strongly expressed in the

perichondrium but only weakly in the cartilage (Mates et al. 2004) was normally distributed in mutant cartilage (Fig 3.8A). Aggrecan, a proteoglycan important for the formation of hydrated aggregates and therefore an important regulator of mechanical properties of the cartilage showed also a normal expression pattern in Col2ILK mice (Fig 3.8B). In agreement with the electron microscopy data collagen II deposition was not altered (Fig 3.8C). Collagen X showed the expected expression pattern along the pre-hypertrophic and the hypertrophic zones in both control and mutant cartilages (Fig 3.8D).

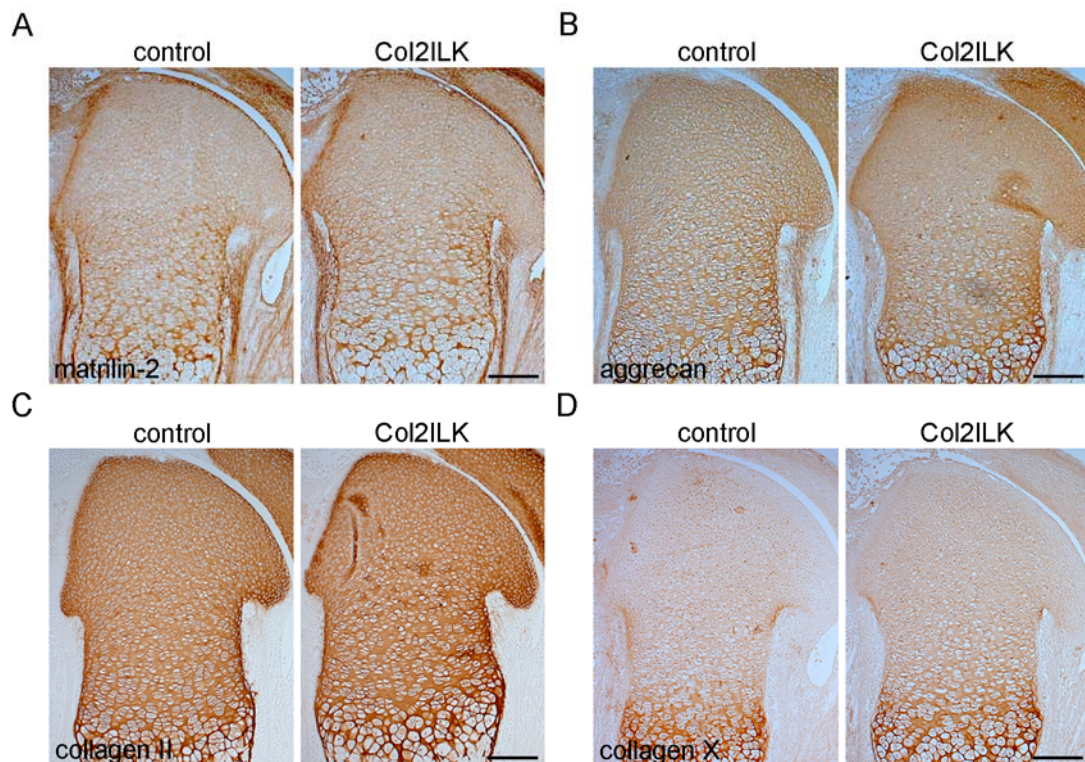


Fig 3.8. Normal ECM expression in Col2ILK cartilage from newborn mice. *A.* Matrilin-2 immunostaining shows a normal distribution along the perichondrium and more weakly in the cartilage. *B.* Aggrecan is present throughout the cartilage in Col2ILK mice. *C.* Collagen type II expression is unaltered in Col2ILK mice. *D.* Collagen type X expression is restricted to the pre-hypertrophic and hypertrophic zones in both control and mutant mice. Scale bars: 100µm.

Histochemical staining for alkaline phosphatase (AP: a marker for osteoblasts, Fig 3.9A) and tartrate-resistant acid-phosphatase (TRAP: a marker for osteoclasts, Fig 3.9B) revealed no differences between wild-type and Col2ILK cartilage.

All these data indicate that ILK is not essential for chondrocyte differentiation and expression or deposition of ECM proteins. These data also demonstrate that the dwarfism phenotype is not caused by an altered osteoblast or osteoclast activity.

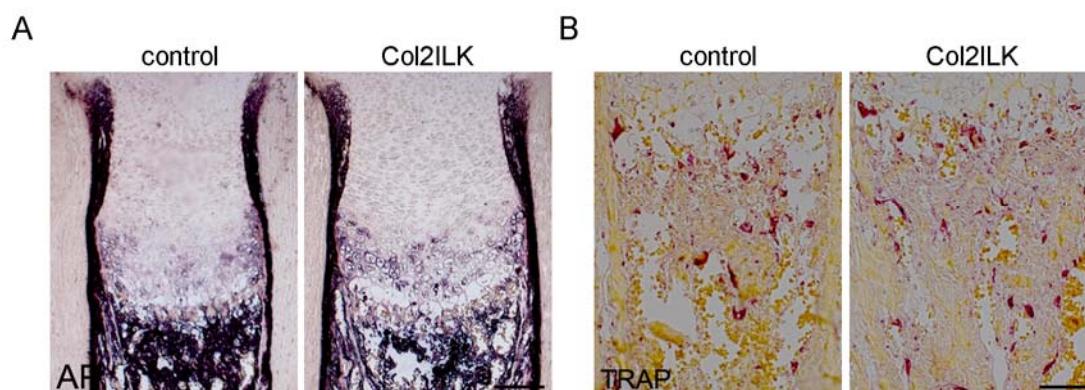


Fig 3.9. Normal osteoblast and osteoclast activity in Col2ILK cartilage. *A. AP staining of tibial sections from control and mutant newborn mice. Osteoblasts (dark blue) are normally distributed along the hypertrophic zones and in the perichondrium. B. TRAP staining of tibial sections from control and mutant newborn mice. Normal osteoclast activity (red) along the hypertrophic zone-bone interface. Scale bars: 100 μ m.*

3.2.6. ILK affects the G1-S transition of the chondrocyte cell cycle

Endochondral bone formation depends on chondrocyte proliferation, hypertrophy and subsequent apoptosis of hypertrophic chondrocytes (1.5.1). Since the number of chondrocytes in the proliferative zone was reduced (Fig 3.5C), the proliferation rate of chondrocytes in the cartilage was investigated. A BrdU incorporation assay, which specifically labels proliferating cells in the synthesis (S) phase of the cell cycle, showed a 29% reduction in BrdU-positive chondrocytes in Col2ILK growth plates (Fig 3.10A). The D-type cyclins have a crucial function in controlling G1 progression and entry into S phase. To test whether the reduced number of BrdU-positive cells is due to diminished cyclin expression, bone sections were stained with an antibody that detects all cyclin-D isoforms (D1, D2 and D3). As shown in Fig 3.10B, the number of cyclin-D-positive nuclei was reduced by 40% in Col2ILK growth plates, suggesting that loss of ILK affects the G1-S transition by regulating cyclin-D expression. Apoptosis, as determined by a TUNEL assay, was not increased in Col2ILK cartilage neither in the proliferative zone nor in the hypertrophic area (Fig 3.10C).

These data indicate that the reduced number of cells in the cartilage is caused by a decreased proliferation rate of chondrocytes in the proliferative zone and not by increased cell death.

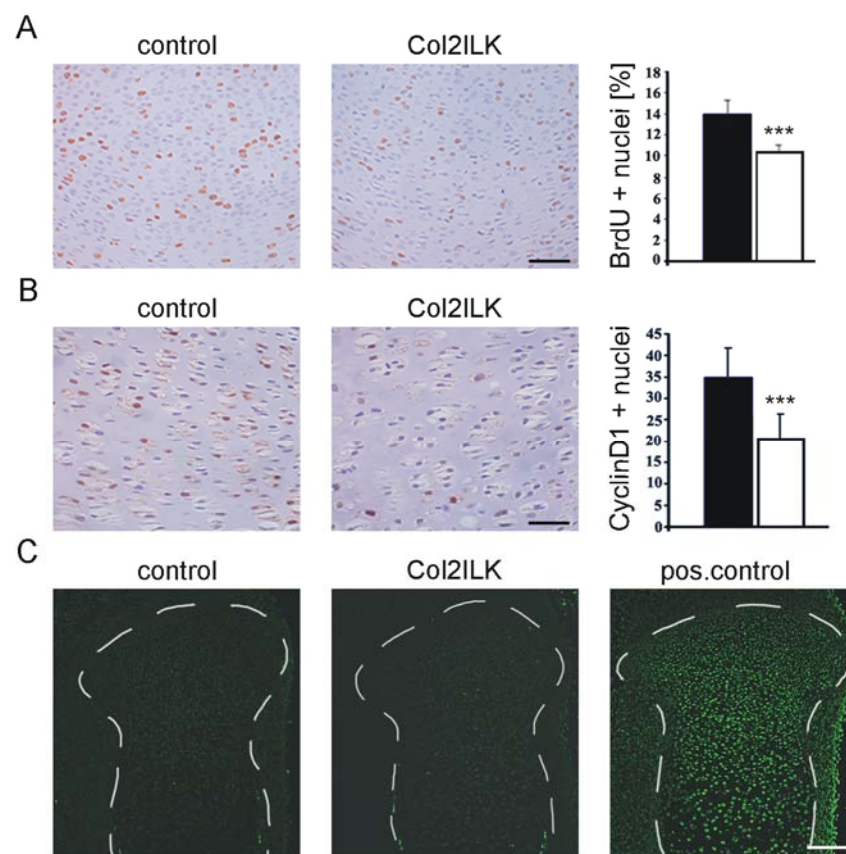


Fig 3.10. Reduced proliferation rates, decreased CyclinD1 expression but no increased apoptosis in Col2ILK cartilage at newborn stage. **A.** BrdU immunostaining of newborn tibial cartilage sections and quantification of BrdU positive cells in the growth plate. The proliferation rate especially in the proliferative zone of mutant cartilage is reduced. Scale bar: 75 μ m. **B.** CyclinD1 immunostaining of newborn tibial cartilage sections and quantification of cells with cyclinD1 positive nuclei. Col2ILK chondrocytes display reduced CyclinD1 expression and a reduced nuclear localization. Scale bar: 50 μ m. (***) indicates $p < 0.0001$. **C.** TUNEL staining of tibial sections at newborn stage demonstrated no increased apoptosis in Col2ILK cartilage. Scale bar: 100 μ m.

3.2.7. ILK modulates the actin cytoskeleton of chondrocytes *in vivo* and *in vitro*

Similar to $\beta 1$ -deficient chondrocytes, Col2ILK chondrocytes displayed an altered cell shape (Fig 3.5C and Fig 3.6A) and showed reduced proliferation rates *in vivo* (Fig 3.10A). Since loss of $\beta 1$ in the cartilage leads to alterations of the f-actin cytoskeleton which could account for differences in the cell shape and also affect cell proliferation, cartilage sections of control and Col2ILK mice were stained for f-actin. While control chondrocytes presented a strong cortical f-actin network, Col2ILK chondrocytes showed an uneven and punctuated f-actin distribution (Fig 3.11A).

To test the role of ILK during actin organization in more detail chondrocytes from control and mutant mice were isolated and analyzed in culture.

ILK-deficient primary chondrocytes displayed a strongly altered cell shape and failed to spread even after 24h of culture while control chondrocytes adhered and spread within the first hours after seeding (Fig 3.11B). F-actin immunostaining revealed a strongly altered cytoskeletal organization in Col2ILK chondrocytes. While control chondrocytes formed f-actin stress fibers that were extending throughout the cell, ILK-deficient chondrocytes did not form elongated stress fibers (Fig 3.11C). Immunostaining against FA proteins such as paxillin, $\beta 1$ integrin or FAK showed the formation of FAs in Col2ILK cells. However, in ILK-deficient chondrocytes FAs were small and their location was restricted to the cell periphery while control cells displayed in general larger FAs that were located also in the cell center (Fig 3.11D-F).

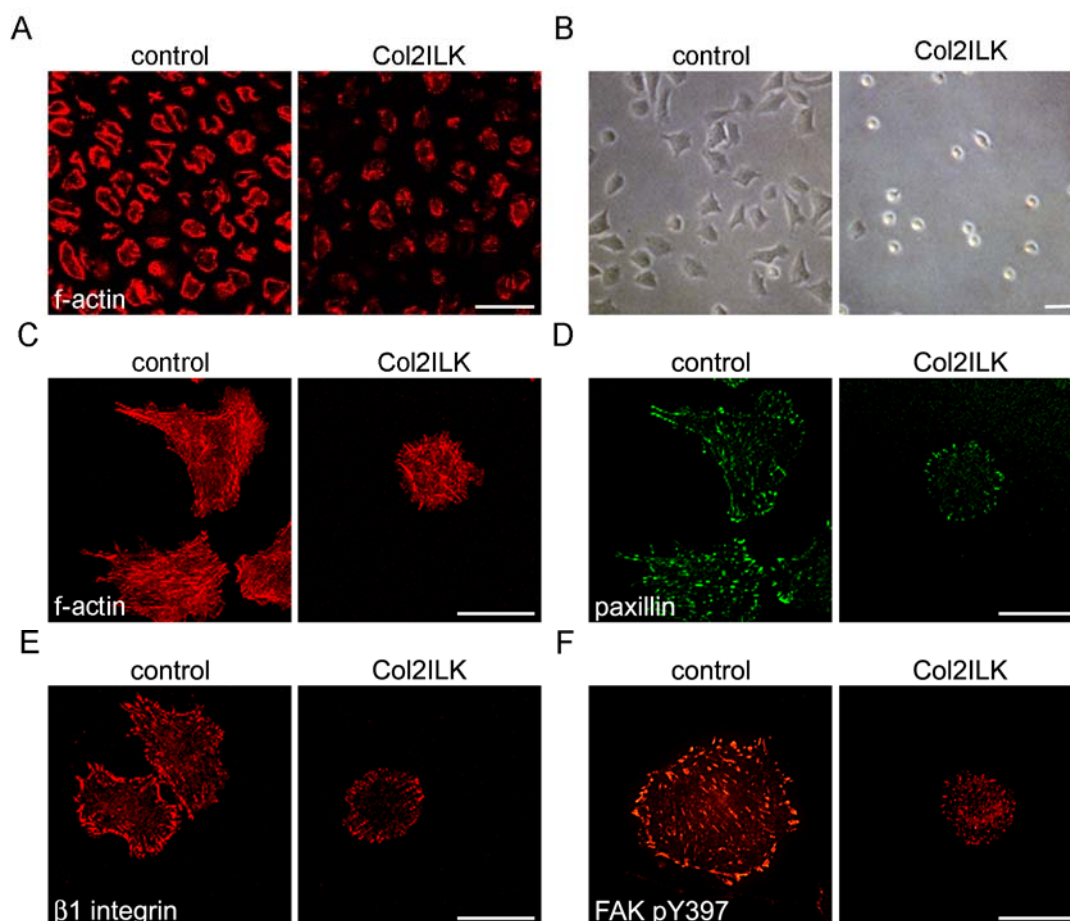


Fig 3.11. Loss of ILK leads to an impaired organization of the f-actin cytoskeleton in chondrocytes *in vivo* and *in vitro*. *A.* Confocal picture of an f-actin immunostaining of tibial sections from newborn cartilage. While control chondrocytes exhibit a strong cortical f-actin organization, ILK-deficient chondrocytes display a punctuated f-actin staining. Scale bar: 40 μ m. *B.* Phase contrast picture of freshly isolated primary chondrocytes after 24h in culture. ILK-deficient chondrocytes have a severe spreading defect. Scale bar: 40 μ m.

C. F-actin immunostaining of primary chondrocytes seeded on FN. D. Paxillin immunostaining of primary chondrocytes. E. β 1-integrin immunostaining of primary chondrocytes. F. Immunostaining of primary chondrocytes against the auto-phosphorylated form of FAK. Scale bars: 20 μ m.

3.2.8. ILK is essential for proliferation and adhesion of primary chondrocytes *in vitro*

To test whether primary chondrocytes would also proliferate less *in vitro*, a BrdU incorporation assay was performed over a time period of 7 days in the presence of growth factors. Similar to the situation *in vivo*, primary Col2ILK chondrocytes proliferated significantly less *in vitro* compared to control chondrocytes (Fig 3.12A). To test, if loss of ILK affects the adhesion of primary chondrocytes to ECM proteins, primary chondrocytes were seeded on FN, VN and collagen type I and allowed to attach for 45min. The adhesion of Col2ILK chondrocytes to FN and collagen type I was reduced by 30% and 32%, respectively, compared to controls (Fig 3.12B); adhesion to vitronectin was less but still significantly reduced (Fig 3.12B). These data show that ILK is essential for proliferation of chondrocytes *in vitro* and important for the normal adhesion of chondrocyte to ECM proteins.

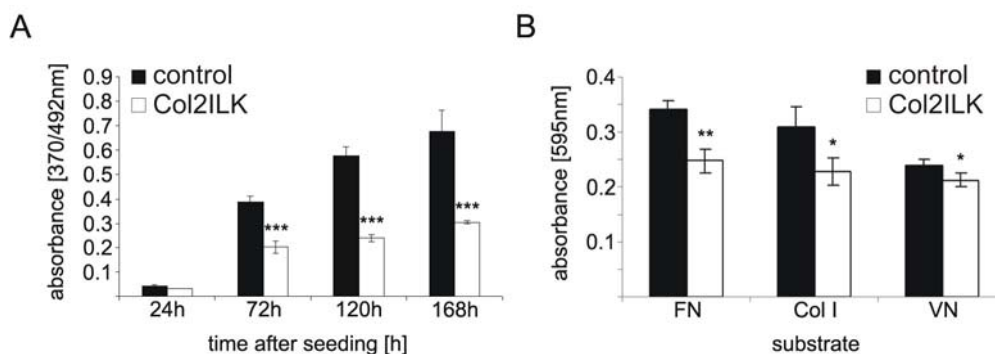


Fig 3.12. Reduced proliferation of Col2ILK chondrocytes and impaired adhesion to ECM proteins. A. Colorimetric quantification of a BrdU incorporation assay. Strongly reduced proliferation rate of ILK-deficient chondrocytes *in vitro*. (***) indicates $p < 0.0001$). B. Colorimetric quantification of cell-substrate adhesion assay. Loss of ILK leads to strongly reduced adhesion of chondrocytes to ECM proteins. (* indicates $p < 0.01$, ** indicates $p < 0.001$).

3.2.9. ILK is dispensable for the phosphorylation of PKB/AKT and GSK-3 β

Since ILK had been implicated in the phosphorylation of PKB/Akt and GSK-3 β , sections of control and mutant newborn mice were immunostained against the phosphorylated form of PKB/Akt (AKT-Ser473). Despite the reduced cell number, altered cell shape, and disorganized columnar structures in the proliferative zone of Col2ILK mice, both control and mutant chondrocytes displayed a robust phosphorylation level of PKB/Akt throughout the

cartilage (Fig 3.13A). Next, protein lysates of freshly isolated chondrocytes were probed for the phosphorylated forms of PKB/Akt (Thr308, Ser473) and GSK-3 β (Ser9/21). In both cases protein lysates from freshly isolated Col2ILK chondrocytes showed similarly high phosphorylation levels as controls (Fig 3.13B, C).

These data demonstrate that in chondrocytes ILK is dispensable as a kinase towards PKB/Akt or GSK-3 β suggesting that the observed phenotype is most likely caused by an altered cytoskeletal f-actin organization and not by modulation of PKB/Akt signalling pathways.

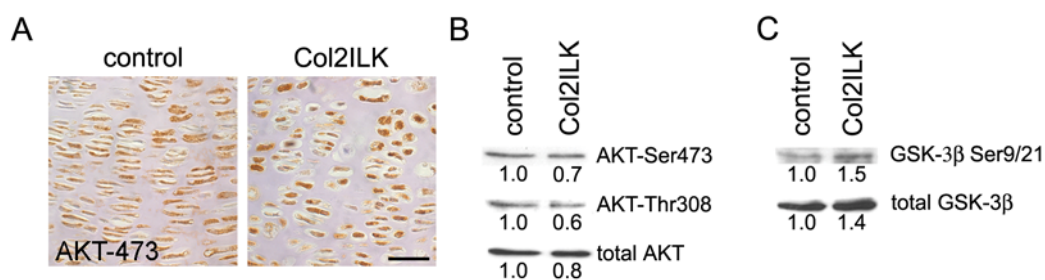


Fig 3.13. Normal phosphorylation levels of PKB/Akt and GSK-3 β in ILK-deficient chondrocytes. *A.* Immunostaining of AKT-Ser473 in the tibial growth plate of control and mutant mice at the newborn stage. Robust phosphorylation levels of PKB/Akt in ILK-deficient chondrocytes. Scale bar: 25 μ m. *B.* Western blot analysis of protein lysates from freshly isolated chondrocytes (including densitometric quantification) showing normal phosphorylation of PKB/Akt and GSK-3 β in ILK-deficient chondrocyte lysates.

3.3. Analysis of ILK function *in vivo*/characterization of keratinocyte-specific ILK knockout mice

3.3.1. Keratinocyte-specific deletion of the *ILK* gene

To delete the *ILK* gene specifically in keratinocytes, ILK flox mice were intercrossed with transgenic mice carrying the Cre-recombinase transgene under the control of a K5 promoter to obtain mice with the genotype ILK (flox/flox)/K5Cre⁺ (ILK-K5). Littermates heterozygous for the ILK flox allele and expressing the K5-cre transgene were used as controls (ILK Co). The deletion of the protein was analyzed by western blot analysis of epidermal protein lysates and immunostaining of back skin sections. While ILK protein levels were decreased but still detectable in the epidermis of newborn mice, the protein was completely absent from P2 epidermis and thereafter (Fig 3.14A). Immunostaining of back skin sections from 2w-old mice demonstrated the loss of ILK from the epidermis, ORS cells and hair matrix, while it was still present in the dermal papilla (Fig 3.14B).

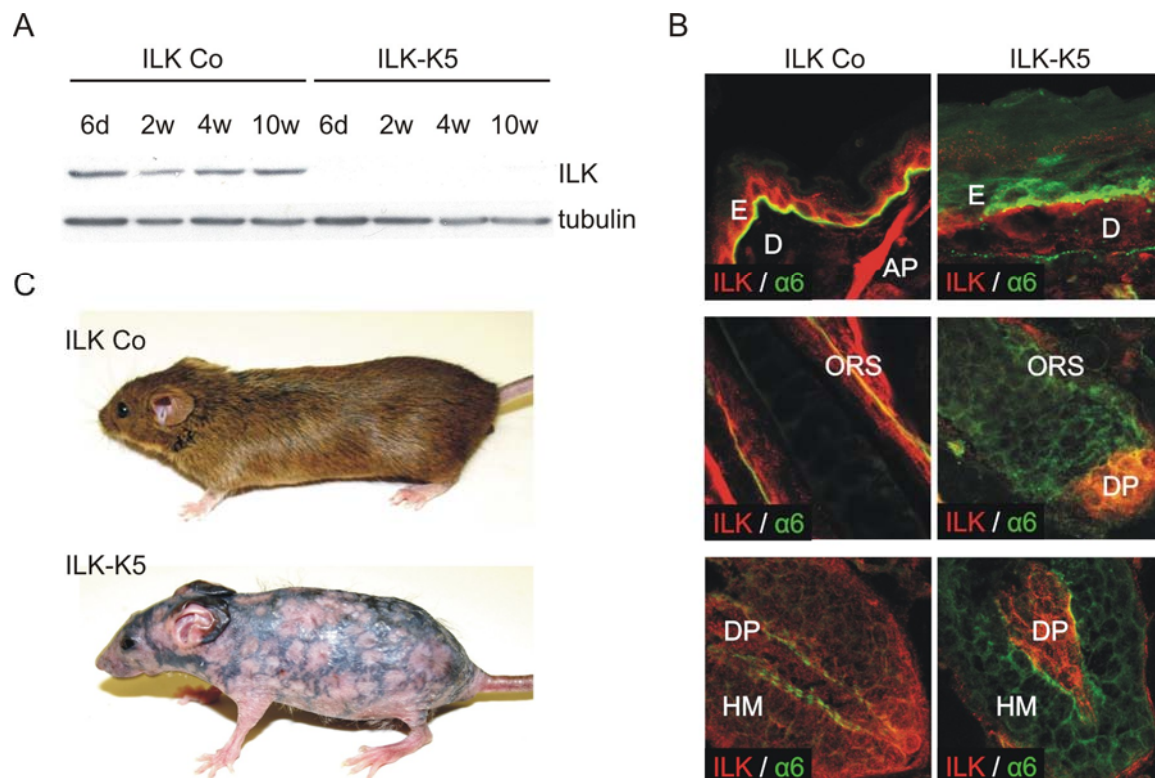


Fig 3.14. Efficient deletion of ILK in the epidermis. *A.* Western blot analysis of epidermal protein lysates from 6d-, 2w-, 4w- and 10w-old mice. *B.* Immunostaining of back skin sections from 2w-old control and ILK-K5 mice. ILK is absent from the epidermis (E) but still detectable in the dermis (D) or the arrector pili muscle (AP). ILK expression is lost in outer root sheet (ORS) cells but not in the dermal papilla (DP). *C.* Control and ILK-K5 mice

at an age of 4w. Deletion of ILK leads to progressive hair loss and reticular pigmentation of the skin. Immunostaining was done by Michal Grzejszczyk and Katrin Lorenz. Pictures in C. were taken by Dr. Takao Sakai.

At birth ILK-K5 mice were indistinguishable from control littermates. After 1-2 weeks when control animals developed a dense hair coat, ILK-K5 mice displayed only scattered hair with partial alopecia. By 4 weeks of age ILK-K5 mice had lost almost all hair and displayed reticular skin pigmentation (Fig 3.14C). However, ILK-K5 mice were of normal size and had a normal life span.

3.3.2. ILK-K5 mice display severe epidermal and HF abnormalities

The epidermis of ILK-K5 mice was normal until P2 but became progressively hyperplastic (Fig 3.15A). While basal keratinocytes were polarized and firmly attached to the BM in control mice they appeared flattened in ILK-K5 mice and frequently detached from the underlying BM (Fig 3.15B). This skin blistering became more severe with age.

In addition to these epidermal defects, loss of ILK severely impaired the development of HFs (Fig 3.15A, C), which diverged into two subpopulations in ILK-K5 mice. At P14 around 66% of the HFs were arrested in their development and showed no hair shaft formation, a misshapen hair matrix and DP (Fig 3.15A, C; ■). About 33% of the HFs were able to complete HF morphogenesis, but were shorter and characterized by a substantial hyperplasia of the ORS (Fig 3.15A, C; ▲). A plausible explanation for the two HF populations is likely the combination of asynchronous HF morphogenesis and the perinatal deletion of the ILK protein. While fully developed HFs might have lost ILK late during morphogenesis, early arrested HFs lost ILK most likely at earlier developmental stages.

No further hair cycle was induced in ILK-K5 mice as demonstrated by histological analysis of back skin section from P28-old mice. By 10w of age all HFs of ILK-K5 mice were resorbed and the melanin deposits gave rise to the reticular skin pigmentation. These data show that ILK is essential for epidermal integrity and HF morphogenesis.

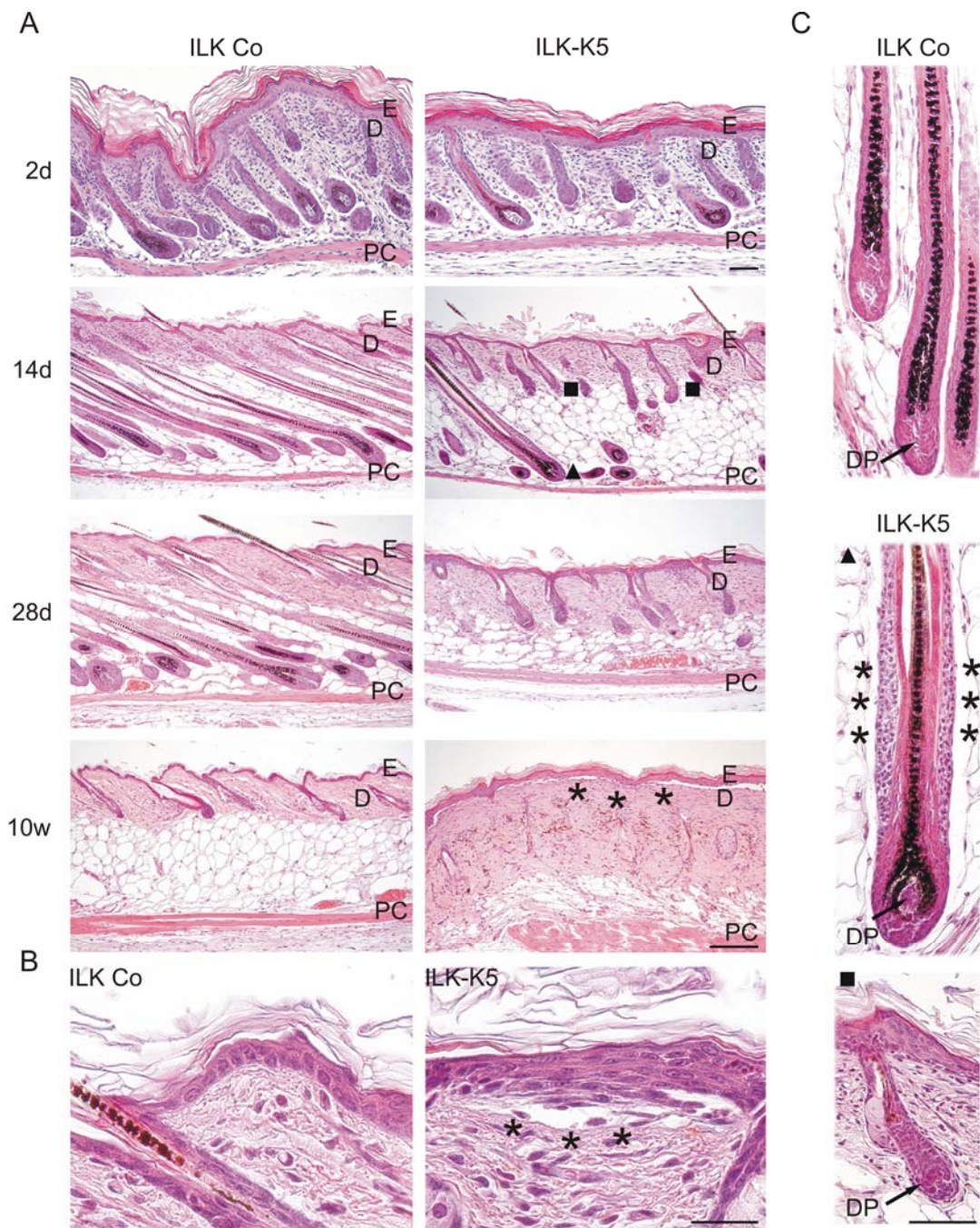


Fig 3.15. Histological analysis of control and ILK-K5 back skin sections. *A.* Hematoxylin/Eosin staining of back skin sections from control and ILK-K5 mice. Loss of ILK leads to skin blistering and the development of two HF populations (■ arrested HFs, ▲ developed HFs). At later stages HFs are completely lost in ILK-K5 mice. D: dermis, E: epidermis, PC: panniculus carnosum. Scale bar: 100µm. *B.* Hematoxylin/Eosin staining of back skin sections from control and ILK-K5 mice at P14. Loss of ILK leads to epidermal detachment (*) from the underlying dermis. *C.* High magnification of HFs from control and ILK-K5 back skin sections at P9. Developed HFs (▲) display a multilayered ORS (*). Scale bar: 50µm. Histology and immunostaining was performed by Michal Grzejszczyk and Katrin Lorenz.

3.3.3. Loss of ILK impairs integrin expression and BM integrity

The detachment of ILK-K5 epidermis from the underlying dermis (Fig 3.15B) indicated an impaired integrin-BM interaction in ILK-deficient keratinocytes. To address this point, back skin sections from 2w-old mice were analyzed by immunostaining for $\beta 1$ and $\beta 4$ integrins as well as the BM marker laminin332. While in control mice $\beta 1$ and $\beta 4$ integrins were expressed exclusively in basal keratinocytes and enriched along the dermal-epidermal junction, these integrin subunits were localized basally but also frequently found on suprabasal keratinocytes (Fig 3.16A) in ILK knockout mice. In addition the BM was severely distorted in ILK-K5 mice. While control skin displayed a linear laminin332 staining along the dermal-epidermal junction, ILK-K5 skin showed an irregular laminin332 staining and areas of massive laminin diffusion into the dermis (Fig 3.16B). These BM defects were confirmed by ultrastructural analyses (in collaboration with Dr. Wilhelm Bloch, University of Cologne) which, however, also revealed that hemidesmosomes could form in ILK-K5 epidermis (Fig 3.16C). Double immunostaining for the BM marker nidogen and phalloidin revealed that in control epidermis f-actin is restricted to the apical and lateral plasma membrane, whereas in ILK-K5 mice f-actin was also present at the basal side facing the BM (Fig 3.16D).

Therefore it can be concluded that loss of ILK is essential for the integrity of the epidermal BM as well as the polarization of the f-actin cytoskeleton in basal keratinocytes.

3.3.4. ILK is not required for keratinocyte proliferation

$\beta 1$ integrin expression is thought to determine the proliferation potential of keratinocytes (Carroll et al. 1995; Jones et al. 1995) and deletion of $\beta 1$ integrins in basal keratinocytes indeed diminishes keratinocyte proliferation *in vivo* (Brakebusch et al. 2000). To test whether ILK is essential for the proliferation of keratinocytes, histological sections were analyzed by Ki67 immunostaining. While no significant differences in the proliferation of basal keratinocytes were observed, we detected a significant number of proliferating cells in suprabasal cell layers (Fig 3.16E). Double immunostaining of integrins and proliferation markers revealed that these suprabasal cells were those cells which still expressed $\beta 1$ and $\beta 4$ integrins (Fig 3.16A, B). These data indicate that the ectopic location of basal keratinocytes most likely caused by an impaired adhesion to the BM contributes to the epidermal thickening. More importantly, these data show that ILK is not required for $\beta 1$ integrins to induce proliferation.

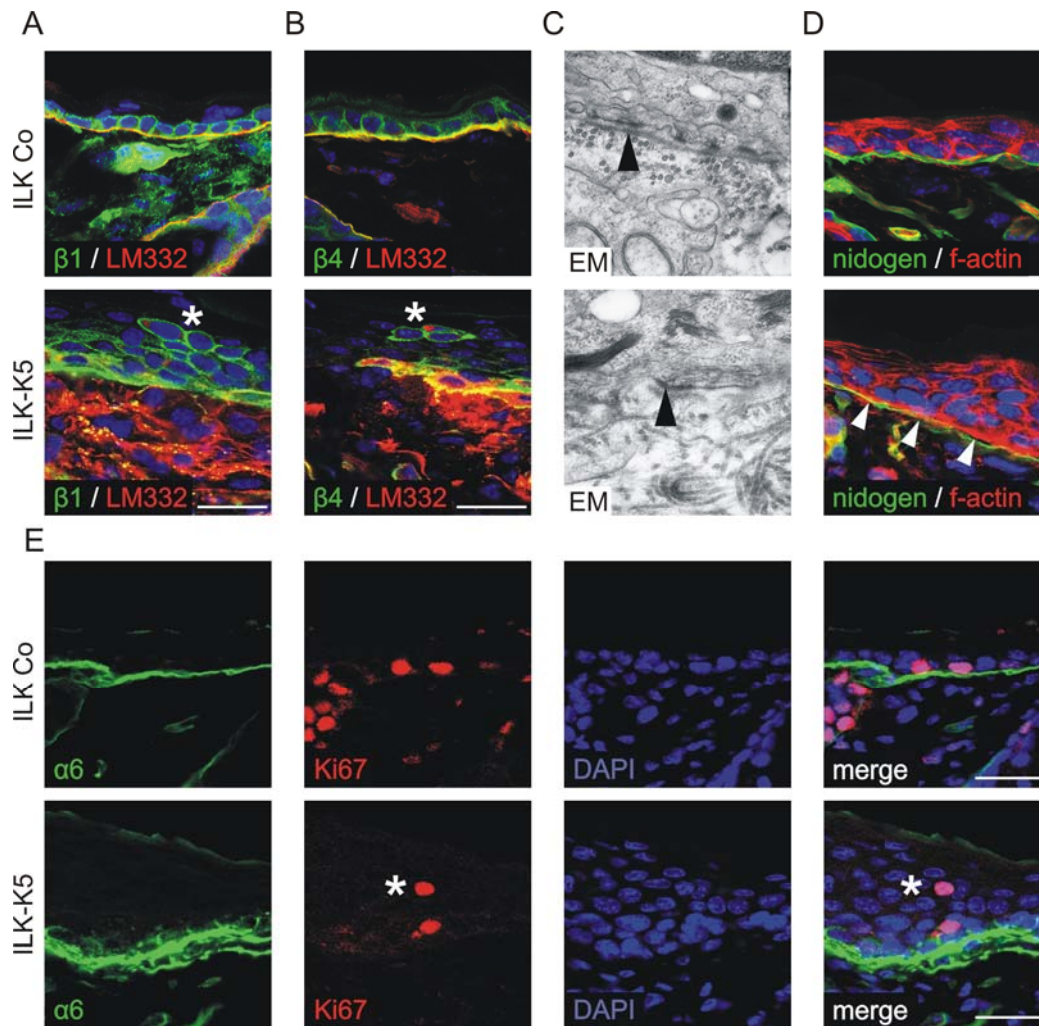


Fig 3.16. Suprabasal integrin expression and impaired BM integrity in the absence of ILK. *A.* Immunostaining of back skin sections from 2w-old mice. $\beta 1$ integrin was frequently localized on suprabasal keratinocytes (*). Laminin332 staining was irregular and indicated massive diffusion of laminin into the dermis. *B.* $\beta 4$ integrin was frequently localized around suprabasal cells. *C.* Electron micrographs of back skin section from 2w-old mice showing the impaired BM structure in ILK-K5 skin. Hemidesmosomes can form in the absence of ILK (arrowhead) *D.* Immunostaining of back skin sections from 2w-old mice immunostained for nidogen and f-actin. F-actin was mislocalized to basal sides in ILK-K5 epidermis (see arrowheads). *E.* Proliferating suprabasal cells were frequently detected in the hyperthickened epidermis of ILK-K5 mice (*). Immunostaining for A, B and D were done by Michal Grzeszczyk and Katrin Lorenz. Electron microscopy was performed by Dr. Wilhelm Bloch (University of Cologne). Scale bar: 25 μ m.

3.3.5. Accumulation of proliferating cells in the ORS of ILK-deficient HFs

Deletion of $\beta 1$ integrin in the epidermis leads to reduced proliferation of epidermal keratinocytes but also hair matrix cells (Brakebusch et al. 2000). To investigate whether altered proliferation is the reason for impaired HF morphogenesis, back skin section of control and ILK-K5 mice at P7 and P14 were stained for the proliferation marker Ki67 or

mice were subjected to BrdU incorporation assays. KI67 immunostaining revealed the presence of an increased number of proliferating cells in the ORS of both developed and growth arrested mutant HF (Fig 3.17A). Quantification of BrdU-positive cells in P7 and P14 HF confirmed this observation. While at P7 the number of proliferating ORS cells was only slightly increased in mutant HF, this difference became more obvious at P14 (Fig 3.17B). Interestingly, at the same time the number of BrdU-positive cells was decreasing in the hair matrix (HM) of ILK-K5 HF (Fig 3.17C) leading to a reduced total number of HM cells (Fig 3.17D). These data suggested that defective morphogenesis of ILK-K5 HF is not caused by reduced proliferation but rather by an impaired downward migration of ORS cells to the hair matrix.

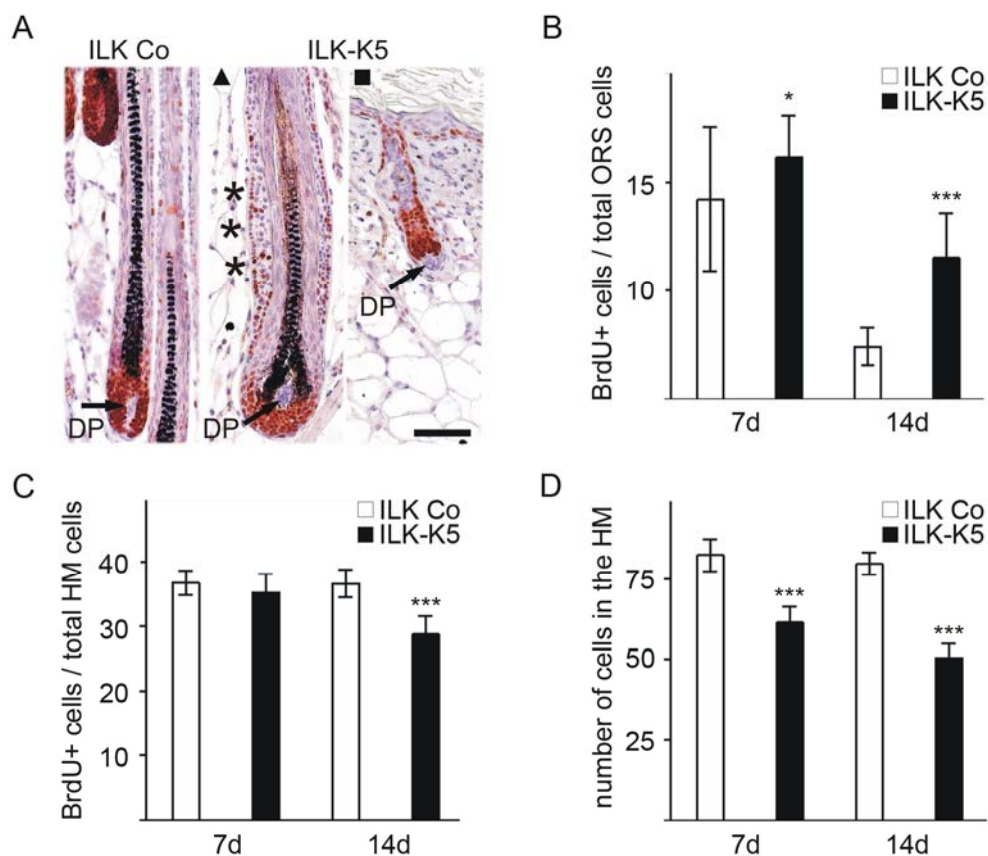


Fig 3.17. ILK-deficient HF accumulate proliferating cells in the ORS. *A.* Ki67 immunostaining of control and mutant HF at P7. Note the accumulation of proliferating cells along the ORS of mutant HF (*). Scale bar: 50 μ m. *B.* Increased number of BrdU-positive cells in the ORS of ILK-K5 HF. *C.* Reduced number of BrdU-positive cells in the HM of ILK-K5 HF. *D.* The total number of cells in the HM is reduced in ILK-K5 HF. Immunostaining was done by Michal Grzejszczyk and Katrin Lorenz.

3.3.6. ILK is essential for directional cell migration

To test the hypothesis that loss of ILK impairs the migration of ORS cells along the BM that lines the HF, primary keratinocytes were isolated from control and ILK-K5 mice and analyzed *in vitro*. Time-lapse microscopy revealed that ILK-deficient keratinocytes are not able to migrate in a persistent manner. Control cells usually formed broad and stable lamellipodia, which allowed single cells to directionally migrate. In contrast, ILK-deficient keratinocytes formed highly unstable lamellipodia which were frequently collapsing. New lamellipodia formed at different locations simultaneously leading to frequent changes of migration direction and hence prohibited a persistent cell migration (Fig 3.18).

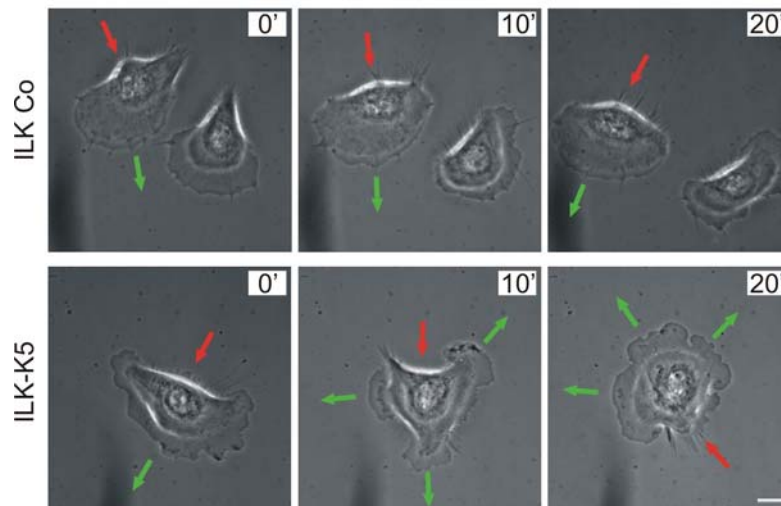


Fig 3.18. ILK is essential for directional migration of keratinocytes. Keratinocytes from control and mutant mice were seeded on a FN/ColII matrix and analyzed by time-lapse microscopy. Control cells were able to perform directional migration, while ILK-K5 cells frequently changed their direction due to highly instable lamellipodia. (Red arrows indicate the retracting area of the cells. Green arrows indicate areas of protrusive activity). Scale bars: 10 μ m. Isolation of keratinocytes was done by Katrin Lorenz.

3.3.7. Loss of ILK is essential for stress fiber formation and establishment of mature FAs in keratinocytes

To test, if the reduced stability of lamellipodia is caused by impaired FC and FA formation which impairs the fixation of this structure to the substrate, primary keratinocytes were analyzed by immunostainings. Visualization of the f-actin cytoskeleton by phalloidin staining and of FAs by FAK immunostaining revealed that ILK-deficient keratinocytes were not able to assemble strong bundles of f-actin (Fig 3.19A). Moreover, the formation of FAs was significantly impaired. Biochemical analysis of protein lysates from adherent control and

mutant keratinocytes revealed a reduced activation of FAK in the absence of ILK (Fig 3.19B) which is in line with the reduced number of FAs in ILK-K5 keratinocytes. To check whether reduced activation of Rac1 contributes to the migration defect of ILK-K5 keratinocytes (Fig 3.18), primary cells were subjected to Rac1 pulldown assays during cell adhesion (Fig 3.19C) or after growth factor stimulation (Fig 3.19D). Interestingly, no significant differences in Rac1 activation levels could be detected.

These data indicate that the reduced migration of ILK-deficient keratinocytes is mainly caused by impaired cell adhesion due to defective FA formation and maturation as well as a disturbed formation of the f-actin cytoskeleton.

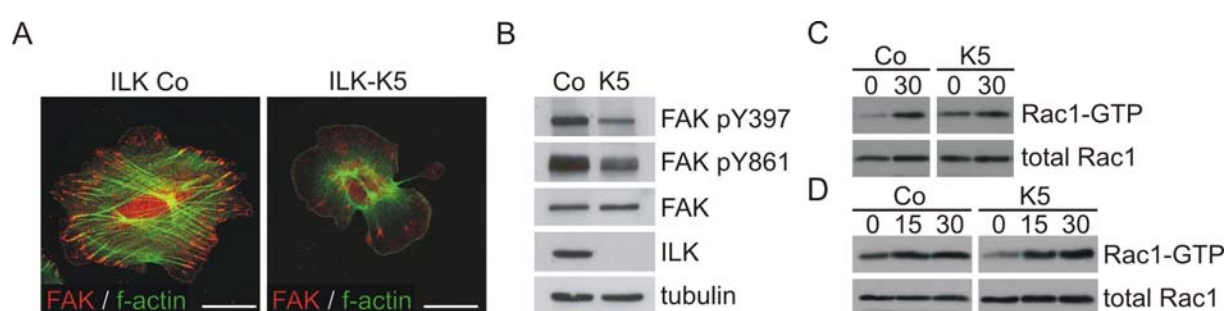


Fig 3.19. Loss of ILK leads to impaired stress fiber formation and FA assembly in keratinocytes. *A.* Immunostaining of control and ILK-K5 primary keratinocytes revealed that loss of ILK impaired FA and stress fiber formation. Moreover most of the ILK-K5 keratinocytes were much smaller. Scale bar: 10 μ m in ILK Co and 20 μ m in ILK-K5. *B.* Biochemical analysis of protein lysates from primary keratinocytes showed reduced activation levels of FAK in ILK-K5 keratinocytes. *C.* Western blot analysis of Rac1 pulldown assays revealed no significant differences in Rac1 activation in control and ILK-K5 primary keratinocytes in suspension (0) or 30min after cell adhesion to a laminin-rich matrix. *D.* Western blot analysis of a Rac1 pulldown assay showing no significant differences after growth factor-induced Rac1 activation in control and ILK-K5 primary keratinocytes. Cells were stimulated for 15min and 30min with 8% FCS. Immunostaining in *A* was done by Katrin Lorenz and Dr. Robert Torka.

3.4. Analysis of ILK function *in vitro*/Characterization of ILK knockout fibroblasts

3.4.1. Generation of immortalized ILK knockout fibroblasts

In order to analyze the importance of ILK during the remodelling of the actin cytoskeleton ILK fibroblasts were generated (Sakai et al. 2003). Cells were isolated from the kidney of an adult ILK (flox/flox) mouse, immortalized by adenoviral transduction of the SV40 large T antigen and several clonal cell lines were established (termed ILK (f/f) hereafter). Subsequently, ILK was deleted by transient adenoviral mediated expression of the Cre-recombinase and clonal knockout cell lines were established, (termed ILK (-/-) hereafter). The establishment of these cell lines was done by Drs. Reinhard Fässler and Takao Sakai (for details see Sakai et al. 2003).

3.4.2. Consequences of ILK deletion in fibroblasts

To confirm loss of ILK protein expression ILK (f/f) and ILK (-/-) cell lines were biochemically analyzed. Western blot analyses of fibroblast cell lysates showed that ILK was absent in the knockout cells while control cells showed robust expression levels of ILK. Known interaction partners of ILK such as Pinch1, α - and β -parvin, paxillin, migfilin and Mig2a/Kindlin-2 were highly expressed in control cells. Pinch2 and γ -parvin, also known to interact with ILK, were not detectable by western blotting. Interestingly, ILK (-/-) fibroblasts showed in addition to the loss of ILK strongly decreased expression levels of Pinch1, α - and β -parvin while the levels of other interaction partners such as paxillin, β 1 integrin, migfilin or Mig2a/Kindlin-2 were unchanged (Fig 3.20A).

To confirm that the observed loss of Pinch1, as well as α - and β -parvin was a direct result of ILK deletion and not an unspecific artefact for example due to cloning, ILK (-/-) cells were infected with a retrovirus carrying an ILK-EGFP controlled by a CMV promoter. Single clones stably expressing ILK-EGFP were generated and analyzed biochemically. Fig 3.20B shows that re-expression of ILK-EGFP in ILK (-/-) fibroblasts fully rescued Pinch1 and parvin expression levels, indicating that the stability of Pinch1 and parvin directly depends on ILK.

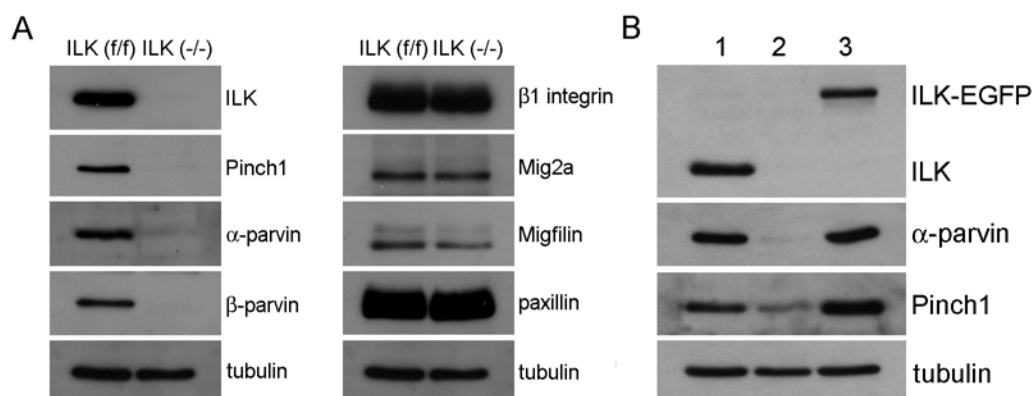


Fig 3.20. Biochemical characterization of ILK (f/f) and ILK (-/-) fibroblast cell lines. *A.* Western blot analysis of protein lysates from ILK (f/f) and ILK (-/-) fibroblasts. Loss of ILK is evident in lysates from ILK (-/-) fibroblasts. Note the reduced levels of Pinch1, α- and β-parvin. *B.* Western blot analysis of protein lysates from ILK (f/f) (lane1), ILK (-/-) (lane2) and ILK (-/-) ILK-EGFP fibroblasts (lane3). Loss of Pinch1 and parvins could be rescued by re-expression of ILK-EGFP.

Similar to ILK-deficient chondrocytes, ILK (-/-) fibroblasts displayed a strong proliferation defect (Fig 3.21). Interestingly, this proliferation defect was especially evident in early passages (passage p1-p15) while later passages (p>15) demonstrated only slightly reduced proliferation rates indicating that ILK (-/-) fibroblasts develop compensatory mechanisms that could overcome the proliferation defect. Since the exact processes responsible for this effect were not known, only cells with low passage numbers (p<15) were used in this study.

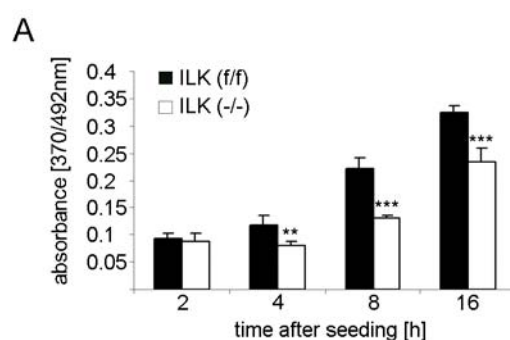


Fig 3.21. Reduced proliferation rate of ILK (-/-) fibroblasts. Colorimetric quantification of a BrdU incorporation assay over a time period of 16h in growth factor containing medium. ILK (-/-) fibroblasts displayed strongly reduced proliferation rates that were especially evident in early passages (** indicates $p<0.01$, *** $p<0,0001$ versus control).

3.4.3. Presence of Pinch1 in FA of ILK (-/-) fibroblasts

The interdependency of ILK, Pinch1 and α-parvin in respect to protein stability has been described before by Wu and colleagues who showed that depletion of Pinch1 from HeLa cells strongly reduced levels of ILK and α-parvin, which was partially reversed by inhibition of the proteasome (Fukuda et al., 2003). Moreover the same group showed that ILK, Pinch1 and α-

parvin form a ternary complex in the cytoplasm which is essential for targeting each protein to FAs (Zhang et al., 2002). If true, loss of ILK should result in a complete loss of Pinch1 from FAs. Interestingly, Pinch1 was not fully degraded in ILK (-/-) cells (Fig 3.20B). The presence of low Pinch1 levels allowed to test by immunostaining with a polyclonal Pinch1 antibody whether it could still localize into FAs of ILK (-/-) cells. In control cells, Pinch1 strongly localized together with other FA markers such as paxillin in FAs (Fig 3.22A). In ILK (-/-) fibroblasts, Pinch1 was almost undetectable due to the strongly reduced protein level. In overnight cultures a fraction of cells contained clear immunosignal of Pinch1 in FAs (Fig 3.22B). These data show for the first time that Pinch1 can be recruited into FAs in the absence of ILK. This has been confirmed in Pinch1 (-/-) murine embryonic fibroblasts where small amounts of ILK were also found in FAs (Stanchi et al., 2006). Nevertheless, the dramatic reduction of Pinch1 expression levels and the very inefficient FA targeting of Pinch1 in ILK (-/-) fibroblasts corroborate the notion that the assembly of the ILK/Pinch/parvin complex is essential for the proper function of the individual proteins.

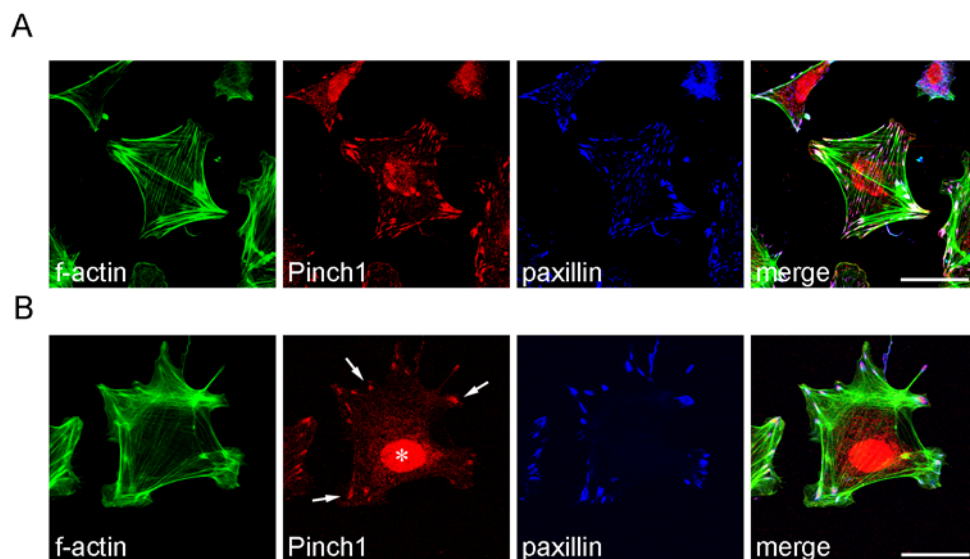


Fig 3.22. Pinch1 localization into FAs of ILK (-/-) fibroblasts. *A.* Confocal image showing the f-actin cytoskeletal network and the Pinch1 localization into FAs in ILK (f/f) fibroblasts. FAs are visualized by paxillin co-staining. *B.* Confocal image showing f-actin cytoskeletal network in a large ILK (-/-) fibroblast and the Pinch1 localization into FAs (indicated by arrows). Nuclear Pinch1 staining (as indicated by *) was found to be largely unspecific, as it is also prominent in Pinch1 (-/-) cells. Scale bars: 20 μ m.

3.4.4. The role of ILK during actin dynamics

To understand the role of ILK during integrin-dependent actin reorganizations, two experiments were established. First, cells were taken into suspension and monitored during

cell spreading on ECM proteins (3.4.5). Second, starved cells were seeded on ECM proteins and stimulated with growth factors (3.4.8). Both experiments are known to induce rapid actin reorganizations.

3.4.5. ILK is essential for actin reorganization during cell spreading

In order to analyze the role of ILK during cell spreading ILK (f/f) and ILK (-/-) fibroblasts were taken into suspension and subsequently seeded on FN. Cells were fixed 20min, 40min and 60min thereafter and the organization of the actin cytoskeleton and FAs were analyzed by immunostaining. After 20min of cell spreading control cells showed a cortical organization of the actin cytoskeleton. At the cell periphery FAs had formed that were positive for the auto-phosphorylated form of FAK indicating the maturation of FCs into FAs (Fig 3.23A). ILK-deficient fibroblasts were smaller and displayed a more diffuse actin cytoskeleton. FAs were present at the periphery of the cell but most of the cells did not show significant FAK phosphorylation at this time point (Fig 3.23A).

After 40min of cell spreading most of the control fibroblasts were polygonal, showed strong bundles of stress fibers at the edge and thin stress fibers in the center of the cell. Most of these actin fibers were anchored to large FAs that were mostly concentrated at the cell borders (Fig 3.23B). In sharp contrast, most of the ILK (-/-) fibroblasts were still round and presented a rather diffuse actin cytoskeleton. FAs were still very small and primarily located at the cell periphery. However, most of the FAs were positive for auto-phosphorylated FAK (Fig 3.23B).

At 60min of cell spreading control cells had developed a robust stress fibers system that was connected to large FAs at the cell edges and smaller FAs in the center of the cell (Fig 3.23C). Fully spread ILK (-/-) fibroblasts only showed a poorly developed stress fiber system. Larger FAs could form but were almost exclusively located at the cell periphery (Fig 3.23C). This phenotype was present on all ECM proteins tested such as FN, VN or a laminin-rich matrix and still evident after overnight culture. However, although the f-actin cytoskeleton was dramatically different between control and knockout cells, the overall ratio of G-actin to F-actin was not affected by the loss of ILK (Fig 3.24).

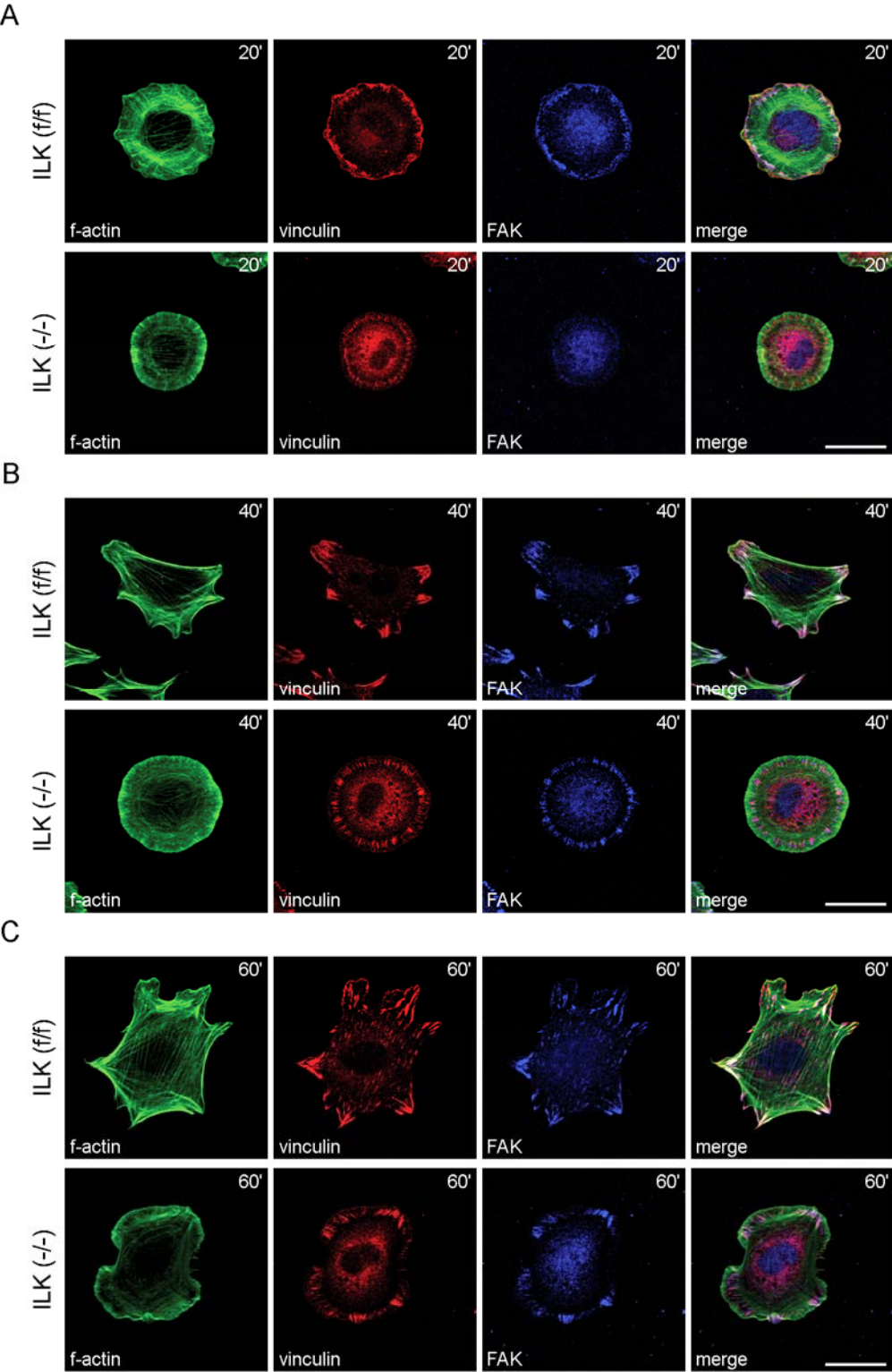


Fig 3.23. Spreading defect of ILK (-/-) fibroblasts. *A.* Confocal pictures of triple immunostainings of ILK (f/f) and ILK (-/-) fibroblasts 20min after cells were seeded on FN-coated LabTek chamber slides. F-actin is shown in green, vinculin in red and FAK in blue. Scale bar: 20μm. *B.* Confocal images of triple immunostainings of ILK (f/f) and ILK (-/-) fibroblasts 40min after cells were seeded on FN. Scale bar: 20μm. *C.* Confocal images of triple immunostainings of ILK (f/f) and ILK (-/-) fibroblasts 60min after cells were seeded on FN. Scale bar: 20μm.

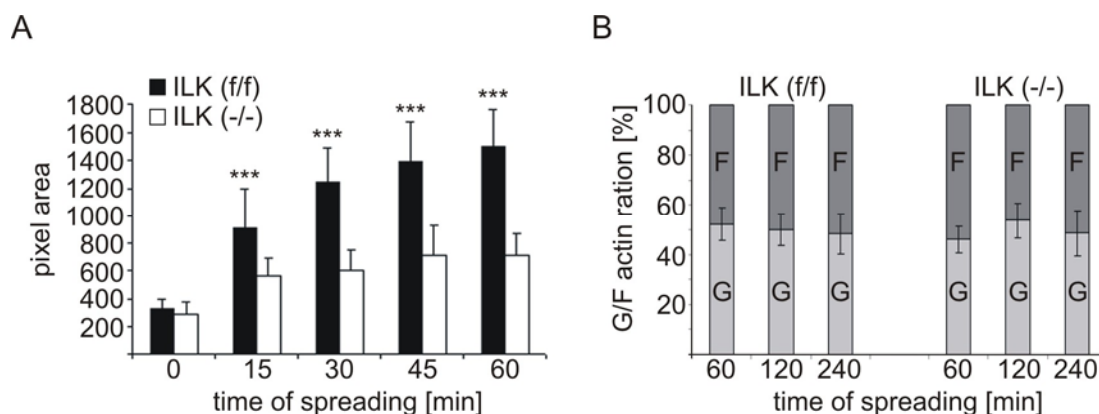


Fig 3.24. Spreading statistic. *A.* ILK (-/-) fibroblasts displayed a reduced cell area during the spreading on FN compared to control cells. *B.* No obvious differences in the G/F-actin ratios of control and ILK (-/-) fibroblasts were detected 60min, 120min and 240min after adhesion to FN.

3.4.6. ILK regulates cell spreading independently of its kinase activity

To confirm that the observed phenotype was exclusively dependent on ILK, a full length ILK that was C-terminally tagged with an EGFP was stably expressed in ILK (-/-) fibroblasts (Fig 3.20B). Cells expressing an amount of ILK that was comparable to wt-levels showed a rescued spreading phenotype, developed a robust stress fiber network and presented large FA throughout the cell (Fig 3.25A). Moreover, the proliferation defect was fully rescued by re-expression of ILK-EGFP (Sakai et al. 2003). ILK that carries a mutation within the kinase domain (E359K) completely rescued the spreading defect (Sakai et al., 2003), indicating that the kinase activity of ILK is dispensable for the regulation of the actin cytoskeleton. It was, however, unclear if the E359K mutation leads to a complete loss of ILK kinase activity. To further analyze this, additional mutations in the C-terminal domain of ILK (described as kinase-dead mutants) were tested. In addition, a double point mutation in the paxillin binding site domain of ILK (ILK-PBS) was analyzed, that was described before to dramatically affect ILK function (Nikolopoulos and Turner 2001).

As shown in Fig 3.25B ILK-PBS was exclusively localized in the cytoplasm and not able to translocate into FAs. Moreover, cell shape, the actin cytoskeleton as well as the structure of FAs was not rescued by this mutant ILK suggesting that the localization of ILK into FAs is essential for its function and that the FA targeting depends on the paxillin-binding motif in ILK. To further test, if the kinase activity of ILK is important three additional mutations were tested. The R211A mutation was described as a PIP3-binding mutant, S343A was shown to affect the activation loop resulting in a complete kinase-dead ILK, whereas mutation S343D

was reported to act as a constitutive active ILK (Persad et al. 2001). All these ILK mutants were fused to EGFP and stably expressed in ILK (-/-) fibroblasts. Interestingly, all ILK mutants were able to rescue the ILK knockout phenotype. The rescued cells were able to develop a strong actin network and formed robust FAs throughout the cell (Fig 3.25C-E). These data indicate that the kinase activity of ILK is not essential for the organization of the actin cytoskeleton.

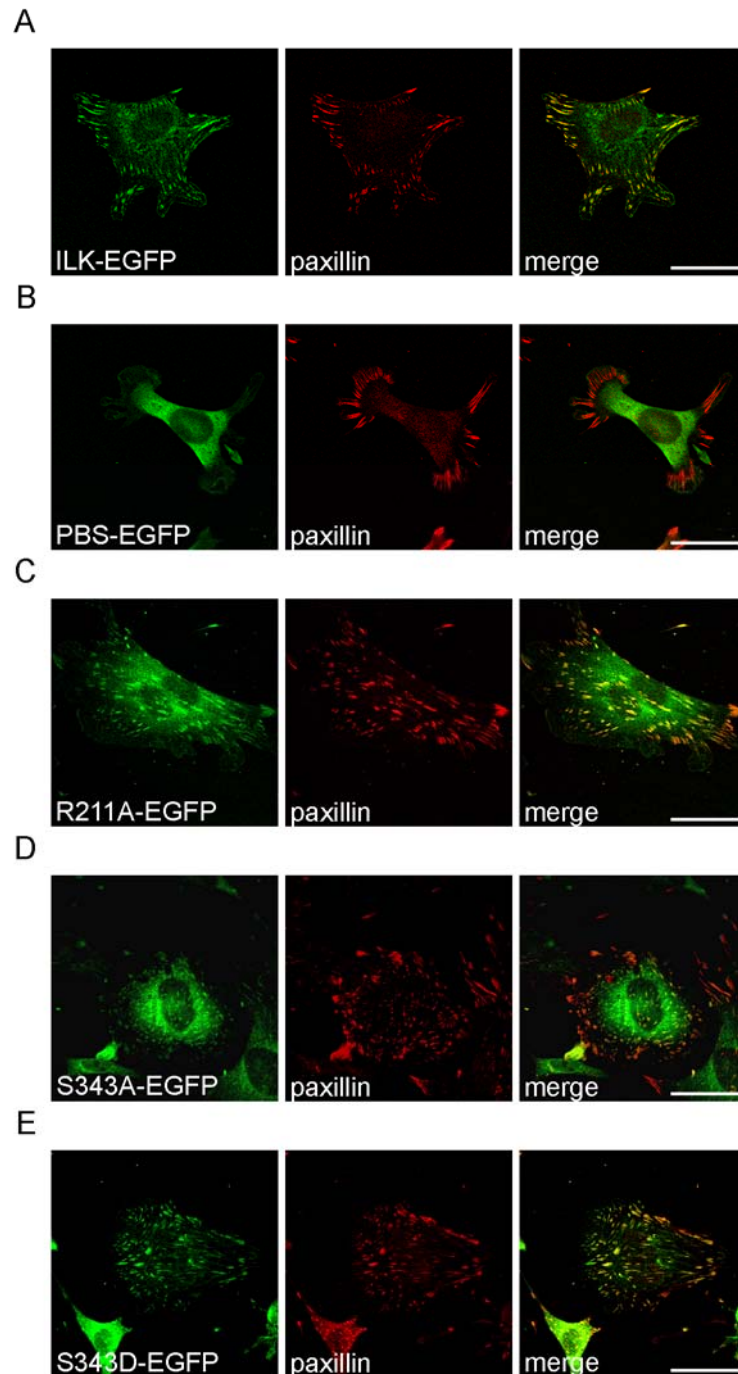


Fig 3.25. ILK kinase activity is dispensable for the regulation of the actin cytoskeleton. *A.* Confocal images of immunostained ILK (-/-) fibroblasts stably expressing ILK-EGFP. *B.* ILK (-/-) fibroblasts stably expressing ILK-

PBS, a double point mutation in the paxillin binding site of ILK. Note, that this mutation does not rescue the ILK knockout phenotype. C. Immunostaining of ILK (-/-) fibroblasts stably expressing the ILK-R211A mutation in the potential PIP3 binding site of ILK. D. Immunostaining of ILK (-/-) fibroblasts stably expressing ILK-S343A. This mutation was reported to result in a complete kinase-dead ILK. E. Immunostaining of ILK (-/-) fibroblasts stably expressing ILK-S343D, a potential constitutive active ILK. EGFP signals are shown in green, paxillin staining in red. Scale bars: 20 μ m.

3.4.7. ILK is essential for fibronectin fibrillogenesis

Although ILK (-/-) cells could form FAs in the cell periphery, they displayed a strongly impaired formation of centrally located FAs. The formation of these structures often coincides with the formation of fibrillar adhesions and is dependent on actin pulling forces, which are essential structures for the assembly of an extracellular FN network. To check whether ILK (-/-) cells could assemble FN fibrils, control and knockout cells were seeded on FN-coated chamber slides and cultured for approximately 12h in the presence of a fluorescently labelled FN (FN-Cy5). Cells were then fixed, immunostained and analyzed by confocal microscopy.

While control cells showed a strong incorporation of the exogenously added FN into a dense FN network (Fig 3.26A), ILK (-/-) cells were completely unable to assemble FN fibrils (Fig 3.26B). ILK (-/-) cells stably expressing ILK-EGFP allowed FN-fibrillogenesis again (Fig 3.26C). These data demonstrate that ILK is essential for FN matrix assembly.

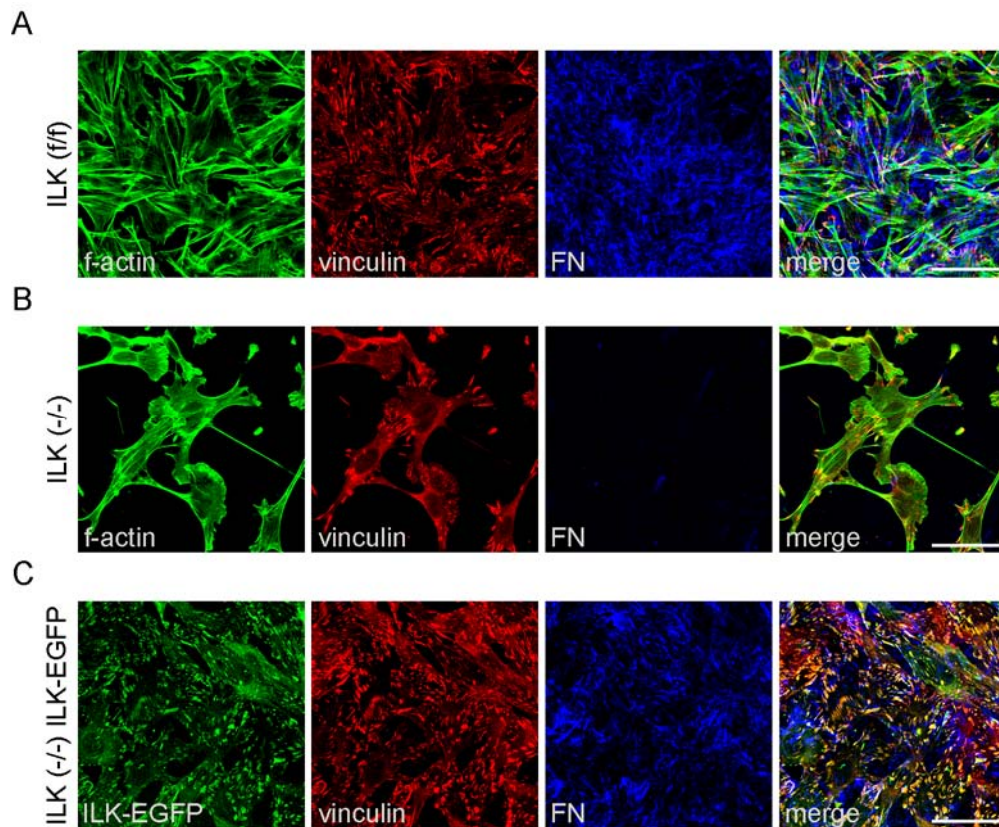


Fig 3.26. Defective FN fibrillogenesis in the absence of ILK. *A.* Merged stack of confocal pictures showing immunostained ILK (f/f) fibroblasts, which incorporated FN-Cy5 into a dense FN network. *B.* Merged stack of confocal pictures showing ILK (-/-) fibroblasts which were not able to assemble FN. *C.* Merged stack of confocal pictures showing ILK (-/-) fibroblasts expressing ILK-EGFP. These cells were able to perform FN fibrillogenesis again. Scale bar: 40 μ m.

3.4.8. Dorsal ruffle (DR) formation

During the cell spreading analysis of ILK (f/f) fibroblasts I realized that these cells can form large but very short lived actin rings. A closer evaluation revealed that those structures were DRs, which are known to occur in certain cell types upon treatment with growth factors such as the epidermal growth factor (EGF) (Chinkers et al. 1979) or the platelet-derived growth factor (PDGF) (Mellstrom et al. 1983) or phorbol esters such as TPA (Schliwa et al. 1984; Kitano et al. 1986). Since DRs form during v-src induced transformation these structures are thought to contribute to rapid actin reorganizations during the onset of cell migration or cell transformation (Boschek et al. 1981). In this study, DR formation was used as a read-out in order to analyze the role of ILK for growth factor-induced actin reorganizations.

3.4.8.1. DR formation during cell spreading

When ILK (f/f) fibroblasts were seeded in the presence of growth factors (10% FCS) on FN and monitored during the cell spreading, around 8-10% of the cells formed DRs, which typically occurred in cells that switched from an isotropic to an anisotropic way of spreading (Fig 3.27). Interestingly these ruffles were hardly observed in ILK (-/-) cells. Similarly ILK (f/f) cells seeded on poly-lysine were also unable to trigger formation of DRs (Fig 3.27B).

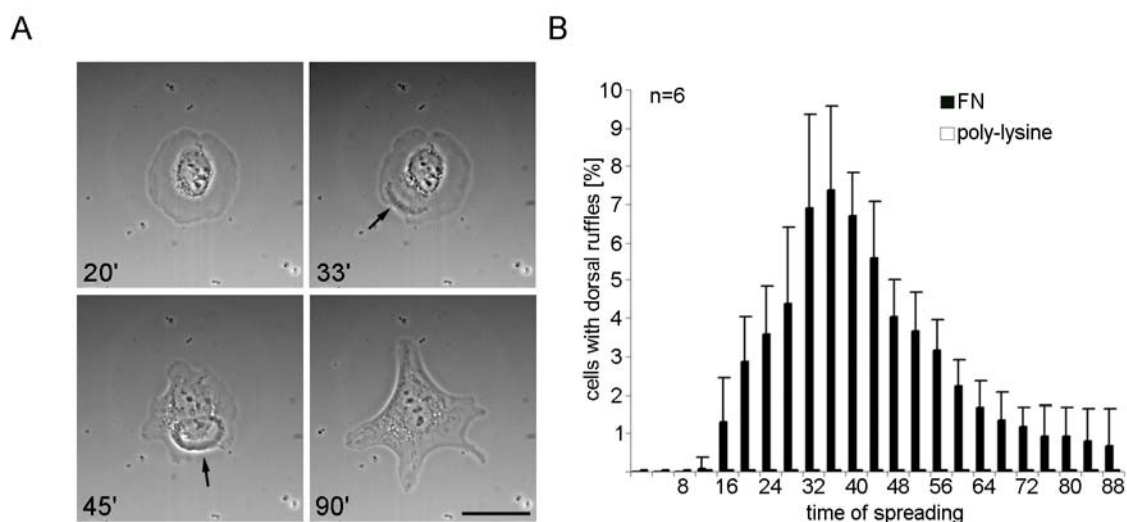


Fig 3.27. DR formation during cell spreading. *A.* Images taken from a time lapse video showing a control ILK (f/f) fibroblast during spreading on FN in the presence of growth factors (arrows indicate the location of the DR). Scale bar: 20 μ m. *B.* Quantification of DR formation in ILK (f/f) control cells during cell spreading on FN and poly-lysine based on 6 independent experiments.

3.4.8.2. Integrin-dependency of DR formation

That ILK (f/f) fibroblasts formed DRs during integrin-mediated adhesion but not after adhesion to poly-lysine indicated that integrin engagement is important for this rapid form of growth factor-induced actin reorganization. To further test this, control cells were starved, seeded on FN or poly-lysine and allowed to spread for 2h. Subsequently, cells were stimulated with EGF. Shortly after EGF stimulation, ILK (f/f) fibroblasts formed DRs that were originating from the cell edges moving onto the dorsal cell body (Fig 3.28A). While approximately 25-30% of the FN-attached cells formed DRs, cells that were seeded on poly-lysine were unable to form DRs after EGF stimulation (Fig 3.28B).

Next, control cells were seeded on different concentrations of FN (2.5-10 μ g/ml) and stimulated with EGF. Cells that were seeded on high concentrations of FN formed significantly more DRs than cells that were seeded on dishes coated with less FN. At a FN concentration of 2.5 μ g/ml cells did adhere but almost completely failed to form DRs (Fig

3.28C). These data show for the first time that integrin engagement is essential for DR formation.

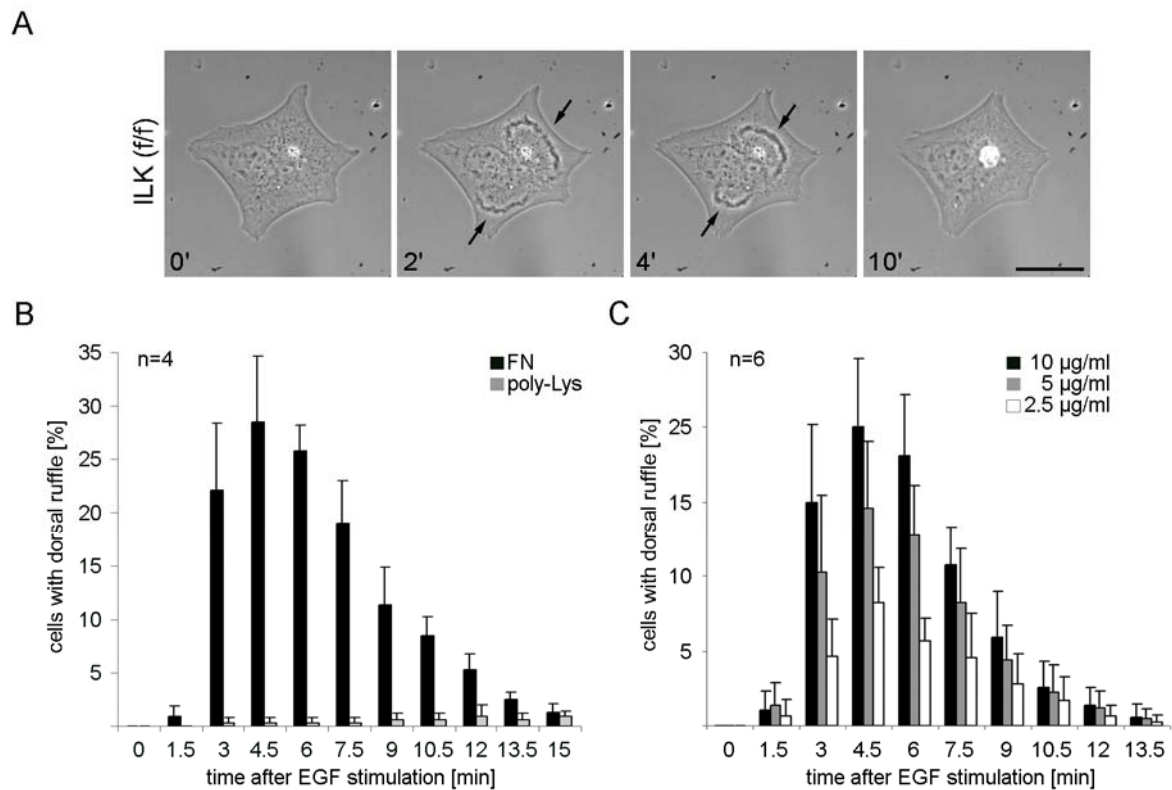


Fig 3.28. Integrin engagement promotes dorsal ruffling after EGF stimulation. *A.* Pictures taken from a movie obtained by time lapse video microscopy. Arrows indicate the location of the DR, which usually forms within the first 4min after EGF stimulation. *B.* Quantification of DR formation after EGF stimulation of ILK (f/f) fibroblasts seeded on FN or poly-lysine based on 4 independent experiments. *C.* Quantification of DR formation after EGF stimulation of ILK (f/f) fibroblasts seeded on different concentrations of FN based on 6 independent experiments.

3.4.9. Localization of vinculin, talin and ILK into DR

It is known for more than 20 years that the FA protein vinculin is present in DRs (Schliwa et al. 1984). This is surprising since FAs are exclusively located at the basal side of 2D-cultured cells. To check whether other integrin-associated proteins also translocate to DRs after EGF treatment, starved control cells were stimulated with EGF, fixed after 4min and subjected to immunostaining. As expected, vinculin localized in FAs at the basal side and into DRs at the dorsal side of the cell (Fig 3.29A). Talin, a $\beta 1$ integrin-binding molecule, showed a similar distribution with a strong staining in the FAs and a weaker but still prominent staining in the DR (Fig 3.29B). Other FAs proteins like FAK or paxillin showed only very weak or no DR localization (Fig 3.29A, B and data not shown).

In order to check if ILK is also present in DRs, ILK (-/-) fibroblasts that stably re-express ILK-EGFP (Fig 3.20B) were monitored during DR formation. In addition, ILK (f/f) fibroblasts were stained with a monoclonal ILK antibody. Both experiments revealed that ILK was mainly localized in FAs but was also capable of translocating into DRs after EGF stimulation (Fig 3.29C and data not shown).

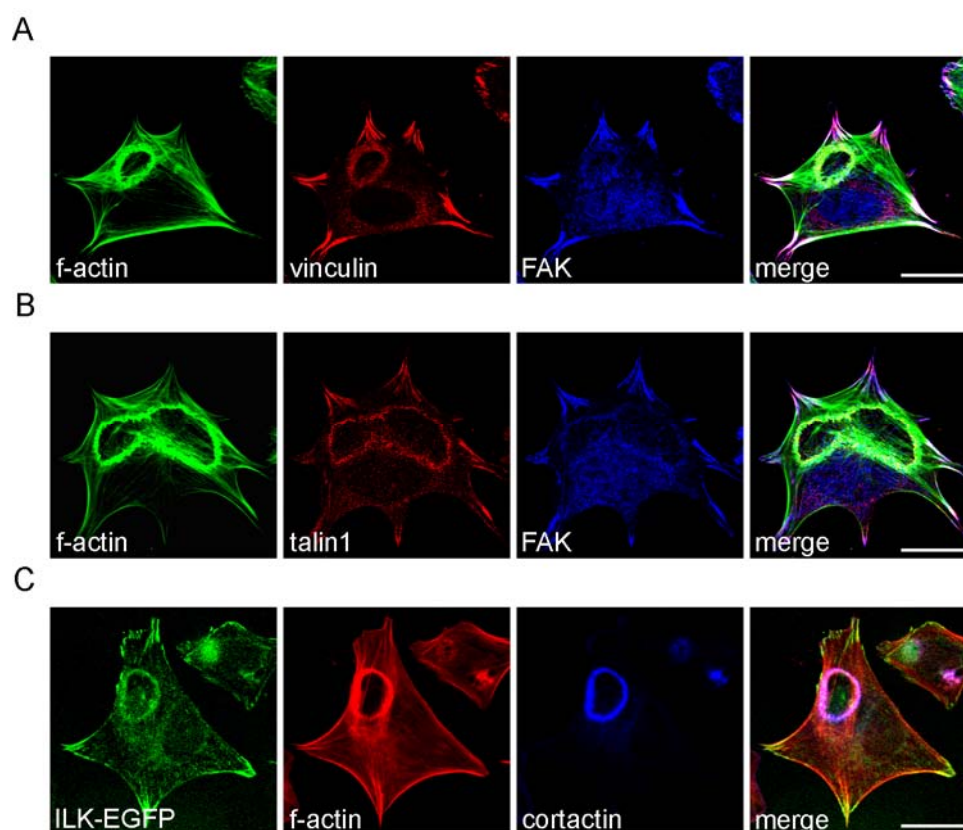


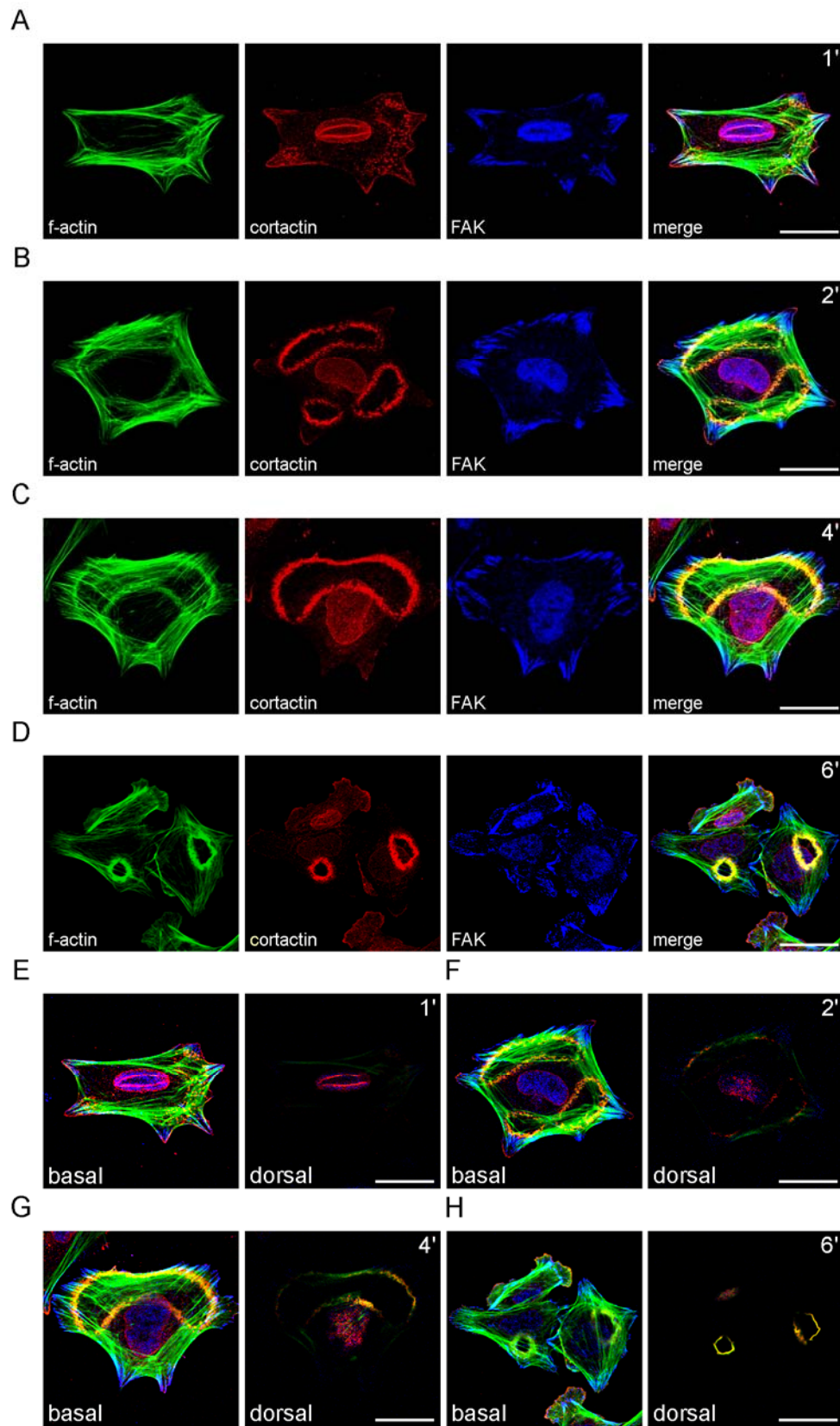
Fig 3.29. Localization of FA proteins into DRs. *A.* Merged stack of a series of confocal pictures showing *f-actin*, *vinculin* and *FAK* immunostaining of ILK (f/f) fibroblasts. Scale bar: 20 μ m. *B.* Merged stack of a series of confocal pictures showing *f-actin*, *talin* and *FAK* immunostaining of ILK (f/f) fibroblasts. Scale bar: 20 μ m. *C.* Merged stack of a series of confocal pictures showing *f-actin* and *cortactin* immunostaining of ILK (-/-) fibroblasts stably expressing ILK-EGFP. Note the localization of *vinculin*, *talin* and ILK in FAs and in DRs. Scale bar: 20 μ m.

3.4.10. DRs originate from the ventral side of the cell

How do FA proteins translocate from FAs at the ventral side of the cell into DRs at the dorsal side? One possibility could be that DRs actually form at the basal side and later translocate to the dorsal side. To test this hypothesis, control cells were stimulated and fixed at early time points during DR formation. Using confocal microscopy, the localization of the DR marker cortactin was investigated. One minute after EGF stimulation, cortactin accumulated in patches at the basal side of the cell. These patches were at this time point not co-localizing

with f-actin and exclusively localized at the basal side of the cell (Fig 3.30A, E) within the same confocal plane as FAs (visualized by FAK immunostaining). 2min after EGF stimulation, the cortactin patches developed into larger structures that became frequently overlapping with f-actin accumulations (Fig 3.30B). However, these structures (resembling early DRs) were still mainly localized to the basal side of the cells (Fig 3.30F). At later time points the distribution of cortactin and f-actin was not clearly restricted to the basal side anymore (Fig 3.30C, G). 6min after EGF stimulation the typical DR was evident in most of the cells. These structures were exclusively localized at the dorsal side of the cell (Fig 3.30D, H). These data indicate that DRs arise at the basal side of the cell and appear only at later time points in dorsal locations.

Fig 3.30. DRs form at the basal side of the cell. *A. Merged stack of confocal images showing ILK (f/f) fibroblasts 1min after EGF stimulation. Small cortactin patches indicate the formation of a DR. B. Merged stack of confocal images showing ILK (f/f) fibroblasts 2min after EGF stimulation. Large f-actin structures began to form. C. ILK (f/f) fibroblasts 4min after stimulation. D. DRs or “actin flowers” 6min after EGF stimulation. E. Images of a basal and a dorsal confocal plane 1min after EGF stimulation taken from (A). Cortactin patches are exclusively basal. F. Images of a basal and a dorsal confocal plane 2min after EGF stimulation taken from (B). F-actin structures are still basal. G. Images of a basal and a dorsal confocal plane 4min after EGF stimulation taken from (C). Certain structures occur at the dorsal side H. Images of a basal and a dorsal confocal plane 6min after EGF stimulation taken from (D). DRs are exclusively at the dorsal side, presenting “actin flowers”. Scale bars: 20 μ m in (A-C, E-G), 30 μ m (D, H)*



3.4.11. ILK is essential for DR formation

ILK (-/-) fibroblasts failed to form DRs during the cell spreading, whereas ILK (f/f) control cells formed numerous DRs on FN (Fig 3.27). To analyze the role of ILK during DR formation in more detail, control and knockout fibroblasts were seeded on FN (10 μ g/ml), allowed to attach and stimulated with EGF. While 25-30% of ILK (f/f) cells showed dorsal ruffling, adherent ILK (-/-) cells formed significantly less DRs (Fig 3.31A).

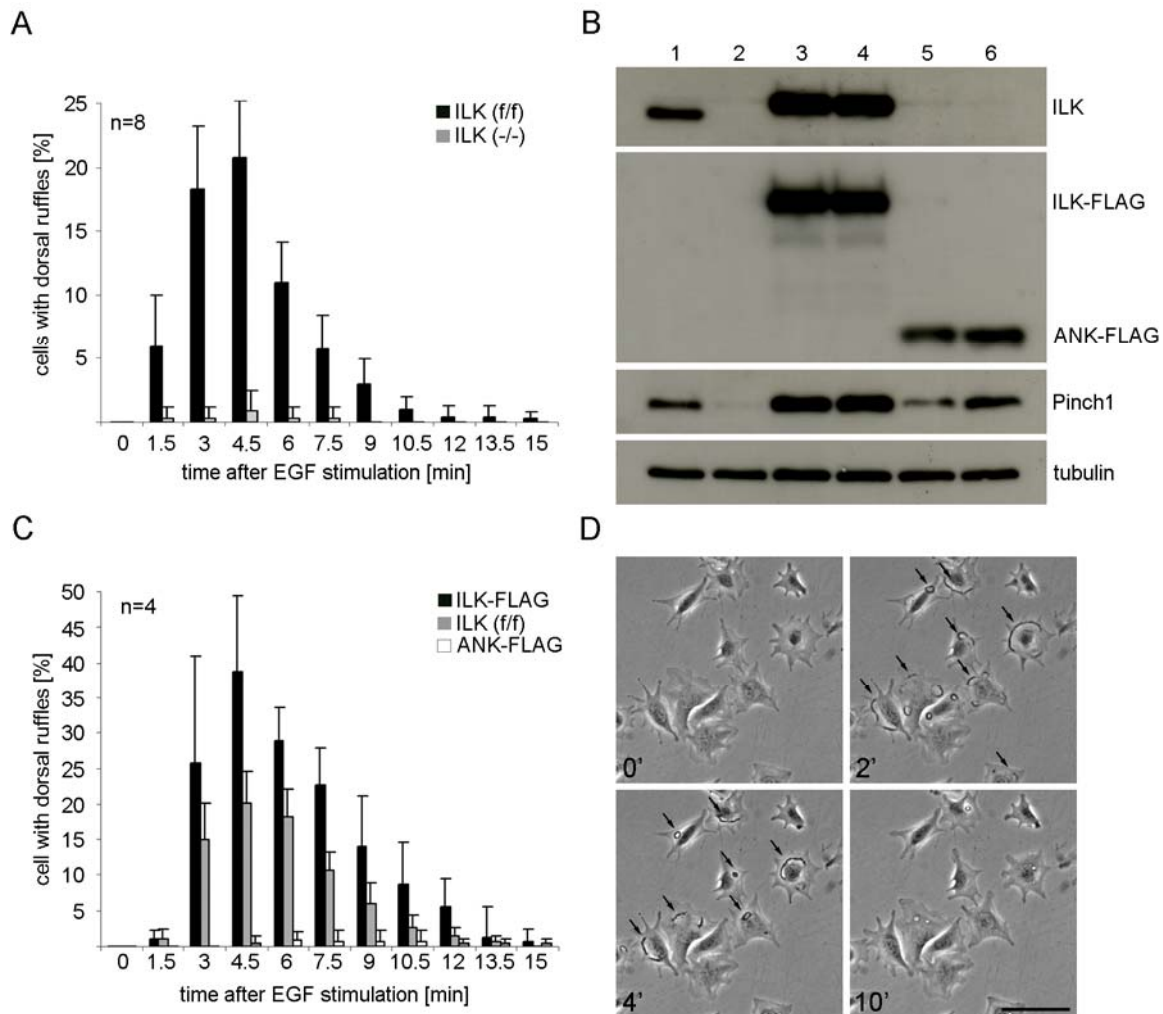


Fig 3.31. ILK is essential for DR formation. *A.* Quantification of DR formation after EGF stimulation of adherent ILK (f/f) and ILK (-/-) fibroblasts based on 8 independent experiments. *B.* Western blot analysis of protein lysates from ILK (f/f) (1), ILK (-/-) (2), ILK-FLAG #1 (3), ILK-FLAG #2 (4), ANK-FLAG #1 (5), ANK-FLAG #2 (6) fibroblasts. Note, that expression of the N-terminal part of ILK is sufficient to rescue Pinch1 degradation. *C.* Quantification of DR formation after EGF stimulation of adherent ILK (f/f), ILK-FLAG and ANK-FLAG fibroblasts. Quantification is based on 4 independent experiments. ILK (-/-) fibroblasts overexpressing ILK-FLAG formed even more DRs. Rescue of the Pinch1 expression level was not sufficient for the induction of dorsal ruffling. *D.* Images taken from a time lapse video showing extensive DR formation (see arrows) after EGF stimulation in ILK-FLAG overexpressing cells. Scale bar: 100 μ m.

Deletion of ILK decreases Pinch1 levels. To exclude that the defective DR formation is due to diminished Pinch1 levels rather than loss of ILK, cell lines were generated that stably expressed an N-terminal part of ILK (tagged with a FLAG tag) but lacked the C-terminal domain (ANK-FLAG) (Fig 3.31B). Stable expression of the truncated ILK stabilized Pinch1 and localized it to FAs (Fig 3.32A, B). The overall phenotype of these cells, the impaired spreading activity and diminished stress fiber formation was, however, unchanged. When stimulated with EGF ANK-FLAG cells were still not able to form DRs (Fig 3.31C).

To further test, if DR formation correlates with ILK expression levels a cell line was generated that overexpressed ILK-FLAG (Fig 3.31B). These cells develop a robust stress fiber network and display strong FA formation (Fig 3.32A). Interestingly, the mild overexpression of ILK led to the formation of significantly more DRs than in control cells, demonstrating that ILK expression directly correlates with DR formation (Fig 3.31C, D)

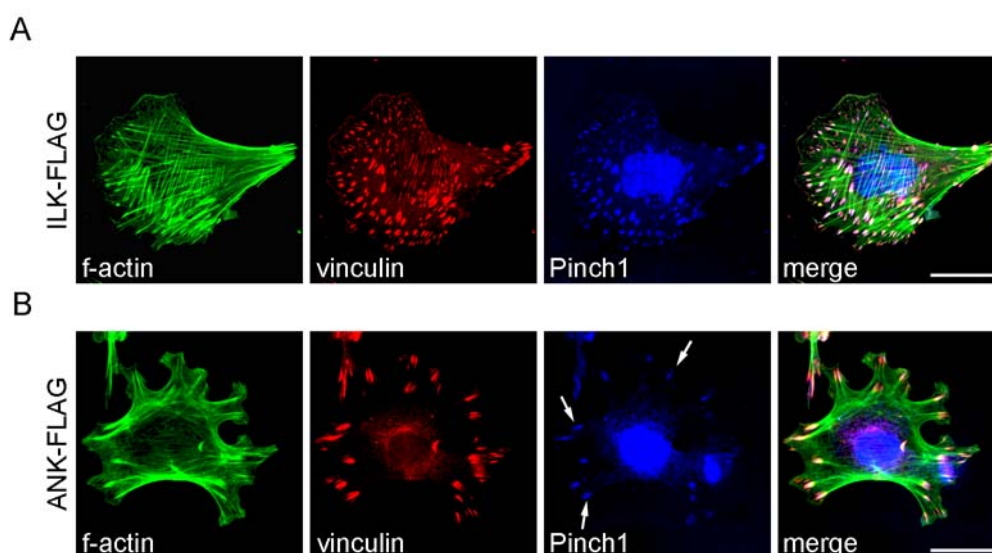


Fig 3.32. Stabilization of Pinch1 by expression of full length ILK and ILK-ANK. *A. Merged stack of confocal images showing immunostaining of ILK (-/-) fibroblasts expressing ILK-FLAG. Pinch1 localized in FAs again. B. Merged stack of confocal images showing immunostaining of ILK (-/-) fibroblasts expressing an N-terminal part of ILK (ILK-ANK). Pinch1 could localize into FAs (arrows). Scale bars: 20 μ m.*

3.4.12. Stabilization of Pinch1 by N-terminal ILK is not sufficient for induction of FN fibrillogenesis in ILK (-/-) fibroblasts

To check if the rescue of Pinch1 degradation and its localization into FAs is sufficient to induce FN fibrillogenesis, ILK (-/-) fibroblasts stably expressing either full length ILK-FLAG or ANK-FLAG were incubated with fluorescently labelled FN (FN-Cy5, 3.4.7). As shown in Fig 3.33, expression of full length ILK-FLAG rescued the FN fibrillogenesis defect of ILK (-

/-) fibroblasts, while expression of the N-terminal ankyrin repeats of ILK was not sufficient to induce FN assembly despite the fact that Pinch1 expression was restored and Pinch1 was targeted to FAs. These data indicate that ILK is a central player for both DR formation and FN fibrillogenesis.

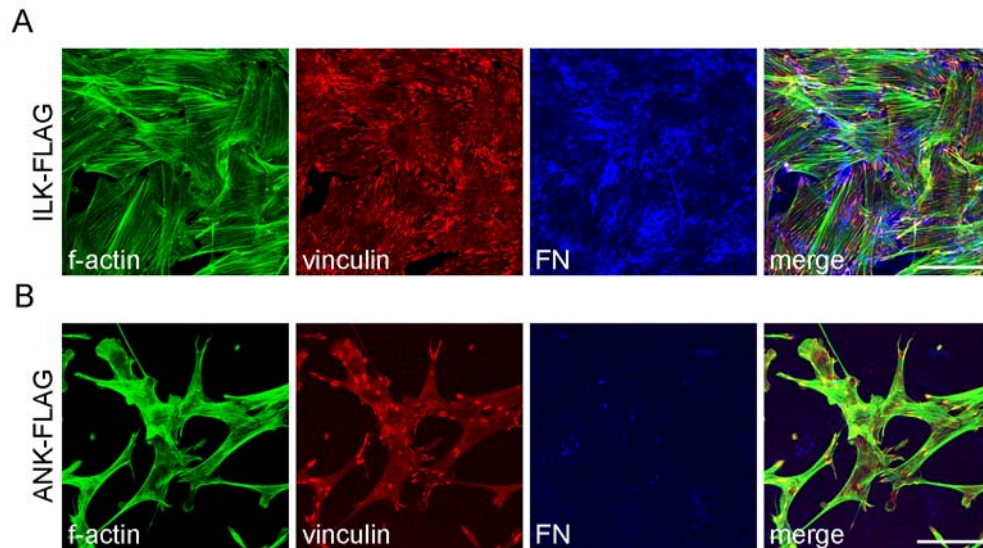


Fig 3.33. Full length ILK is essential for FN-fibrillogenesis. *A. Merged stack of confocal images showing immunostaining of ILK (-/-) fibroblasts stably expressing ILK-FLAG. FN assembly could occur normally. B. Merged stack of confocal images showing immunostaining of ILK (-/-) fibroblasts stably expressing ANK-FLAG. Restoration of Pinch1 expression levels and Pinch1 localization into FAs was not sufficient for triggering FN matrix assembly. Scale bars: 40 μ m.*

3.4.13. Expression of constitutive active Rac1 rescues the DR formation defect

Activation of the small GTPase Rac1 was shown to be crucial for DR formation (Buccione et al., 2004). To confirm the important role of Rac1 during dorsal ruffling in ILK fibroblasts, cell lines were generated that stably expressed either dominant negative Rac1 (RacN17) or constitutive active Rac1 (RacL61). Both constructs contained a myc-tag that allowed for detection of the exogenous protein in western blot analyses and immunostaining. Fig 3.34A shows that transduced RacN17 was diffusely distributed in the cytoplasm of ILK (f/f) fibroblasts. RacL61 which was expressed in ILK (-/-) fibroblasts was found in the cytoplasm as well, but was also localized into peripheral ruffles and DRs that could be induced in these cells with EGF in the absence of ILK (Fig 3.34B). A biochemical analysis revealed that the RacN17 expression level was approximately as high as the endogenous Rac1 level. In contrast, very little amounts of RacL61 were expressed in ILK (-/-) cells that were, however, sufficient to induce quite dramatic morphological changes and dorsal ruffling (Fig 3.34C). Statistical evaluation of DR formation revealed that ILK (-/-) fibroblasts stably expressing

RacL61 formed even more DRs than control cells but slightly delayed. Moreover, DR formation was still dependent on EGF stimulation. Starved ILK (-/-) fibroblasts expressing RacL61 formed almost no DRs indicating that more than just Rac1 activation is necessary for DR formation. Interestingly, when ILK (-/-) RacL61 fibroblasts were seeded on poly-lysine they were unable to form DR after EGF stimulation underscoring the essential role of integrin engagement.

The fact that the loss of ILK can be compensated by the expression of an active Rac1 indicates that ILK itself might be essential for the spatio-temporal activation of Rac1 after EGF stimulation.

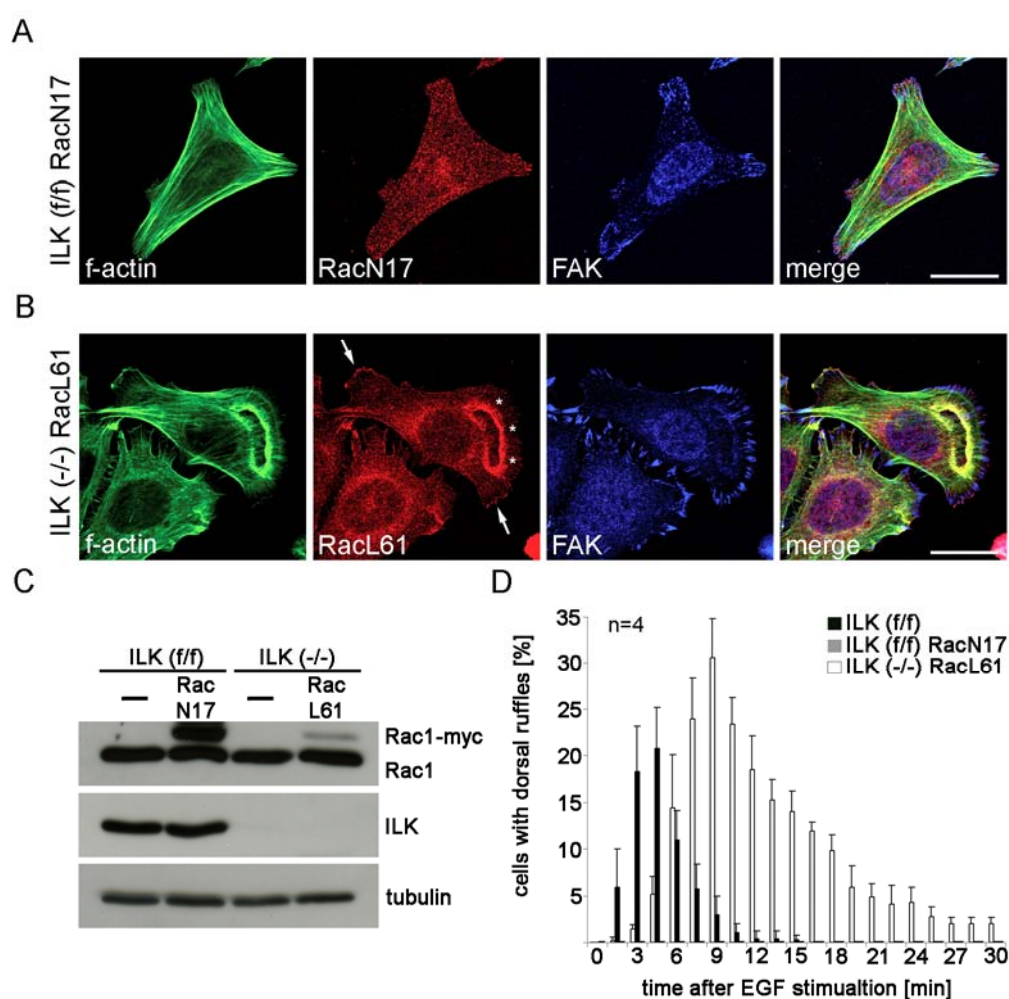


Fig 3.34. Expression of dominant negative and constitutive active Rac1. *A.* Immunostaining of ILK (f/f) fibroblasts stably expressing RacN17. Note, that the overall appearance of these cells is not dramatically changed. Stress fiber and FAs appeared to be rather normal. RacN17 was equally distributed in the cytoplasm. Scale bar: 20 μ m. *B.* Immunostaining of ILK (-/-) fibroblasts expressing RacL61. These cells changed dramatically their morphology. Peripheral ruffles (arrows) and DRs (*) were visible, to which RacL61 itself was localizing. Scale bar: 20 μ m. *C.* Biochemical analysis. The endogenous levels of Rac1 were not changed upon expression of mutant Rac1. Very low levels of RacL61 were sufficient for induction of dorsal ruffling in ILK (-/-)

cells. **D.** *Quantification of DR formation in ILK (f/f), ILK (f/f) RacN17 and ILK (-/-) RacL61 fibroblasts. Defective DR formation of ILK (-/-) fibroblasts could be rescued by expression of RacL61.*

3.4.14. Expression of constitutive active Rac1 is not sufficient to overcome the FN assembly defect of ILK (-/-) fibroblasts

Since expression of RacL61 can rescue the DR formation defect of ILK (-/-) fibroblasts it was tested whether activation of Rac1 could also overcome the FN fibrillogenesis defect of ILK knockout cells. Fig 3.35A shows that expression of RacN17 in ILK (f/f) fibroblasts impaired FN fibrillogenesis although it did not completely block it. The expression of constitutive active Rac1 in ILK (-/-) fibroblasts was not sufficient to allow FN fibrillogenesis to occur (Fig 3.35B) indicating that the essential role of ILK during FN fibrillogenesis is independent of Rac1 activation.

These data demonstrated that ILK plays a crucial role for different integrin-signal transduction pathways, one leading to the Rac1-dependent formation of DR and another leading to the assembly of a FN matrix.

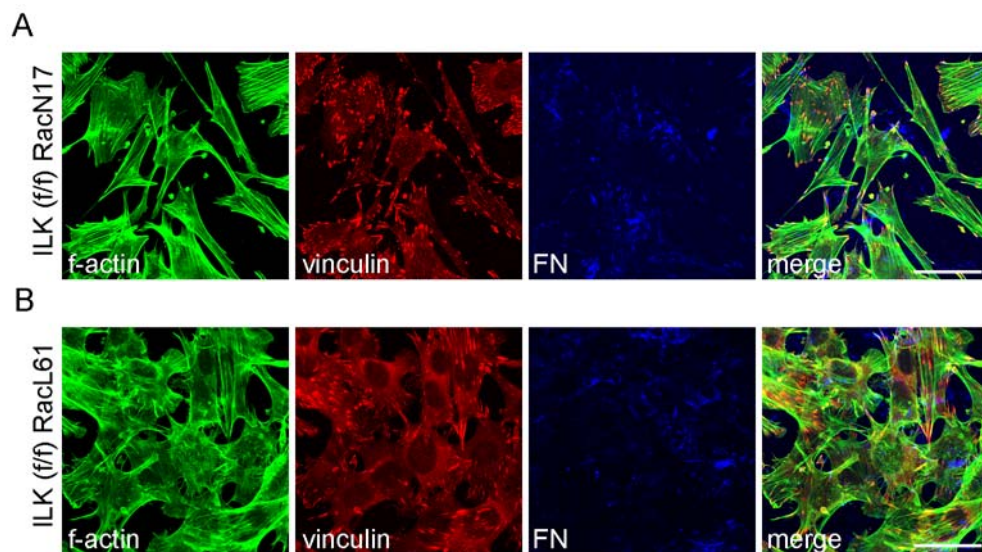


Fig 3.35. Expression of RacL61 is not sufficient to rescue the FN assembly defect of ILK (-/-) fibroblasts. *A. Merged stack of confocal images showing immunostaining of ILK (f/f) fibroblasts stably expressing RacN17. B. Merged stack of confocal images showing ILK (-/-) fibroblasts stably expressing RacL61. Expression of constitutive active Rac1 was not sufficient to overcome the fibrillogenesis defect. Scale bars: 40μm.*

3.4.15. Paxillin is dispensable for DR formation

ILK binds to a number of proteins that could potentially transduce integrin/ILK signalling. As shown before the interaction between paxillin and ILK seemed to be essential for many if not all ILK functions, since ILK (-/-) cells stably expressing a paxillin-binding site mutant ILK-

EGFP still showed a highly disorganized actin cytoskeleton and impaired FA formation (Fig 3.25B). To confirm that paxillin plays a crucial role downstream of ILK, ILK (f/f) fibroblast cell lines were generated that stable express short hairpin RNA (shRNA) directed against the mRNA of mouse-paxillin. Five different shRNA constructs were stably expressed in ILK (f/f) fibroblasts two of which were efficiently reducing the protein levels of paxillin. From these cells, clonal cell lines were generated. In this way, a high knockdown efficiency was permanently achieved. While control cells expressing an unspecific scrambled shRNA sequence displayed unchanged paxillin levels, knockdown cell lines showed an almost complete loss of paxillin with an expression that was less than 5% of the paxillin level in control cells (Fig 3.36A, B). The expression levels of FA proteins which directly bind paxillin such as ILK, α -parvin or FAK were not significantly altered in paxillin knockdown cells. Hic-5, a member of the paxillin family was only expressed at low levels in ILK fibroblasts and slightly reduced in paxillin knockdown cells (Fig 3.36A). Loss of paxillin expression was confirmed by immunostaining and revealed a defective localization of FAK into FAs which was now instead found in the cytoplasm. Moreover, paxillin knockdown cells displayed a disorganized actin cytoskeleton with a strong cortical stress fiber network and altered FAs which appeared slightly larger (Fig 3.36C, D). In agreement with the strongly reduced localization of FAK into FAs tyrosine phosphorylation of FAK was significantly diminished in paxillin knockdown cells (Fig 3.36E). Surprisingly, paxillin knockdown fibroblasts displayed a normal DR formation frequency (Fig 3.36F) indicating that paxillin is not acting downstream of ILK during EGF-induced DR formation.

To check if paxillin is essential for FN fibrillogenesis control and knockdown cell lines were subjected to the FN assembly assay. As shown in Fig 3.37 paxillin knockdown cells displayed an impaired FN fibrillogenesis. This is in line with a previous report showing that FA-targeting of FAK is crucial for FN fibrillogenesis to occur (Ilic et al. 2004).

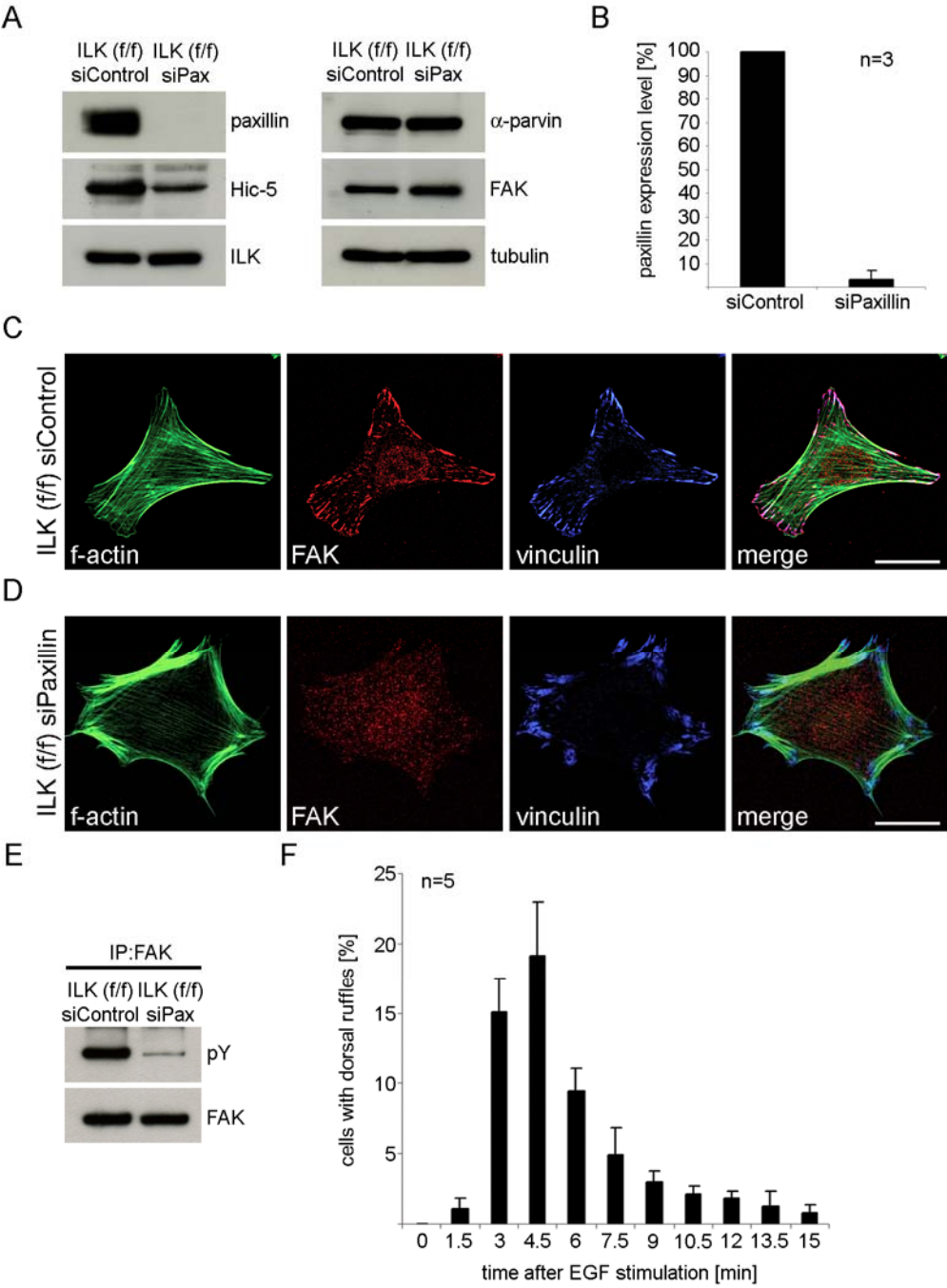


Fig 3.36. Generation and analysis of paxillin knockdown cell lines. *A.* Western blot analysis of protein lysates from ILK (f/f) siControl and ILK (f/f) siPaxillin cell lines. *B.* Quantification of paxillin expression in control and paxillin knockdown cell lines. *C.* Merged stack of confocal images showing organization of the f-actin cytoskeleton and FA structure in control cells. Scale bar: 20 μ m. *D.* Merged stack of confocal images showing defective FAK localization in FAs and altered size of FA in paxillin knockdown cells. Scale bar: 20 μ m. *E.* Western blot analysis of FAK immunoprecipitates from control and knockdown cells. *F.* Quantification of DR formation after EGF stimulation in paxillin knockdown cells based on 5 independent experiments.

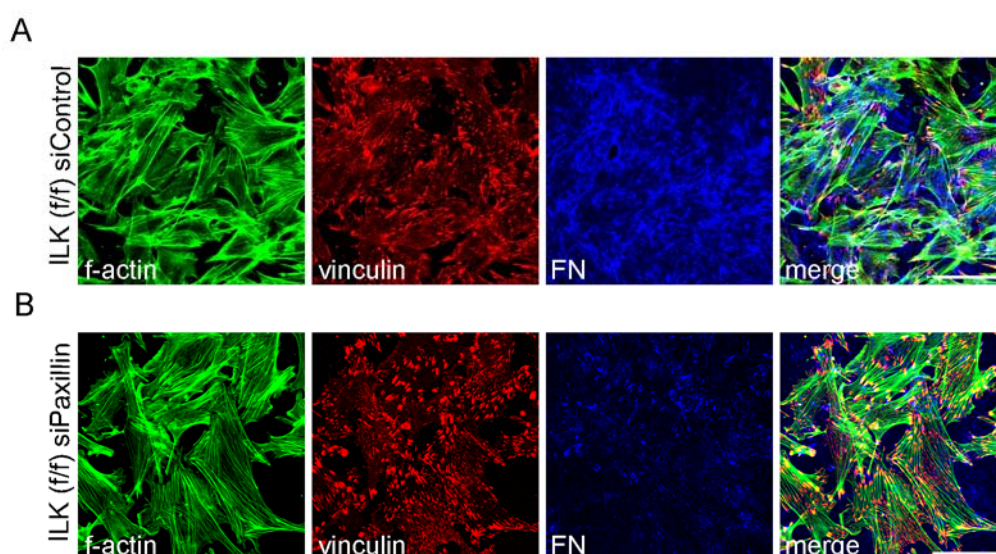


Fig 3.37. Paxillin is necessary for proper FN fibrillogenesis. *A. Merged stack of confocal images showing immunostaining of control ILK (ff) fibroblasts expressing scrambled shRNA. Normal FN fibrillogenesis could occur. B. Merged stack of confocal images showing immunostaining of a paxillin knockdown cell line. FN assembly was impaired but not completely absent. Scale bar: 40 μ m.*

3.4.16. The interaction between paxillin and ILK is not essential for the organization of the actin cytoskeleton

The fact that paxillin knockdown cells displayed a rather normal DR formation frequency was surprising since earlier reports demonstrated that paxillin is essential for the recruitment of ILK as well as α -parvin into FAs (Nikolopoulos and Turner 2000; Nikolopoulos and Turner 2001; Nikolopoulos and Turner 2002). To investigate if loss of paxillin expression indeed impairs recruitment of ILK into FAs (as it was seen with the PBS mutant ILK), cells were seeded on FN-coated coverslips, cultured overnight and immunostained for ILK and α -parvin. Immunostaining of control cells showed that ILK and α -parvin localized together with migfilin or vinculin in FAs (Fig 3.38A, C). Surprisingly, ILK and α -parvin was also present in FAs of paxillin knockdown cells (Fig 3.38B, D). These data show for the first time, that ILK and α -parvin can be recruited into FAs in a paxillin-independent manner. It seems unlikely that the residual paxillin left in the knockdown cells accounted for the recruitment of ILK in FAs, since under the same conditions FAK was diffusively present in the cytoplasm. In order to further dissect the importance of the ILK-paxillin interaction, full length paxillin as well as an ILK-binding mutant paxillin were expressed in the paxillin knockdown background.

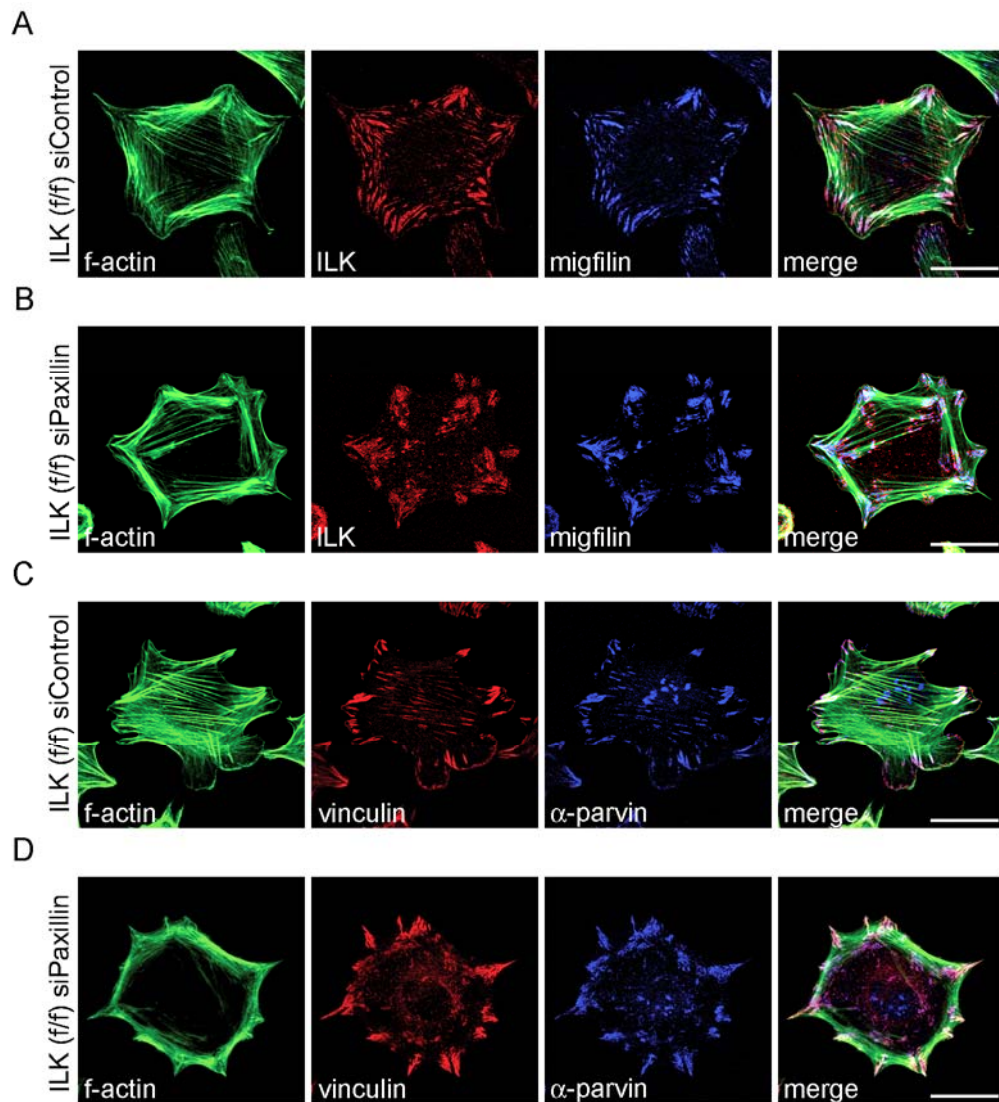


Fig 3.38. Localization of ILK and α -parvin into FAs can occur independently of paxillin. *A.* Immunostaining of control ILK (f/f) fibroblasts showing the localization of ILK and migfilin in FAs. *B.* Immunostaining of paxillin knockdown cells showing normal localization of ILK into FAs. *C.* Immunostaining of control ILK (f/f) fibroblasts showing the localization of vinculin and α -parvin in FAs. *D.* Immunostaining of paxillin knockdown cells showing the localization of α -parvin in FAs. Scale bars: 20 μ m.

3.4.17. The paxillin-ILK interaction is not important for cell spreading and DR formation

Paxillin interacts with ILK via its N-terminally located LD1 domain (1-20aa). Earlier studies have shown that deletion of LD1 in paxillin leads to loss of the paxillin-ILK interaction (Nikolopoulos and Turner 2001). In order to gain further insights into the role of the paxillin-ILK interaction in ILK (f/f) fibroblasts, full length human paxillin and a paxillin LD1-deletion mutant (LD1 Δ -paxillin) expression constructs were introduced into paxillin knockdown cells.

Since human paxillin is not affected by the siRNA construct (directed against mouse paxillin mRNA) both proteins could be stably expressed. Two clonal cell lines were established expressing comparable amounts of paxillin and LD1 Δ -paxillin, respectively. Both constructs rescued the altered FA structure of paxillin knockdown cells, the defective f-actin organization and the FAK localization defect (Fig 3.39). In general, both cell lines were indistinguishable from each other, indicating that the paxillin-ILK interaction alone was not essential for the maintenance of the f-actin cytoskeleton or the assembly of FAs.

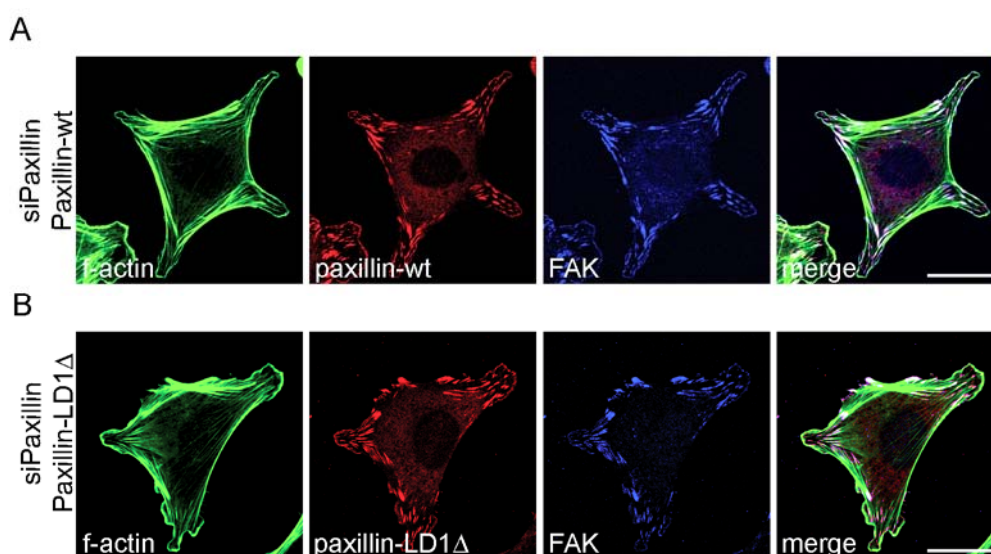


Fig 3.39. Expression of an ILK binding mutant paxillin (LD1 Δ -paxillin) can rescue the morphological defect of paxillin knockdown cells. *A. Immunostaining of paxillin knockdown cells stably expressing a human full length paxillin. Note that FAK localizes in FAs again. B. Immunostaining of paxillin knockdown cells stably expressing LD1 Δ -paxillin. F-actin organization, FA structure and FAK localization in FAs is rescued in these cells. Scale bars: 20 μ m.*

FN fibrillogenesis is completely defective in ILK knockout cells, whereas paxillin knockdown cells display a strongly reduced but not completely inhibited FN assembly (Fig 3.26, Fig 3.37). To check if the direct interaction between ILK and paxillin is necessary for FN fibrillogenesis paxillin knockdown cells expressing full length paxillin or LD1 Δ -paxillin were subjected to the FN assembly assay. As shown in Fig 3.40 paxillin knockdown cells expressing full-length paxillin or LD1 Δ -paxillin performed FN fibrillogenesis like ILK (f/f) control cells.

Altogether, these data indicate that both ILK and paxillin are important for FN assembly but not the direct interaction between ILK and paxillin indicating that these two proteins act independently from each other during FN fibrillogenesis.

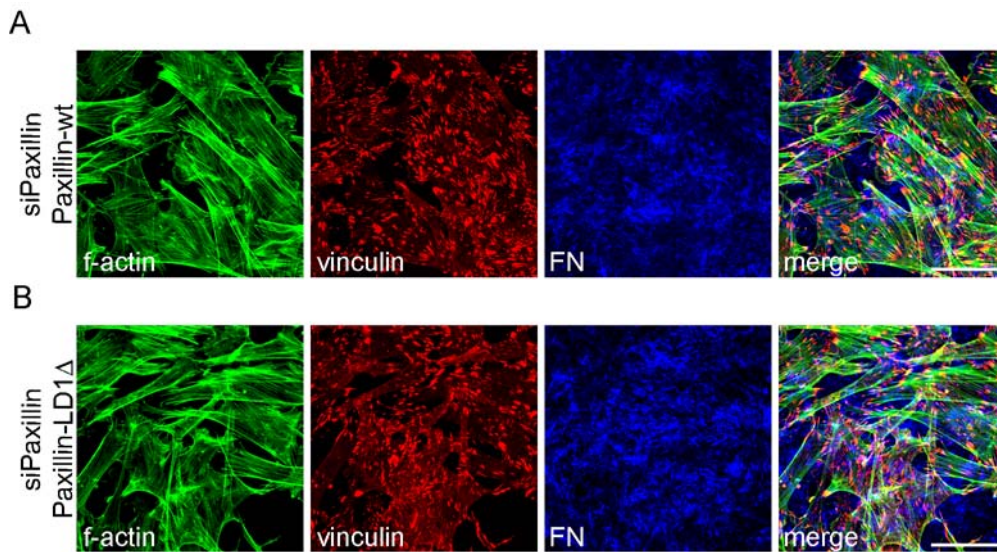


Fig 3.40. The ILK-paxillin interaction is dispensable for FN fibrillogenesis. *A. Merged stack of confocal images showing immunostaining of paxillin knockdown cells expressing full length human paxillin. B. Merged stack of confocal images showing immunostaining of paxillin knockdown cells expressing LD1Δ-paxillin (human). Note, that both cell lines were able to perform FN fibrillogenesis. Scale bars: 40μm.*

3.4.18. FAK is not essential for DR formation

The involvement of FAK for integrin-dependent activation of Rac1 is well documented. The data from paxillin knockdown fibroblasts suggested that the localization of FAK into FAs as well as its tyrosine phosphorylation is not essential for DR formation. To confirm that FAK is not necessary for DR formation, FAK knockdown cell lines were generated. Again five different knockdown constructs were designed and introduced into a retroviral backbone. Viral supernatant was used to infect ILK (f/f) fibroblasts. Two constructs showed a significant decrease of FAK expression levels. Cell lines were cloned exhibiting barely detectable FAK expression levels, while control cells infected with a scrambled shRNA sequence displayed robust FAK expression levels (Fig 3.41A, B). Expression of other FA proteins or FAK interaction partners such as ILK, p130Cas, or paxillin were unchanged in FAK knockdown cells (Fig 3.41A). Loss of FAK expression was additionally confirmed by immunostaining, which also revealed that FAK knockdown cells displayed slightly enlarged FAs (Fig 3.41C,D) as described before (Ilic et al. 1995). As expected, FAK knockdown fibroblasts formed DRs to a normal extent when stimulated with EGF. DR appeared even earlier than in control cells (Fig 3.41E).

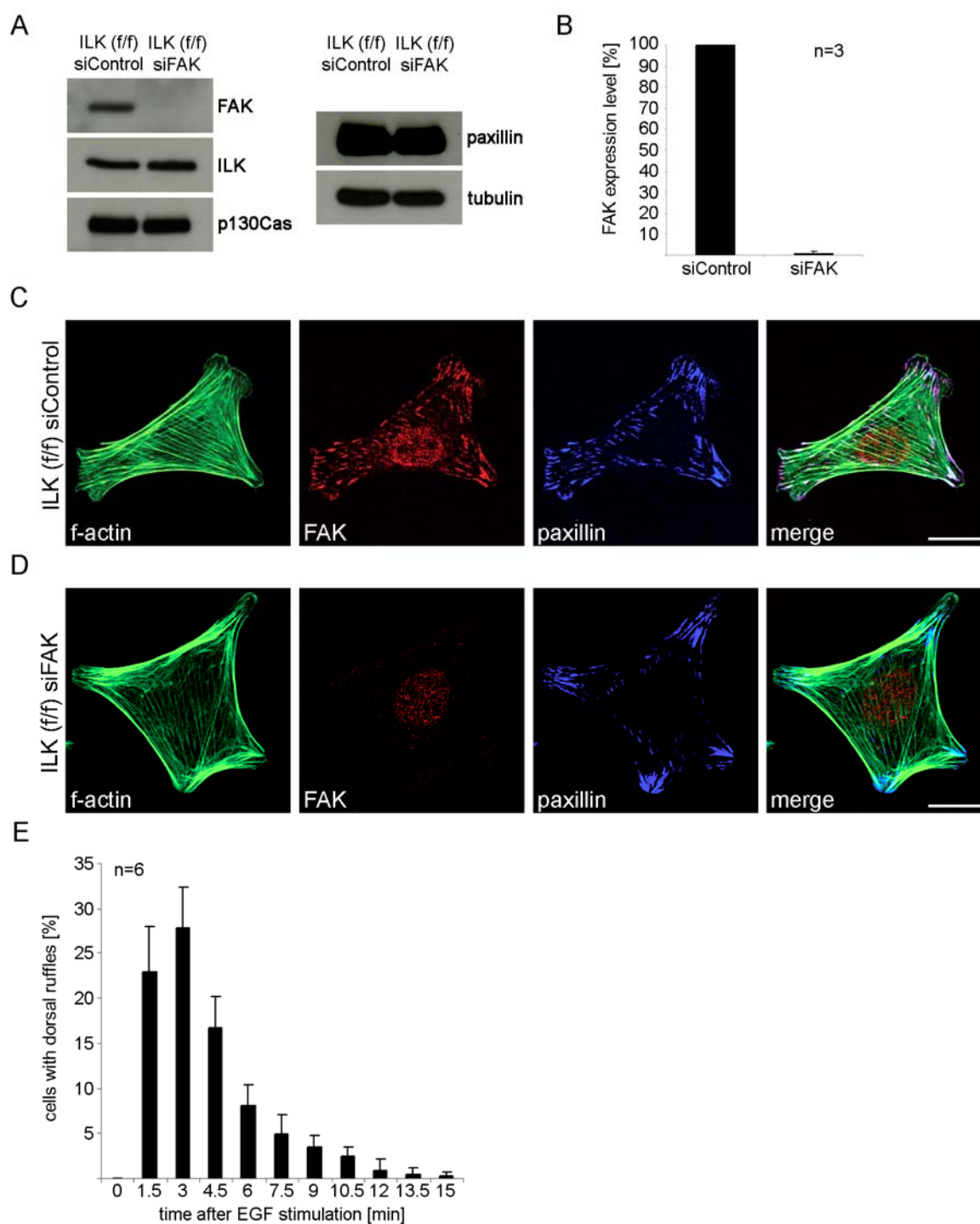


Fig 3.41. Generation and analysis of FAK knockdown cell lines. *A.* Western blot analysis of protein lysates from ILK (f/f) control and ILK (f/f) siFAK cell lines. *B.* Quantification of FAK expression in control and FAK knockdown cell lines. FAK was almost not detectable anymore. Scale bar: 20 μ m. *C.* Merged stack of confocal images showing organization of the f-actin cytoskeleton and FA structure in control cells. Scale bar: 20 μ m. *D.* Merged stack of confocal images showing loss of FAK expression in ILK (f/f) fibroblasts expressing shRNA against FAK mRNA. Note the loss of FAK and the increased size of FAs. *E.* Quantification of DR formation after EGF stimulation in FAK knockdown cells based on 6 independent experiments.

3.4.19. FAK is important for FN fibrillogenesis

FAK has been shown to be essential during FN fibrillogenesis (Ilic et al. 2004). To check if this also the case in ILK (f/f) fibroblasts FAK knockdown cells were analyzed in a FN assembly assay. In line with previous reports FAK knockdown cells displayed an impaired FN fibrillogenesis, while control fibroblasts showed a normal FN matrix assembly.

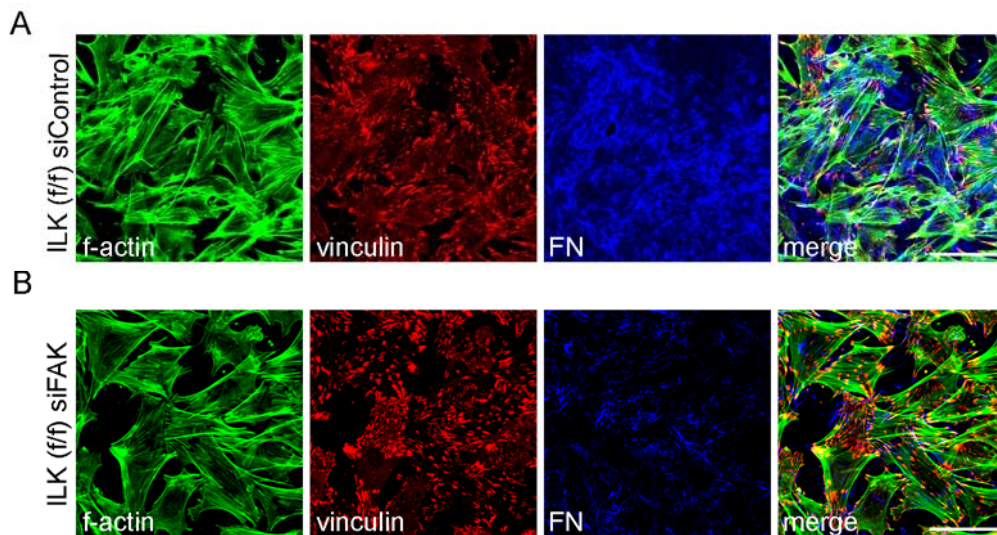


Fig 3.42. FAK is crucial for FN assembly. *A. Merged stack of confocal images showing immunostaining of a control ILK (f/f) fibroblasts expressing scrambled shRNA (same picture as in Fig 3.37). Normal FN fibrillogenesis could occur. B. Merged stack of confocal images showing immunostaining of a FAK knockdown cell line. FN assembly was impaired. Scale bars: 40 μ m.*

3.4.20. Localization of p130Cas, CrkII and ELMO1 in DRs

The formation of peripheral ruffles occurs at the onset of cell migration and is dependent on the assembly of the p130Cas/CrkII complex which mediates an integrin-dependent activation of Rac1 (Klemke et al. 1998). Recent work has identified the ELMO/Dock180 complex downstream of p130Cas/CrkII which is responsible for the activation of Rac1 (Gumienny et al. 2001). To check if the same signalling complex could be involved in DR formation, the localization of these proteins was investigated after EGF stimulation by immunostaining or as in the case of ELMO1 by stable expression of the EGFP-tagged protein in ILK (f/f) fibroblasts.

Fig 3.43 shows that p130Cas, CrkII and ELMO1-EGFP localized into DRs after EGF stimulation. Similar to other FAs proteins like vinculin, talin or ILK (Fig 3.29) p130Cas localized to both FAs and DRs (Fig 3.43A), whereas CrkII was seen mainly cytoplasmic and after EGF stimulation in DRs (Fig 3.43B). Expression of ELMO1-EGFP in ILK (f/f)

fibroblasts revealed a strong localization of this protein into DRs after EGF stimulation (Fig 3.43C), whereas the protein was present in the cytoplasm before stimulation.

These findings suggest that the p130Cas/CrkII complex is involved in DR formation.

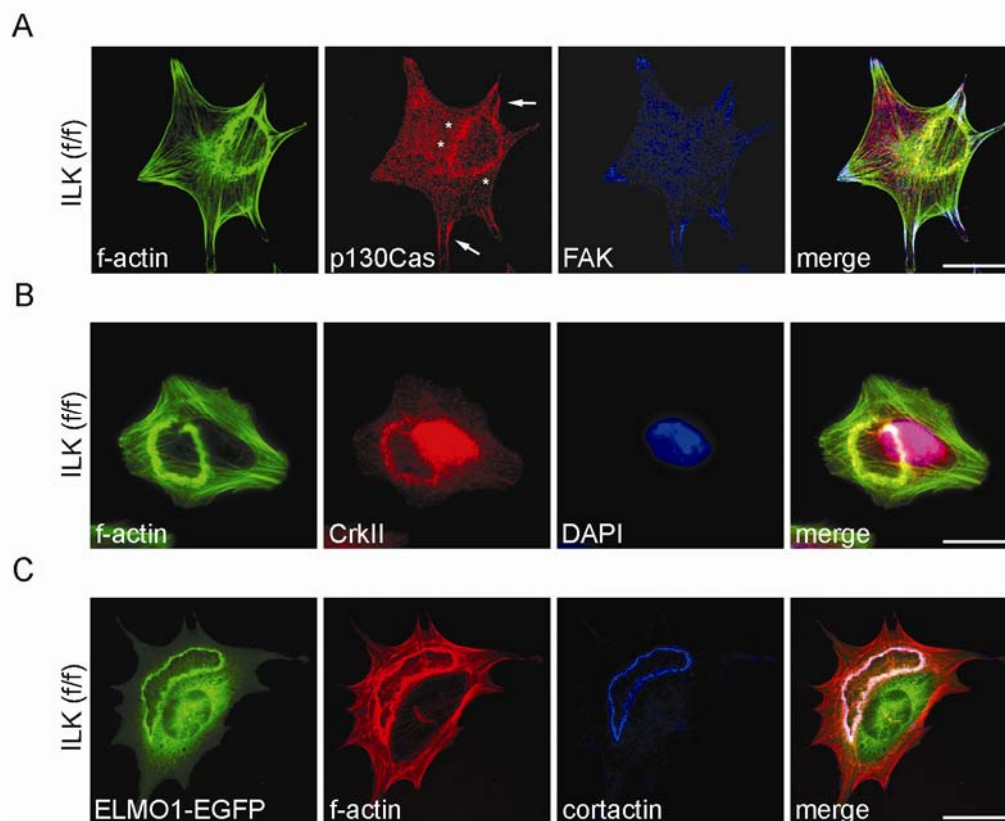


Fig 3.43. Localization of p130Cas, CrkII and ELMO1 into DRs after EGF stimulation. *A.* Merged stack of confocal images showing the localization of p130Cas in DRs in ILK (f/f) fibroblasts. p130Cas is localized in FAs (arrows) as well as DRs (*). *B.* Localization of CrkII in DRs. *C.* Merged confocal stack of images showing immunostaining of ILK (f/f) fibroblasts stably expressing human ELMO1-EGFP. Scale bars: 20 μ m.

3.4.21. p130Cas complexes with ILK and is essential for dorsal ruffling

p130Cas is localized as ILK in FAs and in DRs. In order to check if ILK and p130Cas associate to trigger dorsal ruffling, ILK (-/-) fibroblasts stably expressing full-length ILK-FLAG or ANK-FLAG (Fig 3.31C) were used to perform immunoprecipitation studies. Interestingly, ILK-FLAG is efficiently co-immunoprecipitated with p130Cas but not the N-terminal ANK-FLAG (Fig 3.44A). In the reverse experiment, p130Cas can be co-immunoprecipitated with ILK-FLAG, but not with ANK-FLAG, while both proteins co-immunoprecipitate Pinch1 (Fig 3.44).

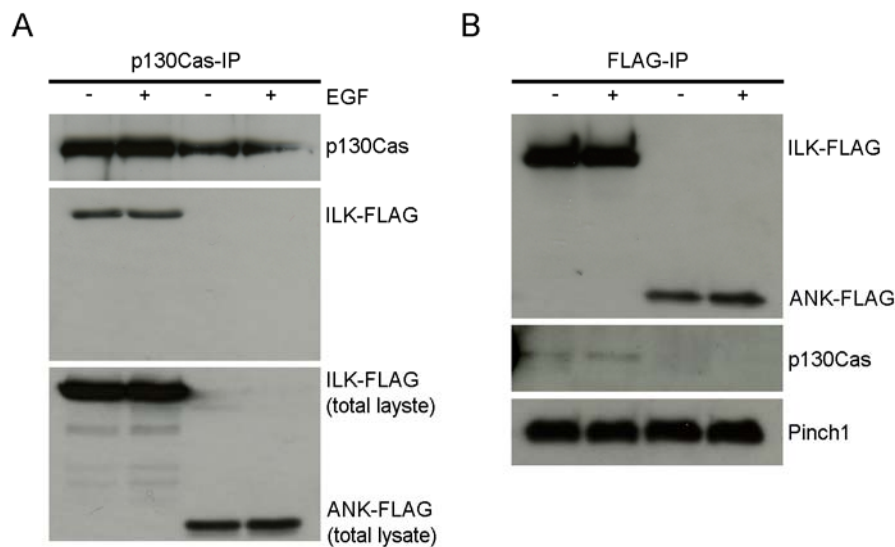


Fig 3.44. Association of ILK and p130Cas. *A. Western blot analysis of a p130Cas-IP. While full length ILK-FLAG can be co-immunoprecipitated with p130Cas, the N-terminal fragment of ILK (ANK-FLAG) does not co-precipitate. B. Western blot analysis of a FLAG-IP. p130Cas can be co-immunoprecipitated with full length ILK-FLAG but not with ANK-FLAG. Note, that both proteins are able to co-precipitate similar amounts of endogenous Pinch1.*

3.4.22. p130Cas expression is essential for dorsal ruffling

To check whether p130Cas is important for dorsal ruffling p130Cas knockdown cell lines were generated. Out of five shRNA constructs, one construct efficiently reduced p130Cas expression levels in ILK (f/f) fibroblasts. While control cells, expressing a scrambled shRNA sequence, showed normal p130Cas levels, a clonal p130Cas knockdown cell line was established with a knockdown efficiency of approximately 85% (Fig 3.45A, B). The expression levels of other proteins directly or indirectly interacting with p130Cas such as ILK, CrkII or FAK were unchanged. The expression levels of Dock180 appeared to be, however, slightly upregulated (Fig 3.45A). Immunostaining confirmed the loss of p130Cas expression from FAs and revealed in agreement with data from primary p130Cas knockout fibroblasts (Honda et al. 1998) that the formation of f-actin stress fibers is impaired in the absence of p130Cas (Fig 3.45C, D). The frequency of DR formation after EGF stimulation was dramatically reduced (Fig 3.45E). In contrast, FN assembly was unchanged in p130Cas knockdown cells (Fig 3.46). These data implicate p130Cas as an essential component of a signalling complex crucial in EGF-induced DR formation.

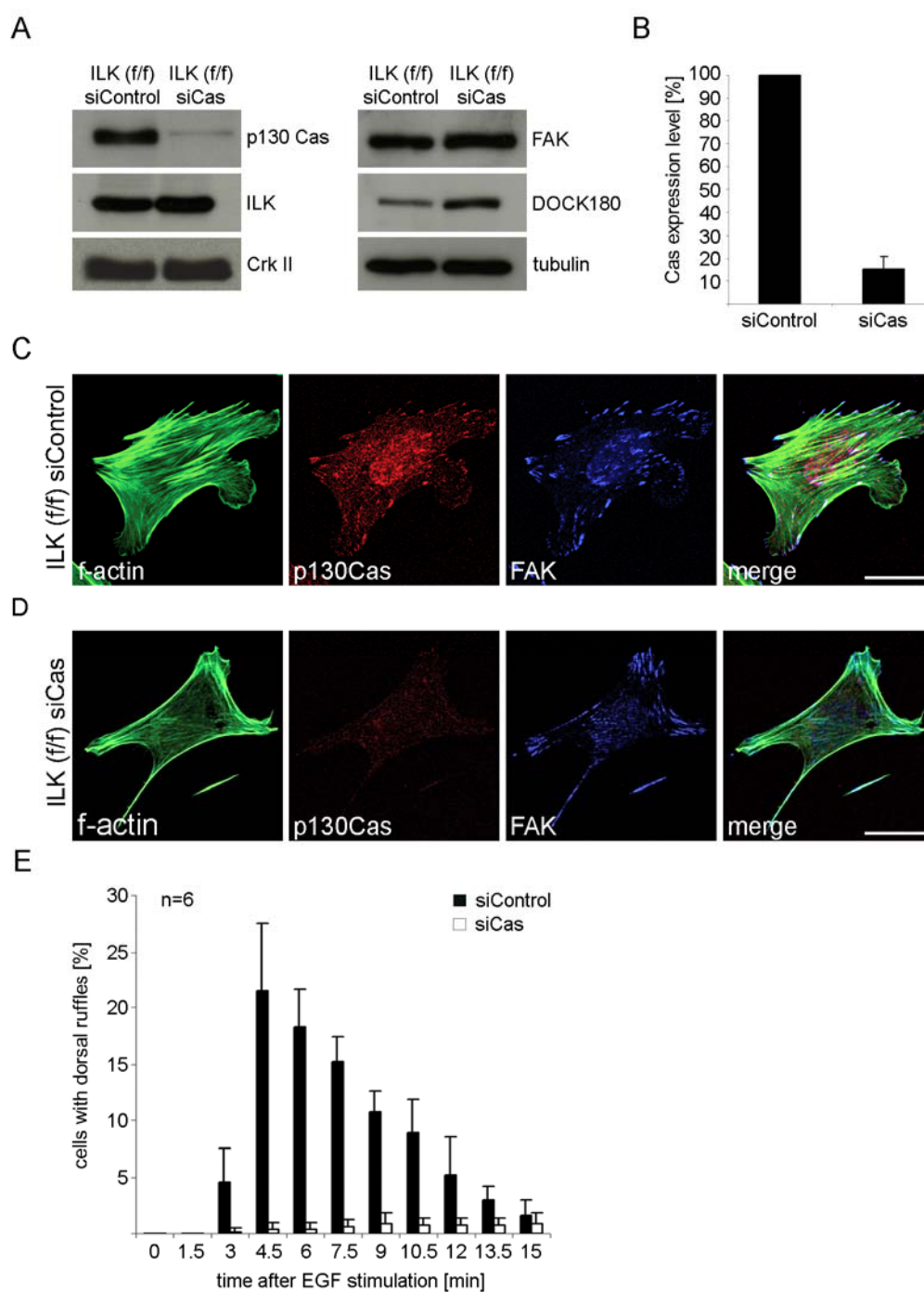


Fig 3.45: Generation and analysis of p130Cas knockdown cell lines. *A.* Western blot analysis of protein lysates from ILK (f/f) siControl and ILK (f/f) p130Cas knockdown cell lines. *B.* Quantification of p130Cas expression in control and p130Cas knockdown cell lines. *C.* Merged stack of confocal images showing the formation of f-actin stress fibers and FAs in control cells. Scale bars: 20µm. *D.* Merged stack of confocal images showing loss of p130Cas expression and impaired stress fiber formation. Scale bar: 20µm. *E.* Quantification of DR formation after EGF stimulation in p130Cas knockdown cells based on 6 independent experiments

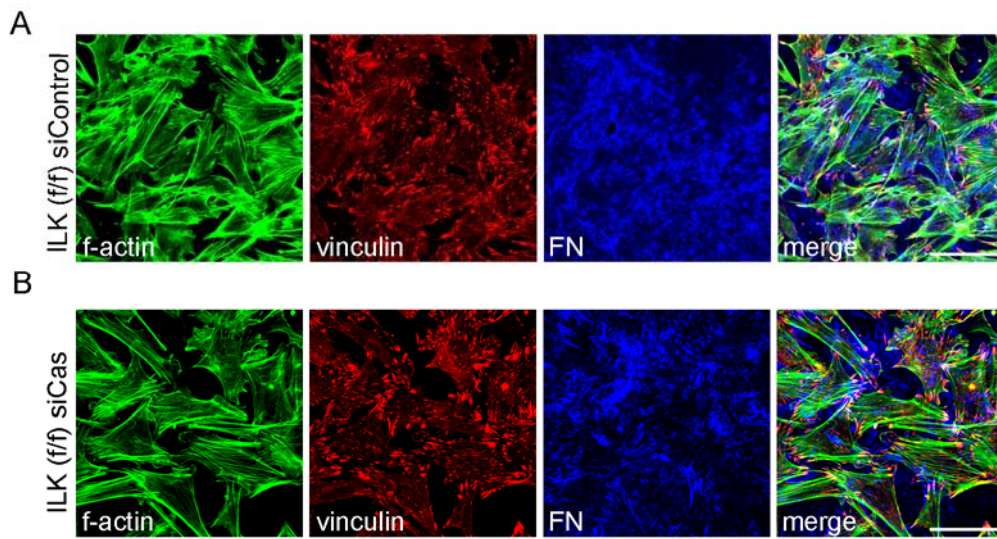


Fig 3.46. Loss of p130Cas does not affect FN fibrillogenesis. *A.* Merged stack of confocal images showing immunostaining of a control ILK (f/f) fibroblasts expressing scrambled shRNA (same picture as in Fig 3.37). Normal FN fibrillogenesis occurred. *B.* Merged stack of confocal images showing immunostaining of a p130Cas knockdown cell line. FN assembly was not affected by loss of p130Cas. Scale bars: 40 μ m.

3.4.23. The GEF Dock180 is indispensable for dorsal ruffling

Rac1 can get activated by a number of GEFs. In order to confirm that the p130Cas/CrkII/ELMO/Dock180 signalling complex is required for dorsal ruffling, ILK (f/f) fibroblasts were depleted of Dock180 by siRNA. Figs. 3.47A, B show the almost complete loss of Dock180 expression. Although Dock180 knockdown cells were spreading much slower than control cells and formed only few lamellipodia during the culture, these cells still formed a normal f-actin cytoskeleton and assembled long stress fibers. Also the formation and appearance of FAs appeared to be normal in Dock180 knockdown cells (Fig 3.47C, D). Furthermore FN assembly occurred normally in these cells (Fig 3.48A, B). However, Dock180 knockdown cells were unable to form DRs after stimulation with EGF, while control cells showed the normal frequency of DR formation. In addition, no DR formation was observed during cells spreading after stimulation with other growth factors such as PDGF or 10% FCS. Similar to fibroblasts expressing dominant negative Rac1 (RacN17) not a single DR was observed (Fig 3.47E). These data strongly indicate that indeed DR formation is regulated in a Dock180-dependent manner.

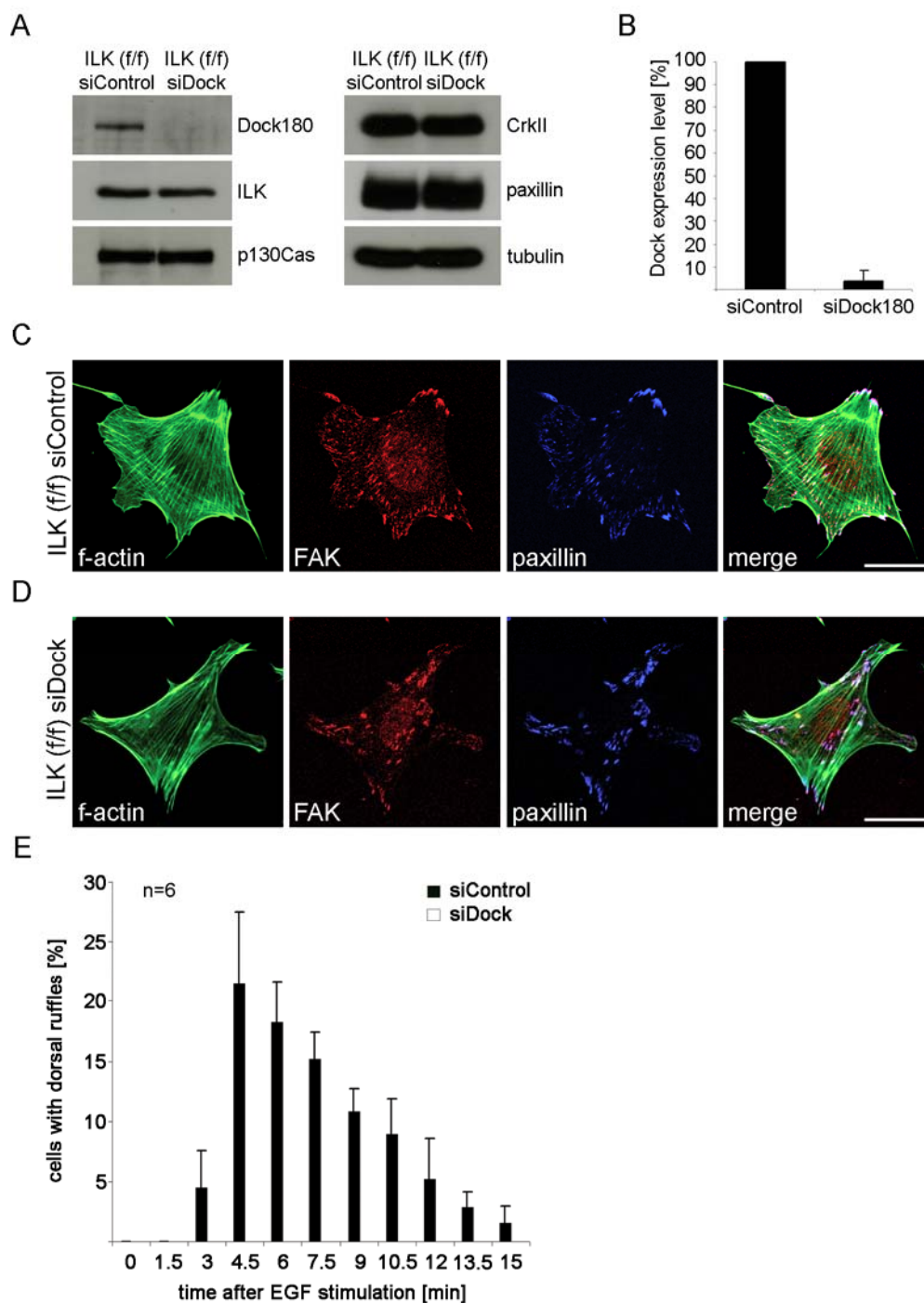


Fig 3.47. Generation and analysis of Dock180 knockdown cell lines. *A.* Western blot analysis of protein lysates from ILK (f/f) control and ILK (f/f) Dock180 knockdown cell lines. *B.* Quantification of Dock180 expression in control and Dock180 knockdown cell lines. *C.* Merged stack of confocal images showing the formation of f-actin stress fibers and FAs in control cells. Scale bar: 20µm. *D.* Merged stack of confocal images showing normal stress fiber and FA formation. Scale bar: 20µm. *E.* Quantification of DR formation after EGF stimulation in control and Dock180 knockdown cells lines based on 6 independent experiments.

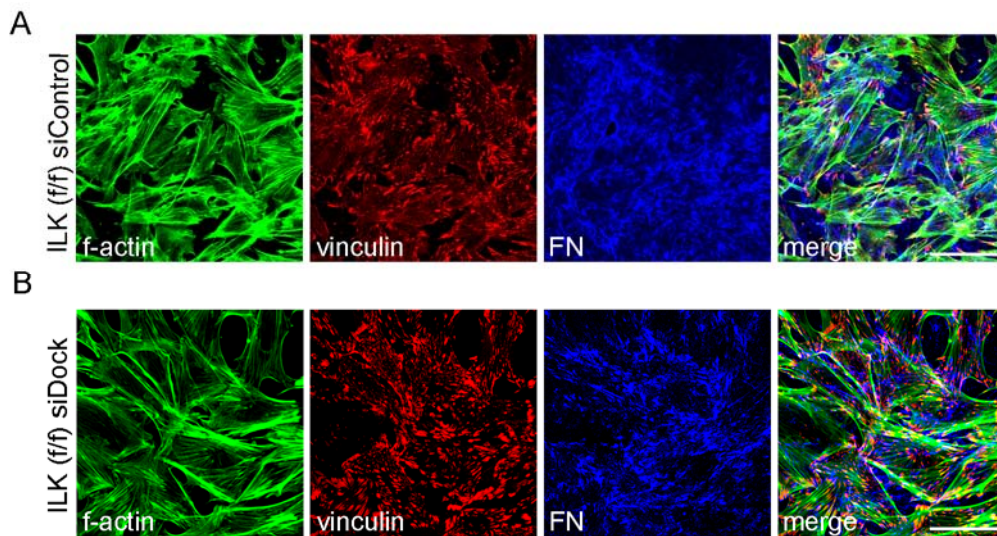


Fig 3.48. Loss of Dock180 does not affect FN fibrillogenesis. *A. Merged stack of confocal images showing immunostaining of a control ILK (ff) fibroblasts expressing scrambled shRNA (same picture as in Fig 3.37). Normal FN fibrillogenesis could occur. B. Merged stack of confocal images showing immunostaining of a Dock180 knockdown cell line. FN assembly is not affected by loss Dock180. Scale bars: 40 μ m.*

3.4.24. Normal plasma membrane organization in ILK (-/-) fibroblasts

The data so far suggested that ILK affects DR ruffle formation by regulating the p130Cas/CrkII activity and consequently the local ELMO1/Dock180-dependent activation of Rac1. An interesting question concerned the mechanism underlying this regulation and the subcellular compartment in which the regulation occurred. It is possible that integrin/ILK signalling facilitates the recruitment of GTPases or GTPase activating molecules into the plasma membrane. Earlier studies have shown that small Rho-GTPases like Rac1 and RhoA are recruited into special structures within the plasma membrane that are characterized by high cholesterol and caveolin-1 levels and hence were named caveolin-rich membrane microdomains. Furthermore, integrin engagement is supposed to be essential for the establishment of caveolin-rich microdomains (also-called “lipid rafts”) at the plasma membrane (del Pozo et al. 2004).

Due to their biochemical properties, lipid rafts can be isolated biochemically by density gradient centrifugation or visualized in culture with fluorescently labelled sphingolipid markers such as cholera-toxin. Although they are thought to be rather heterogenous structures, sphingolipids (especially the gangliosid GM1) are highly enriched in lipid rafts and therefore frequently used as their marker. To check, if p130Cas or Rac1 recruitment could occur in the absence of ILK, a plasma membrane isolation and plasma membrane fractionations were performed. In addition, control and knockout cells were subjected to immunostainings to

visualize cholesterol rich membrane domains during DR formation. As shown in Fig 3.49A, p130Cas (including its phosphorylated form) and Rac1 are normally distributed in ILK (-/-) cells and were detected both in the soluble (s) cytosolic as well as in the particulate (p) plasma membrane fraction. No significant differences before or after EGF stimulation were observed. Moreover, fractionation of the plasma membrane into caveolin-rich membrane fraction (CRM) and non-caveolin-rich membrane fraction revealed that Rac1 and RhoA normally localized into lipid rafts in the absence of ILK indicating that integrins regulate plasma membrane order independently of ILK (Fig 3.49B).

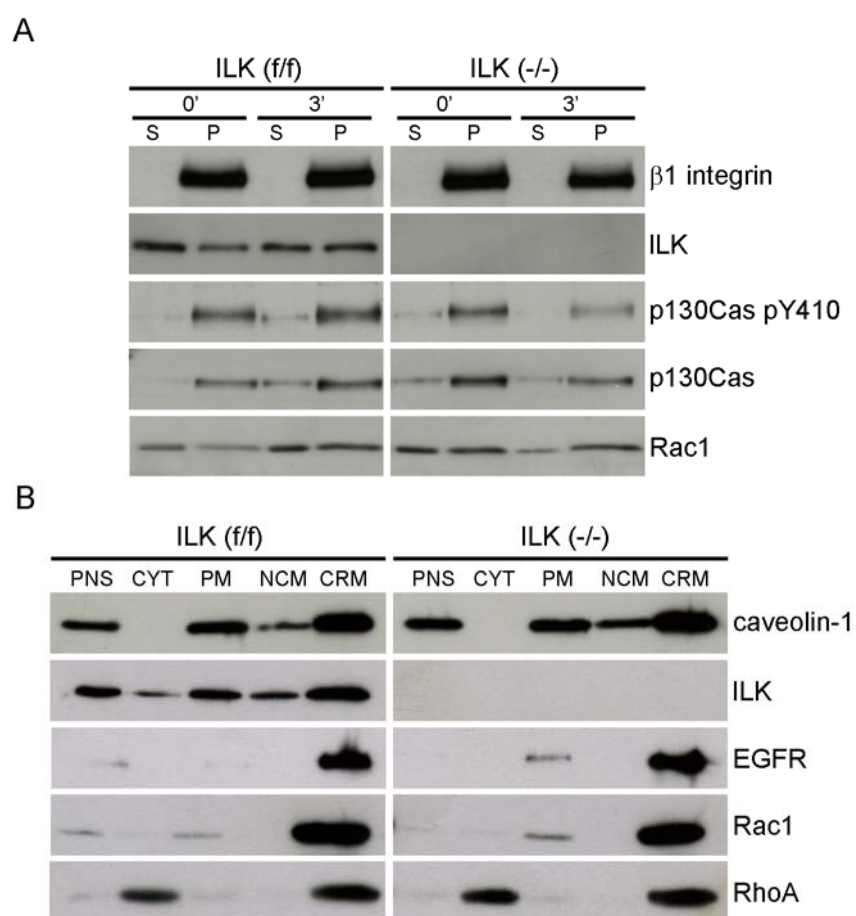


Fig 3.49. Normal localization of p130Cas and Rac1 into the plasma membrane and lipid rafts in ILK (-/-) fibroblasts. **A.** Biochemical analysis of soluble and particulate cell lysates obtained before (0') or 3min (3') after EGF stimulation. No obvious differences could be detected. **B.** Biochemical analysis of plasma membrane preparations. Rac1 can localize normally into the caveolin-rich membrane fraction. PNS: post nuclear supernatant, CYT: cytoplasmic fraction, PM: plasma membrane, NCM: non-caveolin rich membrane fraction, CRM: caveolin-rich membrane fraction. In (B), 2μg protein lysates /lane were loaded.

Lipid rafts are often found at the edges of cells which have been stimulated with growth factors to form peripheral ruffles (del Pozo et al., 2004). In order to test if DRs are cognate

lipid raft structures, ILK (f/f) fibroblasts were stained with cholera-toxin to visualize lipid rafts and cortactin to visualize DRs. While cortactin was strongly localized in DRs, fluorescently labelled cholera-toxin did not stain them (Fig 3.50A). Surprisingly, a higher magnification of the dorsal plasma membrane revealed that cholera-toxin positive areas and cortactin staining were mutually exclusive (Fig 3.50B). In contrast, areas with peripheral ruffles showed colocalization of cholera-toxin and cortactin (Fig 3.50C). A higher magnification further confirmed that at the basal side of the peripheral ruffle, these two markers overlap.

These data demonstrate that DRs are not made from lipid rafts at the plasma membrane. They are rather cytoskeletal structures and are therefore fundamentally different from peripheral ruffles.

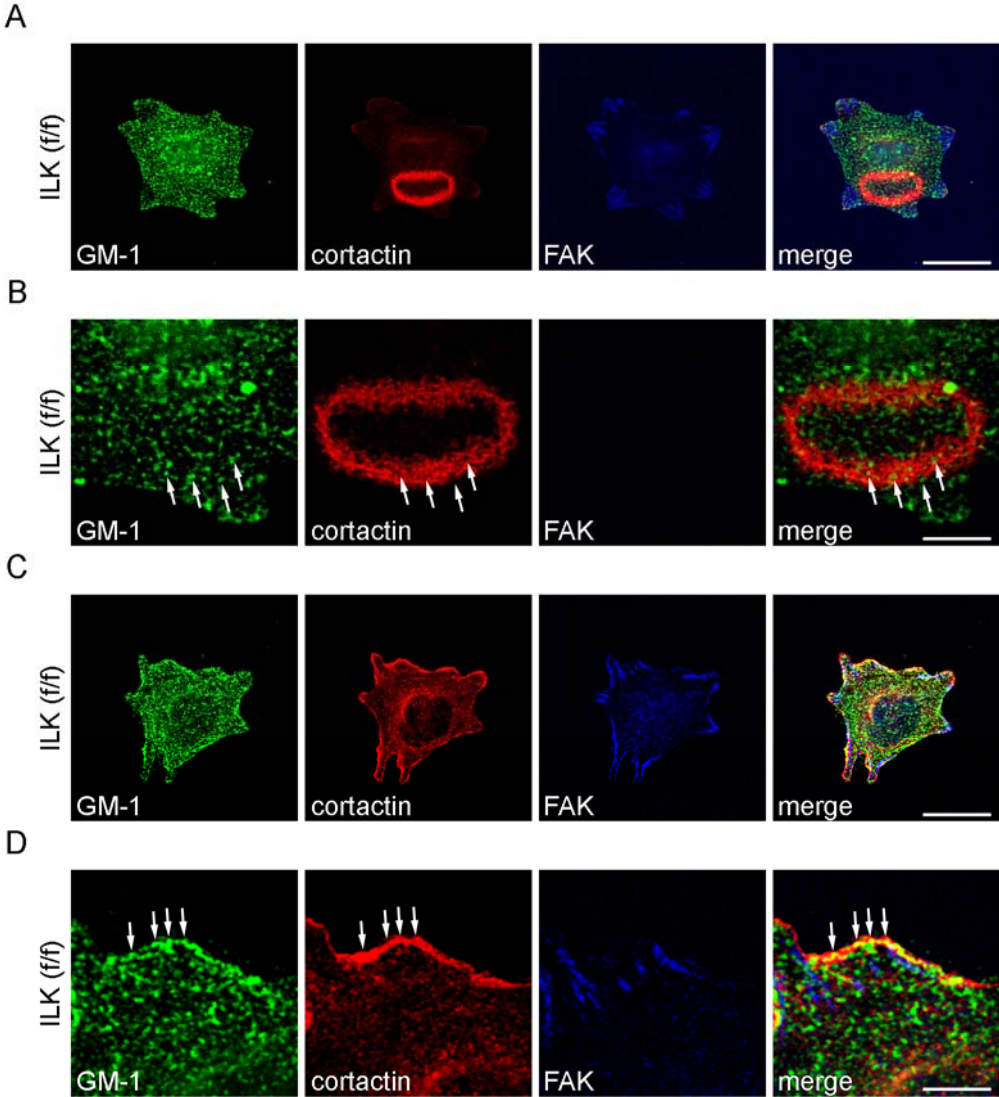


Fig 3.50. DRs and peripheral ruffles are fundamentally different. *A.* Merged stack of a series of confocal images showing an immunostained ILK (f/f) fibroblasts shortly after EGF stimulation forming a DR. **B.**

Magnification of a confocal picture at the dorsal site of the cell. The localization of GM1 and cortactin seemed to be mutually exclusive. Arrows indicate areas of high lipid raft marker intensity that coincides with low staining intensity of cortactin staining C. Merged stack of a series of confocal images showing an immunostained ILK (f/f) fibroblasts shortly after EGF stimulation forming a peripheral ruffle. D. Magnification of a confocal picture at the cell edges at the basal site of the cell. GM1 and cortactin staining overlap (indicated by arrows). Scale bars: 20 μ m (in A, C) and 10 μ m (in B, D).

3.4.25. Cytoskeletal-associated p130Cas is hyperphosphorylated in ILK (-/-) fibroblasts

The experiments above demonstrated that DRs are characterized by their cytoskeletal association. Cytoskeletal structures are typically Triton-X-100 insoluble, which allows to separate them from cytosolic and plasma membrane proteins. To gain deeper insights into the regulation of p130Cas by ILK during dorsal ruffling, the cytoskeletal fraction of ILK (f/f) and ILK (-/-) fibroblasts was prepared before (0min) and after (2min and 6min) EGF stimulation. Very surprisingly, p130Cas was much stronger phosphorylated before stimulation in ILK (-/-) fibroblasts. Stimulation with EGF, however, led to a fast dephosphorylation of p130Cas, such that 6min after stimulation the phosphorylation levels of p130Cas in control and knockout cells were approximately the same. Since p130Cas gets phosphorylated at multiple sites in its substrate binding domain, another phospho-specific antibody was tested on the same lysate. Again, p130Cas was highly phosphorylated in ILK-deficient cells whereas the level of p130Cas phosphorylation in control cells was rather moderate (Fig 3.51A). These biochemical data showed, that cytoskeletal associated p130Cas is hyperphosphorylated in its substrate binding domain when ILK is absent.

The kinase that is thought to be responsible for p130Cas phosphorylation is c-src, which is also known to be essential for growth factor-induced formation of DRs (Boschek et al., 1983, Veracini et al. 2006). To check, if the differences of p130Cas phosphorylation in ILK (-/-) fibroblasts were due to an increased c-src-activity, cells were treated with a src inhibitor (PP1) before the stimulation with EGF. Interestingly, this treatment did not decrease p130Cas phosphorylation in ILK knockout cells, but instead resulted in constitutive and high p130Cas phosphorylation even after EGF stimulation. These data suggest that the p130Cas hyperphosphorylation in ILK (-/-) fibroblasts is not caused by increased c-src kinase activity but rather by decreased activity of protein tyrosine phosphatases. Furthermore, since PP1-treatment inhibited EGF-induced dephosphorylation of p130Cas one would predict that the potential phosphatase(s) should be regulated in a c-src-dependent manner (Fig 3.51B).

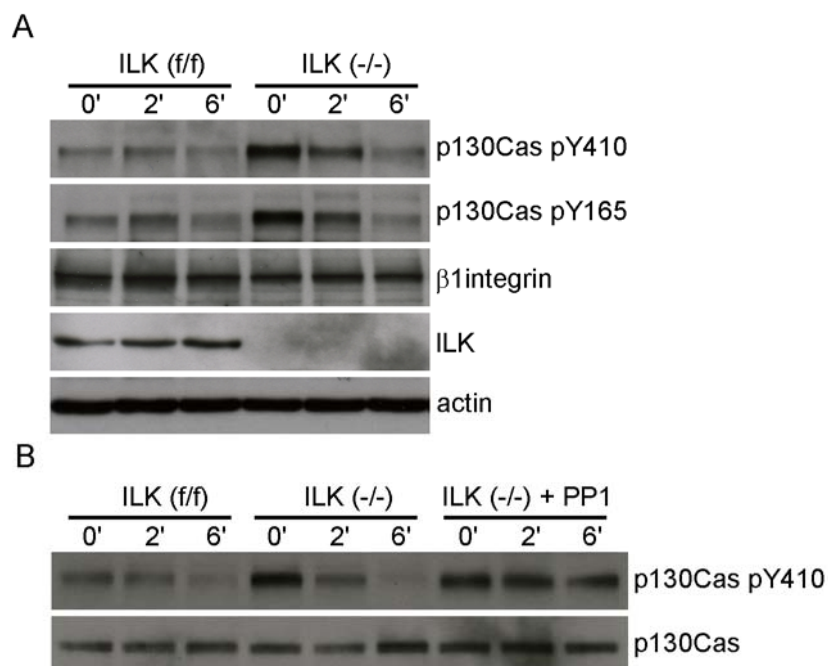


Fig 3.51. Cytoskeletal associated p130Cas is hyperphosphorylated in the absence of ILK. *A. Biochemical analysis of cytoskeletal cell lysates from ILK (f/f) and ILK (-/-) fibroblasts before (0') and after (2', 6') EGF stimulation. B. Biochemical analysis of cytoskeletal cell lysates from ILK (f/f) and ILK (-/-) fibroblasts and from ILK (-/-) fibroblasts which were treated with 5μm of the src inhibitor PP1 prior to EGF stimulation.*

3.4.26. Identification of an ILK-associated protein tyrosine phosphatase by SILAC

To further dissect the mechanism underlying EGF-mediated dorsal ruffling by ILK, ILK-FLAG immunoprecipitates were analyzed by SILAC-based mass-spectroscopy (SILAC-MS) in collaboration with Dr. Matthias Selbach (MPI of Biochemistry, Germany). Cells were cultured in SILAC medium containing isotopically labelled amino acids (Arg0, Arg6 and Arg10) and analyzed during DR formation. Unlabelled cells were lysed before EGF stimulation, Arg6-labelled cells 2min after EGF stimulation and Arg10-labelled cells 6min after EGF stimulation. All cell lysates were pooled and a FLAG-IP was performed. The immunoprecipitate was then analyzed by mass spectroscopy. This very sensitive approach allows identifying proteins which interact with ILK before and after EGF-treatment. Interestingly, out of more than 600 proteins which are co-immunoprecipitated and detected by MS only one protein was found to be strongly enriched after EGF stimulation: this protein turned out to be a src-dependent protein tyrosine phosphatase called LMW-PTP (low

molecular weight - protein tyrosine phosphatase). These findings suggest that EGF stimulation may trigger the recruitment of LMW-PTP to ILK, which in turn affects the phosphorylation of the p130Cas substrate domain.

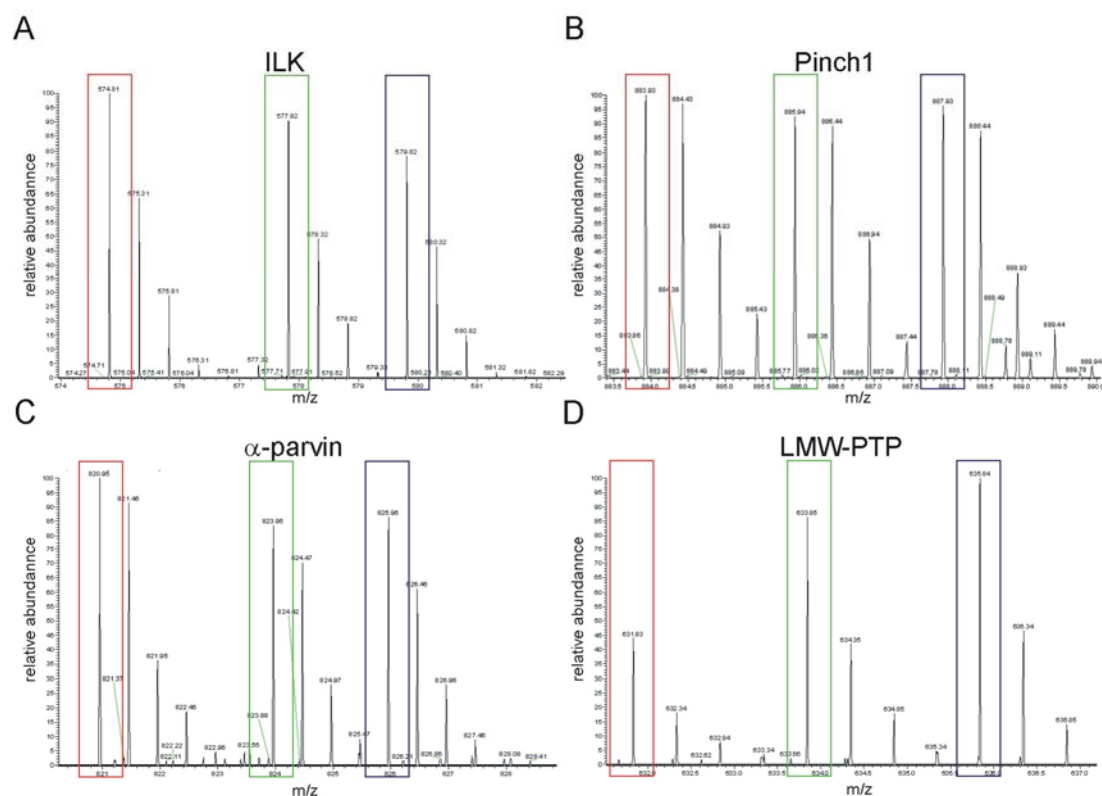


Fig 3.52 Relative abundance of (co)-immunoprecipitated proteins before, 2min and 6min after EGF stimulation. **A.** Control: the ratio of immunoprecipitated ILK was approximately 1:1:1. The red box highlights the signal from protein lysates of unlabelled cells (before stimulation), the green box highlights the signal from protein lysates of Arg6 labelled cells (2min after EGF), the blue box highlight the signal from protein lysates of Arg10 labelled cells (6min after EGF stimulation). **B.** The direct interaction partner Pinch1 is detected in the same ratios as ILK (1:1:1) indicating no dynamic interaction during EGF stimulation. **C.** α -parvin is detected in the same ratios than ILK (A). **D.** In the same lysate as in (A), (B) and (C), LMW-PTP is much more abundant after 2 and 6min as before the stimulation, indicating an increased association of this phosphatase with ILK signalling complexes after EGF treatment.

In the future, the role of the ILK-LMW-PTP interaction during DR formation will be analyzed in more detail. The analysis will include the generation and characterization of LMW-PTP knockdown cell lines as well as p130Cas-LMW-PTP-ILK interaction studies by immunoprecipitations. Furthermore, the phosphorylation levels and the phosphatase activity of LMW-PTP in control and ILK knockout cells will be tested.

4. Discussion

This project was started more than 4 years ago, at a time, when ILK was thought to act as an integrin-associated kinase that modulates Wnt signalling pathways by GSK-3 β phosphorylation, cell survival by PKB/Akt phosphorylation and epithelial-mesenchymal transitions by the regulation of E-cadherin expression (Novak and Dedhar 1999; Persad and Dedhar 2003; Oloumi et al. 2004). Since ILK was also found to be frequently overexpressed in tumours and metastasis, it was regarded as a proto-oncogene and almost all of the ILK-related effects were attributed to its potential kinase activity. The publications about loss-of-functions studies in *Drosophila* and *C. elegans* reporting that ILK's kinase activity is dispensable for invertebrate development were a surprise and raised the first doubts about ILK's molecular function (Zervas et al. 2001; Mackinnon et al. 2002). The present study was initiated to analyse the role of ILK in a mammalian system.

Now, 4 years later, the understanding about the functional properties of ILK has dramatically changed. It is widely accepted that ILK acts mainly as a regulator of integrin-triggered actin dynamics *in vitro* and *in vivo* and is less or not important as a kinase and hence also termed pseudokinase (Boudeau et al. 2006). The data presented in this study significantly contributed to our current understanding of the function of ILK (Grashoff et al. 2003; Sakai et al. 2003; Grashoff et al. 2004).

4.1. The analysis of ILK *in vivo*

4.1.1. General implications about the role of ILK *in vivo*

Deletion of ILK in mice causes embryonic lethality at peri-implantation stage (Sakai et al. 2003). In comparison to other FA proteins this phenotype is exceptionally severe. For example, targeted deletion of talin1, vinculin, paxillin or FAK also results in embryonic lethality, however, at later stages with much milder phenotypes (Fig 4.1.). Loss of talin1 expression impairs mesodermal cell migration at gastrulation which arrests development at E8.5-9.5 (Monkley et al. 2000). Loss of paxillin results in defective somitogenesis and impaired heart development, which closely resembles the phenotype of FN and $\alpha 5$ integrin knockout mice suggesting that paxillin is a crucial mediator of FN- $\alpha 5\beta 1$ signalling (Hagel et al. 2002). Vinculin knockout mice display midline fusion defects, impaired development of the heart and the nervous system and die at E10.5 (Xu et al. 1998). Interestingly, also mice lacking Pinch1 as well as α -parvin – although thought to form a complex with ILK (see below) - die later than ILK-deficient embryos (Li et al. 2005, unpublished observation).

Although several knockout phenotypes could be due to a certain degree of redundancy, loss of talin1 may be compensated by talin2 or α -parvin by β - and γ -parvin, these data demonstrate the central role of ILK as an integrin-associated protein (Fig 4.1).

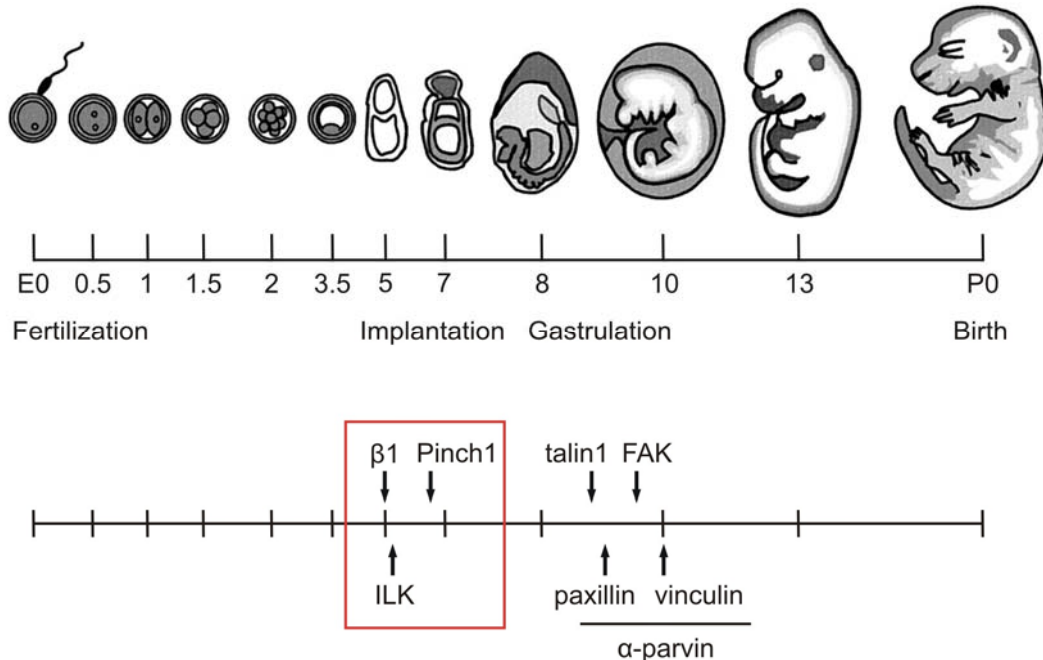


Fig 4.1. Knockout phenotypes of FA proteins. Deletion of *ILK* results in the most severe phenotype demonstrating the essential role of this protein during embryonic development (modified from Bouvard et al., 2001).

4.1.1.1. A comparison of the $\beta 1$ and *ILK* knockout phenotypes

Deletion of the *ILK* and the $\beta 1$ integrin genes, respectively, leads to embryonic lethality at around E5.5 (Fassler and Meyer 1995; Sakai et al. 2003). The analysis of EBs derived from $\beta 1$ - or *ILK*-null ES cells showed that the defects that arrest development differ between the two mouse strains (Fig 4.2).

Deletion of $\beta 1$ integrin abolishes BM formation due to reduced expression of the laminin $\alpha 1$ chain and laminin111 assembly (Aumailley et al. 2000). Addition of exogenous laminin111 rescued the BM assembly defect of $\beta 1$ integrin-null EBs suggesting that $\beta 1$ integrins are not essential for BM assembly *per se*. Once the laminin synthesis defect is overcome, $\beta 1$ -null EBs can also develop an epiblast and cavitate (Li et al. 2002).

Deletion of *ILK* does not impair synthesis of BM components and their assembly. Instead, loss of *ILK* causes an f-actin polarization defect in the epiblast and impairs cavitation which arrests development later as loss of $\beta 1$ integrin expression (Sakai et al. 2003). Since $\beta 1$ -null EBs rescued by the addition of laminin111 can form cavities it is possible that *ILK* regulates epiblasts polarization independently of integrins. It seems, however, more likely that *ILK* also

regulates epiblasts polarization downstream of other integrin subunits which compensate for the loss of $\beta 1$ integrin.

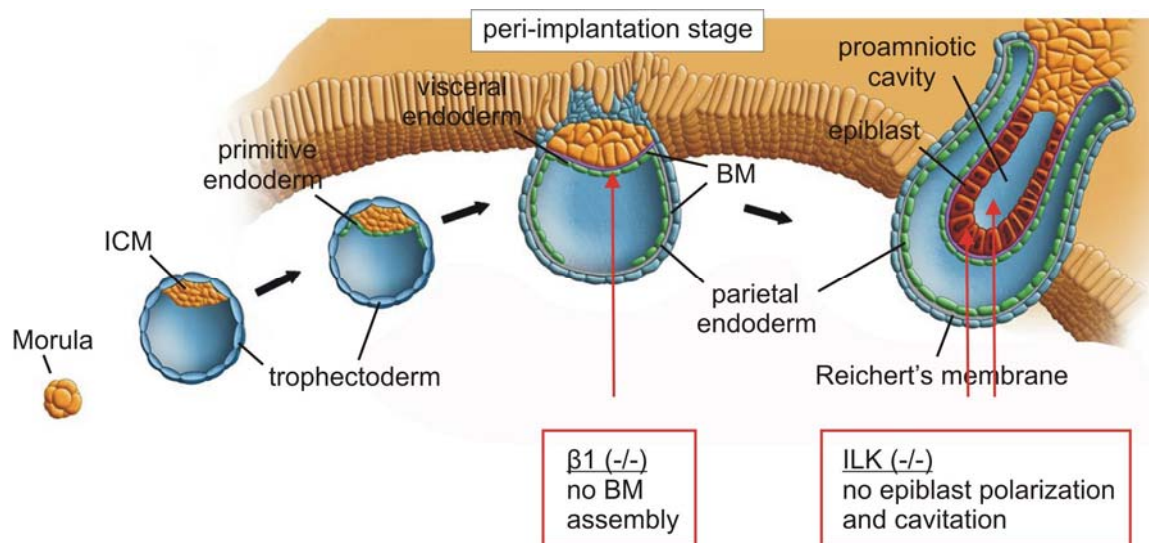


Fig 4.2. No BM assembly in $\beta 1$ -null EBs, abnormal epiblast polarization and cavitation in ILK-null EBs. Loss of $\beta 1$ integrin abrogates BM deposition while loss of ILK affects epiblast polarization and cavitation.

4.1.1.2. The ILK-Pinch-parvin complex-implications from *in vivo* models

Cell culture experiments and biochemical analyses suggested that ILK, Pinch and parvin form a ternary complex which precedes the localization of each these proteins into their subcellular localization (Zhang et al. 2002; Fukuda et al. 2003). Depletion of Pinch1 from HeLa cells by siRNA led to the degradation of ILK and α -parvin and *vice versa*, reduction of ILK resulted in markedly reduced Pinch1 and α -parvin levels, indicating that ILK, Pinch and parvin are mutually dependent in maintaining their stability (Fukuda et al. 2003). Therefore, it was expected that the deletion of ILK, Pinch or parvin in mice would lead to similar if not identical phenotypes. Indeed deletion of ILK or Pinch1 leads in both cases to peri-implantation lethality which is, however, caused by different defects (Sakai et al. 2003; Li et al. 2005).

The majority of EBs generated from Pinch1-null ES cells can form extended cavities and progress much further than ILK-null EBs. Moreover, Pinch1-null EBs display severe cell-cell adhesion defects in the endoderm and the epiblast. Cell-cell adhesion defects were never observed in ILK-deficient EBs although ILK has been implicated in controlling E-cadherin expression either through GSK-3 β phosphorylation or snail activation ((Wu et al. 1998; Tan et al. 2001; Li et al. 2005). Targeted deletion of α -parvin in mice results in embryonic lethality at even later stages (around E8.5-12.5, Motanez and Fässler, unpublished), which could however be due to compensation by β -parvin.

These data suggest that a fraction of the total ILK, Pinch1 and α -parvin proteins may act independently from each other. My observation that Pinch1 can localize to FAs of ILK knockout fibroblasts is supporting such a notion. In agreement with these observations ILK has been detected in FAs of Pinch1 knockout cells (Stanchi et al. 2005). In the future it will be necessary to identify and characterize those cellular processes regulated by ILK in a Pinch- and parvin-independent manner.

4.1.2. Regulation of the ECM by ILK-implications from β 1 integrin and ILK knockout mice

The analysis of EBs revealed that ILK is not required for the deposition and assembly of the first embryonic BM (Sakai et al. 2003). The analysis of Cre/loxP-mediated ILK ablations in mice further confirmed that ILK is not crucial for ECM assembly but indicated that ILK is indispensable for the maintenance of BMs especially after exposure to mechanical stress.

4.1.2.1. No differences in the ECM of the cartilage in the absence of ILK

β 1 integrins play an important role for the modulation of the ECM both in cartilage and skin. Deletion of α 10 or β 1 integrins in chondrocytes leads to reduced collagen fibril density and a disorganized collagen network in the cartilage (Aszodi et al. 2003; Bengtsson et al. 2005). However, the ECM is only mildly affected in newborn mice indicating that the assembly of a collagen network can occur in the absence of collagen-binding integrins. The fact that the matrix defects in β 1-deficient tissues become more pronounced with time could have different reasons. The dramatically altered cell-matrix ratio in the mutant cartilage of adult mice (caused by reduced proliferation) could indirectly affect the organization of the collagen network. Alternatively, integrins could be important during stress-induced remodelling of the ECM. Although muscle contractions are thought to generate mechanical strain on the cartilage already during embryogenesis, the mechanical load that acts on the cartilage during adulthood is disproportional higher (Adams 2006). This may explain, why at the newborn stage only very mild ECM defects were observed, while at alter later stages the matrix is profoundly distorted in the absence of β 1 integrins. Deletion of ILK in chondrocytes does not result in any obvious defects of the ECM at newborn stage (Grashoff et al. 2003). Since these knockout mice die shortly after birth it is unclear whether ILK is similarly important for ECM remodelling in adult cartilages. To address this point, it will be necessary to generate mice with a deletion of ILK only in the appendicular skeleton but not in the palatal shelves to prevent cleft palate formation and perinatal lethality. The use of transgenic mice in which Cre-expression is driven by a Prx-1 promoter should be suitable since Prx-1 (pair-related

homeobox gene 1) is almost exclusively expressed in the early limb bud mesenchyme (Logan et al. 2002).

4.1.2.2. Disruption of the dermal-epidermal BM in the absence of ILK

Deletion of $\alpha 3$ or $\beta 1$ integrin in keratinocytes impairs the integrity of the BM which is in part caused by incomplete processing of BM components such as laminin332 or collagenVII (Brakebusch et al. 2000; DiPersio et al. 2000; Raghavan et al. 2000). Interestingly, only the BM along the dermal-epidermal junction is affected by the loss of $\beta 1$ integrins but not the BM of HFs (Brakebusch et al. 2000). This could be explained by the continuous exposure of the epidermis to mechanical stress which is comparatively lower at the BM of the HF. Deletion of ILK in the epidermis leads to similar BM defects characterized by massive diffusion of BM components into the dermis which becomes more severe with age. Since these knockout mice fail to display obvious defects along the BM of HFs it seems likely that ILK remodels the ECM or maintains the BMs in response to mechanical stress but plays no or only a subtle role for the assembly of these structures *per se*.

This notion is supported by the analyses of mice with a deletion of ILK in podocytes, which form the blood filter in the glomerulus of the kidney. The tight interaction of podocytes with the glomerular BM is critical to maintain the filtration barrier against the high transcapillary pressure gradient. ILK knockout mice are completely normal at birth but die within 19 weeks due to terminal renal failure (El-Aouni et al. 2006). Also these data suggest that ILK is not required for the assembly but rather the maintenance of BMs.

4.1.3. The impact of ILK on cell proliferation

An interesting observation of my study is that loss of ILK profoundly affects cell proliferation. While deletion of ILK in the cartilage leads similarly as the deletion of $\beta 1$ integrin to reduced cell proliferation (Aszodi et al. 2003; Grashoff et al. 2003) loss of ILK in keratinocytes results in increased cell proliferation.

4.1.3.1. Reduced cell proliferation of ILK-deficient chondrocytes

The proliferation defect of $\beta 1$ integrin knockout chondrocytes is caused by at least three distinct defects. First, loss of $\beta 1$ integrin expression results in upregulation of FGFR-3 stimulating the nuclear translocation of STAT proteins which in turn induces the expression of cell cycle inhibitors such as p16 or p21 decelerating cell proliferation (Aszodi et al. 2003). Secondly, loss of $\beta 1$ integrin impairs cytokinesis leading to bi-nucleation of chondrocytes.

Finally, the reduced adhesion as well as the pronounced f-actin defects may constrain cell cycle progression.

Also ILK knockout chondrocytes display proliferation defects (Grashoff et al. 2003). In contrast to the situation in $\beta 1$ knockout mice no cytokinesis defect was observed and the expression of FGFR-3 was also normal in the absence of ILK (Aszodi et al. 2003; Grashoff et al. 2003). Since no obvious changes in GSK-3 β phosphorylation were detected which would indicate a more direct regulation of the cell cycle by ILK (D'Amico et al. 2000) the reduced proliferation rate is most likely caused by the severely impaired organization of the f-actin cytoskeleton as well as the reduced adhesion of chondrocytes. It is well established that cell adhesion itself promotes cell cycle progression. 3T3 cells which are kept in suspension will not proliferate or initiate DNA synthesis until they are allowed to attach (Otsuka and Moskowitz 1975). Another important determinant of cell proliferation could be the cell shape of ILK knockout chondrocytes. Donald Ingber and colleagues could show that the size of cells is sufficient to affect cell proliferation (Huang et al. 1998). Endothelial cells that were attached to small adhesive islands stopped proliferation while the same cells attached to large adhesive areas progressed through the cell cycle. Since ILK-deficient chondrocytes displayed reduced adhesion to the ECM and were in addition significantly smaller than control cells it is tempting to speculate that this together with the distorted actin cytoskeleton could have caused the reduced proliferation rate.

4.1.3.2. Increased cell proliferation in ILK-deficient keratinocytes

In contrast to $\beta 4$ integrins which primarily fulfil an adhesive function at the dermal-epidermal junction (Dowling et al. 1996; van der Neut et al. 1996), $\beta 1$ integrins are thought to play an important role in epidermal cell proliferation. Fiona Watt and colleagues described more than 10 years ago that a high $\beta 1$ integrin expression directly correlates with a high proliferation potential (Jones and Watt 1993; Jones et al. 1995) whereas $\beta 4$ integrin expression did not. Transgenic mice expressing $\beta 1$ integrin in suprabasal cell layers showed hyperproliferation in both basal and suprabasal keratinocytes (Carroll et al. 1995) and consequently deletion of $\beta 1$ integrin in keratinocytes significantly reduced the proliferation rates of basal keratinocytes (Brakebusch et al. 2000; Raghavan et al. 2000).

Surprisingly, ILK-K5 knockout mice did not display reduced proliferation rates in the epidermis but instead showed even a slight increase in cell proliferation. Furthermore, loss of ILK leads to suprabasally located proliferating cells which express basal marker proteins such as keratin 5, $\beta 1$ and $\beta 4$ integrin. A possible explanation for the ectopic location of $\beta 1$ integrin positive cells could be the reduced $\beta 1$ integrin-mediated adhesion followed by the

detachment of proliferating basal keratinocytes. Most importantly, these data demonstrate that ILK is not required for β 1-dependent cell proliferation in keratinocytes.

Altogether our data suggest that ILK does not act as a ubiquitous cell cycle regulator for example by phosphorylating GSK-3 β but rather modulates cell proliferation in a cell type-dependent manner most likely through effects on the actin cytoskeleton.

4.1.4. ILK is dispensable for the phosphorylation of PKB/Akt or GSK-3 β

A number of *in vitro* experiments suggested that ILK regulates the activity of the signalling proteins GSK-3 β and PKB/Akt by direct phosphorylation (Delcommenne et al. 1998; Persad et al. 2001) and thereby modulates a number of signal transduction pathways such as β -catenin translocation to the nucleus (Novak et al. 1998), E-cadherin expression (Wu et al. 1998), the activity of the transcription factor AP-1 (Troussard et al. 1999), the binding of the cAMP responsive element to the cyclinD1 promoter (D'Amico et al. 2000), expression of MMP-9 (Troussard et al. 2000), the expression of the E-cadherin repressor snail (Tan et al. 2001), the activity of NF- κ B and iNOS expression (Tan et al. 2002) and tau phosphorylation (Mills et al. 2003)

One of the most far reaching findings of my studies is that ILK is not essential as a kinase particularly with respect to PKB/Akt or GSK-3 β phosphorylation. Loss of ILK expression in chondrocytes, fibroblasts and keratinocytes did not cause changes in the phosphorylation levels of GSK-3 β as well as PKB/Akt (Sakai et al. 2003; Grashoff et al. 2003). Importantly, our data do not confute that ILK might be able to phosphorylate GSK-3 β or PKB/Akt. They only demonstrate that if ILK is indeed a kinase the catalytic activity is certainly not essential for the phosphorylation of these and likely other proteins and consequently for the regulation of their signalling pathways. The analysis of ILK's kinase activity *in vitro* points to the same direction; re-expression of wt-ILK or three different kinase-dead ILK mutants (R211A, S343A, and E359K) as well as a mutant described to act as a constitutive active ILK (S343D) could all equally rescue the severe phenotype of ILK knockout fibroblasts. It should be noted that these data are in line with the analysis of ILK in invertebrates (Zervas et al. 2001; Mackinnon et al. 2002) which showed that re-expression of kinase-dead ILK versions in ILK-deficient flies and nematodes fully rescues development. Other studies also revealed that ILK is dispensable for PKB/Akt or GSK-3 β phosphorylation. Deletion of ILK in the dorsal forebrain of mice leads to severe cortical lamination defects. However, cortical extracts from ILK knockout mice revealed normal phosphorylation levels of GSK-3 β and PKB/Akt (Niewmierzycka et al. 2005). Depletion of ILK from endothelial cells by siRNA did also not

affect the phosphorylation level of PKB/Akt (Vouret-Craviari et al. 2004). Finally, the same group which demonstrated the important role of ILK in PKB/Akt phosphorylation recently reported that siRNA-depletion of ILK or the inhibition of ILK kinase activity by small molecular inhibitors affected phosphorylation of PKB/Akt only in cancer cell lines but not in untransformed epithelial and mesenchymal cells (Troussard et al. 2006).

If ILK has any crucial catalytic activity *in vivo* remains to be investigated and several experiments will be necessary to fully understand the role of ILK as a kinase. First, the generation of ILK-kinase-dead mice will allow addressing the importance of ILK's catalytic activity under physiological conditions. Secondly, the role of the ILK kinase activity under pathological conditions could be tested with control and kinase-dead ILK mutant mice in a tumour model. Finally, the determination of the ILK crystal structure would be certainly helpful to understand how ILK could act as a kinase lacking crucial amino acids which are essential for the catalytic activity of other kinases (Legate et al. 2006).

4.1.5. ILK is essential for the regulation of the f-actin cytoskeleton

The most obvious consequence of ILK deletion *in vivo* and *in vitro* is the impaired organization of the f-actin cytoskeleton and the associated cell shape changes. ILK-null EBs failed to polarize the f-actin cytoskeleton in the epiblasts which coincided with malformations of the epiblast cells that were almost indistinguishable from cells of the inner cell mass (Sakai et al. 2003). In the cartilage, the usually cortical f-actin staining around growth plate chondrocytes appeared discontinuous in ILK knockout mice and the flattened chondrocytes which develop typical columnar structures in normal growth plates were largely missing in the absence of ILK (Grashoff et al. 2003). In the epidermis, loss of ILK impaired the polarization and the cell shape of basal keratinocytes corresponding to f-actin mislocalizations. All cell types that were analyzed *in vitro*, primary chondrocytes, primary keratinocytes and immortalized fibroblastic cell lines, displayed dramatic alterations of the cell shape that were in all cases associated with abnormal stress fiber and FA formation (Grashoff et al. 2003; Sakai et al. 2003). Therefore, our data identify ILK as one of the most crucial integrin-associated regulators of the f-actin cytoskeleton (Grashoff et al. 2004; Legate et al. 2006).

4.2. The analysis of ILK *in vitro*

To understand in more detail how ILK regulates the f-actin cytoskeleton, immortalized control and ILK knockout fibroblasts were subjected to two different experiments. First, the dynamics of f-actin reorganization in response to cell adhesion was analyzed in cell spreading assays. Second, the ability of ILK (f/f) fibroblasts to form DRs was exploited to study the role of ILK during growth factor induced f-actin reorganizations.

4.2.1. ILK is essential for stress fiber formation and cell spreading

In all cell lines tested, deletion of ILK caused a pronounced cell spreading defect associated with poor stress fiber and FA formation (Grashoff et al. 2003; Sakai et al. 2003). A detailed analysis in fibroblasts revealed that this phenotype is caused by several defects. First, deletion of ILK leads to reduced adhesion of fibroblasts to ECM proteins such as FN, VN or collagen type I contributing to the delayed onset of cell spreading (Sakai et al. 2003). Since the formation of stress fibers and FAs never reaches full maturity the reduced cell spreading cannot be caused exclusively by the cell adhesion defect. This notion is supported by the observation that endothelial cells which were depleted of ILK by siRNA showed an increase in cell adhesion but still displayed a prominent cell spreading defect (Vouret-Craviari et al. 2004).

Second, although the formation of talin-, vinculin- and paxillin-containing FCs occurred normally in the absence of ILK their maturation into large FAs or fibrillar adhesions was significantly impaired and associated with abnormal stress fiber formation. One reason for the defective FA maturation and stress fiber formation could be the lack of force generation in ILK (-/-) fibroblasts.

Previous reports demonstrated that the size of FAs correlates with the mechanical force applied to the adhesion site (Riveline et al., 2001; Galbraith et al., 2002). On the other hand, the formation of stress fibers only occurs when cells are appropriately anchored to the substrate. Therefore, both the formation of FAs and stress fibers depends on the generation of mechanical forces (Riveline et al. 2001; Hinz and Gabbiani 2003). The mechanical strain is usually generated intracellularly by actin-myosin-dependent pulling forces. The activation of the small GTPase RhoA activates the Rho-associated kinase (ROCK), which in turn (i) phosphorylates and thereby inhibits the myosin light chain (MLC) phosphatase and (ii) activates MLC kinase. Both events increase MLC phosphorylation and actin myosin contractility. Alternatively, it has been shown that external forces can induce FA assembly in a ROCK-independent manner through processes that involve mDial activation and most

likely actin polymerization (Riveline et al. 2001). However, since we observed neither gross differences in the activation levels of RhoA nor in the phosphorylation status of MLC or differences in G/F actin levels in ILK (-/-) cells it seems unlikely that the defective FA maturation is caused by a loss of actin-myosin contractility. It could instead be that ILK is mechanically required for the anchorage of f-actin fibers at FAs, especially when internal or external forces are applied to the actin cytoskeleton (Fig 4.3). This would also explain why ILK (-/-) cells failed to form fibrillar adhesions whose formation critically depends on the generation of actin-myosin pulling forces

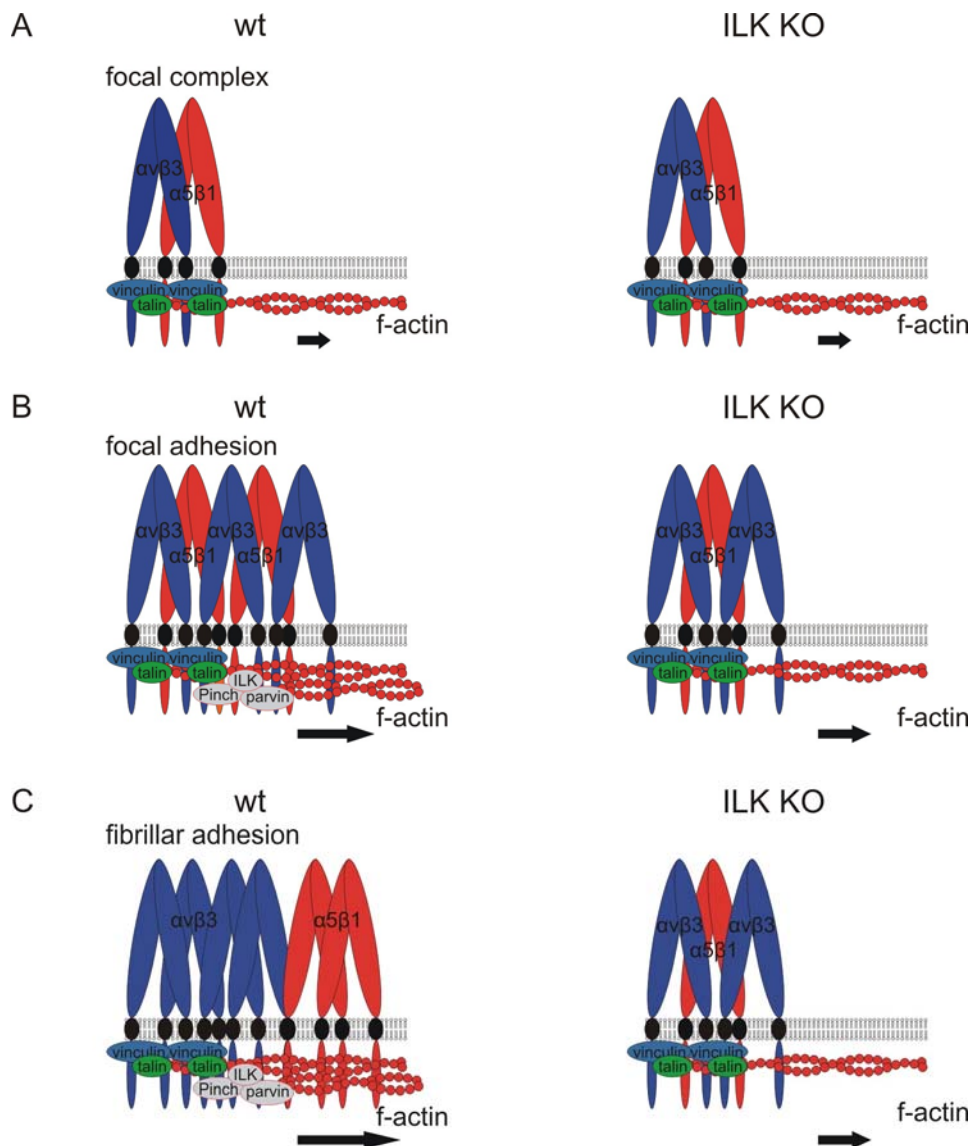


Fig 4.3. Requirement of ILK for the generation of pulling forces in FAs. *A.* The mechanical forces required for the formation of FCs are rather low and FCs develop normally in ILK (-/-) fibroblasts. *B.* The maturation of FAs is accompanied by an increase in actin-myosin-dependent pulling forces. The formation of mature FAs is disturbed in the absence of ILK. *C.* The formation of fibrillar adhesions requires very higher actin-myosin pulling forces. Fibrillar adhesions are completely absent in ILK-deficient fibroblasts.

The hypothesis that ILK is essential for the generation and/or transmission of pulling forces along the f-actin-integrin connection would provide an explanation for the impaired FA and fibrillar adhesion formation *in vitro* and would be in line with the observation that several *in vivo* phenotypes are triggered by mechanical stress (see also 4.1.2).

Deletion of ILK in *Drosophila* causes a disruption of the f-actin network from the plasma membrane (Fig 1.11), which is likely induced by embryonic muscle contractions since the initial anchorage of f-actin bundles to the plasma membrane is not affected (Zervas et al. 2001). The identification of ILK as a mechanosensing molecule in cardiac muscle cells of zebra fish (*Danio rerio*) further supports the idea that ILK is a mechanoresponsive protein (Bendig et al. 2006).

In the future, it will be important to directly address the role of ILK in mechanotransduction. The microscopical analysis of control and knockout fibroblasts as well as the biochemical analysis of ILK-FLAG cells on stretchable substrates might already give insight into the molecular role of ILK as a mechanosensitive molecule.

4.2.2. ILK is required for FN fibrillogenesis

FN is major constituent of the ECM and already expressed in mouse blastocysts. Since FN is ubiquitously expressed in embryonic and adult tissues and frequently altered under pathological conditions such as cancer, thrombosis or fibrosis and because integrin-binding to FN is critical for FN matrix assembly it is widely believed that FN-integrin interactions play important roles in developmental and disease (Miyamoto et al. 1998). How FN matrix assembly is regulated and which integrin binding proteins are involved in this regulation is largely unclear. First implications about the involvement of ILK in this process came from studies in epithelial cells, where overexpression of ILK resulted in markedly increased FN matrix assembly (Wu et al. 1998). Conversely, depletion of ILK from endothelial cells led to significantly reduced FN fibrillogenesis (Vouret-Craviari et al. 2004). The data of my studies emphasize the central role of ILK during FN matrix assembly but also demonstrate that other FA proteins such as paxillin or FAK are critical.

4.2.2.1. The involvement of ILK, paxillin and FAK in FN fibrillogenesis

The deletion of ILK in fibroblasts caused a complete loss of FN fibrillogenesis and the fact that reconstitution of Pinch1 could not rescue this defect suggests that ILK is a central molecule in this process. Since depletion of FAK and paxillin from the parental ILK (f/f) cells caused a similar reduction in FN fibril assembly one could speculate that ILK regulates

fibrillogenesis through its binding to paxillin which in turn could directly interact with FAK. The expression of a mutant paxillin lacking the LD1 domain, however, did not affect FN matrix assembly. This suffices to suggest that at least the direct interaction between ILK and paxillin is not required for FN fibrillogenesis and opens the possibility that ILK and paxillin act independently from each other. While ILK might be essential for the generation of actin pulling forces, paxillin and FAK could be important for the efficient recruitment of additional proteins such as tensin into fibrillar adhesions. Tensin can interact directly with FAK and is thought to be central for FN matrix assembly (Davis et al. 1991; Pankov et al. 2000).

An alternative role for FAK during fibrillogenesis was suggested by Dusko Ilic and colleagues. They speculated that the interaction between FAK and p130Cas could be essential for FN matrix assembly (Ilic et al. 2004). My data indicate that p130Cas is not critical for FAK-dependent FN assembly since fibrillogenesis was not impaired in p130Cas knockdown cells. Since the knockdown efficiency in p130Cas knockdown cells is about 85%, it is however possible, that the residual p130Cas is sufficient to induce FN-fibrillogenesis.

It is important to note here that paxillin was earlier described to be abundant in FAs but almost completely excluded from fibrillar adhesions (Zamir et al. 2000). This was not the case in ILK (f/f) fibroblasts where paxillin was also found in fibrillar adhesions. A recent report confirmed our observation showing that in porcine aortic endothelial cells non-phosphorylated paxillin can localize into fibrillar adhesions where it colocalizes with tensin (Zaidel-Bar et al. 2007).

Taken together, we identified a number of FA proteins which are critical for FN matrix assembly including ILK, paxillin and FAK. Surprisingly, the direct ILK-paxillin interaction was not required for FN fibrillogenesis. In the future it will be important to analyze the role of the ILK-Pinch1-parvin complex during FN matrix assembly in more detail. Especially the analysis of α -parvin knockout cells could be interesting, since α -parvin was shown to localize into fibrillar adhesions (Olski et al. 2001). Since β -parvin should prevent the degradation of ILK and Pinch1 in the α -parvin knockout background these cells could be a suitable model system to test the role of parvins in FN matrix assembly. Furthermore, since FN-integrin interactions are essential during vasculogenesis (Francis et al. 2002) it would be especially interesting to analyze the role of ILK, Pinch1 and parvin during vascular development *in vivo*.

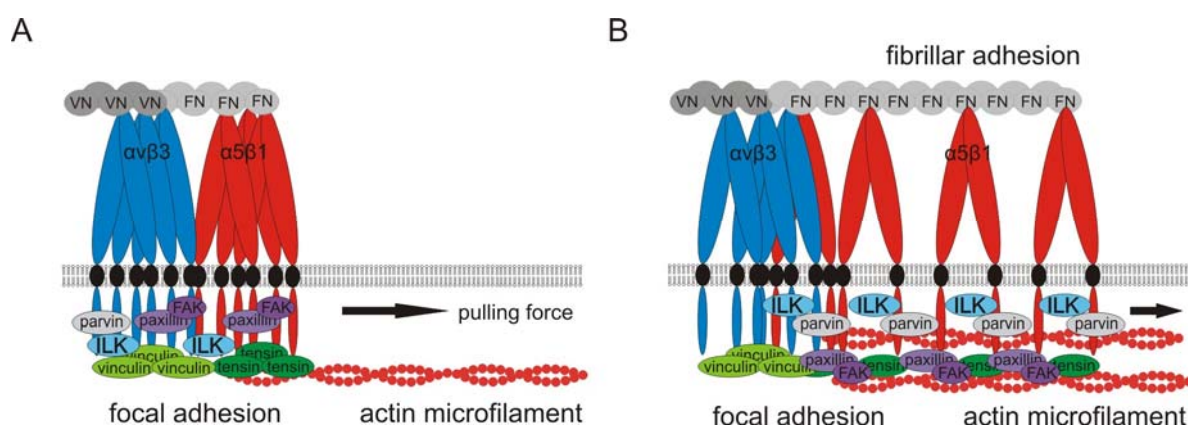


Fig 4.4. The role of FA proteins during FN fibrillogenesis. ILK, paxillin and FAK are all crucial for FN matrix assembly. The direct interaction between ILK and paxillin is not required. (Taken from Yamada et al. 2003 and modified).

4.2.3. ILK mediates integrin-RTK crosstalk during DR formation

It is well established that integrin- and RTK-signalling interact to regulate many cellular functions (Giancotti and Tarone 2003). However, most of our knowledge about integrin-RTK crosstalk stems from experiments on cell proliferation, whereas the impact of this crosstalk on cytoskeletal reorganizations is less well understood. This is in part due to the fact that current model systems used to analyze f-actin dynamics such as cell spreading or cell migration assays are highly complex and rather difficult to interpret. Cell proliferation can easily be evaluated by counting the cell number, while cell migration is assayed with numerous read outs including cell migration speed, cell migration persistence, cell polarization, actin polymerization, stress fiber formation, microtubular dynamics, MTOC orientation, structure and turnover of FAs and FCs at the leading front or retracting edge, etc. In my PhD work I used the DR formation assay to study actin dynamics in an integrin and RTK-dependent manner.

4.2.3.1. DR formation is integrin-dependent

DRs were first described more than 25 years ago as growth factor induced actin structures. Treatment of fibroblasts or transformed epithelial cells with EGF, PDGF, and HGF but also with phorbol esters such as TPA induced the formation of ring-like structures within minutes. Furthermore, forced expression of a constitutive active src also induced the formation of DR (Chinkers et al. 1979; Boschek et al. 1981; Mellstroom et al. 1983; Schliwa et al. 1984; Kitano et al. 1986). Extensive work over the last 20 years suggest that DR are structures which play important roles during cell transformation or cell migration (Buccione et al. 2004).

The data presented in this study provide evidence that growth factor induced DR formation requires integrin engagement and hence results from an integrin-RTK crosstalk.

The first indication about the importance of integrin engagement during dorsal ruffling came from spreading assays which revealed that control cells formed DR after cell adhesion to FN but not when cells were seeded on poly-lysine. Moreover, growth factor induced dorsal ruffling was only seen in cells that were seeded on FN but not in cells attached to poly-lysine. Finally, the DR formation frequency correlated with the amount of FN presented to control cells. The importance of integrin engagement became especially obvious during the analysis of cells which express constitutive active Rac1 (RacL61). Although activation of Rac1 is a strong stimulus for dorsal ruffling (Wang et al. 2006) cells expressing RacL61 would only form DRs when adherent to FN but not on poly-lysine.

Several reports described the formation of DRs in cells that were either seeded on uncoated glass coverslips (Legg et al. 2006) or on poly-lysine (Wang et al. 2006). It should be noted that in these experiments the cells were cultured overnight on the coverslips before growth factor stimulation. It is therefore almost certain that the cells secreted their own FN matrix to which they adhered via integrins (Legg et al. 2006). Other studies cultured the cells overnight in the presence 10% FCS, starved them of growth factors and subsequently triggered DR formation with growth factors (Wang et al. 2006). Since FCS is rich in ECM proteins also these cells adhered most likely to FCS-derived ECM proteins.

4.2.3.2. DRs originate at the ventral side of the cell

Shortly after the observation that vinculin is a FA protein (Geiger 1979) Manfred Schliwa and colleagues described the localization of vinculin in DRs (Schliwa et al. 1984). Surprisingly, it was never checked whether other FA proteins are capable of localizing into these structures. The observation that in addition to vinculin also talin, ILK and p130Cas are present in DRs indicates that certain integrin-associated proteins are not only functional but also physically connected to DRs. This observation prompted us to check where DRs actually form. Surprisingly, immediately after growth factor stimulation of starved cells all cortactin patches resembling ruffle precursors were exclusively localized along the ventral cell body, whereas at later time points the typical dorsal location was observed. In between these time points the f-actin ring was in most of the cases neither exclusively ventral nor dorsal but detectable in both locations. These data suggest that DRs form at the basal side of the cells and move to the dorsal surface at later time points.

An obvious question is how these structures translocate from the ventral to the dorsal side of the cell. Since DRs usually appear at the cell edges where the cell body is rather thin, it is

possible that the high actin polymerisation leads to a growth of the actin ring towards the dorsal cell surface. The observation that DRs are Triton-X-insoluble actin structures and do not colocalize with membrane markers such as GM1 supports the notion that during this process DRs are not tightly associated with the plasma membrane.

Certainly, further experiment will be necessary to clarify the development of DRs and their transition from ventral to dorsal locations. It should be possible to follow the formation of a DR at the basal side in more detail by total internal reflection microscopy (TIRF) with living cells using cortactin-EGFP as a DR reporter construct. Alternatively, cells could be analyzed by internal reflection microscopy to monitor processes at the basal side of the cell during DR formation.

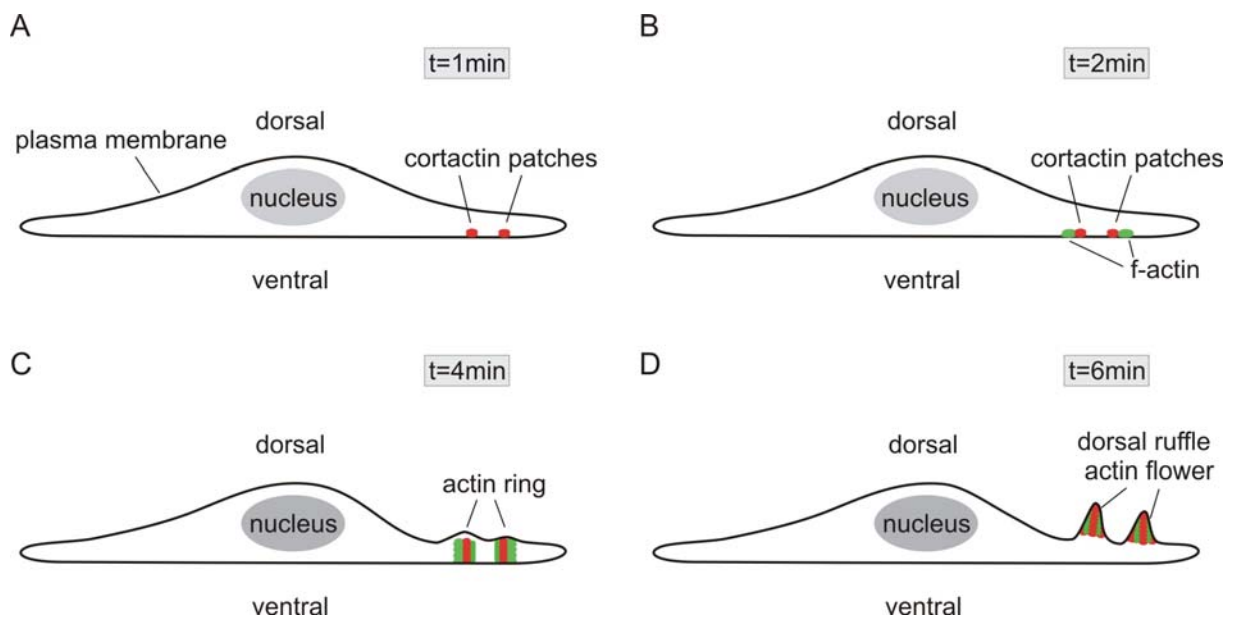


Fig 4.5. Model of DR formation in ILK (f/f) fibroblasts. *A.* Shortly after EGF stimulation cortactin patches form at the ventral side of the cell. *B.* Approximately 2min after stimulation f-actin is found at the cortactin patches, most likely due to local f-actin polymerization. *C.* The high f-actin polymerization drives the growth towards the dorsal side of the cell. *D.* 6min after stimulation the typical actin flowers or waves can be observed on the dorsal surface.

4.2.3.3. ILK is indispensable for DR formation

Loss of ILK leads to impaired DR formation. ILK (-/-) fibroblasts, adherent to FN or polylysine, formed very few or no DRs after EGF stimulation. Also when cells were analyzed during spreading on FN almost no DRs could be detected. However, when ILK-EGFP was re-expressed in the knockout cells DR formation was rescued. Interestingly, overexpression of ILK-FLAG in ILK (-/-) cells caused a marked increase in the DR formation frequency while reconstitution of Pinch1 protein levels by expression of an N-terminal ILK fragment (ANK-

FLAG) did not restore the capacity to form DRs. In addition, expression of constitutive active Rac1 in ILK (-/-) cells restored dorsal ruffling, which was, however, still dependent on integrin-mediated cell adhesion and growth factor stimulation.

These data suggest that in addition to its function as an important adaptor protein ILK is able to induce signal transduction pathways in response to integrin and growth factor stimulation, which lead to dynamic changes of the f-actin cytoskeleton.

4.2.3.4. Integrin/ILK-dependent DR formation does not require paxillin or FAK

To get insights into the molecular mechanism that is exploited by integrins and ILK to induce DRs, a number of knockdown cell lines were established and tested for their capability to form DRs after growth factor stimulation. These experiments revealed that ILK acts independently of paxillin and FAK, but seems to induce DRs in a p130Cas/Crk and ELMO1/Dock180-dependent manner.

The observation that paxillin knockdown cells formed DRs to a normal extent was unexpected since earlier studies showed that the recruitment of ILK and α -parvin into FAs and hence their function was dependent on paxillin binding (Nikolopoulos and Turner 2000; Nikolopoulos and Turner 2001). The localization of ILK and α -parvin into FAs could occur in paxillin knockdown cells whereas the translocation of FAK into FAs was inhibited. The role of the paxillin-ILK interaction was further tested by the expression of a paxillin-deletion mutant which lacked the ILK-binding LD1 domain. The expression of the LD1-lacking paxillin version rescued the entire phenotype of paxillin knockdown cells including the defective FA formation or the impaired FN fibrillogenesis indicating that the direct interaction between paxillin and ILK is less important than previously thought (Nikolopoulos and Turner, 2001). An explanation for the the severe phenotype observed in ILK (-/-) cells which express the paxillin-binding-mutant ILK (Nikolopoulos and Turner 2001 and this study) could be that the double point mutation in the ILK paxillin-binding-motif might have additional consequences than solely the loss of paxillin binding. Such additional abnormalities may include aberrant folding of the mutant ILK protein.

The translocation of FAK from FAs into the cytoplasm as well as the strongly reduced FAK phosphorylation levels in paxillin knockdown cells immediately suggested that this protein is not critical for DR formation. This was confirmed by the generation and analysis of FAK knockdown cells which displayed a normal DR formation frequency.

4.2.3.5. Integrin/ILK-dependent DR formation requires p130Cas and Dock180

p130Cas is, similarly like FAK or cortactin, highly phosphorylated upon integrin-mediated cell adhesion (Nojima et al. 1995; Vuori and Ruoslahti 1995). Upon binding to CrkII, p130Cas is thought to regulate a number of integrin-dependent processes such as cell migration (Klemke et al. 1998), cell invasion or survival (Cho and Klemke 2000). p130Cas can bind a variety of proteins, including phosphatases (PTP-PEST, PTP1B) or kinases (FAK, c-src) which are thought to tightly regulate the phosphorylation status of the protein. The exact mechanisms of p130Cas phosphorylation, however, is unclear although c-src is thought to play a central role during in p130Cas phosphorylation (Chodniewicz and Klemke 2004). Previous reports demonstrated that p130Cas and CrkII are essential for Rac1-dependent formation of peripheral ruffles which, similarly as DRs, form in an integrin-dependent manner. Although peripheral ruffles and DRs are thought to be regulated by distinct mechanisms (Suetsugu et al. 2003) I tested the involvement of p130Cas in DR formation. The analysis of p130Cas knockdown cells demonstrated that p130Cas expression is necessary for DR formation in ILK (f/f) fibroblasts. Immunostaining of control cells revealed that p130Cas and CrkII can localize to DRs. A biochemical analysis of ILK (-/-) cells stably expressing full length ILK-FLAG or the truncated ANK-FLAG indicated that ILK and p130Cas can associate in common subcellular fractions.

The activation of Rac1 by p130Cas is mediated by the ELMO1/Dock180 pathway (Gumienny et al. 2001). ELMO1 is capable of binding to CrkII and Dock180, which is a GEF for Rac1. Immunostaining revealed that p130Cas, CrkII and also ELMO1 localize into DRs and depletion of Dock180 from ILK (f/f) cells completely abolished DR formation after growth factor stimulation. These data suggest that the assembly of the p130Cas/CrkII and ELMO1/Dock180 complex is a prerequisite for DR formation.

4.2.4. Hyperphosphorylation of p130Cas in the cytoskeletal fraction of ILK-deficient cells

The coupling of p130Cas and CrkII and therefore the initiation of the p130Cas/CrkII/ELMO1/Dock180 complex is believed to be regulated by phosphorylation of the p130Cas substrate domain (Chodniewicz and Klemke 2004). However, the exact mechanism of p130Cas phosphorylation and CrkII-binding is not known. Stimulation of p130Cas with low concentrations of EGF (2ng/ml) were shown to induce tyrosine phosphorylation of p130Cas, whereas stimulation with high EGF concentrations (80ng/ml) caused a rapid dephosphorylation (Ojaniemi and Vuori 1997). Although p130Cas can directly

interact with phosphatases such as PTP1B or PTP-PEST it is not known whether these phosphatases control p130Cas dephosphorylation after EGF stimulation.

To check if loss of ILK has any impact on p130Cas phosphorylation levels, protein lysates of the plasma membrane, plasma membrane fractions as well as cytoskeletal fractions were analyzed. While no differences in the phosphorylation state of p130Cas could be seen in plasma membrane preparations, there was a strong increase in the phosphorylation of the p130Cas substrate domain in the cytoskeletal fraction of ILK (-/-) cells. The fact the inhibition of c-src was unable to decrease but instead increased p130Cas phosphorylation levels suggested that the hyperphosphorylation was not caused by an elevated kinase activity but rather by a reduced phosphatase activity. These results prompted us to search for ILK interaction partners before and after EGF stimulation. By analysing immunoprecipitates of ILK-FLAG lysates with SILAC-based mass-spectroscopy we could identify the phosphatase LMW-PTP which shows a strongly increased accumulation in ILK-FLAG immunoprecipitates after EGF stimulation.

LMW-PTP is a 18kDa phosphatase that exists in spatially and functionally distinct subcellular fractions (Cirri et al. 1998; Raugei et al. 2002). In the cytosol, LMW-PTP is non-phosphorylated and able to dephosphorylate the PDGF-receptor. The cytoskeletal-associated LMW-PTP becomes phosphorylated after growth factor stimulation by c-src and is thought to mediate dephosphorylation of p190RhoGAP (Chiarugi et al. 2000a). LMW-PTP associates with the cytoskeleton only in cells that are attached to FN but not in cells that are seeded on poly-lysine suggesting that integrin engagement modulates the activity of this phosphatase (Chiarugi et al. 2000a; Chiarugi et al. 2000b). I could show that LMW-PTP associates with ILK-FLAG after EGF stimulation, which is the first implication of LMW-PTP in DR formation. It is possible that ILK is needed for activation and/or localization of LMW-PTP after growth factor stimulation thereby integrating integrin-mediated cell adhesion into RTK signalling pathways (Fig 4.6).

In the future it will be important to test this model by generating LMW-PTP knockdown cell lines and by analyzing LMW-PTP phosphorylation and phosphatase activity at the cytoskeletal fraction in control and ILK knockout cells.

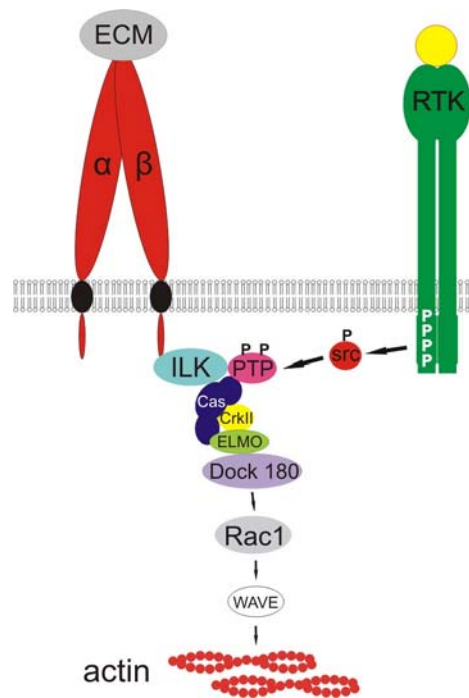


Fig 4.6. Model of ILK-dependent DR formation. ILK associates with integrins and forms a complex with p130Cas. EGF stimulation leads to src-dependent phosphorylation of LMW-PTP which translocates in the cytoskeletal fraction and associates with ILK. The subsequent dephosphorylation of p130Cas is essential for the formation of the p130as/CrkII/ELMO/Dock180 complex which leads to the activation of Rac1 and f-actin polymerization.

5. Summary

Integrins are ubiquitously expressed cell surface receptors which mediate the interaction of cells with the extracellular matrix. The interaction between integrins and their ligands is considered to provide the physical support for cells in order to maintain adhesion, to permit traction forces and to organize signalling complexes which regulate a variety of cellular processes including cell differentiation, cell proliferation or cell survival. Furthermore integrins connect cell matrix adhesions with the actin cytoskeleton which is essential for the regulation of cell migration or the establishment of cell polarity. Since integrins lack actin-binding sites and do not have any catalytic activity their signal transduction depends on intracellular proteins which are recruited to the cytoplasmic tail. One of these integrin-binding proteins is Integrin-linked kinase (ILK) which directly interacts with $\beta 1$ and $\beta 3$ integrins.

Overexpression studies revealed that ILK recruits adaptor and signalling proteins to the integrin adhesion sites and stimulates downstream signalling cascades through direct phosphorylation of numerous target proteins including PKB/Akt and GSK-3 β . However, loss of function studies in *C.elegans* and *Drosophila* indicated that the kinase activity might be far less important than previously thought. To describe the physiological role of ILK in a mammalian system this study was initiated. The overall goal was to describe the consequences of a constitutive ILK deletion and of tissue specific ablations of the protein in the cartilage and in the epidermis of mice. Additionally we wanted to establish an *in vitro* model system that allows studying the role of ILK as a kinase and as an adaptor protein in more detail.

The data presented in this study identify ILK as one of the major integrin-associated regulators of the f-actin cytoskeleton *in vivo* and *in vitro* and demonstrate that ILK modulates actin dynamics as an adaptor and as a signalling protein. Moreover, my experiments indicate that ILK is not important as a kinase.

The analysis of constitutive ILK knockout mice and ILK-deficient embryoid bodies revealed that loss of ILK leads to peri-implantation lethality caused by incomplete epiblast differentiation and cavitation. The impaired epiblast polarization is associated with abnormal f-actin accumulations at the endodermal-epiblast basement membrane (Sakai et al 2003).

Deletion of ILK in the cartilage of mice resulted in chondrodysplasia and perinatal death due to respiratory distress. ILK-deficient chondrocytes displayed an abnormal cell shape and reduced cell proliferation associated with a disorganized f-actin cytoskeleton *in vivo* and *in*

vitro. The phosphorylation levels of PKB/Akt or GSK-3 β , however, were unaffected (Grashoff et al. 2003).

Deletion of ILK in the epidermis of mice resulted in an integrin-mediated adhesion defect leading to epidermal detachment and disintegration of the epidermal-dermal basement membrane. Impaired downward migration of outer root sheath cells along the basement membrane of hair follicles resulted in an almost complete hair loss of ILK knockout mice. The f-actin polarization in the epidermis as well as stress fiber formation in cell culture was severely impaired in ILK-deficient keratinocytes (Lorenz, Grashoff, Torika et al. resubmitted for publication).

The analysis of ILK knockout fibroblasts *in vitro* revealed that ILK is required for the formation of focal and fibrillar adhesions and the establishment of a normal f-actin stress fiber network. Loss of ILK led to strongly reduced Pinch1 and parvin protein levels, impaired the cell shape and the cell spreading and fully inhibited FN matrix assembly. Loss of ILK also affected the formation of DRs which develop after integrin and growth factor stimulation. My data suggest that ILK induces actin polymerization through local activation of Rac1 in a p130Cas- and Dock180-dependent manner (Grashoff et al., manuscript in preparation)

In summary, ILK regulates the organization of the f-actin cytoskeleton in several ways: on the one hand by stabilizing and recruiting actin binding proteins to the integrin adhesion site and on the other hand by stimulating actin polymerization in response to integrin and growth factor stimulation.

6. References

- Adair, B. D., J. P. Xiong, C. Maddock, S. L. Goodman, M. A. Arnaout and M. Yeager (2005). "Three-dimensional EM structure of the ectodomain of integrin $\{\alpha\}V\{\beta\}_3$ in a complex with fibronectin." J Cell Biol **168**(7): 1109-18.
- Adams, M. A. (2006). "The mechanical environment of chondrocytes in articular cartilage." Biorheology **43**(3-4): 537-45.
- Assoian, R. K. and X. Zhu (1997). "Cell anchorage and the cytoskeleton as partners in growth factor dependent cell cycle progression." Curr Opin Cell Biol **9**(1): 93-8.
- Aszodi, A., J. F. Bateman, E. Gustafsson, R. Boot-Handford and R. Fassler (2000). "Mammalian skeletogenesis and extracellular matrix: what can we learn from knockout mice?" Cell Struct Funct **25**(2): 73-84.
- Aszodi, A., E. B. Hunziker, C. Brakebusch and R. Fassler (2003). "Beta1 integrins regulate chondrocyte rotation, G1 progression, and cytokinesis." Genes Dev **17**(19): 2465-79.
- Aumailley, M., M. Pesch, L. Tunggal, F. Gaill and R. Fassler (2000). "Altered synthesis of laminin 1 and absence of basement membrane component deposition in (beta)1 integrin-deficient embryoid bodies." J Cell Sci **113 Pt 2**: 259-68.
- Bader, B. L., H. Rayburn, D. Crowley and R. O. Hynes (1998). "Extensive vasculogenesis, angiogenesis, and organogenesis precede lethality in mice lacking all alpha v integrins." Cell **95**(4): 507-19.
- Bendig, G., M. Grimmmler, I. G. Huttner, G. Wessels, T. Dahme, S. Just, N. Trano, H. A. Katus, M. C. Fishman and W. Rottbauer (2006). "Integrin-linked kinase, a novel component of the cardiac mechanical stretch sensor, controls contractility in the zebrafish heart." Genes Dev **20**(17): 2361-72.
- Bengtsson, T., A. Aszodi, C. Nicolae, E. B. Hunziker, E. Lundgren-Akerlund and R. Fassler (2005). "Loss of alpha10beta1 integrin expression leads to moderate dysfunction of growth plate chondrocytes." J Cell Sci **118**(Pt 5): 929-36.
- Bennett, J. S. (2005). "Structure and function of the platelet integrin alphaIIb beta3." J Clin Invest **115**(12): 3363-9.
- Bi, W., J. M. Deng, Z. Zhang, R. R. Behringer and B. de Crombrughe (1999). "Sox9 is required for cartilage formation." Nat Genet **22**(1): 85-9.
- Bianchi, E., S. Denti, A. Granata, G. Bossi, J. Geginat, A. Villa, L. Rogge and R. Pardi (2000). "Integrin LFA-1 interacts with the transcriptional co-activator JAB1 to modulate AP-1 activity." Nature **404**(6778): 617-21.
- Blagoev, B. and M. Mann (2006). "Quantitative proteomics to study mitogen-activated protein kinases." Methods **40**(3): 243-50.
- Blanpain, C. and E. Fuchs (2006). "Epidermal stem cells of the skin." Annu Rev Cell Dev Biol **22**: 339-73.

- Boudeau, J., D. Miranda-Saavedra, G. J. Barton and D. R. Alessi (2006). "Emerging roles of pseudokinases." Trends Cell Biol **16**(9): 443-52.
- Boschek, C. B., B. M. Jockusch, R. R. Friis, R. Back, E. Grundmann and H. Bauer (1981). "Early changes in the distribution and organization of microfilament proteins during cell transformation." Cell **24**(1): 175-84.
- Boulter, E., D. Grall, S. Cagnol and E. Van Obberghen-Schilling (2006). "Regulation of cell-matrix adhesion dynamics and Rac-1 by integrin linked kinase." Faseb J **20**(9): 1489-91.
- Bouvard, D., C. Brakebusch, E. Gustafsson, A. Aszodi, T. Bengtsson, A. Berna and R. Fassler (2001). "Functional consequences of integrin gene mutations in mice." Circ Res **89**(3): 211-23.
- Brakebusch, C. and R. Fassler (2003). "The integrin-actin connection, an eternal love affair." Embo J **22**(10): 2324-33.
- Brakebusch, C., R. Grose, F. Quondamatteo, A. Ramirez, J. L. Jorcano, A. Pirro, M. Svensson, R. Herken, T. Sasaki, R. Timpl, S. Werner and R. Fassler (2000). "Skin and hair follicle integrity is crucially dependent on beta 1 integrin expression on keratinocytes." Embo J **19**(15): 3990-4003.
- Brancaccio, M., S. Guazzone, N. Menini, E. Sibona, E. Hirsch, M. De Andrea, M. Rocchi, F. Altruda, G. Tarone and L. Silengo (1999). "Melusin is a new muscle-specific interactor for beta(1) integrin cytoplasmic domain." J Biol Chem **274**(41): 29282-8
- Brandau, O., A. Meindl, R. Fassler and A. Aszodi (2001). "A novel gene, tendin, is strongly expressed in tendons and ligaments and shows high homology with chondromodulin-I." Dev Dyn **221**(1): 72-80.
- Braun, A., R. Bordoy, F. Stanchi, M. Moser, G. G. Kostka, E. Ehler, O. Brandau and R. Fassler (2003). "PINCH2 is a new five LIM domain protein, homologous to PINCH and localized to focal adhesions." Exp Cell Res **284**(2): 239-50.
- Brown, N. H. (1994). "Null mutations in the alpha PS2 and beta PS integrin subunit genes have distinct phenotypes." Development **120**(5): 1221-31.
- Brown, N. H. (2000). "Cell-cell adhesion via the ECM: integrin genetics in fly and worm." Matrix Biol **19**(3): 191-201.
- Brummelkamp, T. R., R. Bernards and R. Agami (2002). "A system for stable expression of short interfering RNAs in mammalian cells." Science **296**(5567): 550-3.
- Buccione, R., J. D. Orth and M. A. McNiven (2004). "Foot and mouth: podosomes, invadopodia and circular dorsal ruffles." Nat Rev Mol Cell Biol **5**(8): 647-57.
- Cabodi, S., L. Moro, E. Bergatto, E. Boeri Erba, P. Di Stefano, E. Turco, G. Tarone and P. Defilippi (2004). "Integrin regulation of epidermal growth factor (EGF) receptor and of EGF-dependent responses." Biochem Soc Trans **32**(Pt3): 438-42.
- Calderwood, D. A., Y. Fujioka, J. M. de Pereda, B. Garcia-Alvarez, T. Nakamoto, B. Margolis, C. J. McGlade, R. C. Liddington and M. H. Ginsberg (2003). "Integrin beta

- cytoplasmic domain interactions with phosphotyrosine-binding domains: a structural prototype for diversity in integrin signaling." *Proc Natl Acad Sci U S A* **100**(5): 2272-7.
- Carman, C. V. and T. A. Springer (2003). "Integrin avidity regulation: are changes in affinity and conformation underemphasized?" *Curr Opin Cell Biol* **15**(5): 547-56.
- Carroll, J. M., M. R. Romero and F. M. Watt (1995). "Suprabasal integrin expression in the epidermis of transgenic mice results in developmental defects and a phenotype resembling psoriasis." *Cell* **83**(6): 957-68.
- Cary, L. A. and J. L. Guan (1999). "Focal adhesion kinase in integrin-mediated signaling." *Front Biosci* **4**: D102-13.
- Chang, D. D., C. Wong, H. Smith and J. Liu (1997). "ICAP-1, a novel beta1 integrin cytoplasmic domain-associated protein, binds to a conserved and functionally important NPXY sequence motif of beta1 integrin." *J Cell Biol* **138**(5): 1149-57.
- Chiarugi, P., P. Cirri, L. Taddei, E. Giannoni, G. Camici, G. Manao, G. Raugei and G. Ramponi (2000). "The low M(r) protein-tyrosine phosphatase is involved in Rho-mediated cytoskeleton rearrangement after integrin and platelet-derived growth factor stimulation." *J Biol Chem* **275**(7): 4640-6.
- Chiarugi, P., M. L. Taddei, P. Cirri, D. Talini, F. Buricchi, G. Camici, G. Manao, G. Raugei and G. Ramponi (2000). "Low molecular weight protein-tyrosine phosphatase controls the rate and the strength of NIH-3T3 cells adhesion through its phosphorylation on tyrosine 131 or 132." *J Biol Chem* **275**(48): 37619-27.
- Chicurel, M. E., R. H. Singer, C. J. Meyer and D. E. Ingber (1998). "Integrin binding and mechanical tension induce movement of mRNA and ribosomes to focal adhesions." *Nature* **392**(6677): 730-3.
- Chinkers, M., J. A. McKanna and S. Cohen (1979). "Rapid induction of morphological changes in human carcinoma cells A-431 by epidermal growth factors." *J Cell Biol* **83**(1): 260-5.
- Cho, S. Y. and R. L. Klemke (2000). "Extracellular-regulated kinase activation and CAS/Crk coupling regulate cell migration and suppress apoptosis during invasion of the extracellular matrix." *J Cell Biol* **149**(1): 223-36.
- Chodniewicz, D. and R. L. Klemke (2004). "Regulation of integrin-mediated cellular responses through assembly of a CAS/Crk scaffold." *Biochim Biophys Acta* **1692**(2-3): 63-76.
- Chu, H., I. Thievessen, M. Sixt, T. Lammermann, A. Waisman, A. Braun, A. A. Noegel and R. Fassler (2006). "gamma-Parvin is dispensable for hematopoiesis, leukocyte trafficking, and T-cell-dependent antibody response." *Mol Cell Biol* **26**(5): 1817-25.
- Cirri, P., P. Chiarugi, L. Taddei, G. Raugei, G. Camici, G. Manao and G. Ramponi (1998). "Low molecular weight protein-tyrosine phosphatase tyrosine phosphorylation by c-Src during platelet-derived growth factor-induced mitogenesis correlates with its subcellular targeting." *J Biol Chem* **273**(49): 32522-7.

References

- Cotsarelis, G., T. T. Sun and R. M. Lavker (1990). "Label-retaining cells reside in the bulge area of pilosebaceous unit: implications for follicular stem cells, hair cycle, and skin carcinogenesis." Cell **61**(7): 1329-37.
- Coxon, A., P. Rieu, F. J. Barkalow, S. Askari, A. H. Sharpe, U. H. von Andrian, M. A. Arnaout and T. N. Mayadas (1996). "A novel role for the beta 2 integrin CD11b/CD18 in neutrophil apoptosis: a homeostatic mechanism in inflammation." Immunity **5**(6): 653-66.
- D'Amico, M., J. Hult, D. F. Amanatullah, B. T. Zafonte, C. Albanese, B. Bouzahzah, M. Fu, L. H. Augenlicht, L. A. Donehower, K. Takemaru, R. T. Moon, R. Davis, M. P. Lisanti, M. Shtutman, J. Zhurinsky, A. Ben-Ze'ev, A. A. Troussard, S. Dedhar and R. G. Pestell (2000). "The integrin-linked kinase regulates the cyclin D1 gene through glycogen synthase kinase 3beta and cAMP-responsive element-binding protein-dependent pathways." J Biol Chem **275**(42): 32649-57.
- Danen, E. H., J. van Rheenen, W. Franken, S. Huvneers, P. Sonneveld, K. Jalink and A. Sonnenberg (2005). "Integrins control motile strategy through a Rho-cofilin pathway." J Cell Biol **169**(3): 515-26.
- Davis, S., M. L. Lu, S. H. Lo, S. Lin, J. A. Butler, B. J. Druker, T. M. Roberts, Q. An and L. B. Chen (1991). "Presence of an SH2 domain in the actin-binding protein tensin." Science **252**(5006): 712-5.
- del Pozo, M. A., N. B. Alderson, W. B. Kiosses, H. H. Chiang, R. G. Anderson and M. A. Schwartz (2004). "Integrins regulate Rac targeting by internalization of membrane domains." Science **303**(5659): 839-42.
- Delcommenne, M., C. Tan, V. Gray, L. Rue, J. Woodgett and S. Dedhar (1998). "Phosphoinositide-3-OH kinase-dependent regulation of glycogen synthase kinase 3 and protein kinase B/AKT by the integrin-linked kinase." Proc Natl Acad Sci U S A **95**(19): 11211-6.
- Deng, C., A. Wynshaw-Boris, F. Zhou, A. Kuo and P. Leder (1996). "Fibroblast growth factor receptor 3 is a negative regulator of bone growth." Cell **84**(6): 911-21.
- Deng, J. T., C. Sutherland, D. L. Brautigan, M. Eto and M. P. Walsh (2002). "Phosphorylation of the myosin phosphatase inhibitors, CPI-17 and PHI-1, by integrin-linked kinase." Biochem J **367**(Pt 2): 517-24.
- Deng, J. T., J. E. Van Lierop, C. Sutherland and M. P. Walsh (2001). "Ca²⁺-independent smooth muscle contraction. a novel function for integrin-linked kinase." J Biol Chem **276**(19): 16365-73.
- DiPersio, C. M., R. van der Neut, E. Georges-Labouesse, J. A. Kreidberg, A. Sonnenberg and R. O. Hynes (2000). "alpha3beta1 and alpha6beta4 integrin receptors for laminin-5 are not essential for epidermal morphogenesis and homeostasis during skin development." J Cell Sci **113** (Pt 17): 3051-62.
- Dowling, J., Q. C. Yu and E. Fuchs (1996). "Beta4 integrin is required for hemidesmosome formation, cell adhesion and cell survival." J Cell Biol **134**(2): 559-72.

- Erlebacher, A., E. H. Filvaroff, S. E. Gitelman and R. Derynck (1995). "Toward a molecular understanding of skeletal development." Cell **80**(3): 371-8.
- Fassler, R. and M. Meyer (1995). "Consequences of lack of beta 1 integrin gene expression in mice." Genes Dev **9**(15): 1896-908.
- Francis, S. E., K. L. Goh, K. Hodivala-Dilke, B. L. Bader, M. Stark, D. Davidson and R. O. Hynes (2002). "Central roles of alpha5beta1 integrin and fibronectin in vascular development in mouse embryos and embryoid bodies." Arterioscler Thromb Vasc Biol **22**(6): 927-33.
- Fukuda, T., K. Chen, X. Shi and C. Wu (2003). "PINCH-1 is an obligate partner of integrin-linked kinase (ILK) functioning in cell shape modulation, motility, and survival." J Biol Chem **278**(51): 51324-33.
- Gardner, H., J. Kreidberg, V. Koteliensky and R. Jaenisch (1996). "Deletion of integrin alpha 1 by homologous recombination permits normal murine development but gives rise to a specific deficit in cell adhesion." Dev Biol **175**(2): 301-13.
- Gaus, K., S. Le Lay, N. Balasubramanian and M. A. Schwartz (2006). "Integrin-mediated adhesion regulates membrane order." J Cell Biol **174**(5): 725-34.
- Geiger, B. (1979). "A 130K protein from chicken gizzard: its localization at the termini of microfilament bundles in cultured chicken cells." Cell **18**(1): 193-205.
- Georges-Labouesse, E., N. Messaddeq, G. Yehia, L. Cadalbert, A. Dierich and M. Le Meur (1996). "Absence of integrin alpha 6 leads to epidermolysis bullosa and neonatal death in mice." Nat Genet **13**(3): 370-3.
- Giancotti, F. G. (1997). "Integrin signaling: specificity and control of cell survival and cell cycle progression." Curr Opin Cell Biol **9**(5): 691-700.
- Giancotti, F. G. and G. Tarone (2003). "Positional control of cell fate through joint integrin/receptor protein kinase signaling." Annu Rev Cell Dev Biol **19**: 173-206.
- Goldmann, W. H. (2000). "Kinetic determination of focal adhesion protein formation." Biochem Biophys Res Commun **271**(2): 553-7.
- Grashoff, C., A. Aszodi, T. Sakai, E. B. Hunziker and R. Fassler (2003). "Integrin-linked kinase regulates chondrocyte shape and proliferation." EMBO Rep **4**(4): 432-8.
- Grashoff, C., I. Thievensen, K. Lorenz, S. Ussar and R. Fassler (2004). "Integrin-linked kinase: integrin's mysterious partner." Curr Opin Cell Biol **16**(5): 565-71.
- Gumienny, T. L., E. Brugnera, A. C. Tosello-Trampont, J. M. Kinchen, L. B. Haney, K. Nishiwaki, S. F. Walk, M. E. Nemergut, I. G. Macara, R. Francis, T. Schedl, Y. Qin, L. Van Aelst, M. O. Hengartner and K. S. Ravichandran (2001). "CED-12/ELMO, a novel member of the CrkII/Dock180/Rac pathway, is required for phagocytosis and cell migration." Cell **107**(1): 27-41.
- Guo, W. and F. G. Giancotti (2004). "Integrin signalling during tumour progression." Nat Rev Mol Cell Biol **5**(10): 816-26.

References

- Hagel, M., E. L. George, A. Kim, R. Tamimi, S. L. Opitz, C. E. Turner, A. Imamoto and S. M. Thomas (2002). "The adaptor protein paxillin is essential for normal development in the mouse and is a critical transducer of fibronectin signaling." *Mol Cell Biol* **22**(3): 901-15.
- Hannigan, G. E., C. Leung-Hagesteijn, L. Fitz-Gibbon, M. G. Coppelino, G. Radeva, J. Filmus, J. C. Bell and S. Dedhar (1996). "Regulation of cell adhesion and anchorage-dependent growth by a new beta 1-integrin-linked protein kinase." *Nature* **379**(6560): 91-6.
- Hayashi, Y., B. Haimovich, A. Reszka, D. Boettiger and A. Horwitz (1990). "Expression and function of chicken integrin beta 1 subunit and its cytoplasmic domain mutants in mouse NIH 3T3 cells." *J Cell Biol* **110**(1): 175-84.
- Hill, M. M., J. Feng and B. A. Hemmings (2002). "Identification of a plasma membrane Raft-associated PKB Ser473 kinase activity that is distinct from ILK and PDK1." *Curr Biol* **12**(14): 1251-5.
- Hinz, B. and G. Gabbiani (2003). "Mechanisms of force generation and transmission by myofibroblasts." *Curr Opin Biotechnol* **14**(5): 538-46.
- Hmama, Z., K. L. Knutson, P. Herrera-Velitz, D. Nandan and N. E. Reiner (1999). "Monocyte adherence induced by lipopolysaccharide involves CD14, LFA-1, and cytohesin-1. Regulation by Rho and phosphatidylinositol 3-kinase." *J Biol Chem* **274**(2): 1050-7.
- Hodivala-Dilke, K. M., K. P. McHugh, D. A. Tsakiris, H. Rayburn, D. Crowley, M. Ullman-Cullere, F. P. Ross, B. S. Collier, S. Teitelbaum and R. O. Hynes (1999). "Beta3-integrin-deficient mice are a model for Glanzmann thrombasthenia showing placental defects and reduced survival." *J Clin Invest* **103**(2): 229-38.
- Holtkotter, O., B. Nieswandt, N. Smyth, W. Muller, M. Hafner, V. Schulte, T. Krieg and B. Eckes (2002). "Integrin alpha 2-deficient mice develop normally, are fertile, but display partially defective platelet interaction with collagen." *J Biol Chem* **277**(13): 10789-94.
- Honda, H., H. Oda, T. Nakamoto, Z. Honda, R. Sakai, T. Suzuki, T. Saito, K. Nakamura, K. Nakao, T. Ishikawa, M. Katsuki, Y. Yazaki and H. Hirai (1998). "Cardiovascular anomaly, impaired actin bundling and resistance to Src-induced transformation in mice lacking p130Cas." *Nat Genet* **19**(4): 361-5.
- Horwitz, A., K. Duggan, C. Buck, M. C. Beckerle and K. Burridge (1986). "Interaction of plasma membrane fibronectin receptor with talin--a transmembrane linkage." *Nature* **320**(6062): 531-3.
- Huang, S., C. S. Chen and D. E. Ingber (1998). "Control of cyclin D1, p27(Kip1), and cell cycle progression in human capillary endothelial cells by cell shape and cytoskeletal tension." *Mol Biol Cell* **9**(11): 3179-93.
- Huang, X., M. Griffiths, J. Wu, R. V. Farese, Jr. and D. Sheppard (2000). "Normal development, wound healing, and adenovirus susceptibility in beta5-deficient mice." *Mol Cell Biol* **20**(3): 755-9.
- Huang, X. Z., J. F. Wu, D. Cass, D. J. Erle, D. Corry, S. G. Young, R. V. Farese, Jr. and D. Sheppard (1996). "Inactivation of the integrin beta 6 subunit gene reveals a role of

- epithelial integrins in regulating inflammation in the lung and skin." *J Cell Biol* **133**(4): 921-8.
- Humphries, M. J., P. A. McEwan, S. J. Barton, P. A. Buckley, J. Bella and A. P. Mould (2003). "Integrin structure: heady advances in ligand binding, but activation still makes the knees wobble." *Trends Biochem Sci* **28**(6): 313-20.
- Hynes, R. O. (2002). "Integrins: bidirectional, allosteric signaling machines." *Cell* **110**(6): 673-87.
- Hynes, R. O. and Q. Zhao (2000). "The evolution of cell adhesion." *J Cell Biol* **150**(2): F89-96.
- Ilic, D., Y. Furuta, S. Kanazawa, N. Takeda, K. Sobue, N. Nakatsuji, S. Nomura, J. Fujimoto, M. Okada and T. Yamamoto (1995). "Reduced cell motility and enhanced focal adhesion contact formation in cells from FAK-deficient mice." *Nature* **377**(6549): 539-44.
- Ilic, D., B. Kovacic, K. Johkura, D. D. Schlaepfer, N. Tomasevic, Q. Han, J. B. Kim, K. Howerton, C. Baumbusch, N. Ogiwara, D. N. Streblov, J. A. Nelson, P. Dazin, Y. Shino, K. Sasaki and C. H. Damsky (2004). "FAK promotes organization of fibronectin matrix and fibrillar adhesions." *J Cell Sci* **117**(Pt 2): 177-87.
- Jones, P. H., S. Harper and F. M. Watt (1995). "Stem cell patterning and fate in human epidermis." *Cell* **80**(1): 83-93.
- Jones, P. H. and F. M. Watt (1993). "Separation of human epidermal stem cells from transit amplifying cells on the basis of differences in integrin function and expression." *Cell* **73**(4): 713-24.
- Jenkins, A. L., L. Nannizzi-Alaimo, D. Silver, J. R. Sellers, M. H. Ginsberg, D. A. Law and D. R. Phillips (1998). "Tyrosine phosphorylation of the beta3 cytoplasmic domain mediates integrin-cytoskeletal interactions." *J Biol Chem* **273**(22): 13878-85
- Karaplis, A. C., A. Luz, J. Glowacki, R. T. Bronson, V. L. Tybulewicz, H. M. Kronenberg and R. C. Mulligan (1994). "Lethal skeletal dysplasia from targeted disruption of the parathyroid hormone-related peptide gene." *Genes Dev* **8**(3): 277-89.
- Karsenty, G. and E. F. Wagner (2002). "Reaching a genetic and molecular understanding of skeletal development." *Dev Cell* **2**(4): 389-406.
- Kessler, C., H. J. Holtke, R. Seibl, J. Burg and K. Muhlegger (1990). "Non-radioactive labeling and detection of nucleic acids. I. A novel DNA labeling and detection system based on digoxigenin: anti-digoxigenin ELISA principle (digoxigenin system)." *Biol Chem Hoppe Seyler* **371**(10): 917-27.
- Kiss, E., A. Muranyi, C. Csontos, P. Gergely, M. Ito, D. J. Hartshorne and F. Erdodi (2002). "Integrin-linked kinase phosphorylates the myosin phosphatase target subunit at the inhibitory site in platelet cytoskeleton." *Biochem J* **365**(Pt 1): 79-87.
- Kitano, Y., N. Okada and J. Adachi (1986). "TPA-induced alteration of actin organization in cultured human keratinocytes." *Exp Cell Res* **167**(2): 369-75.

- Klemke, R. L., J. Leng, R. Molander, P. C. Brooks, K. Vuori and D. A. Cheresh (1998). "CAS/Crk coupling serves as a "molecular switch" for induction of cell migration." J Cell Biol **140**(4): 961-72.
- Kieffer, J. D., G. Plopper, D. E. Ingber, J. H. Hartwig and T. S. Kupper (1995). "Direct binding of F actin to the cytoplasmic domain of the alpha 2 integrin chain in vitro." Biochem Biophys Res Commun **217**(2): 466-74.
- Knezevic, I., T. M. Leisner and S. C. Lam (1996). "Direct binding of the platelet integrin alphaIIb beta3 (GPIIb-IIIa) to talin. Evidence that interaction is mediated through the cytoplasmic domains of both alphaIIb and beta3." J Biol Chem **271**(27): 16416-21.
- Kolanus, W., W. Nagel, B. Schiller, L. Zeitlmann, S. Godar, H. Stockinger and B. Seed (1996). "Alpha L beta 2 integrin/LFA-1 binding to ICAM-1 induced by cytohesin-1, a cytoplasmic regulatory molecule." Cell **86**(2): 233-42.
- Komori, T., H. Yagi, S. Nomura, A. Yamaguchi, K. Sasaki, K. Deguchi, Y. Shimizu, R. T. Bronson, Y. H. Gao, M. Inada, M. Sato, R. Okamoto, Y. Kitamura, S. Yoshiki and T. Kishimoto (1997). "Targeted disruption of Cbfa1 results in a complete lack of bone formation owing to maturational arrest of osteoblasts." Cell **89**(5): 755-64.
- Kreidberg, J. A., M. J. Donovan, S. L. Goldstein, H. Rennke, K. Shepherd, R. C. Jones and R. Jaenisch (1996). "Alpha 3 beta 1 integrin has a crucial role in kidney and lung organogenesis." Development **122**(11): 3537-47
- Lai, L. P. and J. Mitchell (2005). "Indian hedgehog: its roles and regulation in endochondral bone development." J Cell Biochem **96**(6): 1163-73.
- Law, D. A., L. Nannizzi-Alaimo and D. R. Phillips (1996). "Outside-in integrin signal transduction. Alpha IIb beta 3-(GP IIb IIIa) tyrosine phosphorylation induced by platelet aggregation." J Biol Chem **271**(18): 10811-5.
- Legate, K. R., E. Montanez, O. Kudlacek and R. Fassler (2006). "ILK, PINCH and parvin: the tIPP of integrin signalling." Nat Rev Mol Cell Biol **7**(1): 20-31.
- Legg, J. A., G. Bompard, J. Dawson, H. L. Morris, N. Andrew, L. Cooper, S. A. Johnston, G. Tramontanis and L. M. Machesky (2006). "N-WASP Involvement in Dorsal Ruffle Formation in Mouse Embryonic Fibroblasts." Mol Biol Cell.
- Leung-Hagesteijn, C., A. Mahendra, I. Naruszewicz and G. E. Hannigan (2001). "Modulation of integrin signal transduction by ILKAP, a protein phosphatase 2C associating with the integrin-linked kinase, ILK1." Embo J **20**(9): 2160-70.
- Li, J., R. Mayne and C. Wu (1999). "A novel muscle-specific beta 1 integrin binding protein (MIBP) that modulates myogenic differentiation." J Cell Biol **147**(7): 1391-8.
- Li, S., R. Bordoy, F. Stanchi, M. Moser, A. Braun, O. Kudlacek, U. M. Wewer, P. D. Yurchenco and R. Fassler (2005). "PINCH1 regulates cell-matrix and cell-cell adhesions, cell polarity and cell survival during the peri-implantation stage." J Cell Sci **118**(Pt 13): 2913-21.
- Li, S., D. Edgar, R. Fassler, W. Wadsworth and P. D. Yurchenco (2003). "The role of laminin in embryonic cell polarization and tissue organization." Dev Cell **4**(5): 613-24.

- Li, S., D. Harrison, S. Carbonetto, R. Fassler, N. Smyth, D. Edgar and P. D. Yurchenco (2002). "Matrix assembly, regulation, and survival functions of laminin and its receptors in embryonic stem cell differentiation." J Cell Biol **157**(7): 1279-90.
- Liddington, R. C. and M. H. Ginsberg (2002). "Integrin activation takes shape." J Cell Biol **158**(5): 833-9.
- Liliental, J. and D. D. Chang (1998). "Rack1, a receptor for activated protein kinase C, interacts with integrin beta subunit." J Biol Chem **273**(4): 2379-83
- Liu, S., S. M. Thomas, D. G. Woodside, D. M. Rose, W. B. Kiosses, M. Pfaff and M. H. Ginsberg (1999). "Binding of paxillin to alpha4 integrins modifies integrin-dependent biological responses." Nature **402**(6762): 676-81.
- Liu, S., D. A. Calderwood and M. H. Ginsberg (2000). "Integrin cytoplasmic domain-binding proteins." J Cell Sci **113** (Pt 20): 3563-71.
- Logan, M., J. F. Martin, A. Nagy, C. Lobe, E. N. Olson and C. J. Tabin (2002). "Expression of Cre Recombinase in the developing mouse limb bud driven by a Prxl enhancer." Genesis **33**(2): 77-80.
- Lukashev, M. E., D. Sheppard and R. Pytela (1994). "Disruption of integrin function and induction of tyrosine phosphorylation by the autonomously expressed beta 1 integrin cytoplasmic domain." J Biol Chem **269**(28): 18311-4.
- Mackenzie, I. C. (1997). "Retroviral transduction of murine epidermal stem cells demonstrates clonal units of epidermal structure." J Invest Dermatol **109**(3): 377-83.
- Mackinnon, A. C., H. Qadota, K. R. Norman, D. G. Moerman and B. D. Williams (2002). "C. elegans PAT-4/ILK functions as an adaptor protein within integrin adhesion complexes." Curr Biol **12**(10): 787-97.
- Mann, M. (2006). "Functional and quantitative proteomics using SILAC." Nat Rev Mol Cell Biol **7**(12): 952-8.
- Mariotti, A., P. A. Kedeshian, M. Dans, A. M. Curatola, L. Gagnoux-Palacios and F. G. Giancotti (2001). "EGF-R signaling through Fyn kinase disrupts the function of integrin alpha6beta4 at hemidesmosomes: role in epithelial cell migration and carcinoma invasion." J Cell Biol **155**(3): 447-58.
- Mates, L., C. Nicolae, M. Morgelin, F. Deak, I. Kiss and A. Aszodi (2004). "Mice lacking the extracellular matrix adaptor protein matrilin-2 develop without obvious abnormalities." Matrix Biol **23**(3): 195-204.
- Mayer, U., G. Saher, R. Fassler, A. Bornemann, F. Echtermeyer, H. von der Mark, N. Miosge, E. Poschl and K. von der Mark (1997). "Absence of integrin alpha 7 causes a novel form of muscular dystrophy." Nat Genet **17**(3): 318-23.
- Mellstrom, K., A. S. Hoglund, M. Nister, C. H. Heldin, B. Westermark and U. Lindberg (1983). "The effect of platelet-derived growth factor on morphology and motility of human glial cells." J Muscle Res Cell Motil **4**(5): 589-609.

- Mills, J., M. Digicaylioglu, A. T. Legg, C. E. Young, S. S. Young, A. M. Barr, L. Fletcher, T. P. O'Connor and S. Dedhar (2003). "Role of integrin-linked kinase in nerve growth factor-stimulated neurite outgrowth." *J Neurosci* **23**(5): 1638-48.
- Miyamoto, S., B. Z. Katz, R. M. Lafrenie and K. M. Yamada (1998). "Fibronectin and integrins in cell adhesion, signaling, and morphogenesis." *Ann N Y Acad Sci* **857**: 119-29.
- Monkley, S. J., X. H. Zhou, S. J. Kinston, S. M. Giblett, L. Hemmings, H. Priddle, J. E. Brown, C. A. Pritchard, D. R. Critchley and R. Fassler (2000). "Disruption of the talin gene arrests mouse development at the gastrulation stage." *Dev Dyn* **219**(4): 560-74.
- Moro, L., M. Venturino, C. Bozzo, L. Silengo, F. Altruda, L. Beguinot, G. Tarone and P. Defilippi (1998). "Integrins induce activation of EGF receptor: role in MAP kinase induction and adhesion-dependent cell survival." *Embo J* **17**(22): 6622-32.
- Muller, U., D. Wang, S. Denda, J. J. Meneses, R. A. Pedersen and L. F. Reichardt (1997). "Integrin alpha8beta1 is critically important for epithelial-mesenchymal interactions during kidney morphogenesis." *Cell* **88**(5): 603-13.
- Naik, U. P., P. M. Patel and L. V. Parise (1997). "Identification of a novel calcium-binding protein that interacts with the integrin alphaIIb cytoplasmic domain." *J Biol Chem* **272**(8): 4651-4.
- Naito, Y., T. Yamada, K. Ui-Tei, S. Morishita and K. Saigo (2004). "siDirect: highly effective, target-specific siRNA design software for mammalian RNA interference." *Nucleic Acids Res* **32**(Web Server issue): W124-9.
- Naviaux, R. K., E. Costanzi, M. Haas and I. M. Verma (1996). "The pCL vector system: rapid production of helper-free, high-titer, recombinant retroviruses." *J Virol* **70**(8): 5701-5.
- Niewmierzycka, A., J. Mills, R. St-Arnaud, S. Dedhar and L. F. Reichardt (2005). "Integrin-linked kinase deletion from mouse cortex results in cortical lamination defects resembling cobblestone lissencephaly." *J Neurosci* **25**(30): 7022-31.
- Nikolopoulos, S. N. and C. E. Turner (2000). "Actopaxin, a new focal adhesion protein that binds paxillin LD motifs and actin and regulates cell adhesion." *J Cell Biol* **151**(7): 1435-48.
- Nikolopoulos, S. N. and C. E. Turner (2001). "Integrin-linked kinase (ILK) binding to paxillin LD1 motif regulates ILK localization to focal adhesions." *J Biol Chem* **276**(26): 23499-505.
- Nikolopoulos, S. N. and C. E. Turner (2002). "Molecular dissection of actopaxin-integrin-linked kinase-Paxillin interactions and their role in subcellular localization." *J Biol Chem* **277**(2): 1568-75.
- Nojima, Y., N. Morino, T. Mimura, K. Hamasaki, H. Furuya, R. Sakai, T. Sato, K. Tachibana, C. Morimoto, Y. Yazaki and et al. (1995). "Integrin-mediated cell adhesion promotes tyrosine phosphorylation of p130Cas, a Src homology 3-containing molecule having multiple Src homology 2-binding motifs." *J Biol Chem* **270**(25): 15398-402.
- Novak, A. and S. Dedhar (1999). "Signaling through beta-catenin and Lef/Tcf." *Cell Mol Life Sci* **56**(5-6): 523-37.

- Novak, A., S. C. Hsu, C. Leung-Hagesteijn, G. Radeva, J. Papkoff, R. Montesano, C. Roskelley, R. Grosschedl and S. Dedhar (1998). "Cell adhesion and the integrin-linked kinase regulate the LEF-1 and beta-catenin signaling pathways." Proc Natl Acad Sci U S A **95**(8): 4374-9.
- Otey, C. A., F. M. Pavalko and K. Burridge (1990). "An interaction between alpha-actinin and the beta 1 integrin subunit in vitro." J Cell Biol **111**(2): 721-9.
- O'Toole, T. E., Y. Katagiri, R. J. Faull, K. Peter, R. Tamura, V. Quaranta, J. C. Loftus, S. J. Shattil and M. H. Ginsberg (1994). "Integrin cytoplasmic domains mediate inside-out signal transduction." J Cell Biol **124**(6): 1047-59.
- Ojaniemi, M. and K. Vuori (1997). "Epidermal growth factor modulates tyrosine phosphorylation of p130Cas. Involvement of phosphatidylinositol 3'-kinase and actin cytoskeleton." J Biol Chem **272**(41): 25993-8.
- Oloumi, A., T. McPhee and S. Dedhar (2004). "Regulation of E-cadherin expression and beta-catenin/Tcf transcriptional activity by the integrin-linked kinase." Biochim Biophys Acta **1691**(1): 1-15.
- Olski, T. M., A. A. Noegel and E. Korenbaum (2001). "Parvin, a 42 kDa focal adhesion protein, related to the alpha-actinin superfamily." J Cell Sci **114**(Pt 3): 525-38.
- Otsuka, H. and M. Moskowitz (1975). "Arrest of 3T3 cells in G1 phase in suspension culture." J Cell Physiol **87**(2): 213-9.
- Pankov, R., E. Cukierman, B. Z. Katz, K. Matsumoto, D. C. Lin, S. Lin, C. Hahn and K. M. Yamada (2000). "Integrin dynamics and matrix assembly: tensin-dependent translocation of alpha(5)beta(1) integrins promotes early fibronectin fibrillogenesis." J Cell Biol **148**(5): 1075-90.
- Pasquet, J. M., M. Noury and A. T. Nurden (2002). "Evidence that the platelet integrin alphaIIb beta3 is regulated by the integrin-linked kinase, ILK, in a PI3-kinase dependent pathway." Thromb Haemost **88**(1): 115-22.
- Persad, S., S. Attwell, V. Gray, N. Mawji, J. T. Deng, D. Leung, J. Yan, J. Sanghera, M. P. Walsh and S. Dedhar (2001). "Regulation of protein kinase B/Akt-serine 473 phosphorylation by integrin-linked kinase: critical roles for kinase activity and amino acids arginine 211 and serine 343." J Biol Chem **276**(29): 27462-9.
- Persad, S. and S. Dedhar (2003). "The role of integrin-linked kinase (ILK) in cancer progression." Cancer Metastasis Rev **22**(4): 375-84.
- Pfaff, M., S. Liu, D. J. Erle and M. H. Ginsberg (1998). "Integrin beta cytoplasmic domains differentially bind to cytoskeletal proteins." J Biol Chem **273**(11): 6104-9.
- Quelo, I., C. Gauthier, G. E. Hannigan, S. Dedhar and R. St-Arnaud (2004). "Integrin-linked kinase regulates the nuclear entry of the c-Jun coactivator alpha-NAC and its coactivation potency." J Biol Chem **279**(42): 43893-9.
- Radeva, G., T. Petrocelli, E. Behrend, C. Leung-Hagesteijn, J. Filmus, J. Slingerland and S. Dedhar (1997). "Overexpression of the integrin-linked kinase promotes anchorage-independent cell cycle progression." J Biol Chem **272**(21): 13937-44.

- Raghavan, S., C. Bauer, G. Mundschau, Q. Li and E. Fuchs (2000). "Conditional ablation of beta1 integrin in skin. Severe defects in epidermal proliferation, basement membrane formation, and hair follicle invagination." *J Cell Biol* **150**(5): 1149-60.
- Ramirez, A., A. Page, A. Gandarillas, J. Zanet, S. Pibre, M. Vidal, L. Tusell, A. Genesca, D. A. Whitaker, D. W. Melton and J. L. Jorcano (2004). "A keratin K5Cre transgenic line appropriate for tissue-specific or generalized Cre-mediated recombination." *Genesis* **39**(1): 52-7.
- Raugei, G., G. Ramponi and P. Chiarugi (2002). "Low molecular weight protein tyrosine phosphatases: small, but smart." *Cell Mol Life Sci* **59**(6): 941-9.
- Reddy, K. B., P. Gascard, M. G. Price, E. V. Negrescu and J. E. Fox (1998). "Identification of an interaction between the m-band protein skelemin and beta-integrin subunits. Colocalization of a skelemin-like protein with beta1- and beta3-integrins in non-muscle cells." *J Biol Chem* **273**(52): 35039-47.
- Ridley, A. J., H. F. Paterson, C. L. Johnston, D. Diekmann and A. Hall (1992). "The small GTP-binding protein rac regulates growth factor-induced membrane ruffling." *Cell* **70**(3): 401-10.
- Rietzler, M., M. Bittner, W. Kolanus, A. Schuster and B. Holzmann (1998). "The human WD repeat protein WAIT-1 specifically interacts with the cytoplasmic tails of beta7-integrins." *J Biol Chem* **273**(42): 27459-66.
- Riveline, D., E. Zamir, N. Q. Balaban, U. S. Schwarz, T. Ishizaki, S. Narumiya, Z. Kam, B. Geiger and A. D. Bershadsky (2001). "Focal contacts as mechanosensors: externally applied local mechanical force induces growth of focal contacts by an mDia1-dependent and ROCK-independent mechanism." *J Cell Biol* **153**(6): 1175-86.
- Rojiani, M. V., B. B. Finlay, V. Gray and S. Dedhar (1991). "In vitro interaction of a polypeptide homologous to human Ro/SS-A antigen (calreticulin) with a highly conserved amino acid sequence in the cytoplasmic domain of integrin alpha subunits." *Biochemistry* **30**(41): 9859-66.
- Rosenberger, G., I. Jantke, A. Gal and K. Kutsche (2003). "Interaction of alphaPIX (ARHGEF6) with beta-parvin (PARVB) suggests an involvement of alphaPIX in integrin-mediated signaling." *Hum Mol Genet* **12**(2): 155-67.
- Saiki, R. K., D. H. Gelfand, S. Stoffel, S. J. Scharf, R. Higuchi, G. T. Horn, K. B. Mullis and H. A. Erlich (1988). "Primer-directed enzymatic amplification of DNA with a thermostable DNA polymerase." *Science* **239**(4839): 487-91.
- Sajid, M., Z. Hu, M. Lele and G. A. Stouffer (2000). "Protein complexes involving alpha v beta 3 integrins, nonmuscle myosin heavy chain-A, and focal adhesion kinase from in thrombospondin-treated smooth muscle cells." *J Investig Med* **48**(3): 190-7.
- Sakai, K., L. Hiripi, V. Glumoff, O. Brandau, R. Eerola, E. Vuorio, Z. Bosze, R. Fassler and A. Aszodi (2001). "Stage-and tissue-specific expression of a Col2a1-Cre fusion gene in transgenic mice." *Matrix Biol* **19**(8): 761-7.

- Sakai, T., S. Li, D. Docheva, C. Grashoff, K. Sakai, G. Kostka, A. Braun, A. Pfeifer, P. D. Yurchenco and R. Fassler (2003). "Integrin-linked kinase (ILK) is required for polarizing the epiblast, cell adhesion, and controlling actin accumulation." Genes Dev **17**(7): 926-40.
- Schaller, M. D., C. A. Otey, J. D. Hildebrand and J. T. Parsons (1995). "Focal adhesion kinase and paxillin bind to peptides mimicking beta integrin cytoplasmic domains." J Cell Biol **130**(5): 1181-7.
- Scharffetter-Kochanek, K., H. Lu, K. Norman, N. van Nood, F. Munoz, S. Grabbe, M. McArthur, I. Lorenzo, S. Kaplan, K. Ley, C. W. Smith, C. A. Montgomery, S. Rich and A. L. Beaudet (1998). "Spontaneous skin ulceration and defective T cell function in CD18 null mice." J Exp Med **188**(1): 119-31.
- Schliwa, M., T. Nakamura, K. R. Porter and U. Euteneuer (1984). "A tumor promoter induces rapid and coordinated reorganization of actin and vinculin in cultured cells." J Cell Biol **99**(3): 1045-59.
- Schmits, R., T. M. Kundig, D. M. Baker, G. Shumaker, J. J. Simard, G. Duncan, A. Wakeham, A. Shahinian, A. van der Heiden, M. F. Bachmann, P. S. Ohashi, T. W. Mak and D. D. Hickstein (1996). "LFA-1-deficient mice show normal CTL responses to virus but fail to reject immunogenic tumor." J Exp Med **183**(4): 1415-26.
- Schneller, M., K. Vuori and E. Ruoslahti (1997). "Alphavbeta3 integrin associates with activated insulin and PDGFbeta receptors and potentiates the biological activity of PDGF." Embo J **16**(18): 5600-7.
- Schon, M. P., A. Arya, E. A. Murphy, C. M. Adams, U. G. Strauch, W. W. Agace, J. Marsal, J. P. Donohue, H. Her, D. R. Beier, S. Olson, L. Lefrancois, M. B. Brenner, M. J. Grusby and C. M. Parker (1999). "Mucosal T lymphocyte numbers are selectively reduced in integrin alpha E (CD103)-deficient mice." J Immunol **162**(11): 6641-9.
- Schwartz, M. A. and M. H. Ginsberg (2002). "Networks and crosstalk: integrin signalling spreads." Nat Cell Biol **4**(4): E65-8.
- Shattil, S. J., T. O'Toole, M. Eigenthaler, V. Thon, M. Williams, B. M. Babior and M. H. Ginsberg (1995). "Beta 3-endonexin, a novel polypeptide that interacts specifically with the cytoplasmic tail of the integrin beta 3 subunit." J Cell Biol **131**(3): 807-16.
- Smart, E. J., Y. S. Ying, C. Mineo and R. G. Anderson (1995). "A detergent-free method for purifying caveolae membrane from tissue culture cells." Proc Natl Acad Sci U S A **92**(22): 10104-8.
- Smyth, N., H. S. Vatansever, P. Murray, M. Meyer, C. Frie, M. Paulsson and D. Edgar (1999). "Absence of basement membranes after targeting the LAMC1 gene results in embryonic lethality due to failure of endoderm differentiation." J Cell Biol **144**(1): 151-60.
- Solowska, J., J. L. Guan, E. E. Marcantonio, J. E. Trevithick, C. A. Buck and R. O. Hynes (1989). "Expression of normal and mutant avian integrin subunits in rodent cells." J Cell Biol **109**(2): 853-61.
- St-Jacques, B., M. Hammerschmidt and A. P. McMahon (1999). "Indian hedgehog signaling regulates proliferation and differentiation of chondrocytes and is essential for bone formation." Genes Dev **13**(16): 2072-86.

- Stanchi, F., R. Bordoy, O. Kudlacek, A. Braun, A. Pfeifer, M. Moser and R. Fassler (2005). "Consequences of loss of PINCH2 expression in mice." J Cell Sci **118**(Pt 24): 5899-910.
- Suetsugu, S., D. Yamazaki, S. Kurisu and T. Takenawa (2003). "Differential roles of WAVE1 and WAVE2 in dorsal and peripheral ruffle formation for fibroblast cell migration." Dev Cell **5**(4): 595-609.
- Tang, S., Y. Gao and J. A. Ware (1999). "Enhancement of endothelial cell migration and in vitro tube formation by TAP20, a novel beta 5 integrin-modulating, PKC theta-dependent protein." J Cell Biol **147**(5): 1073-84.
- Takagi, J., B. M. Petre, T. Walz and T. A. Springer (2002). "Global conformational rearrangements in integrin extracellular domains in outside-in and inside-out signaling." Cell **110**(5): 599-11.
- Tan, C., P. Costello, J. Sanghera, D. Dominguez, J. Baulida, A. G. de Herreros and S. Dedhar (2001). "Inhibition of integrin linked kinase (ILK) suppresses beta-catenin-Lef/Tcf-dependent transcription and expression of the E-cadherin repressor, snail, in APC^{-/-} human colon carcinoma cells." Oncogene **20**(1): 133-40.
- Tan, C., A. Mui and S. Dedhar (2002). "Integrin-linked kinase regulates inducible nitric oxide synthase and cyclooxygenase-2 expression in an NF-kappa B-dependent manner." J Biol Chem **277**(5): 3109-16.
- Tronik-Le Roux, D., V. Roullot, C. Poujol, T. Kortulewski, P. Nurden and G. Marguerie (2000). "Thrombasthenic mice generated by replacement of the integrin alpha(IIb) gene: demonstration that transcriptional activation of this megakaryocytic locus precedes lineage commitment." Blood **96**(4): 1399-408.
- Troussard, A. A., P. Costello, T. N. Yoganathan, S. Kumagai, C. D. Roskelley and S. Dedhar (2000). "The integrin linked kinase (ILK) induces an invasive phenotype via AP-1 transcription factor-dependent upregulation of matrix metalloproteinase 9 (MMP-9)." Oncogene **19**(48): 5444-52.
- Troussard, A. A., P. C. McDonald, E. D. Wederell, N. M. Mawji, N. R. Filipenko, K. A. Gelmon, J. E. Kucab, S. E. Dunn, J. T. Emerman, M. B. Bally and S. Dedhar (2006). "Preferential dependence of breast cancer cells versus normal cells on integrin-linked kinase for protein kinase B/Akt activation and cell survival." Cancer Res **66**(1): 393-403.
- Troussard, A. A., C. Tan, T. N. Yoganathan and S. Dedhar (1999). "Cell-extracellular matrix interactions stimulate the AP-1 transcription factor in an integrin-linked kinase- and glycogen synthase kinase 3-dependent manner." Mol Cell Biol **19**(11): 7420-7.
- Tu, Y., F. Li, S. Goicoechea and C. Wu (1999). "The LIM-only protein PINCH directly interacts with integrin-linked kinase and is recruited to integrin-rich sites in spreading cells." Mol Cell Biol **19**(3): 2425-34.
- Tu, Y., F. Li and C. Wu (1998). "Nck-2, a novel Src homology2/3-containing adaptor protein that interacts with the LIM-only protein PINCH and components of growth factor receptor kinase-signaling pathways." Mol Biol Cell **9**(12): 3367-82.

- Tu, Y., Y. Huang, Y. Zhang, Y. Hua and C. Wu (2001). "A new focal adhesion protein that interacts with integrin-linked kinase and regulates cell adhesion and spreading." J Cell Biol **153**(3): 585-98.
- Tu, Y., S. Wu, X. Shi, K. Chen and C. Wu (2003). "Migfilin and Mig-2 link focal adhesions to filamin and the actin cytoskeleton and function in cell shape modulation." Cell **113**(1): 37-47.
- Turner, C. E. (2000). "Paxillin and focal adhesion signalling." Nat Cell Biol **2**(12): E231-6.
- Ui-Tei, K., Y. Naito, F. Takahashi, T. Haraguchi, H. Ohki-Hamazaki, A. Juni, R. Ueda and K. Saigo (2004). "Guidelines for the selection of highly effective siRNA sequences for mammalian and chick RNA interference." Nucleic Acids Res **32**(3): 936-48.
- van der Neut, R., P. Krimpenfort, J. Calafat, C. M. Niessen and A. Sonnenberg (1996). "Epithelial detachment due to absence of hemidesmosomes in integrin beta 4 null mice." Nat Genet **13**(3): 366-9.
- Velyvis, A., Y. Yang, C. Wu and J. Qin (2001). "Solution structure of the focal adhesion adaptor PINCH LIM1 domain and characterization of its interaction with the integrin-linked kinase ankyrin repeat domain." J Biol Chem **276**(7): 4932-9.
- Veracini, L., M. Franco, A. Boureux, V. Simon, S. Roche and C. Benistant (2006). "Two distinct pools of Src family tyrosine kinases regulate PDGF-induced DNA synthesis and actin dorsal ruffles." J Cell Sci **119**(Pt 14): 2921-34.
- Vikkula, M., M. Metsaranta and L. Ala-Kokko (1994). "Type II collagen mutations in rare and common cartilage diseases." Ann Med **26**(2): 107-14.
- Vinogradova, O., A. Velyvis, A. Velyviene, B. Hu, T. Haas, E. Plow and J. Qin (2002). "A structural mechanism of integrin alpha(IIb)beta(3) "inside-out" activation as regulated by its cytoplasmic face." Cell **110**(5): 587-97.
- Vouret-Craviari, V., E. Boulter, D. Grall, C. Matthews and E. Van Obberghen-Schilling (2004). "ILK is required for the assembly of matrix-forming adhesions and capillary morphogenesis in endothelial cells." J Cell Sci **117**(Pt 19): 4559-69.
- Vuori, K. and E. Ruoslahti (1995). "Tyrosine phosphorylation of p130Cas and cortactin accompanies integrin-mediated cell adhesion to extracellular matrix." J Biol Chem **270**(38): 22259-62.
- Wagner, N., J. Lohler, E. J. Kunkel, K. Ley, E. Leung, G. Krissansen, K. Rajewsky and W. Muller (1996). "Critical role for beta7 integrins in formation of the gut-associated lymphoid tissue." Nature **382**(6589): 366-70.
- Wang, D., Y. C. Tan, G. E. Kreitzer, Y. Nakai, D. Shan, Y. Zheng and X. Y. Huang (2006). "G proteins G12 and G13 control the dynamic turnover of growth factor-induced dorsal ruffles." J Biol Chem **281**(43): 32660-7.
- Wang, H. and S. K. Dey (2006). "Roadmap to embryo implantation: clues from mouse models." Nat Rev Genet **7**(3): 185-99.

- Wary, K. K., A. Mariotti, C. Zurzolo and F. G. Giancotti (1998). "A requirement for caveolin-1 and associated kinase Fyn in integrin signaling and anchorage-dependent cell growth." *Cell* **94**(5): 625-34.
- Weir, E. C., W. M. Philbrick, M. Amling, L. A. Neff, R. Baron and A. E. Broadus (1996). "Targeted overexpression of parathyroid hormone-related peptide in chondrocytes causes chondrodysplasia and delayed endochondral bone formation." *Proc Natl Acad Sci U S A* **93**(19): 10240-5.
- White, D. E., R. D. Cardiff, S. Dedhar and W. J. Muller (2001). "Mammary epithelial-specific expression of the integrin-linked kinase (ILK) results in the induction of mammary gland hyperplasias and tumors in transgenic mice." *Oncogene* **20**(48): 7064-72.
- Wixler, V., D. Geerts, E. Laplantine, D. Westhoff, N. Smyth, M. Aumailley, A. Sonnenberg and M. Paulsson (2000). "The LIM-only protein DRAL/FHL2 binds to the cytoplasmic domain of several alpha and beta integrin chains and is recruited to adhesion complexes." *J Biol Chem* **275**(43): 33669-78.
- Williams, B. D. and R. H. Waterston (1994). "Genes critical for muscle development and function in *Caenorhabditis elegans* identified through lethal mutations." *J Cell Biol* **124**(4): 475-90.
- Wu, C., S. Y. Keightley, C. Leung-Hagesteijn, G. Radeva, M. Coppolino, S. Goicoechea, J. A. McDonald and S. Dedhar (1998). "Integrin-linked protein kinase regulates fibronectin matrix assembly, E-cadherin expression, and tumorigenicity." *J Biol Chem* **273**(1): 528-36.
- Xiong, J. P., T. Stehle, B. Diefenbach, R. Zhang, R. Dunker, D. L. Scott, A. Joachimiak, S. L. Goodman and M. A. Arnaout (2001). "Crystal structure of the extracellular segment of integrin alpha Vbeta3." *Science* **294**(5541): 339-45.
- Xiong, J. P., T. Stehle, R. Zhang, A. Joachimiak, M. Frech, S. L. Goodman and M. A. Arnaout (2002). "Crystal structure of the extracellular segment of integrin alpha Vbeta3 in complex with an Arg-Gly-Asp ligand." *Science* **296**(5565): 151-5.
- Xu, W., H. Baribault and E. D. Adamson (1998). "Vinculin knockout results in heart and brain defects during embryonic development." *Development* **125**(2): 327-37.
- Yamada, K. M., R. Pankov and E. Cukierman (2003). "Dimensions and dynamics in integrin function." *Braz J Med Biol Res* **36**(8): 959-66.
- Yamaji, S., A. Suzuki, Y. Sugiyama, Y. Koide, M. Yoshida, H. Kanamori, H. Mohri, S. Ohno and Y. Ishigatsubo (2001). "A novel integrin-linked kinase-binding protein, affixin, is involved in the early stage of cell-substrate interaction." *J Cell Biol* **153**(6): 1251-64.
- Yang, J. T., H. Rayburn and R. O. Hynes (1993). "Embryonic mesodermal defects in alpha 5 integrin-deficient mice." *Development* **119**(4): 1093-105.
- Yang, J. T., H. Rayburn and R. O. Hynes (1995). "Cell adhesion events mediated by alpha 4 integrins are essential in placental and cardiac development." *Development* **121**(2): 549-60.
- Zaidel-Bar, R., R. Milo, Z. Kam and B. Geiger (2007). "A paxillin tyrosine phosphorylation switch regulates the assembly and form of cell-matrix adhesions." *J Cell Sci* **120**(Pt 1): 137-48.

- Zamir, E. and B. Geiger (2001). "Molecular complexity and dynamics of cell-matrix adhesions." J Cell Sci **114**(Pt 20): 3583-90.
- Zamir, E., M. Katz, Y. Posen, N. Erez, K. M. Yamada, B. Z. Katz, S. Lin, D. C. Lin, A. Bershadsky, Z. Kam and B. Geiger (2000). "Dynamics and segregation of cell-matrix adhesions in cultured fibroblasts." Nat Cell Biol **2**(4): 191-6.
- Zent, R., C. A. Fenczik, D. A. Calderwood, S. Liu, M. Dellos and M. H. Ginsberg (2000). "Class- and splice variant-specific association of CD98 with integrin beta cytoplasmic domains." J Biol Chem **275**(7): 5059-64.
- Zervas, C. G., S. L. Gregory and N. H. Brown (2001). "Drosophila integrin-linked kinase is required at sites of integrin adhesion to link the cytoskeleton to the plasma membrane." J Cell Biol **152**(5): 1007-18.
- Zhang, Y., K. Chen, L. Guo and C. Wu (2002). "Characterization of PINCH-2, a new focal adhesion protein that regulates the PINCH-1-ILK interaction, cell spreading, and migration." J Biol Chem **277**(41): 38328-38.
- Zhang, Y., K. Chen, Y. Tu, A. Velyvis, Y. Yang, J. Qin and C. Wu (2002). "Assembly of the PINCH-ILK-CH-ILKBP complex precedes and is essential for localization of each component to cell-matrix adhesion sites." J Cell Sci **115**(Pt 24): 4777-86.
- Zhang, Y., K. Chen, Y. Tu and C. Wu (2004). "Distinct roles of two structurally closely related focal adhesion proteins, alpha-parvins and beta-parvins, in regulation of cell morphology and survival." J Biol Chem **279**(40): 41695-705.
- Zhu, J., K. Motejlek, D. Wang, K. Zang, A. Schmidt and L. F. Reichardt (2002). "beta8 integrins are required for vascular morphogenesis in mouse embryos." Development **129**(12): 2891-903.

7. Publications

Sakai, T., S. Li, D. Docheva, **C. Grashoff**, K. Sakai, G. Kostka, A. Braun, A. Pfeifer, P. D. Yurchenco and R. Fässler (2003). "Integrin-linked kinase (ILK) is required for polarizing the epiblast, cell adhesion, and controlling actin accumulation." Genes Dev **17**(7): 926-40.

Grashoff, C., A. Aszodi, T. Sakai, E. B. Hunziker and R. Fässler (2003). "Integrin-linked kinase regulates chondrocyte shape and proliferation." EMBO Rep **4**(4): 432-8.

Grashoff, C., I. Thievensen, K. Lorenz, S. Ussar and R. Fässler (2004). "Integrin-linked kinase: integrin's mysterious partner." Curr Opin Cell Biol **16**(5): 565-71.

Gimona, M., **C. Grashoff** and P. Kopp (2005). "Oktoberfest for adhesion structures." EMBO Rep **6**(10): 922-6.

Lorenz, K.*, **C. Grashoff***, R. Torka*, T. Sakai, L. Langbein, W. Bloch, M. Aumialley and R. Fässler (2007). "ILK is required for epidermal and hair follicle morphogenesis". Re-submitted for publication.

*: equal contribution

8. Acknowledgements

First and foremost, I would like to thank Prof. Dr. Reinhard Fässler for the outstanding support and the excellent supervision over the last 4 years. I would like to thank for all inspiring advises, constructive suggestions and always fair and honest criticisms. I always greatly appreciated the intensive and motivating discussions about all aspects of our research. The last 4 years have been the most valuable time of my scientific life and I am grateful for this experience.

I would like to thank Prof. Dr. Alexander Pfeifer for the extremely helpful and supportive mentoring of this PhD thesis. I am grateful for all his scientific and personal advices and much obliged for the help with numerous retroviral preparations which were essential for this project.

I would like to express my gratitude to Prof. Dr. Michael Schleicher and Prof. Dr. Martin Biel for examining this thesis. I also would like to thank Prof. Dr. Schleicher for his help during fellowship applications.

I would like to thank Dr. Carsten Culmsee for examining this thesis and for the uncomplicated team play during many practical courses.

I thank Dr. Attila Aszodi for his excellent teaching and expert advices during the analysis of Col2ILK mice. It would have been impossible to analyze these mice in such a short time without him. I always appreciated his honest criticisms about my work.

I would like to thank Dr. Walter Göhring for all the technical help, Stefan Benkert and Catharina Cramnert for teaching and practical help in the HistoLab and Heidi Sebald for many, many viruspreps.

I would especially like to thank my parents Hans-Jochen und Helga Grashoff, my dear sister Katrin Grashoff and my grandma Elfriede Stössel for the continuous encouragement and support during my studies and this PhD thesis.

Finally, I would like to thank Anna for her love and support every day.

9. Curriculum vitae

Personal details

Name: Carsten Grashoff
Date of birth: 18.03.1977 in Northeim
Nationality: German
Marital status: married
Affiliation: Max-Planck-Institute of Biochemistry
Department of Molecular Medicine
Address: Am Klopferspitz 18, 82152 Martinsried, Germany

Education

1983-1987: Primary school, Osterode-Dorste, Germany
1987-1996: Grammar school, Gymnasium Osterode, Germany
1996-1997: Military Service, Niedersachsenkaserne Dörverden, Germany

Scientific Education

1997-2002: Study of Applied Science, Technical University Bergakademie
Freiberg, Germany
2001-2002: Diploma-Thesis, Robert-Koch-Institute Berlin, Germany
2002-2007: Dissertation, Max-Planck-Institute of Biochemistry, Germany
Department of Molecular Medicine

Honors/Awards

2003 Greorgius-Agricola Medal of the Technical University Bergakademie
Freiberg
2004 Max-Planck-Institute of Biochemistry Junior Research Award

München, den 08.02.2007